2808914299

REFERENCE ONLY

UNIVERSITY OF LONDON THESIS

Degree PhD Year 2006 Name of Author SMARAGDI NAMINI Sonella

COPYRIGHT
This is a thesis accepted for a Higher Degree of the University of London. It is an unpublished typescript and the copyright is held by the author. All persons consulting the thesis must read and abide by the Copyright Declaration below.

COPYRIGHT DECLARATION
I recognise that the copyright of the above-described thesis rests with the author and that no quotation from it or information derived from it may be published without the prior written consent of the author.

LOANS
Theses may not be lent to individuals, but the Senate House Library may lend a copy to approved libraries within the United Kingdom, for consultation solely on the premises of those libraries. Application should be made to: Inter-Library Loans, Senate House Library, Senate House, Malet Street, London WC1E 7HU.

REPRODUCTION
University of London theses may not be reproduced without explicit written permission from the Senate House Library. Enquiries should be addressed to the Theses Section of the Library. Regulations concerning reproduction vary according to the date of acceptance of the thesis and are listed below as guidelines.

A. Before 1962. Permission granted only upon the prior written consent of the author. (The Senate House Library will provide addresses where possible).

B. 1962 - 1974. In many cases the author has agreed to permit copying upon completion of a Copyright Declaration.

C. 1975 - 1988. Most theses may be copied upon completion of a Copyright Declaration.

D. 1989 onwards. Most theses may be copied.

This thesis comes within category D.

☐ This copy has been deposited in the Library of UCL

☐ This copy has been deposited in the Senate House Library, Senate House, Malet Street, London WC1E 7HU.

C:\Documents and Settings\lproctor\Local Settings\Temporary Internet Files\OLK8\Copyright - thesis (2).doc

A Study of the role of Desert hedgehog in the peripheral nervous system

Soheila SharghiNamini

Department of Anatomy and Developmental Biology

University College London

A thesis presented for the degree of Doctor of Philosophy

University of London, 2006

UMI Number: U593166

All rights reserved

INFORMATION TO ALL USERS
The quality of this reproduction is dependent upon the quality of the copy submitted.

In the unlikely event that the author did not send a complete manuscript
and there are missing pages, these will be noted. Also, if material had to be removed,
a note will indicate the deletion.

UMI U593166
Published by ProQuest LLC 2013. Copyright in the Dissertation held by the Author.
Microform Edition © ProQuest LLC.
All rights reserved. This work is protected against
unauthorized copying under Title 17, United States Code.

ProQuest LLC
789 East Eisenhower Parkway
P.O. Box 1346
Ann Arbor, MI 48106-1346

DEDICATED TO BELOVED SISTERS AFAGH AND JILA

ACKNOWLEDGEMENTS

I would to thank Prof. Rhona Mirsky and Prof. Kristjan R. Jessen for giving me the opportunity to work on these project and for their guidance and support throughout the course. I am indebted to Mark Turmaine for his immense help in processing tissues for EM throughout this project. I would like to thank past and present members of the laboratory particularly Dr. David B. Parkinson, Dr. Maria Duran-Alonso, Dr. Maurizio D'Antonio, Dr. Ambily Bhaskaran, Anna Droggiti, and Ashwin Woodhoo for their assistance and support. I would also like to thank Mary Rahman for her endless technical support, Prof. P. Brophy, Dr. S. Davies, Dr. E. Peles, Dr. J. Roes and Dr. J. Archelos for the gift of antibodies, and Prof. A. P. McMahon and Prof. I. Griffiths for provision of mutant mice.

Finally, I thank my family specially my partner for their endless encouragement and support throughout this journey.

CONTENTS

ABSTRACT

This work shows that *desert hedgehog (dhh)*, a signalling molecule expressed by Schwann cells, is essential for the structural and functional integrity of peripheral nerve. *Dhh*-null nerves display multiple abnormalities that affect myelinating and non-myelinating Schwann cells, axons, vasculature and immune cells. Myelinated fibres of these mice have a significantly increased (>2x) number of Schmidt-Lanterman incisures (SLI) and connexin (Cx)29, a molecular component of SLI, is strongly up-regulated. Crossing *dhh*-null mice with myelin basic protein (MBP)-deficient *shiverer (shi)* mice, which also have increased SLI numbers, results in further increased SLI, suggesting that Dhh and MBP control SLI by different mechanisms. Unmyelinated fibres are also affected, containing many fewer axons per Schwann cell in transverse profiles, while the total number of unmyelinated axons is reduced by approximately a third. In *dhh*-null mice, the blood-nerve barrier is permeable and neutrophils and macrophage numbers are elevated, even in uninjured nerves. *Dhh*-null nerves also lack the largest diameter myelinated fibres, have elevated numbers of degenerating myelinated axons and contain regenerating fibres. Transected *dhh* nerves degenerate faster than wildtype controls.

This demonstrates that a single identified glial signal, Dhh, plays a critical trophic role in maintaining the integrity of peripheral nervous tissue, in line with its critical role in nerve sheath development (Parmantier *et al.*, 1999). The complexity of the defects raises a number of important questions about the Dhh-dependent cell-cell signalling network in peripheral nerves.

ABBREVIATIONS

APS	Ammonium peroxodisulphate
B-FABP	Brain fatty acid binding protein
BMP	Bone morphogenetic proteins
BSA	Bovine serum albumin
Caspr	Contactin associated protein
CNS	Central nervous system
DMEM	Dulbecco's modified Eagles medium
Dhh	Desert hedgehog
DRG	Dorsal root ganglia
ECM	Extracellular matrix
ET	Endothelin
FCS	Fetal calf serum
FGF	Fibroblast growth factor
GAP-43	Growth associated protein 43
Gal-C	Glycolipid galactocerebroside
GDNF	Glial derived neurotrophic factor
GGF	Glial growth factor
HGF	Hepatocyte growth factor
IGF	Insulin growth factor
Ihh	Indian hedgehog
LIF	Leukaemia inhibitory factor
LPA	Lysophosphatidic acid
MAG	Myelin-associated glycoprotein

MAL	Myelin and lymphocyte protein
MBP	Myelin basic protein
MEM	Minimum essential medium
MUPP1	Multi-PDZ domain protein
NF155	Neurofascin protein-155
NGF	Nerve growth factor
Nrg1	Neuroregulin-1
NT-3	Neurotrophin-3
P75NTR	Low affinity p75 neurotrophin receptor
PDGF-BB	Platelet-derived growth factor-BB
PLP	Proteolipid protein
PMP-22	Peripheral myelin protein
P_0	Major peripheral myelin protein zero
PNS	Peripheral nervous system
PTKs	Protein tyrosine kinase molecules
SCF	Stem cell factor
Shh	Sonic hedgehog
SLI	Schmidt-Lanterman Incisures
TGF-β	Transforming growth factor-beta
TNFα	Tumour necrosis factor-alpha

Chapter 1

Chapter 3

Chapter 4

Chapter 5

Chapter 6

CHAPTER I

GENERAL INTRODUCTION

One of the major classes of glia within the nervous system is that of the myelinating glia which includes oligodendrocytes in the central nervous system (CNS), and Schwann cells in the peripheral nervous system (PNS). The glial cells in the PNS also include non-myelinating Schwann cells as well as enteric and satellite cells. The nerve fibres in the PNS are surrounded by specialised connective tissues which are organised in three different layers; epineurium (outer layer), perineurium (Middle layer), and endoneurium (inner layer).

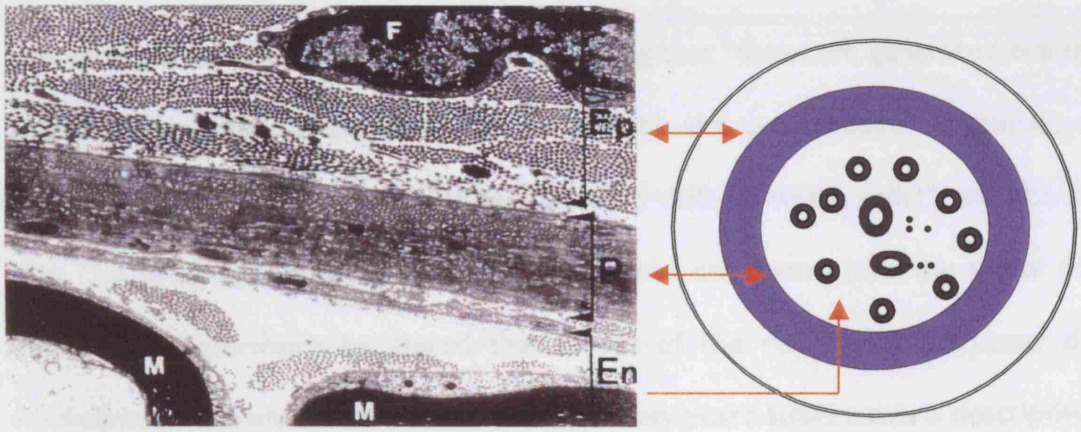

Figure I.1 Electron microscopy and schematic depiction of the organization of epi-, peri-, and endoneurial connective tissue shown in a transverse section from normal nerve. Epineurium (Ep) consists mainly of collagen fibrils and of scattred fibroblasts (F) lacking a basal lamina. The perineurium (P) consists of six to eight layers of compacted concentric layers of flattened cells with a continuous basal lamina on each side. Parts of two myelinated axons in the intrafascicular space, surrounded by endoneurial (En) collagen fibrils, can be seen in the lower part of the micrograph. Abbreviation: M, myelin sheath – From Parmantier *et al.*, 1999, *Neuron* **23,** 713-724.

The epineurium is mainly formed of collagen fibrils as well as scattered fibroblasts lacking a basal lamina. The perineurium is formed from compacted layer of flattened cells (usually six to eight) of epithelial-like morphology arranged around the nerve, where cells are linked together by tight junctions and gap junctions (Thomas *el al.*, 1984). Myelinating glial cells provide multilamellar spiral structures of specialised membrane that ensheathes axons to insulate and facilitate rapid saltatory conduction. The myelin sheath itself can be divided into two domains, compact myelin and non-compact myelin including the paranodal regions (Fig 1.2) and Schmidt-Lanterman incisures (SLI). In the CNS, a single oligodendrocyte will wrap around many axons whereas in the PNS, a single Schwann cell associated with and myelinates only a single axonal segment.

Theodore Schwann, the pioneer of cell theory, gave the first description of the cells that would later bear his name in 1839, by stating that "fibres are generated in a similar manner to muscle; that is they are formed by the coalescence of primary cells, therefore the nervous fibres would be secondary cells (Schwann cells)", and also stated that "by progressive development they become converted into the white fibres" (myelin). Furthermore he stated that "most of the cell nuclei disappear during formation of the white substance". About seventy years later, a more descriptive and detailed version of Schwann cells that we know today, was introduced by Ramon Y Cajal, the founder of modern neurobiology. The development of the metallic impregnation technique by Camillo Golgi in 1873, allowed Cajal to identify the Schwann cell, node of Ranvier (NR), SLI and that the cytoplasm was continuous within myelin rather than being a separate entity. The presence of non-myelinated fibres was also described by Cajal, which were originally identified in 1837 by Robert Remak. Cajal also identified the astrocytes among neuronal cells later but failed to recognize

the source of myelin in the CNS due to technical limitations. The advent of the electron microscope allowed the ultrastructural and functional profile of both Schwann cell forms to be revealed (Geren and Raskind, 1953).

NEURAL CREST

The neural crest is a transient group of migratory cells that has originated from the neural primordium (Dupin *et al.*, 2003; Le Douarin and Smith, 1988), where it delaminates from the dorsal neural tube during embryonic development. Most neural crest cells are multipotent and they give rise to a large spectrum of cell types, including glial cells, neurons of sensory and autonomic ganglia as well as a range of non-neuronal tissues like melanocytes, chromaffin cells, smooth muscle cells, and cartilage. A number of studies in the chick proposed that a small population of Schwann cells in the proximal part of the peripheral nerve may originate from the ventral neural tube *in* vivo (Loring and Erickson, 1987; Lunn *et al.*, 1987; Rickmann *et al.*, 1985; Weston, 1963). More recent works suggested that glial cells populating ventral roots are of neural crest origin (Carpenter and Hollyday, 1992a; Bhattacharyya *et al.*, 1994; Golding and Cohen, 1997). Moreover, studies on boundary cap (BC) cells, which originate from neural crest, suggest that they provide an alternative source of precursors for the completion of proximal PNS construction after the cessation of neural crest migration (Maro *et al.*, 2004). Taken all together these data suggest that the vast majority of Schwann cells are derived from neural crest but that a small minority may be ventrally derived.

The induction of the neural crest

At the early stage of neural development, neural tissue is induced in the outer layer (ectodermal) of the embryo, causing division of the layer into three different regions: neural plate which give rise to CNS formation, non-neural ectoderm which forms the epidermis; and the cells at the border between, which mostly become the neural crest (Gammill and Bronner-Fraser, 2003). The early development of neural crest begins as the neural plate folds towards the midline to form the neural tube through the fusion of opposite sides of the ectoderm in border region. In this way, neural crest progenitors come to lie in the dorsal neural tube (Le Douarin and Kalcheim, 1999). Although the neural folds are viewed as pre-migratory neural crest, only a small proportion of these cells will migrate and that on its own involves several signalling events (Gammill and Bronner-Fraser, 2003). It has been shown by a number of groups that signalling between newly induced neural tissue and the nearby non-neural ectoderm is involved in the formation of the neural plate border and neural crest cells (Moury and Jacobson, 1989; Serbedzija *et al.,* 1994; Selleck and Bronner-Fraser, 1995; Mancilla and Mayor, 1996; Streit and Stern, 1999). Furthermore, signals from paraxial mesoderm are also involved in inducing the border region (Selleck and Bronner-Fraser, 1995; Monsoro-Burg *et al.,* 2003). The formation of neural crest precursors at the neural plate border involves a number of secreted factors and signalling events. Wnt proteins, Bone Morphogenetic Proteins (BMPs) and Fibroblast Growth Factors (FGFs) have all been shown in different assays to take part in to promoting the tissue interactions that induce neural crest (Gammill and Bronner-Fraser, 2003). Another factor, called Noelin-1, appears to be crucial in the timing of neural crest formation, as it can prolong the window of neural crest production (Barembaum *et al.,* 2000). Wnt proteins are required for neural crest induction in amphibians and zebrafish. Studies in

mouse embryos lacking both Wnt1 and Wnt3a showed that, although these genes are not required for neural crest induction, they might have a role in the proliferation of neural crest precursors (Ikeya *et al.*, 1997). Studies in birds however, indicate that Wnt6 seems to be the inducing signal from non-neural ectodermal tissue (Garcia-Castro *et al.*, 2002). Work by Selleck *et al.* (1998) stated that neural crest formation requires BMP signals only after the initial induction step, indicating that BMP's role is in maintenance of the induction process, or for initiation of migration (Sela-Donenfeld and Kalcheim, 1999). In amphibians, FGF signalling can induce neural crest in neuralized ectoderm (LaBonne and Bronner-Fraser, 1989; Mayor *et al.*, 1995). Furthermore, studies in the chick have also shown that FGF can act as a neural inducer (Storey *et al.*, 1998; Streit *et al.*, 2000), and that FGF signalling is required for neural induction (Streit *et al.*, 2000).

Neural crest migration patterns

The earliest investigation into the migratory path of neural crest involved injection of tritiated thymidine into the donor tissue. This becomes incorporated into DNA (Weston, 1963). The downfall of this technique was its limitation in labelling the subsequent progeny due to dilution of the label with each cell division. Nevertheless, it permitted the identification of two main routes of neural crest migration in the trunk region: ventromedial migration to give rise to cells in the dorsal root ganglia (DRG), sympathetic ganglia, adrenomedullary cells, aortic plexuses and Schwann cells (Weston, 1963; Le Douarin and Teillet, 1974; Erickson *et al.*, 1992), and at a later stage, dorsolaterally to give rise to melanocytes (Erickson *et al.*, 1992; Erickson and Goins, 1995). However, it was the design of an elegant chimeric avian model, based on the differences in cell size or/and staining properties of the cells found in chick and quail,

by Le Douarin that led to further investigation into the pattern of the neural crest migration (Le Douarin, 1973; 1982). Ventromedial neural crest migration is linked to the maturation of the somites. Somites bud from the segmental plate to form ball-like epithelial structures and each one becomes compartmentalized, consisting of an epithelial dermomyotome and mesenchymal sclerotome. It is at this stage of somite development that trunk neural crest cells invade the somite (Guillory and Bronner-Fraser, 1986). The pattern of neural crest cell invasion is largely mediated by inhibitory signals that actively exclude cells from the caudal half of each somite. Experimental evidence in which somites were inverted in an anterior-posterior direction, showed that neural crest will migrate only through the original anterior portion of the somite (Bronner-Fraser and Stern, 1991), suggesting that somitic mesoderm determines the segmental organization of trunk neural crest cell migration (Krull, 2001). Over the past few years, several inhibitory molecules in the posterior somite that could influence segmentation have been identified. These molecules include (i) extracellular matrix molecules (ECM) like collagen IX, versican, chondrotin 6-sulfate protoglycan, (ii) T-cadherin, (iii) ephrin B2, and (iv) peanut lectin agglutinin (PNA) (Oakley and Tosney, 1991; Ranscht and Bronner-Fraser, 1991; Ring *et al.*, 1996; Debby-Brafman *et al.*, 1999).

Multipotentiality of neural crest

The ability of neural crest to generate divergent types of differentiated cells is of great interest to developmental biologists. A major finding from *in vitro* clonal analysis of neural crest cell progeny is that the neural crest is composed of a heterogeneous population of cells featured with different proliferation and differentiation potentials (Sieber-Blum, 1990; Dupin *et al.*, 1998; Le Douarin and Kalcheim, 1999). This was deduced from experiments that illustrated that randomly selected quail neural crest

cells from 9-13 somite embryos at the mesencephalic level gave rise to clones that were different in size and phenotypic composition. Rare totipotent progenitors were also identified which were able to generate neurons, glial cells, melanocytes and mesenchymal derivatives, such as cartilage nodules and fibroblasts, indicating that some neural crest cells are fully commited to give rise to only one cell type whereas others yield a diverse progeny, hence their multipotentiality at the time of migration (Baroffio *et al.*, 1988; Dupin *et al.*, 1990; Baroffio *et al.*, 1991). Neural crest cell plasticity was examined in the quail-chick system by ablating a particular region of the neural tube or neural folds before the onset of neural crest cell migration in one embryo and replacing it by the equivalent region from a stage-matched embryo in the other. These grafting experiments revealed that the fate of the neural crest cells is not determined before they migrate, but their plasticity would remain until they receive differentiation signals, during or at the end of their migration (Le Douarin, 1986; Le Douarin and Kalcheim, 1999; Sieber-Blum, 1990; Le Douarin, 2004). This observation was supported by experiments analysing the fate commitment of progenitors where it has been shown that culturing neural crest cells away from neural tube for 30-36 hours results in fate restriction in more than 70% of the progenitors (Henion and Weston, 1997), hence, as migration proceeds, neural crest cells face restriction of their potentiality. Furthermore, it has been shown that neural crest cells are capable of extensive self-renewal in culture; they have therefore been referred to as stem cells (Stemple and Anderson, 1992). Procedures have been sought to select multipotent cells from early embryonic nerves, based on the expression of p75 low affinity NGF receptors but absence of expression of the major myelin protein protein zero (P0). On the basis of these experiments, the existence of a population of neural crest stem cells in peripheral nerves system has been suggested (Morrison et al., 1999).

The effects of growth factors on the development of different neural crest derivatives using *in vivo* and *in vitro* models has also been investigated (Anderson, 1997). Stem cell factor (SCF) and endothelin-3 (ET3) and their respective receptors c-kit and ETRB, are involved in melanocyte lineage differentiation in the skin (Opdecamp *et al.*, 1998; Yoshida *et al.*, 2001). Enteric gangliogenesis by neural crest cells depends upon glial-derived neurotrophic factor (GDNF) acting via its receptors *ret* and GFRα1, as well as ET3 and ETRB. Both GDNF and ET3 are produced by the gut mesenchyme through which neural crest cells migrate and differentiate (Airaksinen and Saarma, 2002; Kruger *et al.*, 2003). GDNF may be involved in the directional migration of crest cells through the gastrointestinal tract (Young *et al.*, 2001), and ETRB signalling may be required to modulate the response of neural crest progenitors to migratory signals such as GDNF (Kruger *et al.*, 2003). In mouse mutants as well as in humans, absence of these signals causes Hirschsprung's disease where the ability of neural crest cells to colonize the hindgut is impaired (Iwashita *et al.*, 2003). In the PNS, both neurons and glia differentiate in the same environment, so the understanding of how they choose to adapt to either neuronal or glial fate has been of interest. It is likely that lateral or juxtacrine inhibition is an important mechanism in this context, and both Notch activation and Neuroregulin 1 (Nrg1) signalling have been implicated in this process. Both of these signals inhibit neurogenesis in the neural crest. It has been suggested that expression of Notch ligands or Nrg1 by early neurons would suppress further neurogenesis in neighbouring cells, an effect that might act indirectly to promote gliogenesis. *In vivo* studies have shown that cell-intrinsic changes in responsiveness to neurogenic signals, such as BMPs, influence the type and number of neurons that stem cells can generate (Qian *et al.*, 2000; White *et al.*, 2001). Proneural basic helix-loop-helix (bHLH) transcription factors reinforce neurogenesis by activating the expression

of a cascade of neuronal genes, as well as inhibiting the expression of glial genes (Nieto *et al.*, 2001; Sun *et al.*, 2001). In order for gliogenesis to take place, it is likely that neurogenesis needs to be terminated. It is possible that this partly takes place by Notch activation (Morrison *et al.*, 2000). Furthermore, exposure of cells isolated from embryonic day 14 (E14) nerves to the soluble form of a Notch ligand (Delta) for only 24 hours causes the loss of neuronal potential even in the presence of BMP2 (Morrison, 2001). This response seems to be regulated by the relative expression of Notch and its inhibitor Numb, whereby Numb expressing cells undergo a neuronal fate and, non expressing cells will become glial cells. Consequently, overexpression of Numb in crest cell cultures promotes neuronal differentiation (Wakamatsu *et al.*, 2000; Kubu *et al.*, 2002). Transplantation of uncultured neural cells from E14 sciatic nerve or gut into developing peripheral nerves in vivo demonstrated that, sciatic nerve neural cells gave rise only to glia (i.e Schwann cell precursor), while gut neural cells gave rise primarily to neurons. These results suggest that neural diversity is generated by combination of factors involving regional environmental differences and cell-intrinsic differences encoded in developing neural cells (Bixby *et al.*, 2002).

DEVELOPMENT OF THE SCHWANN CELL LINEAGE

Schwann cells develop in a specific manner that involves a series of different stages beginning with the formation of the neural crest (Le Douarin *et al.*, 1991; Anderson, 1997). There are three main transitional stages from neural crest cells to the generation of mature Schwann cells: first, the formation of Schwann cell precursors from neural crest, second, the formation of immature Schwann cells from Schwann cell precursors, and finally the reversible generation of myelinating and nonmyelinting Schwann cells (Mirsky and Jessen, 1996; Jessen and Mirsky, 1999; 2005).

Schwann cell precursors

The earliest stage of glial differentiation in peripheral nerve trunks is the Schwann cell precursor which represents the large majority of cells in the limb nerves of rat between E14 and E15 (E12- E13 in the mouse). Most of these cells are localised at the periphery of nerve bundles but a small proportion of cells are seen within larger nerve branches (Jessen *et al.*, 1994). Schwann cell precursors are always in close contact with axons and their long, flattened processes form junctions with the processes of the neighbouring cells. This leads to the formation of bundles that hold axons of similar diameter at this age. Unlike older nerves, these early nerves contain no extracellular matrix within them (Jessen *et al.*, 1994; Jessen and Mirsky, 2005). At this stage, Schwann cell precursors express a number of markers that distinguish them from migrating crest cells, these are; growth-associated protein 43 (GAP-43), the brain fatty acid binding protein (B-FABP), and mRNA for the myelin proteins P0, proteolipid protein (PLP), and peripheral myelin protein (PMP-22), (Jessen *et al.*, 1994; Kurtz *et al.*, 1994; Lee *et al.*, 1997; Hagedorn *et al.*, 1999; Britsch *et al.*, 2001). Schwann cell precursors also express mRNA for cadherin 19 and desert hedgehog (Parmantier *et al.*, 1999; Takahashi and Osumi, 2005). Furthermore, unlike immature Schwann cells, the precursors undergo rapid apoptotic death if dissociated from the axons (Jessen *et al.*, 1994), an effect that can be rescued by incubation with Nrg1 (Dong *et al.*, 1995), an axonal signal responsible for Schwann cell precursor survival (Jessen and Mirsky, 1999). Analysis of cell morphology *in vitro* showed that instead of the bi- or tri-polar shape of immature Schwann cells, precursors are more flattened with less polarized shape and tend to grow in clusters. Furthermore, in vitro studies indicated that Schwann cell precursors are highly motile and that unlike immature Schwann cells, share the characteristically high migration rates of neural crest cells (Jessen *et al.*, 1994).

From E17-E18 in the rat (E15-E16 in the mouse), almost all cells in peripheral nerve are early (immature) Schwann cells and are recognisable by cytoplasmic expression of the calcium binding protein S100 (Jessen *et al.*, 1994). At the same time as S100 expression, immature Schwann cells start expressing surface lipid 04 (Dong *et al.*, 1999), and these cells proliferate extensively around E19-E20 in the rat sciatic nerve (Stewart *et al.*, 1993). One of the characteristics of immature Schwann cells that most clearly distinguishes them from Schwann cell precursors, is their ability to survive after being removed from the axon, having establishing autocrine survival loops (Dong *et al.*, 1999; Meier *et al.*, 1999). Investigation to identify the components of this survival circuit suggested that the main survival activity is the combined effect of three growth factors; neurotrophin-3 (NT-3), insulin-like growth factor-2 (IGF-2), and PDGF-BB (Dong *et al.*, 1999; Meier *et al.*, 1999). Two other factors that may contribute towards autocrine Schwann cells survival are Leukaemia inhibitory factor (LIF) and lysophosphatidic acid (LPA) (Dowsing *et al.*, 1999; Weiner and Chun, 1999).

The development of immature Schwann cells proceeds further when the cells choose to become either myelinating or non-myelinating Schwann cells. Differentiation to either phenotype requires the formation of a basal lamina upon contact with axons (Bunge *et al.*, 1986). Those immature Schwann cells that are to become myelinating, start to express the glycolipid galactocerebroside at E19 in rat, at about the same time as they form a 1:1 relationship with axons. The proliferation of Schwann cells has stopped at this point, and they begin to differentiate by expressing high levels of myelin protein. Non-myelinating Schwann cells in comparison, develop later. The expression of galactocerebroside in these cells in the third postnatal week (Diner, 1965; Jessen *et al.*, 1985; Jessen *et al.*, 1987b).

Neuronal differentiation and axon sprouting is independent of the Schwann cell precursor

The sciatic nerve is composed of a mixed population of sensory and motor neuron derived axons which originate from the lumbar (L) spinal segments L4-6. The differentiation of DRG neurons starts at E11 in the rat and is complete by E15 (Lawson *et al.*, 1974). Projection of axons from motor neurons of the ventral neural tube also begins at E11, and at E12 these form loose bundles with those from the DRG in early nerve roots (Reynolds *et al.*, 1991). At E13, the growing nerves enter the proximal part of the developing hindlimb, and most remain tightly bundled, with a few branches projecting to superficial tissues. The extension and branching of the nerve into the most of the hindlimb takes place by E15, followed by innervation of the majority of the distal aspect of the hindlimb by E19 (Reynolds *et al.*, 1991).

The close interaction between Schwann cells and axons has been investigated in a number of animal models (Harrison, 1924; Weston, 1963; Loring and Erickson, 1987; Carpenter and Hollyday, 1992a; 1992b). It has been suggested that Schwann cell precursors migrate ahead of the axon and may act as a pioneer cells in guiding axonal outgrowth (Nokes and Bennett, 1987; Serbedzija *et al.*, 1990). However, this theory was later excluded by findings in transgenic mice lacking neuregulin 1 (Nrg1) or its receptor ErbB3, that although Schwann cells precursors and Schwann cells are absent in these mice, axons grow towards their target area in a fairly normal way, although the more detailed aspects of target innervation are affected (Meyer and Birchmeier, 1995; Riethmacher *et al.*, 1997). Furthermore, the absence of Schwann cells precursors and Schwann cells in the Splotch mouse does not prevent peripheral axons from projecting essentially normally, despite motor neuron migration from the spinal cord in to the periphery (Grim *et al.*, 1992; Vermeren *et al.*, 2003). In contrast, it appears that

neurite outgrowth from the ventral motor axons is required for guiding Schwann cells to peripheral nerves (Bhattacharyya *et al.*, 1994).

Neuroregulins and their interactions in axon Schwann cell signaling

The partnership between the Nrg family of proteins and the ErbB subfamily of receptor protein tyrosine kinase molecules (PTKs) proved to be important in both neural and cardiac development (Adlkofer and Lai, 2000; Garratt *et al.*, 2000a). Four genes of the Nrg family have been identified to date; Nrg1, Nrg2, Nrg3, and Nrg4 (Adlkofer and Lai, 2000; Garratt *et al.*, 2000a). Nrg1 is the best known gene in the group and has many isoforms discovered independently under various names: neu differentiation factor (NDF) (Wen *et al.*, 1992), or heregulin (Holmes *et al.*, 1992), glial growth factor (GGF) (Marchionni *et al.*, 1993), and acetylcholine receptor inducing activity (ARIA) (Falls *et al.*, 1993). The term neuregulin is a combined name originating from two independent groups who were seeking a ligand for the ErbB2 receptor, and reported Nrg1 as NDF (Wen *et al.*, 1992), or heregulin (Holmes *et al.*, 1992). Nrg1 has been shown to be involved as a regulator of many different features of Schwann cell development starting from the neural crest to adult cells (Adlkofer and Lai, 2000; Lemke, 2001). Nrg2 and Nrg3 are expressed in the nervous system. However, their role during nerve development is not clear (Adlkofer and Lai, 2000).

Nrg1 signaling is initiated by binding to and activating members of the EGF-receptor subfamily of PTKs known as ErbBs. The name originated from the avian virus oncogene v-Erb-B, present in avian erythroblastosis virus and encoding for a mutant EGF receptor (EGFR) (Adlkofer and Lai, 2000). There are four known receptors of this class; ErbB1, ErbB2, ErbB3, and ErbB4 (Lemke, 1996). They are large molecules, 170-

185 kDa, with a single transmembrane domain, two cysteine-rich regions in the extracellular domain and a long tyrosine rich intracellular domain (Adlkofer and Lai, 2000). ErbB2 was originally identified as the Nrg1 receptor, however it is now known that the activation of ErbB2 takes place indirectly via heterodimeric association with ErbB3 or ErbB4 receptors, that bind Nrg1 with high affinity (Carraway 3rd and Cantley, 1994; Sliwkowski *et al.*, 1994; Riese *et al.*, 1995). Furthermore, studies have shown that ErbB2/ErbB4 or ErbB2/ErbB3 heterodimers are the preferred binding receptors for Nrg1 signals, whereas Nrg2 mainly activates the ErbB1/ErbB3 heterodimer and the ErbB4 homodimer (Carraway *et al.*, 1997; Crovello *et al.*, 1998; Pinkas-Kramarski *et al.*, 1998; Jones *et al.*, 1999).

The gene structure of Nrg1 has been elucidated recently (Stefansson *et al.*, 2002). The gene is located on the short arm of chromosome 8, and although it consists of 1.3 megabases, only 0.3% encodes for protein. Nrg1 has at least 15 different isoforms that arise as a result of alternative splicing and the use of multiple promoters (Lemke, 1996). Nrg1 contains a N-terminal domain which is either Ig-like or cysteine rich, an EGF domain, a transmembrane domain, and an intracellular C-terminal domain (Adlkofer and Lai, 2000). Alternative splicing at the C-terminal region of the EGF-like domain produces "α" and "β" forms, which modulate the binding affinities for ErbB receptors (Pinkas-Kramarski *et al.*, 1998; Jones *et al.*, 1999). The Nrg1 isoform of greatest importance for Schwann cell development is the membrane bound type III Nrg1β isoform, that is expressed on axonal surfaces (Jessen and Mirsky, 2005).

Indication of the importance of Nrg in the Schwann cell lineage came originally from in vitro experiments where GGF was identified as a Schwann cell mitogen (Raff *et al.*,

1978; Marchionni *et al.*, 1993). Moreover, it has been shown that, at least *in vitro*, Nrg1 indirectly directs the neural crest towards a glial choice by inhibiting the generation of neurons (Shah *et al.*, 1994; Shah and Anderson, 1997). In addition, in vitro studies on Schwann cell precursors have shown that Nrg1 can promote the survival and differentiation of these cells (Dong *et al.*, 1995). Studies on null transgenic mice underline the requirement of Nrg1, ErbB2, and ErbB3 function in the Schwann cell lineage (Lee *et al.*, 1995; Meyer and Birchmeier, 1995; Riethmacher *et al.*, 1997). Since Nrg1 and ErbBs are also expressed in the heart, Nrg1, ErbB2, and ErbB4 null mutant mice die at E10.5 due to failed development of ventricular trabeculae within the heart (Gassmann *et al.*, 1995; Lee *et al.*, 1995; Meyer and Birchmeier, 1995). Nevertheless, even at this embryonic age, there is a significant reduction in the number of Schwann cell precursors in emerging peripheral nerves (Meyer and Birchmeier, 1995). About 20% of mice lacking ErbB3 are able to survive until birth and the analysis of the late stage embryos showed a complete loss of Schwann cell precursors and immature Schwann cells. A study of DRG and motor neurons of ErbB3 mutant embryos, that lack Schwann cell precursors, showed that, despite initial normal number of cells at E12.5, there is a reduction of about 80% in both type of neurons of later embryonic stages (Riethmacher *et al.*, 1997). The importance of developing Schwann cells for neuronal survival was further investigated by an elegant approach to rescue the cardiac defect. Woldeyesus and colleagues as well as Lee and colleagues, created transgenic mouse lines that lacked ErbB2 in peripheral glia, although ErbB2 cDNA expressed under the control of the heart specific promoters Nkx2.5 or the heart muscle actin promoters rescued the cardiac defect. In addition to the lack of Schwann cell precursor and immature Schwann cells in these mice, there was a severe loss of both

motor and sensory neurons. Nerves also fail to fasciculate and become properly organized (Woldeyesus *et al.*, 1999; Morris *et al.*, 1999).

Neuregulin and myelination

Following the transition of Schwann cell precursors to the immature phenotype, their survival becomes relatively independent of axonal Nrg1, due to the activation of an autocrine loops as discussed above. Nevertheless, they are still able to respond to the factor (Jessen and Mirsky, 1999). Sensory and motor neurons express Nrg1 in the adult nervous system (Chen *et al.*, 1994; Bermingham-McDonogh *et al.*, 1997), which may raise the possibility of Nrg1 involvement in the maintenance of the myelin sheath. The Nrg signaling system in myelinating Schwann cells was further investigated by the use of Cre-loxP technology and removing the ErbB2 receptor late in embryonic Schwann cell development by a Krox20-cre allele. This resulted in a reduction in the number of Schwann cells as well as in myelin thickness (Garratt *et al.*, 2000b). In line with this, using heterozygote null Nrg1 mice, Michailov and colleagues have shown that myelin thickness and conduction velocity are reduced in these animals. By comparison, overexpression of Nrg1 type III increased the myelin thickness resulting in a lower g-ratio (axon diameter/ fibre diameter) (Michailov *et al.*, 2004). Despite these interesting findings, the mechanisms which connect axonal diameter and Nrg1 expression are still not clear. It remains to reconcile these observation with the earlier findings that addition of GGF, an isoform of Nrg1, to co-cultures of DRG neurons and Schwann cells prevents myelination in a dose dependent manner; whereas, its addition to an already myelinated co-culture, results in demyelination (Zanazzi *et al.*, 2001). These observations are compatible with that of Carroll and colleagues who showed that

neuregulin and ErbB expression was elevated following nerve axotomy coinciding with the onset of Schwann cell DNA synthesis (Carroll *et al.*, 1997).

Endothelins and their role in Schwann cell generation

It has been shown that *in vitro* and *in vivo*, Schwann cell precursors die rapidly by apoptosis due to the loss of axonal contact unless exogenous Nrg1 is provided. Under these conditions, Schwann cell precursors continue their lineage progression towards immature Schwann cells (Dong *et al.*, 1995). Other survival factors include Endothelins (ETs) which more importantly act as a regulator of the timing of Schwann cell generation both *in vivo* and *in vitro* (Brennan *et al.*, 2000). ETs are a small polypeptide factors related to the sarafotoxins. ET1, 2, and 3 are encoded by three different genes which share strong sequence and structural homology (Yanagisawa *et al.*, 1988). Culturing Schwann cell precursors in the presence of Nrg1 and ET delayed the emergence of Schwann cells compared to that seen in Nrg1 alone (Brennan *et al.*, 2000). In the presence of ET alone, Schwann cells precursors only progressed to Schwann cells at a very slow rate. These *in vitro* observations were supported by the decreased transition time from precursors to Schwann cells in mutant rats lacking functional endothelin B receptor (Ceccherini *et al.*, 1995; Brennan *et al.*, 2000). Nevertheless, it has been shown that most Schwann cell precursors change to Schwann cells after 7 days exposure to ET in the absence of Nrg, demonstrating that ETs do not block Schwann cell generation but delay the process (Brennan *et al.*, 2000). Interestingly, this shows that Nrg is not required for the generation of Schwann cells from the precursors, but that Nrgl and ET are involved in controlling the rate of this process. Further work has shown that AP-2 transcription factors, AP-2α in particular, may be involved as negative regulators of Schwann cell generation (Stewart *et al.*,

2001). Out of three different genes in this family, only AP-2α and AP-2γ are expressed by Schwann cell precursors during early development, but their expression declines as precursors begin to generate Schwann cells *in vivo* and *in vitro*. Enforced expression of AP-2α *in vitro*, delays the generation of Schwann cells (Stewart *et al.*, 2001).

Schwann Cell Survival

Cell death is an event that takes place during the development of the majority of mammalian tissues including the nervous system. Evidence has shown that death or survival of glial cells is likely to be regulated by locally produced trophic factors that modulate the interaction between axons and glia in preparation for myelination (Barres and Raff, 1994). The survival of Schwann cell precursors, as mentioned earlier, is dependent on axonal signals and Nrg1 production (Dong *et al.*, 1995; Grinspan *et al.*, 1996; Syroid *et al.*, 1996; Trachtenberg *et al.*, 1996), and survival of immature Schwann cells depends on autocrine Schwann cell signals (Cheng *et al.*, 1998; Meier *et al.*, 1999). Major components of autocrine Schwann cell survival circuits are IGF-2, (NT3), and platelet-derived growth factor-BB (PDGF-BB). It has been shown that IGF is involved in inactivation of c-Jun terminal kinases which prevents caspase mediated apoptosis (Campana *et al.*, 1999; Delaney *et al.*, 1999; Syroid *et al.*, 1999; Cheng *et al.*, 2000). Autocrine survival signals are likely to be a major explanation for why Schwann cells are able to survive for a considerable time after nerve injury, although their numbers decline and they become less responsive to extrinsic signals (Li *et al.*, 1998; Sulaiman and Gordon, 2002). Furthermore, there are also factors that play an active role in inducing Schwann cell death during development and after nerve injury. Two such factors that are directly involved during this process are nerve growth factor (NGF) and the transforming growth factor-beta (TGFβ) (Soilu-Hanninen et al., 1999;

Parkinson et al., 2001; D'Antonio 2004-PhD thesis, UCL). NGF acts via the low affinity neutrophin receptor p75 (p75NTR) to promote Schwann cell death. In neonatal mice lacking p75NTR, Schwann cell death was reduced after nerve injury, and similar results were observed in adult mice three weeks after nerve crush (Ferri and Bisby, 1999; Syroid *et al.*, 2000; Khursigara *et al.*, 2001). Furthermore, cultured Schwann cells from these mice survive better than normal Schwann cells when deprived of serum and growth factors (Soilu-Hanninen et al., 1999; Syroid *et al.*, 2000). Studies on the Schwann cell response to NGF have identified receptor interacting protein-2 (RIP-2), a protein that interacts with p75. Expression of dominant negative RIP-2 *in vitro* makes Schwann cells sensitive to NGF-induced cell death, whereas, in the presence of RIP-2, Schwann cell death in response to NGF is prevented (Khursigara *et al.*, 2001).

TGFβ like NGF, can induce apoptotic cell death in neonatal Schwann cells *in vitro* as well as *in vivo* (Parkinson *et al.*, 2001). TGFβs are a small family of multi-functional growth factors and there are three mammalian isoforms; TGFβ1 TGFβ2, and TGFβ3 (Kingsley, 1994). Addition of TGFβ to freshly isolated neonatal Schwann cells induced cell death which could be prevented by the combined presence of Nrg1 and autocrine factors. In the presence of serum, a combination of TGFβ and tumour necrosis factor (TNF)α, will induce apoptosis in cells, and is much more effective than TGFβ alone (Skoff *et al.*, 1998). Moreover, injection of TGFβ increases Schwann cell death in injured nerve (Parkinson *et al.*, 2001). Genetic elimination of type II TGFβ receptor from Schwann cells also reduces normal developmental Schwann cell death (D'Antonio PhD thesis-UCL 2005). It has been shown that the phosphorylation of c-Jun via JNK is involved in this process, an active form of c-Jun kills Schwann cells and a dominant negative form of c-Jun inhibits TGFβ-induced death (Parkinson *et al.*, 2001). It has been shown that using JNK blockers; SP600125 and JBD (JNK-interacting protein 1, JIP-1),

reduces the activity of TGFβ death pathway in Schwann cells (Parkinson DB, unpublished data). Furthermore, myelinating Schwann cells from postnatal day 4 nerves are protected from TGFβ-induced cell death as TGFβ is unable to phosphorylate c-Jun in myelinated Schwann cells ((Parkinson *et al.*, 2002a; 2004). Enforced expression of the transcription factor Krox20 *in vitro*, is sufficient to impede cell death by inactivating the JNK-c-Jun pathway. It is possible that the scaffold protein JIP-1 is involved in Krox-20 mediated Jun down-regulation (Parkinson *et al.*, 2004). TGFβ is expressed by Schwann cells and neurons during development and in the adult (Stewart *et al.*, 1995). Following nerve injury in neonatal and adult mice, TGFβ1 expression in the distal stump of injured nerve was elevated, whereas TGFβ3 expression was reduced, indicating the possible role for TGFβ1 in early response to nerve damage (Scherer *et al.*, 1993; Parkinson *et al.*, 2001).

Schwann cell proliferation

The ability of Schwann cells to proliferate is a critical property both, of course, during development but also after nerve injury. Schwann cells proliferate in response to a variety of growth factors present in neurons. Extensive use of DRG neurons and Schwann cell co-cultures to examine axon-induced proliferation, have established Nrg1 as the primary axonal mitogen for Schwann cells (Morrissey *et al.*, 1995). Purified cultures of Schwann cells have also been used to measure DNA synthesis and proliferation. With the exception of Nrg1 and Hepatocyte growth factor (HGF), the mitogenic response of cultured Schwann cells to growth factors is minimal in the absence of cAMP elevation (Mirsky and Jessen, 2001; Jessen and Mirsky, 2004). In the presence of cAMP, several growth factors, including FGF-1and -2, TGFβs, PDGF-BB and Reg-2 act as Schwann cell mitogens in serum purified cultures. Additional presence

of IGF will potentiate the effect of most Schwann cell mitogens including Nrg1. Once Schwann cells have begun to mature, IGF switches to a new role of a differentiating factor and enhances P0 and MBP expression (Stewart *et al.*, 1996; Cheng and Feldman, 1997; Cheng *et al.*, 1999; Conlon *et al.*, 2001). Studies on injured nerve indicate that proliferation is regulated by mechanisms different from those in nerve development. Thus, Schwann cells fail to proliferate in cyclin-D1 null mice during Wallerian degeneration, and cultured Schwann cells from these mice did not respond to growth factors, although proliferation during development is normal (Kim *et al.*, 2000; Atanasoski *et al.*, 2001).

TRANSCRIPTION FACTORS IN SCHWANN CELL DEVELOPMENT

Eukaryotic organisms are composed of a large number of tissue types. It is now clear that gene regulation at the level of transcription, forms the basis of such diverse phenotypes. This is achieved in response to particular signals, transcription factors and related proteins, that bind to a short DNA sequence elements located in the promoter or enhancers. The identification of the mechanisms that regulate gene transcription in a particular cell type, tissue or in respond to a particular signal is fundamental to our understanding of eukaryotic development. To date several transcription factors have been identified and classified according to the structure of the DNA binding domain. The development of Schwann cells involves two distinct and sometimes overlapping patterns of transcription factor expression. Those that are present during neural crest formation, migration, and Schwann cell precursor development, and can be considered as early transcription factors which includes Sox-10 and Pax-3, and those that involved in Schwann cell differentiation, here termed late transcription factors and including

Oct-6 and Krox-20 (Monuki *et al.*, 1989; Topilko *et al.*, 1994; Kioussi *et al.*, 1995; Bermingham Jr *et al.*, 1996; Jaegle *et al.*, 1996).

Early transcription factors

Sox10

Sox proteins are a subgroup of proteins that contain a high-mobility-group (HMG) domain as their DNA binding domain. They are also have similarity (usually >50% amino acid homology) to the HMG domain of male-sex-determinig factor, SRY, which is also known as the Sry box (Wegner, 1999). In PNS, Sox10 expression is initially detected in neural crest cells as they dissociate from the neural tube. This is maintained during their migration and although the expression continues in the glial and melanocyte lineage, it is turned off in many other neural crest cell derivatives (Wegner, 2000; Britsch *et al.*, 2001). Expression of Sox10 in CNS increases steadily and reaches its maximum level during adulthood, where it is mostly found in oligodendrocytes (Wegner, 2000; Kuhlbrodt *et al.*, 1998).

Genetic inactivation of Sox10 in mice causes a combination of neural crest defects. Mutation is embryonic lethal in the homozygous state and the embryos fail to produce melanoblasts (Herbarth *et al.*, 1998; Southard-Smith *et al.*, 1998). In the heterozygous state, spontaneous mutations of Sox10 interfere with the development of melanocytes and of enteric nervous system, causing changes in pigmentation and megacolon ((Herbarth *et al.*, 1998; Southard-Smith *et al.*, 1998). These mutations have been identified in mice as *Dominant megacolon* (*Dom*) mutation, and in human as Waardenburg syndrome type 4 ((Herbarth *et al.*, 1998; Kuhlbrodt *et al.*, 1998; Pingault *et al.*, 1998; Southard-Smith *et al.*, 1998; 1999). Furthermore, certain heterozygous mutations in the human Sox10 gene are associated with defects in both the CNS and

PNS, growth retardation, and in a few cases, peripheral neuropathy with hypomyelination and deafness (Pingault *et al.*, 1998; Touraine *et al.*, 2000). The role of Sox10 in the development of peripheral glia has been analysed further by the generation of a targeted Sox10 mutation in mice, where the complete open frame of Sox10 was replaced by a lacZ sequence (Britsch *et al.*, 2001). In heterozygous mice, defects in pigmentation and megacolon were observed, which were similar to *Dom* and WS4 mutants. In homozygous Sox10 null mice however, early peripheral glial cells are missing, and there is also a reduction in the expression of the Nrg1 receptor, ErbB3, which is likely to have a severe effect on glial development (Britsch *et al.*, 2001). The reduced levels of ErbB3 in Sox10 null mice might, to a lesser extent, explain the reduced glia number in peripheral nerve trunks, in these mice, as Nrg1 and its receptor ErbB3 are important for survival, proliferation and early differentiation (Britsch *et al.*, 2001; Dong *et al.*, 1995). The lack of glia in the DRGs of Sox10 null mice however does not follow the same argument, as DRG glia develop normally in mice whose Nrg1 signal has been inactivated (Meyer and Birchmeier, 1995; Woldeyesus *et al.*, 1999; Garratt *et al.*, 2000a). It has been shown that Sox10 functions as a transcriptional modulator for Pax3, Oct6, and Krox20 (Kuhlbrodt *et al.*, 1998). Moreover, Sox10 controls expression of myelin protein genes including P0 promoter (Peirano *et al.*, 2000a). This is in agreement with recent studies that have demonstrated that Sox10, in synergy with Krox20, strongly activates Connexin32 (Cx32) expression *in vitro* by binding to its promoter (Bondurand *et al.*, 2001).

Pax-3

Pax-3 is a member of the murine Paired box (Pax) DNA binding domain transcription factor family which was identified originally as a *Drosophila* segmentation gene, and

encodes a 479 amino acid protein containing both paired domain and paired type homeodomain (Goulding *et al.*, 1991). Pax3 mRNA is expressed during early development in the dorsal part of the neural tube (roof plate), in neural crest, and in somatic mesoderm (Goulding *et al.*, 1991). Mutations in a number of Pax genes have been shown to result in developmental defects in humans and mice (Mansouri *et al.*, 1996). In humans, disruption of the Pax-3 gene causes Waadenburg syndrome (WS) type I and 3 and, the fusion of Pax-3 with the Forkhead gene is related to the childhood cancer rhabdomyosarcoma (Galili *et al.*, 1993; Shapiro *et al.*, 1993). In mice, there are two naturally occurring Pax-3 mutants, *splotch* (*Sp*) with deletion in the homeodomain (Epstein *et al.*, 1991), and *splotch delayed* (*Spd*) which have a point mutation in the paired domain (Moase and Trasler, 1990; Franz, 1993). There is a significant loss or reduction of embryonic Schwann cells, particularly in hind limb nerves, in *Sp* (Grim *et al.*, 1992) and *Spd* (Franz, 1993) mice, possibly due to defects in neural crest migration rather than the defects in the Schwann cells themselves. In addition, these mice also show a reduced number of neurons in spinal and sympathetic ganglia and in melanocytes (Gruss and Walther, 1992). These observations suggest that Pax-3 has a role in the early emergence and development of neural crest derivatives and that it is required for Schwann cell development. Expression studies confirm the presence of Pax-3 throughout embryonic development in the cells of the Schwann cell lineage (Kioussi *et al.*, 1995; Blanchard *et al.*, 1996), indicating that Pax-3 is not restricted to the early developmental stages. Furthermore, microinjection of exogenous Pax-3 into Schwann cells in vitro causes decreased expression of myelin genes like P0 and myelin basic protein (MBP), and increased expression of markers characteristic of non-myelinating Schwann cells (Kioussi *et al.*, 1995). These observations suggest that Pax-3 is involved in determining the choice between the

myelinating and non-myelinating phenotype of a Schwann cell, favouring the generation of a non-myelinating phenotype by suppressing the myelin-forming genes.

Late Transcription Factors

Oct-6

The Oct-6 transcription factor is a member of a family of nuclear proteins characterised by the highly conserved POU domain. The POU domain was defined following the discovery of these proteins in three different systems, Pit-1, Oct-6, and Unc (Latchman, 1999). Oct-6 was isolated from three different systems concurrently; sciatic nerve, testes and embryonic stem cells of the central nervous system (He *et al.*, 1989; Monuki *et al.*, 1989; Meijer *et al.*, 1990; Suzuki *et al.*, 1990). The initial experiments to show the role of Oct-6 gene in Schwann cell development showed that treatment of cultured Schwann cells with agents that elevate intracellular cAMP concentrations led to upregulation of the Oct-6 gene, referred to by these cultures as "SCIP" for "suppressed cAMP inducible POU" (Monuki *et al.*, 1989). The gene expression of Oct-6 is initiated around E12 in mouse sciatic nerve and persists until at least postnatal day 12 (p12) (Blanchard *et al.*, 1996). Its expression is gradually upregulated when Schwann cell precursors progress to an immature Schwann cell phenotype phenotype during late embryonic life (Jaegle and Meijer, 1998). Oct-6 expression reaches its peak at around birth in sciatic nerve, when myelin gene expression is initiated and is then followed by a gradual down-regulation in Schwann cells (Monuki *et al.*, 1990; Scherer *et al.*, 1994; Blanchard *et al.*, 1996; Arroyo *et al.*, 1998). The loss of axonal contact in transected and crushed nerves sees the rapid up-regulation of the gene (Scherer *et al.*, 1994). In cultured Schwann cells, elevated levels of cAMP induce Oct-6 expression that preceds the expression of myelin genes

(Scherer *et al.*, 1994; Monuki *et al.*, 1989). *In vivo* studies on Oct-6 deficient mice have shown that Schwann cells establish a 1:1 relationship with axons but myelination is delayed by about 14 days in the majority of null mice (Bermingham Jr *et al.*, 1996; Jaegle *et al.*, 1996). The reason for delayed myelination in Oct-6 null mice has been explained by the fact that in Oct-6 null mice expression of the transcription protein Krox-20, that is necessary for myelination, is delayed. Oct-6 null mice myelinate eventually due to the presence of an additional transcription factor called Brn-2 which is closely related to Oct-6 and which can partially compensate for its lack (Jaegle *et al.*, 1996). The Brn-2 expression pattern is similar to that of Oct-6, however Brn-2 deficient mice do not show any abnormalities in myelination. Brn-2 gene activation is independent of Oct-6 and overexpression of Brn-2 in Oct-6 deficient Schwann cell under the control of Oct-6 Schwann cell enhancer, activates Krox-20 and partially rescues the developmental delay phenotype. However, distruption of Oct-6 and Brn-2, results in a much more severe phenotype than that seen with disruption of Oct-6 alone with further delayed myelination (Ghazvini *et al.*, 2002; Sim *et al.*, 2002; Jaegle *et al.*, 2003).

Krox-20

The name Krox-20 (Egr-2/ NGF-IB) originates from *krüppel* box and encodes for a zinc transcription factor containing three zinc finger motifs. Krox-20 was isolated from 3T3 fibroblast cell lines as well as pheochromocytoma (PC12) following induction by NGF (Hazel *et al.*, 1988; Milbrandt., 1988; Ryseck *et al.*, 1989). The expression of Krox-20 is predominantly nuclear (Herdegen *et al.*, 1993), and detected in different tissues including heart, muscle, thymus, testes, spleen, lung, CNS, and PNS (Chavrier *et al.*, 1988; Watson and Milbrandt, 1988). In CNS, the expression is described in neocortex, striatum, hypothalamus, amygdala and olfactory bulb (Bhat *et al.*, 1992; Mack *et al.*,

1992; Herdegen *et al.*, 1993). Krox-20 is an essential component of hindbrain segmentation during CNS development (Wilkinson *et al.*, 1989a). Krox-20's expression is restricted to rhombomeres (r) 3 and 5, which are either partially formed or eliminated in Krox-20 deficient mice (Schneider-Maunoury *et al.*, 1993). Krox-20 is also reported to interact with NGFI-A binding proteins, Nab1 and Nab2 , a family of co-repressors that as well as negatively regulating the transcriptional activity of the family of zinc finger transcription factors, are positive regulators towards Schwann cell differentiation (Swirnoff *et al.*, 1998; Le *et al.*, 2005).

In the PNS, Krox-20 has a fundamental role in the development of myelinating Schwann cells (Topilko *et al.*, 1994). The expression of Krox-20 in cells that are destained to myelinate, starts at E15.5 in mouse, approximately 20-30 hours after induction of Oct-6 protein and is dependent on continuous axonal contact (Topilko *et al.*, 1994; Blanchard *et al.*, 1996; Zorick *et al.*, 1996; 1999). From this point onwards, the expression of Krox-20 remains unchanged in myelinating Schwann cells throughout life (Topilko *et al.*, 1994). Analysis of the PNS in Krox-20 null mice reveals a permanent block in myelination, although Schwann cells still establish a 1:1 relationship with axons and wrap their membrane one and a half turns around the axons before becoming stalled (Topilko *et al.*, 1994). These mice express the Schwann cell marker S100 and the early myelination marker MAG (myelin-associated glycoprotein), but expression of P0 and MBP (myelin basic protein), are strongly reduced suggesting that Krox-20 is essential for completion of the myelination process (Topilko *et al.*, 1994). The expression of Oct-6 appears normal and on time in Krox-20 null mice. These data support the theory that Schwann cells are stalled at a particular stage in development, most likely to be the pro-myelinating phase, where they continues to cycle as they

would in the late embryonic/ newborn animals well into the second postnatal week. The importance of Krox-20 in regulating myelination was further reinforced by gene array technology and using adenovirally enforced expression of Krox-20 in cultured Schwann cells. Under these conditions, many genes including lipid and myelin-related genes, as well as other genes of unknown function are up-regulated by Krox-20 (Nagarajan *et al.*, 2001). Furthermore it has been demonstrated that enforced expression of Krox-20 on its own is sufficient to introduce a range of phenotypic changes in cultured Schwann cells characteristic of quiescent myelinating ones (Parkinson *et al.*, 2002a; 2003; 2004). These experiments show that in addition to the up-regulation of myelin-related genes like P0 and periaxin, and down-regulation of L1, Nrg1-induced proliferation, and TGFβ induced cell death is also prevented. All of this represents changes that occur in vivo as immature Schwann cells start to myelinate. Recent evidence has showed that one of the mechanisms behind these changes is the ability of Krox-20 to inactivate the JNK/c-Jun pathway which is otherwise required for proliferation and death (Parkinson *et al.*, 2003). Surprisingly, Krox-20 is also able to induce expression of myelin genes like P0 and periaxin in an unrelated cell type, NIH 3T3 cells. Together, these findings suggest that Krox-20 acts as a global regulator or "master regulatory gene" for the transition between immature Schwann cells and myelinating cells (Jessen and Mirsky, 2004; Parkinson *et al.*, 2004). The mechanisms by which Krox-20 is regulated by axons are not yet clear. Recently analysis of Oct-6 and Krox-20 promoters has identified the presence of Schwann cell specific enhancer (SCE) elements which are regulated by axonally regulated transcription factors. The Krox-20 promoter contains two elements, the immature Schwann cell element (ISE), located upstream of the transcription initiation site, which is active in immature Schwann cells from E15, and a myelinating Schwann cell element (MSE) situated

downstream of the Krox-20 transcription initiation site which is active from E18 onwards in myelinating cells and also dependent on Oct-6 for its activation. Both enhancers are re-expressed in regenerating nerves (Ghislain *et al.*, 2002).

Krox-24

Krox-24, also known as Egr-1, NGFI-A, Zif268, or tis8 (Lau and Nathans, 1987; Lim *et al.*, 1987; Milbrandt, 1987; Sukhatme *et al.*, 1987; Lemaire *et al.*, 1988) is another member of the zinc finger transcription factor family which is expressed in different tissues including heart, lung, muscle, bone, CNS and PNS (Christy *et al.*, 1988; Lemaire *et al.*, 1988; Sukhatme *et al.*, 1988; McMahon *et al.*, 1990). In the CNS, Krox-24 is expressed at low levels in the neonate and reaches high levels in the mature cortex, suggesting a necessity in cortical maturation (Watson and Milbrandt, 1990). In the PNS, Krox-24 is closely related to Krox-20 and binds to some of the sequences recognised by Krox-20 (Topilko *et al.*, 1997). Krox-24 is expressed in mouse Schwann cells as early as E11/12 and this expression persists in non-myelinating cells in adult nerves, but upregulates after nerve injury (Topilko *et al.*, 1997). Analysis of Krox-24 null mice revealed that myelination occurs normally, but there is an increased cell death after nerve transection in comparison to wild type nerves (Topilko *et al.*, 1998). The expression of Krox-24 in Schwann cells is regulated by the class B helix-loop-helix (HLH) factor Mash2 (Kury *et al.*, 2002). Mash2 has been identified in a subset of adult Krox-20 positive Schwann cells; it is down-regulated after nerve transection and prevents Schwann cell proliferation in cultures (Kury *et al.*, 2002).

Other HLH genes in Schwann cells are the Id genes. All four HLH Id genes are expressed during Schwann cell development. Id1 and Id3 specifically, are expressed at

higher levels in adult nerve than in early postnatal nerves (peak of myelination), and both are up-regulated after nerve transection (Stewart *et al.*, 1997a; Thatikunta *et al.*, 1999).

NF-κB

NF-κB is a nuclear protein that interacts with a defined site in the kappa immunoglobulin enhancer. It is originally identified in B lymphocytes, where it stimulates transcription of the immunoglobulin κ light chain (Sen and Baltimore, 1986). NF-κB also has a role in limb formation and neural survival and plasticity (Bushdid *et al.*, 1998; Mattson *et al.*, 2000). Recently, it has been shown that NF-κB has a role in myelination (Nickols *et al.*, 2003). NF-κB is upstream of Oct-6 and expressed before Oct-6 in myelinating cocultures of neurons and Schwann cell. Its inhibition reduces myelination, indicating a role for NF-κB in this process (Nickols *et al.*, 2003).

MYELIN AND MYELINATION

Myelin is the layer of fatty material that surrounds the axons of most vertebrates neurons. Myelin has two major roles; one is to insulate and the other is to allow faster transmission of the nervous impulse long the axons it surrounds. These impulses are introduced by depolarization of the internodal axonal membrane. In the PNS, the formation of myelin is carried out by the differentiation of the plasma membrane which are rich in lipids and Schwann cells (Mugnaini, 1982). Myelinating Schwann cells are also secrete continuous basal lamina which covers the total length of each myelinated fibre. The access to the entire myelin structure is by cytoplasmic channels of SLIs (Raine, 1984). Analysis of myelinated fibres using freeze-fracture EM has revealed the presence

of tight junctions, adherens junction, and gap junctions in the SLIs (Sandri *et al.*, 1982; Tetzlaff, 1982; Scherer, 1996).

The relationship between axons and myelin has been studied for decades; while axons are involved in regulating myelinating phenotype of cells, myelination also influences neuronal survival and maturation. However, not much known about the molecules that are involved in this process. Myelination increases the diameter of axons (Windebank *et al.*, 1985) which is a determinant of conduction velocity (Arbuthnott *et al.*, 1980) as it is approximately proportional to the fibre diameter (Waxman and Bennett, 1972). It is important to note that myelination also increases the phosphorylated state of neurofilaments, which are the major axonal cytoskeleton components, and this in turn increases the neurofilament spacing and hence increases axonal diameter (de Waegh *et al.*, 1992; Hsieh *et al.*, 1994).

Structure of myelin

Segmental compact myelin is organised in internodes and near the ends of internodes, the Schwann cell plasma membranes abruptly open out from compact myelin into cytoplasm-filled channels termed "paranodal loops" (Pedraza *et al.*, 2001). These loops are a major site of myelin axon adhesion via a series of septate-like junctions which provide a diffusible barrier and prevent lateral diffusion of membrane proteins (Peles and Salzer, 2000) Nodes of Ranvier are located between two adjacent paranodes and are involved in mediating saltatory conduction (Hodgkin and Huxley, 1952). In unmyelinated axons, conduction velocity is directly proportional to the square root of the diameter of the axon. The need for rapid nerve conduction therefore explains development of "giant axons' in invertebrates such as squid. Myelin increases the

velocity of action potentials up to ten times in comparison to a similar size unmyelinated axon (Ritchie, 1982; Jacobson, 1993). Compact myelin accounts for the majority of the myelin in the internode. Using Electron microscopy, myelin appears as a lamellar structure that wraps a central axon with alternating dark and light lines. Non-compacted myelin, on the other hand, provides cytoplasmic continuity over the length of the myelinating Schwann cell and includes the cytoplasmic channels at the abaxonal and adaxonal surfaces of the myelinating cell and SLI, that radially traverse the compact myelin. The paranodal axonal membrane contains contactin-associated protein (Caspr), also known as paranodin, which is a cell adhesion molecule that may connect the axonal and glial membranes (Einheber *et al.,* 1997; Menegoz *et al.,* 1997; Peles *et al.,* 1997). The 10-15 nm area of the internode adjacent to the paranodal loop is known as the juxtaparanodal region and the axonal membrane in that area is enriched in delayed-rectifier potassium channels as well as Caspr2, a homologue of Caspr (Peles and Salzer, 2000). The axonal membrane of the node of Ranvier however, is rich in voltage-gated Na channels, hence its direct responsibility for saltatory conduction (Scherer and Paul, 2004). Furthermore, the nodal axolemma is surrounded by Schwann cell microvilli, which extend from the outer border of the adjacent myelin internodes and contain F-actin (Trapp et al., 1989a; Zimmermann, 1996), ezrin, radixin and moesin which are members of ERM family of proteins (Scherer and Paul, 2004). Moreover, freeze- fracture electron microscopy analysis has demonstrated the presence of tight junctions, adherens junctions, and gap junctions in the SLI (Sandri *et al.,* 1982; Tetzlaff, 1982; Scherer, 1996). The idea that gap junctions might provide a shortcut for the diffusion of small molecules across the non-compacted regions of myelin, was confirmed by injections of dye into the prenuclear region of myelinating Schwann cells and the diffusion of the dye was monitored by video microscopy (Balice-

Gordon *et al.*, 1998). The labelling was first observed in the abaxonal cytoplasmic region and then in SLI, and finally in the NR.

Schmidt – Lanterman Incisures (SLI)

SLI are cytoplasmic channels within the myelin sheath that were described independently over a century ago by Schmidt, and Lanterman as funnel-shaped discontinuities apparent in the myelin sheaths of normal peripheral nerve fibres (Hall and Williams, 1970). There are several SLI per internode in myelinated nerve fibres and their number shows a linear increase with increase in fibre diameter (Hall and Williams, 1970; Ghabriel and Allt, 1981; Poliak and Peles, 2003). There is strong evidence that SLIs are a feature of developing, regenerating and remyelinated fibres. In developing peripheral nerves, SLIs were detected from the first postnatal day in the mouse at a stage where myelin sheaths were composed of only 5 compact lamellae (Hall and Williams, 1970), and in regenerated peripheral nerves of the rat 30 days after nerve crush (Hiscoe, 1947). Moreover, in normal adult fibres the increase in the number of SLI per internode in relation to fibre diameter produces a gradual reduction in the inter-incisural distances in larger fibres. This was described by Hiscoe to be due to two events; (i) intercalation of additional incisures associated with increase in fibre diameter, (ii) elongation of the whole internode. Furthermore, in regenerated fibres the inter-incisural distances were much shorter than those of normal adult fibres and slightly shorter than those seen in young animals (Ghabriel and Allt, 1981). Incisures are less frequent in the paranodal and nuclear region of the internode (Webster, 1965). Moreover, the length from the node to the first incisure is greater than the length between two incisures in fibres of all diameters (Hiscoe, 1947). In the CNS of higher vertebrates SLIs do not occur so frequently.

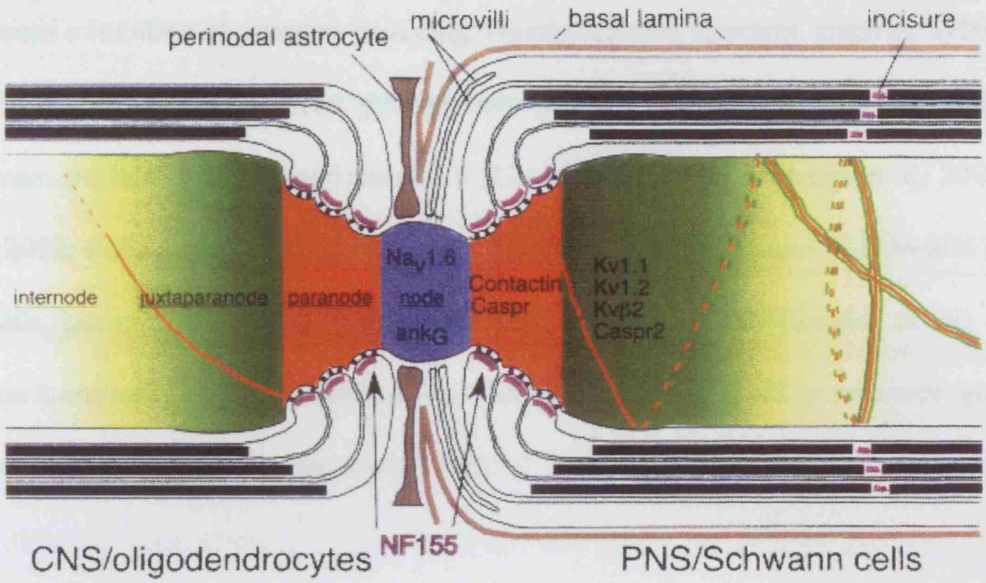

Figure 1.2 Schematic depiction of the node, paranode, juxtaparanode, and internode in CNS and PNS myelin sheaths surrounding a single myelinated axon. Each region are characterized by their expression of a different set of molecules in both the CNS and the PNS. At nodes, ankyrin-G is depicted encircling the cytoplasmic aspect of the Na channels. At paranodes, Contactin associated protein (Caspr) and contactin multimers interact with NF155– Modified from Scherer et al., Myelin Biology and disorders, 2004.

The functions of SLIs are not very clear. There has been a suggestion that SLI facilitate communication between the abaxonal and adaxonal Schwann cell compartments via gap junctions (Balice-Gordon *et al.*, 1998), thus they may be essential for the maintenance and metabolism of myelin (Robertson, 1962). Radial diffusion of small ions through SLIs are documented, and such diffusion is thought to occur through reflexive gap-junctions and not through the cytoplasm of SLI (Balice-Gordon *et al.*, 1998). It is therefore interesting that gap-junctions have not been reported by electron microscopy to be part of the structure of SLI, although incisures express the gap-junction protein connexin-32. Furthermore, blocking of gap-junction function blocks the diffusion process of ions (Balice-Gordon *et al.*, 1998; Scherer *et al.*, 1995b). Nevertheless diffusion seems to be normal in Cx-32 null mice, perhaps indicating the

presence of gap junctions made from other connexins (Balice-Gordon *et al.*, 1998). SLI express a number of proteins including; F-actin, tubulin, spectrin, ankyrin, S100, Cx29 and Cx32, myelin associated glycoprotein (MAG), neurofascin (NF)155, multi-PDZ domain protein (MUPP1) and claudin 5 (Gould *et al.*, 1995; Altevogt *et al.*, 2002; Li *et al.*, 2002; Poliak *et al.*, 2002). Increased numbers of SLI are seen in Schwann cells of myelin basic protein (MBP)-deficient *shiverer (shi)* mice (Gould *et al.*, 1995), *Caspr/paranodin* null mice (Bhat *et al.*, 2001), and in the CNS in *ceramide galactosyl transferase* null mice (Dupree *et al.*, 1998).

Myelination

The process of myelination, carried out by oligodendrocytes in the CNS, and Schwann cells in the PNS, represents a remarkable example of cell-cell co-operation. In the PNS, all Schwann cells have the potential to myelinate, but only those that make contacts with larger diameter axons will be induced to adopt a myelinating phenotype.

During development of the Schwann cell lineage, those immature Schwann cells that are destined to become myelinating Schwann cells begin to express the glycolipid galactocerebroside (Gal-C) at around E19 (Jessen *et al.*, 1985). Large diameter axons segregate and form a 1:1 relationship between axons and Schwann cells. The non-myelinating Schwann cells however, enclose themselves individually around pockets containing smaller diameter axons (Webster, 1971). Proliferation ceases soon after Schwann cells form a 1:1 relationship with axons. Reduction of proliferation starts at birth in the Schwann cells of the sciatic nerves of mouse and rat (Mirsky *et al.*, 2002; Jessen and Mirsky, 2004).

During myelination, Schwann cells polarize along the axons with an outer/abaxonal plasma membrane in contact with the extracellular matrix, and interacting with the endoneurial fluid. The abaxonal plasma membrane directs the formation of a basal lamina which is necessary for myelination (Bunge *et al.*, 1986), while the inner/ adaxonal plasma membrane is enriched in MAG (Trapp *et al.*, 1984a; 2004). The adaxonal membrane radially and longitudinally ensheaths the axon and plays a role in directing axonal Na+ channels to NR (Pedraza *et al.*, 2001). Expansion of mesaxon membrane initiates spiral growth of the myelin internode and creates a lead edge for wrapping at the adaxonal surface. The major dense line of mature myelin is formed by the fusion of two intracellular lipid bilayers and compression of the cytoplasm, while the interperiod line is formed by the two extracellular surfaces of the Schwann cell membrane (Alberts *et al.*, 1994; Trapp *et al.*, 2004). During this compaction MAG is removed and addition of P0 takes place (Trapp, 1988a). The appearance of the first wrappings of the myelin sheath around axons sees strong elevation in expression of the major myelin proteins including: the P0, peripheral PMP22, MBP, PLP, MAG, plasmolipin, myelin and lymphocyte protein (MAL), P2, periaxin (Prx), and CNPase (Jessen and Mirsky, 1999; Jessen and Mirsky, 2005).

Myelin Composition

The major function of compact myelin is to insulate axons, and to acquire this structure, Schwann cells are able to elaborate a highly lipid-rich plasma membrane rich in galactosphingolipids and saturated long-chain fatty acids, and wrap this membrane tightly around the axon many times (Mugnaini, 1982). Myelin membrane consists of about 75% lipids and 25% proteins in both CNS and PNS. There are no myelin-specific lipids, but many of the proteins are myelin specific.

Lipids

All the major classes of lipid including neutral lipids, phosphoglycerides and sphingolipids are present in myelin membrane. The dry mass of both CNS and PNS myelin is characterised by a high percentage of lipid, 70 –85%, and low protein, 15-30% content, unlike other cell membranes (Taylor *et al.*, 2004). There are no myelin-specific lipids but certain lipids are substantially enriched. During CNS myelination, the concentration of galactocerebroside is directly proportional to myelin accumulation, hence, the rate of myelination could be measured by the rate of cerebroside synthesis (Singh and Pfeiffer, 1985; Muse *et al.*, 2001). A fifth of galactocerebroside in myelin is coverted to sulfatide, however, it has been shown that mice deficient in an enzyme necessary for galactocerebroside and sulfatide biosynthsis (UDP- galactose:ceramide galactosyltransferase) have normal myelin (Coetzee *et al.*, 1996a, 1996b; 1998). Gangliosides, a class of glycosphingolipids, constitute 0.1-0.3% of myelin lipids and although are ubiquitously expressed, they are quatitatively enriched in the exoplasmic leaflet of the plasma membrane in the nervous system (Svennerholm, 1980). Myelin has large quantities of cholestrerol and ethanolamine-containning plasmogens as well as lecithin. In addition, myelin has minor lipid components which include at least three fatty acid esters of cerebroside and the glycerol-based galactosyldiglycerides diacylglycerylgalactoside and monoalkylmonoacylglycerylgalactoside (Taylor *et al.*, 2004). Cholesterol constitutes about 30% of myelin lipids (Benjamins and Smith, 1984). Cholesterol is synthesized in the endoplasmic reticulum and transported to the plasma membrane via the Golgi apparatus. Since cholesterol is potentially toxic, its levels have to be controlled; this is accomplished by the transcriptional regulation of enzymes involved in the cholesterol synthesis pathway, cellular uptake, and storage in esterified form, and cellular efflux (Simons and Ikonen, 2000). In peripheral nerve, myelin is

enriched more in sphingomyelin than in brain myelin (Norton, and Cammer, 1984), and has a high content of monogalactosylsphingolipids, cerebrosides and sulfatides (Garbay *et al.*, 2000). Oleic acid in particular, is abundant in PNS myelin comprising about 40% of the fatty acids in sciatic nerves (Pratt *et al.*, 1969; Fressinaud *et al.*, 1986). Myelin proteins are encoded in the CNS and PNS by an overlapping but non identical set of genes. Abundant proteins that have been identified in myelin by biochemical methods include P0, MBP, P2 protein and peripheral myelin protein-22 (PMP-22) in PNS myelin (Greenfield *et al.*, 1973), proteolipid protein (PLP) and MBP in CNS myelin (Lees and Brostoff, 1984). Furthermore, immunocytochemistry confirmed an enrichment of PNS myelin with P0, PMP-22, and P2, as well as PLP and MBP both of which are major components of compact CNS myelin (Snipes *et al.*, 1992; Trapp *et al.*, 1979). Natural mutants and transgenic mice have been widely used to address the function of these proteins and their importance during Schwann cell development which will be explained below.

Protein Zero (P_0)

P_0 is the main protein in PNS myelin, accounting for more than 50% of the total; it is highly glycosylated (Greenfield *et al.*, 1973). The P_0 gene encodes a single RNA species of 1.9 kb that gives rise to a 29-residue signal peptide, a 124-residue extracellular domain, a 26-residue transmembrane domain and a 69-residue intracellular domain (Sakamoto *et al.*, 1987; Kirschner *et al.*, 2004). It codes for a tetramere-forming 28-30 kDa transmembrane glycoprotein of the immunoglobulin (Ig) superfamily, whose expression is largely specific to Schwann cells (Lemke and Axel, 1985; Lemke *et al.*, 1988a; Wegner, 2000). The presence of an Ig-like domain, also found in cell adhesion molecules such as N-CAM (Edelman, 1983), is an indication of P_0 involvement in

adhering myelin layers together (Lemke and Axel, 1985). The homophilic adhesive nature of P_0 has been demonstrated by transfection assays where increased cell-cell attachment occurs (D'Urso *et al.*, 1990; Filbin *et al.*, 1990; Schneider-Schaulies *et al.*, 1990). The only structural evidence to date comes from the crystal structure of P_0, suggesting that four P0 molecules form a tetramer in cis that interacts homophilically in trans with tetramers in apposing myelin lamellae to form the intraperiod line and perform an adhesive function (Shapiro *et al.*, 1996).

P_0 is expressed in the Schwann cell lineage, but its mRNA has been also detected in the notochord, otic placode and vesicle, enteric neural crest, and olfactory ensheathing cells (Lee *et al.*, 2001). The basal level of P_0 mRNA, first appears before birth in a sub-population of neural crest cells, indicating glial fate, and remains in Schwann cell precursors and immature Schwann cells (Bhattacharyya *et al.*, 1991; Lee *et al.*, 1997). Following birth, the expression level of P_0 mRNA and protein synthesis in myelinating Schwann cells rises 30-40 fold and peaks during the second post-natal week before its levels fall in the adult (Lemke and Axel, 1985; Trapp, 1988a; Stahl *et al.*, 1990; Baron *et al.*, 1994). To induce and maintain high levels of P0 expression, myelin forming Schwann cells require continuous axonal contact (Trapp, 1988a; Lemke *et al.*, 1988a; Jessen and Mirsky, 1991; Gupta *et al.*, 1993; Scherer *et al.*, 1994). To date, the strongest evidence for direct regulation of the P_0 gene is by the Sox-10 transcription factor, and it has been claimed that this constitutes the best link so far established between a glial transcription factor and the regulation of a myelin gene (Peirano and Wegner, 2000b). *In vitro*, Sox-10 increases the level of endogenous P_0 expression and activates the P_0 promoter, although these experiments have only been carried out in a cell line. Furthermore, the P_0 promoter contains multiple Sox-10 binding sites which are

functionally important for Sox-10 dependent activation of P_0 (Peirano *et al.*, 2000a). The use of transgenic mice has provided more information on the function of the P0 protein. A series of P_0 null mice develop axonal degeneration, indicating a possible role for P_0 in axon protection and maintenance (Giese *et al.*, 1992; Martini *et al.*, 1995; Frei *et al.*, 1999). Furthermore, it has been shown that complete disruption of P_0 expression leads to uncompaction of the myelin sheath (Giese *et al.*, 1992). To date, more than 80 mutations have been identified in the P_0 gene many of them in the extracellular domain (Wrabetz *et al.*, 2004). In humans, a number of P0 mutations have been characterised in a variety of demyelinating diseases including the mild variant of Charcot-Marie-Tooth disease (CMTB), Dejerine-Sottas syndrome (DSS), and congenital hypomyelination (CH) (Eichberg, 2002). Moreover, work on P_0 gene overexpression has highlighted the importance of gene dosage and stoichiometry of different myelin genes in the production of a stable myelin sheath (Wrabetz *et al.*, 2000). In transgenic mice overexpressing P_0 increasing dysmyelination occurs with increased P_0 gene dosage. It has also been confirmed that increased P_0 gene dosage causes a reduction in P_0 protein expression as well as a reduction in the normal levels of MBP, suggesting that myelin assembly employs a process linking the various constituents in a mechanism that closely controls the final stoichiometry.

Myelin Basic Protein (MBP)

MBP is the second most abundant protein accounting for 2-16% of peripheral myelin (Greenfield *et al.*, 1973). The MBP gene is about 105 Kb in length in mouse and about 180 Kb in human (Campagnoni *et al.*, 1993; Pribyl *et al.*, 1993). There are three transcription start sites in the gene, giving rise to three sets of mRNAs encoding two families of proteins. The generation of classic MBP mRNAs is primarily from

transcription start site 3 in myelin-forming cells. The second family of MBP is the *golli-MBPs*, which are generated from the first transcription start site of the gene. These proteins are expressed in the nervous system at significantly lower levels than MBP, and also throughout the immune system (Campagnoni *et al.*, 1993). The classic MBP consists of at least six different isoforms generated by alternative splicing and ranging from 14 to 21.5 kDa. They are located on the intracellular face of compact myelin in the major dense line (Lemke and Barde, 1998). MBP proteins are targeted by oligodendrocytes and Schwann cells to the sheath via free ribosomes located close to the site of myelination (Colman *et al.*, 1982; Trapp *et al.*, 1987; Ainger *et al.*, 1993). It is believed that MBPs together with the P0 glycoprotein, paticipates in maintenance of the major dense line and compaction of the PNS myelin sheath (Omlin *et al.*, 1982; Martini *et al.*, 1995). In the mouse, the MBP gene, distributed over a 32 kbp region of chromosome 18, comprises seven exons, of which exons 2, 5, and 6 are alternatively spliced, accounting for all six forms of mouse MBP identified in the CNS (de Ferra *et al.*, 1985; Roach *et al.*, 1985; Takahashi *et al.*, 1985; Newman *et al.*, 1987). The *shiverer* "*Shi*" mouse is a naturally occurring mutant that has been shown to be deficient in MBP. These mice show a number of behavioural patterns including a generalized action tremor starting around p12, convulsions and early death. In these mice there is an almost complete lack of myelin in the CNS and the major dense line fails to form, while in the PNS, although myelin appears to have normal thickness, lamellar structure and periodicity, there is an increase in the number of SLIs (Privat et al., 1979; Kirschner and Ganser, 1980; Rosenbluth, 1980; Gould *et al.*, 1995). One reason for the difference in CNS and PNS myelin might be due to the amount of MBP in the CNS. Unlike PNS, MBP forms 30% of myelin protein in CNS and hence may play a role in myelin stability. Furthermore, generation of double mutant mice deficient for both P0

and MBP showed severe hypomyelination, and a thin myelin sheath devoid of major dense lines, indicating their importance for normal myelination (Martini *et al.*, 1995).

PMP22

The peripheral myelin protein 22 (PMP22) belongs to a family of membrane proteins characterised by four hydrophobic domains and conserved amino acid motifs (Jetten and Suter, 2000). It is 22 kDa and a minor component of the myelin sheath in PNS. During embryonic development and in the adult, PMP22 is widely expressed in neural and non-neural tissues (Kuhn *et al.*, 1993; De Leon *et al.*, 1994; Baechner *et al.*, 1995; Taylor *et al.*, 1995). During PNS development of the rat, PMP22 is found in peripheral nerves and in DRG from E12 onwards (Hagedorn *et al.*, 1999). In mouse however, the expression of PMP22 in DRG is very weak or absent (Paratore *et al.*, 2002). Its expression in myelinating Schwann cells is upregulated with the onset of myelination (Snipes *et al.*, 1992; Notterpek *et al.*, 1999). PMP22 is localized in the plasma membrane of both non-myelinating and myelinating Schwann cells as well as in compact myelin (Snipes *et al.*, 1992; Haney *et al.*, 1996). In injured nerve, PMP22 is rapidly down-regulated in the degenerated nerve, but is upregulated in the regenerating nerve (De Leon *et al.*, 1991; Welcher *et al.*, 1991; Snipes *et al.*, 1992; Kuhn *et al.*, 1993), suggesting a requirement of axons for induction and expression of PMP22 (Maier *et al.*, 2002).

The human PMP22 gene spans approximately 40 kbp and contain 6 exons (Patel *et al.*, 1992; Suter *et al.*, 1994). It is located on chromosome 17 and its gene organisation has similarity with the mouse and rat genes, located on chromosome 11. On the transcriptional level, two different promoters, P1 and P2, have been identified (Suter *et al.*, 1994). P1 is a classic promoter with TATA and CAAT boxes, and appears to regulate myelinating Schwann cell-specific expression. Unlike P1, P2 lacks these

features and is highly GC-rich, similar to the promoters of house-keeping genes (Suter *et al.*, 1994). It has been shown that PMP22 and P0 are co-localised in compact myelin and regulated in a similar way during development, myelination and after nerve injury. Furthermore, the idea of the association between PMP22 with a P_0 tetrameric complex may well be true since mutations in both genes result in similar inherited demyelinating neuropathies (Snipes and Suter, 1995; Scherer, 1997; D'Urso *et al.*, 1999; Wrabetz *et al.*, 2004). Most of the information about the role of PMP22 comes from point mutations. The best studied point mutations are the *trembler* (*Tr*) (G150D), and *Tr-J* (L16P) mutations in mice. Examination of affected peripheral nerves in these animals reveals hypomyelination, uncompaction, and increased number of Schwann cells in both models (Suter *et al.*, 1992a; 1992b; 1993). Furthermore, these mutations are in hydrophobic regions of the PMP22 protein, suggesting the importance of the transmembrane domains for myelin compaction and maintenance of mature myelin (Suter *et al.*, 1992b; Suh *et al.*, 1997). In cells transfected with the Trembler allele only, PMP22 colocalizes with the endoplasmic reticulum and there is some overlap with the Golgi (D'Urso *et al.*, 1998), suggesting that the Tr mutation is retained in the ER, does not accumulate in the Golgi, and is not incorporated into myelin like the wild-type protein (Snipes and Orfali, 1998). Tr-J mice with Leu16Pro mutation, also have defects in protein transport (Notterpek *et al.*, 1997; Tobler *et al.*, 1999). It is the mutation that has been described in human CMT1 (Valentijn *et al.*, 1992). The idea that P0 and PMP22 might have similar roles during myelination was addressed by generating PMP22 knock-out mice (Adlkofer *et al.*, 1995). These mice were viable and identified at p14 due to walking difficulties; other abnormalities also observed included body tremor and stress-induced convulsions. Morphological analysis displayed a mild delayed onset of myelination followed by hypermyelination and demyelinating peripheral neuropathies in

both the homozygous and heterozygous state, characterised by tomacula, onion bulbs and aberrant Schwann cell proliferation and death (Adlkofer et al., 1995; 1997; Sancho *et al.*, 1999; 2001). Overexpression of PMP22 in mice induces peripheral neuropathies with four copies or more of the transgene; where there are seven copies hypomyelination is severe (Huxley *et al.*, 1996; 1998). Delays in the onset of myelination have also been observed in these mice (Magyar et al., 1996; Sereda *et al.*, 1996). Furthermore, Schwann cells of *Tr* mutants and mice with seven copies of PMP22 gene are able to form 1:1 association with axons, although many fibres were not completely surrounded by Schwann cell cytoplasm (Robertson *et al.*, 1999). Analysis of transgenic rats that overexpress PMP22 in Schwann cells demonstrated that myelination is arrested at the promyelinating stage and not delayed, suggesting an accumulation of PMP22 in a late Golgi-cell membrane compartment that causes a defect in myelin assembly (Niemann *et al.*, 2000). Beside CMT there are two human diseases that have been associated with PMP22 gene mutations, Dejerine-Sottas syndrome (DSS) and hereditary neuropathy with liability to pressure palsies (HNPP) (Keller and Chance, 1999; Wrabetz *et al.*, 2004). The variation and extent of neuropathies studied in both animal models and patients with PMP22 gene mutations indicates that, like mutations in P0, PMP22 could act via at least two different mechanisms, gain or loss of function. In the case of gain of function, the protein is likely to be degraded creating an abnormal or toxic function that disturbs the cell biology leading to a more severe phenotypes. Loss of function is more likely to be responsible for the milder phenotypes observed (Wrabetz *et al.*, 2004). In general, these observations highlight two important roles for PMP22 in PNS; in establishing a complete Schwann cell-axon association and involvement in maturation of compact myelin.

Proteolipid protein (PLP)

PLP, an integral membrane protein of compact myelin, is the major myelin protein of the adult CNS where it is likely to have a structural role in maintaining the intraperiod line (Duncan *et al.*, 1987). The PLP gene, localized on chromosome X, spanning about 17 kb, consists of seven exons and a single promoter region (Stoffel *et al.*, 1984; Diehl *et al.*, 1986; Macklin *et al.*, 1987). PLP is highly conserved with four transmembrane domains and functions in oligodendrocyte development, myelin compactation and axonal integrity. There are two isoforms of proteolipid protein, PLP (24kDa), and DM20 (20 kDa). PLP expression makes up 40% of total myelin protein in the CNS whereas in PNS the expression level is much lower. The localization of PLP and DM20 in PNS myelin is still not clear as in some reports they are believed to be cytoplasmic, outside of the compact myelin (Puckett *et al.*, 1987; Bizzozero *et al.*, 1989; Griffiths *et al.*, 1989), while in others they are reported in compact myelin (Agrawal and Agrawal, 1991; Garbern *et al.*, 1997). DM20 is the most abundant isoform in PNS and has been also detected in non-myelinating Schwann cells (Pham-Dinh *et al.*, 1991; Ikenaka *et al.*, 1992; Griffiths *et al.*, 1995). Two transcription initiation sites have been identified in the PLP gene (Milner *et al.*, 1985), and both are employed in the CNS, where the site downstream is predominantly used in the PNS (Kamholz *et al.*, 1992). During development of oligodendrocytes, DM20 is initially expressed at higher level but is later overtaken by PLP at the peak of myelination (Schindler *et al.*, 1990; Timsit *et al.*, 1992; 1995; Hudson, 2004). Gene targeting of the PLP locus has been used to generate null mice lacking both PLP and DM20 as well as mice that are deficient in PLP isoform only (Boison and Stoffel, 1994; Boison *et al.*, 1995; Klugmann *et al.*, 1997; Stecca *et al.*, 2000; Uschkureit *et al.*, 2001; Sporkel *et al.*, 2002). In all transgenics, oligodendrocytes develop normally and they assemble myelin, but the intraperiod line in PLP/DM20 null

mice have defects with reduced conduction velocity, axonal swelling and loss of compact myelin in small diameter axons (Yool *et al.*, 2002). Age-related degeneration is also occurs in PLP/DM20 and PLP null mice (Boison and Stoffel, 1994; Boison *et al.*, 1995; Klugmann *et al.*, 1997; Stecca *et al.*, 2000; Sporkel *et al.*, 2002; Yool *et al.*, 2002). In humans, mutation in PLP and/or DM20 causes Pelizaeus-Merzdacher disease (PMD), an X-linked recessive disorder which in some cases cause dysmyelinating neuropathy. Severity and onset of the disease ranges widely and depends on the type of PLP mutation (Yool *et al.*, 2002). The effect of PLP gene dosage on CNS myelination is therefore an indication of a direct interaction between the oligodendrocyte and axon in which proteolipids are involved.

Myelin-Associated Glycoprotein (MAG)

On the basis of the rat cDNA, MAG is a type I membrane glycoprotein consisting of an N-terminal extracellular domain, a single transmembrane domain and a short cytoplasmic domain (Arquint *et al.*, 1987; Lai *et al.*, 1987b; Salzer *et al.*, 1987). The molecular weight of MAG is about 100 kDa with a gene that spans approximately 16 kb and composing of 13 exons. MAG exists as two isoforms resulting from alternative splicing producing a small MAG (S-MAG) with 67 kDa and a large MAG (L-MAG) with 72 kDa. L-MAG is predominant during CNS development reaching a peak by p22 and then declining, whereas S-MAG comes up at later stages of oligodenrocyte development and becomes predominant in adult brain. In the PNS, S-MAG is predominant throughout development and reaching peak levels at p6-10 (Lai *et al.*, 1987a; Tropak *et al.*, 1988; Inuzuka *et al.*, 1991). MAG accounts for 1% of the total myelin protein in the CNS, and about 0.1% in the PNS (Quarles *et al.*, 1973; Figlewicz *et al.*, 1981). It is found in the periaxonal region and at the inner mesaxons and is not

present within the compacted myelin. In the PNS, MAG is found mainly in non-compact myelin including paranodal loops, SLI, and inner mesaxon (Trapp and Quarles, 1982; Owens and Bunge, 1989; Trapp *et al.*, 1989b). Moreover, MAG has been detected on Schwann cells prior to the onset of myelination (Trapp, 1988a; Owens and Bunge, 1989), indicating an additional role before myelin formation. MAG contains an extracellular portion of five Ig-like domains, as seen with P0, which have been proposed to participate in the adhesion of the myelinating glial cell to the axon. The adhesive function of MAG has been demonstrated experimentally using different approaches. The use of antibody against MAG, for example, prevents the binding of oligodendrocytes to neurons (Poltorak *et al.*, 1987), and incorporation of purified endogenous or recombinant MAG into liposomes demonstrate binding to different cell types like DRG and neurons (Poltorak *et al.*, 1987; Johnson *et al.*, 1989; Afar *et al.*, 1991). One of the earliest indications of MAG involvement in mediating interaction between axon and myelin sheath was provided with naturally occurring "*quaking*" mouse mutant. In this mouse, although the mutation occurs in QK1 gene, it directly affects expression of MAG mRNA and protein as well as MAG localization most probably, through defects in alternative splicing and abnormal levels of L-MAG and S-MAG (Trapp, 1988a; Bartoszewicz *et al.*, 1995). MAG deficient mice have delayed myelin formation in the CNS unlike PNS where the changes are subtle. Aanalysis of PNS in aged mice lacking MAG showed that although myelin seems normal up to ten weeks of age, degenerating axons and myelin sheaths were observed in the PNS of older animals, suggesting that MAG may also be involved in long-term maintanence of myelin (Fruttiger *et al.*, 1995b; Yin *et al.*, 1998; Weiss *et al.*, 2001). In addition, MAG inhibits extension of neurites from older ganglia in vitro, indicating that MAG has an inhibitory effect on axonal growth for mature neurons. This is in agreement with other

studies that reported that regeneration following sciatic nerve injury is enhanced in MAG null mice (DeBellard *et al.*, 1996; Li *et al.*, 1996; Tang *et al.*, 1997; Shen *et al.*, 1998).

Periaxin (Prx)

Prx, a member of PDZ domain protein family, is a PNS specific protein that is primarily expressed by myelinating Schwann cells. Prx is 170 kDa and represents about 5% of the total myelin protein (Shuman *et al.*, 1983). The name periaxin originated in accordance with its localisation close to the periaxonal membrane of myelinated Schwann cells (Gillespie *et al.*, 1994; Scherer *et al.*, 1995a). The Prx gene is localized in mouse on chromosome 7, spanning 20.6 kbp and encodes two mRNAs of 4.6 and 5.2 kb for the two periaxin forms: L-periaxin (147 kDa) and S-periaxin (16 kDa) (Gillespie *et al.*, 1997). S-periaxin (the large mRNA), a truncated protein, is produced by a retained intron mechanism that introduces a stop codon. L-periaxin is localized to the plasma membrane of myelinating Schwann cells, although initially targeted to the nucleus of early Schwann cells, and S-periaxin is expressed diffusely in the cytoplasm (Dytrych *et al.*, 1998). The reason behind nuclear localization of Prx is not clear yet but one possibility is the involvement of nuclear localization signal of an unusual tripartite type for translocating L-periaxin into the nucleus of Schwann cells. It is also possible that L-periaxin may have a role in co-transcriptional regulation in embryonic nerve (Sherman and Brophy, 2004). In human PNS, L-periaxin (the small mRNA) is dominant isoform in myelinating Schwann cells (Boerkoel *et al.*, 2001). L-Periaxin is detectable in Schwann cells at early stages of development, E14, when it is localized to the nuclei of Schwann cells at this time and remains for 3 days of Schwann cell development (Sherman and Brophy, 2000). It is expressed before significant levels of Krox-20 are

detectable (Parkinson *et al.*, 2003). The expression of periaxin is axonally regulated, in a similar way to other myelin genes and down-regulates following nerve injury (Scherer *et al.*, 1995).

To identify the proteins that L-periaxin interacts with, yeast two hybrid screens identified dystrophin-related protein 2 (DRP2), a member of the dystrophin-like protein family, as an interacting protein. This family of proteins which comprises dystrophin, utrophin, and dystrobrevin, are components of complexes with the plasma membrane protein dystroglycan. Immunocytochemical studies have showed that the L-periaxin-DRP2 complex is clustered in specific patches at Schwann cell plasma membrane which is likely promoted or stabilized by dimerization of L-periaxin at its PDZ domain (Gillespie *et al.*, 2000; Sherman *et al.*, 2001). The interaction between L-periaxin and DRP2 was further investigated in periaxin-null mice (Sherman *et al.*, 2001). These mice are also able to form and assemble myelin at an early age, however, by 6 weeks of age the sciatic nerves contain some tomacula (focal thickenings) and infoldings of internodal myelin (Gillespie *et al.*, 2000). With ageing, periaxin null mice show severe demyelination and associated reduced nerve conduction velocities (Gillespie *et al.*, 2000). Mutations in the periaxin gene have also been reported in human neuropathies including DSS (Boerkoel *et al.*, 2001), and an autosomal recessive form of CMT termed CMT4 (Guilbot *et al.*, 2001). Further investigation of periaxin null animals demonstrated that the internodal distances are decreased, which causes slower conduction velocity (Court *et al.*, 2004). Together these data suggest that periaxin is involved in stability and/or protein turnover towards formation of mature myelinating Schwann cell and more interestingly has a role in controlling the internodal length which itself influences nerve conduction velocity.

P2

The basic P2 protein was first isolated from bovine nerve roots (London, 1971). It is a member of a family of fatty acid-binding proteins, with a high affinity for oleic acid, retinoic acid and retinol (Uyemura *et al.*, 1984). It has a product of 14.8 kDa cytosolic protein expressed on the cytoplasmic side of the compact myelin membranes (Trapp *et al.*, 1984b; Narayanan *et al.*, 1988) and accounts for less than 1% of total myelin protein in PNS (Greenfield *et al.*, 1973; Kadlubowski *et al.*, 1984). It has been proposed that P2 may serve as a lipid carrier and may therefore be involved in the assembly, remodelling, and maintenance of myelin (Garbay *et al.*, 2000).

2',3'-cyclic nucleotide 3'-phosphodiesterase (CNPase)

CNPase was first identified in CNS myelin (Kurihara and Tsukada, 1967; Olafson *et al.*, 1969) and represents less than 0.5% of PNS myelin proteins (Uyemura *et al.*, 1972). CNPase is expressed in the periaxonal region, outer myelin sheath, Schwann cell surface membrane, outer mesaxon, SLI, and in the Schwann cell cytoplasm (Yoshino *et al.*, 1983; 1985; Trapp *et al.*, 1988b). CNPase is found as two isoforms, CNP1 (46 kDa) and CNP2 (48 kDa) within glial cells as well as other non-neuronal tissues (Braun *et al.*, 2004). The generation of CNPase null mice showed normal myelin development at younger age but adults develop axonal swellings and neurodegenerative disorder, suggesting a possible role for CNPase in axonal survival (Lappe-Siefke *et al.*, 2003). Moreover, based on structural analysis, it has been revealed that CNP has similarities with some bacterial RNA ligases indicating a role for CNPase in RNA regulation, degradation and metabolism (Mazumder *et al.*, 2002).

Plasmolipin and Myelin and Lymphocyte protein (MAL/MVP17)

Plasmolipin and MAL are, as with PLP and PMP22, members of the tetraspan myelin proteins. Plasmolipin is mostly expressed in the kidney and the nervous system (Hamacher *et al.*, 2001). The gene encodes a single 1.7 kb mRNA, resulting in a 157 aa, 18 kDa protein (Fischer and Sapirstein, 1994). In the PNS, plasmolipin mRNA expression is confined to myelinating Schwann cells, and its regulation during development shows a correlation with myelination (Gillen *et al.*, 1996; Bosse *et al.*, 2001). It has been shown that after nerve injury, the expression of plasmolipin is induced in the distal stump even after prevention of regeneration using ligation of the proximal nerve stump (Bosse *et al.*, 2001). This suggest an additional role different from myelin biogenesis and maintenance.

Plasmolipin shares some sequence similarities with MAL/ MVP17. MAL is a 17 kDa proteolipid which is expressed in CNS by oligodenrocytes and PNS by Schwann cells, as well as kidney, spleen and brain (Kim *et al.*, 1995; Schaeren-Wiemers *et al.*, 1995). In the PNS, MAL expression is highest in myelinating Schwann cells and it co-localizes with MBP and PLP (Frank *et al.*, 1999). Immunocytochemistry with MAL antibodies has also detected expression in immature Schwann cells and it persists in adult non-myelinating Schwann cells (Frank *et al.*, 1999).

Connexin 32

The connexins are a family of highly related genes that encode a group of channel forming proteins (Bruzzone *et al.*, 1996; White and Paul, 1999). Connexins are a subunit of connexon, a protein structure that forms a gap junction which is a channel that allows ions and small molecules, usually <1000 Da, to move between

adjacent cells. Each connexin gene is named according to the organism which it is derived from and the predicted molecular mass of the protein that it encodes. There are 21 different connexin genes in mammals (Willecke *et al.*, 2002). All connexin genes encode proteins with a similar four transmembrane domain topology (Bruzzone *et al.*, 1996; White and Paul, 1999; Scherer and Paul, 2004). The first connexin to be cloned was Cx32 (Paul, 1986; Kumar and Gilula, 1986). It is highly conserved across all mammalian species, and the coding region is contained within a single exon. It is expressed in a number of tissues including myelin forming cells of the CNS and PNS, where it appears to be regulated by transcription factors Sox10 and Krox20 respectively (Bondurand et al., 20001; Musso *et al.*, 2001). In the PNS, Cx32 is located in the paranodal regions and SLI, and has been proposed to form gap junctions between different membrane layers of the myelin sheath to provide a shortcut for the diffusion across the non-compacted regions of the sheath (Paul, 1995; Scherer *et al.*, 1995b). In Cx32 null mice, myelination occurs normally but they develop a late-onset demyelinating peripheral neuropathy, characterized by progressive onion bulb formation, thinly myelinated axons, and abnormal organisation of the non-compacted myelin membranes (Anzini *et al.*, 1997; Scherer *et al.*, 1998). In humans, the gene encoding Cx32 is located on chromosome X, and to date, more than 80 mutations in this gene have been identified. Some of these are found in non-coding regions and are associated with a form of CMTX disease (Bergoffen *et al.*, 1993; Bruzzone *et al.*, 1994; Ionasescu *et al.*, 1994; Bondurand *et al.*, 2001).

Connexin 29 (Cx29)

As it mentioned earlier, although both Schwann cells and oligodendrocytes express Cx32, in its absence only the PNS undergoes demyelination. Cx29 has been recently

identified using RT-PCR and degenerate primers, on CNS cDNA, in an attempt to find another connexin that could function in replacemet of Cx32 (Altevogt and Paul, 2000). The expression of Cx29 appears to be restricted to myelinated glia (Sohl *et al.*, 2001; Altevogt *et al.*, 2002). It is localised in the myelin sheaths of small myelinated axons in the CNS, and particularly in the juxaparanodal region of myelinating Schwann cells (Altevogt *et al.*, 2002). Light microscopy obsrvations have indicated that Cx29 expression is targeted to SLI and paranodal loops where colocalizes with MAG. Immunogold labelling for Cx29 however, did not reveal gap junctions at incisures or in linking successive loops of paranodal myelin, and to date there is no reported gap junctions at SLI or between paranodal loops in the PNS (Li *et al.*, 2002). Interestingly, in PNS myelinated axons, immunohistochemical co-localization studies have showed that Cx29 in the adaxonal Schwann cell membrane and Kv1.2, potassium channels in the axonal membrane overlap. This is intriguing because Cx29 and Kv1.2 are expressed in different cells (Altevogt *et al.*, 2002). There are no data to support the presence of gap junctions between axons and their myelin sheath.

Integrins

Integrins are cell surface glycoproteins that mediate interactions between cells and the extracellular matrix (ECM) (Hynes, 1992; 2002; ffrench-Constant, 2004). They are also involved in regulating survival, proliferation, migration, and differentiation. Integrins comprise a family of heterodimers, composed of α and β subunits, each encoded by separate genes, and associated using non-covalent bonds. Each subunit has a short cytoplasmic domain, except for $\beta 4$, that may interact with adaptor molecules and cytoskeleton components like vinculin and talin. To date, 20 different subunits are known and at least 22 α/β heterodimers have been described (Hynes, 1992; Archelos

et al., 1999). Each integrin heterodimer molecule has the specificity to interact with one or more ligands usually members of the ECM and transmembrane proteins of the Ig superfamily like L1 and Thy-1. This is referred as *in-trans* binding. The interaction with cell-surface/cytoskeletal proteins such as tetraspan molecules like CD9 is referred to as *in-cis* binding (Previtali *et al.*, 2001).

In the PNS, several different integrins are expressed throughout Schwann cell development in a pattern that are varies according to the developmental stages. Studies on chick neural crest have shown that its differentiation to Schwann cell precursor is accompanied by the expression of α6β1 (laminin receptor) integrin (Lallier *et al.*, 1992). Conversely, the expression of α1β1 which is detectable in the neural crest, becomes down-regulated in Schwann cell precursors but is high postnatally in non-myelin forming Schwann cells (Perris, 1997; Stewart *et al.*, 1997b). At least seven integrin heterodimers have been identified in the mature Schwann cells of chick, rodent, and human. These are α1β1, α6β1, αvβ8, α2β1, α6β4, αvβ3, and α5β1 (Previtali *et al.*, 2001). Studies have suggested a major role for at least two integrins, the laminin receptors α6β1 and α6β4, as myelination is dependent on basal lamina assembly (Eldridge *et al.*, 1989). It has been shown that mutations in laminin-2 causes peripheral neuropathy in both human and mouse (Matsumura *et al.*, 1997). During embryonic development in mice, β1 subunit of α6β1 is detectable at E12.5, but α6 subunit switches partner from β1 to β4 at the onset of myelination, when both β1 and β4 are expressed (Giancotti *et al.*, 1992). Levels of β4 subunit expression in humans and rats progressively increase during postnatal nerve development and myelination and is localised to the abaxonal surface of myelin forming Schwann cells and is axon dependent (Einheber *et al.*, 1993; Feltri *et al.*, 1994; Niessen *et al.*, 1994). To

characterize the role of the β4 subunit, mutant mice lacking β4 were generated. Although these mutants die shortly after birth, cultured DRG showed that myelination can occur in the absence of β4 integrin (Frei *et al.*, 1999). The use of Cre/loxp system in Schwann cells to overcome the embryonic lethality of β1 integrin knockout animals showed that the lack of β1 causes a severe dysmyelinating neuropathy due to the lack of a correct interactions with axons (Feltri *et al.*, 2002). However, some Schwann cells can bypass the lack of interaction and synthesise myelin with a delay, possibly due to a compensatory mechanism via dystroglycan or α6β4 (Feltri *et al.*, 2002). Further investigation of these mice showed that β1 integrin is not required in the embryonic stages of development, as migration, proliferation, and survival of precursor cells occur normally. Although these data suggest that Schwann cells require β1 integrins for proper contact with axons, more experiments are required to understand the role of integrin during Schwann cell development.

Laminin

Laminin are heterotrimeric glycoproteins with three subunits; α-, β-, and γ-subunit, where each is encoded by a different gene and composed of five α-subunits, four β-subunits, and 3 γ-subunits (Feltri and Wrabetz, 2005). Both myelin forming and non-myelin forming Schwann cell synthesise basal lamina (Billings-Gagliardi *et al.*, 1974; Bignami *et al.*, 1984). They express a large amount of laminin, which is the main component of basal lamina (Cornbrooks *et al.*, 1983; Podratz *et al.*, 2001). Studies have showed that laminin deposition on the Schwann cell surface is sufficient for myelination even in the absence of a structured basal lamina (Podratz *et al.*, 2001). The main form of laminin expressed by Schwann cells consists of β1 and β2 light chains and the α2 heavy chain (also known as merosin) (Reichardt and Tomaselli, 1991). Mutation in

merosin causes peripheral neuropathy in mouse, known as dy/dy, and in human knwn as merosin-deficient congenital muscular dystrophy (CMD) (Xu *et al.*, 1994; Sunada *et al.*, 1995), where both were recognised by abnormal bundles of naked axons, as well as discontinuous basal lamina (Bradley and Jenkison, 1973; Madrid *et al.*, 1975; Uziyel *et al.*, 2000). These data indicate the important role of laminin-integrin complex towards Schwann cell myelination.

Spectrin and ankyrin

The spectrins are a family of submembranous scaffolding proteins. They are a component of the cytoskeleton which maintains the structural integrity of the membrane (Bennett and Baines, 2001). They are composed of two large polypeptide chains, α-spectrin and β-spectrin and are associated laterally to form antiparallel heterodimers which form hetrotetramers that cross-link membrane proteins and actin filaments into a flexible and stable network. However, this binding of spectrin depends on a large intracellular attachment protein called ankyrin which binds to β-spectrin as well as the cytoplasmic domain of cell membrane proteins. One of the best examples are the erythroid spectrins which are necessary to maintain the highly deformable and elastic properties of circulating red blood cell membrane (Marchesi and Steers,1968; Delaunay, 2002). In comparison, the roles of non-erythroid spectrins are not well understood. Ankyrins however, belong to the membrane skeletal family of proteins that seem to be associated with the L1/CAM family of cell adhesion molecules (Bennett and Lambert, 1999). They were initially found in human erythrocytes linking cytoplasmic domain of the anion exchanger and the spectrin/actin network on the innersurface of the plasma membrane (Bennett and Lambert, 1999). Ankyrin binding proteins include the voltage dependent sodium channel (Srinivasan *et al.*, 1988), Na/K

ATPase (Nelson and Veshnock, 1987), Na/Ca^{2+} exchanger (Li *et al.*, 1993), the IP3 receptor and ryanodine receptor calcium release channels (Bourguignon et al., 1993; Bourguignon et al., 1995), CD44 (Kalomiris and Bourguignon, 1988), and the L1/neurofascin/NrCAM family of cell adhesion molecules (Davis *et al.*, 1993; Davis and Bennett, 1994; Dubreuil *et al.*, 1996; Zhang *et al.*, 1998). In mammals there are three members of the ankyrin gene family; ankyrin R (ANK1) (Lux *et al.*, 1990; Lambert *et al.*, 1990), which are expressed in erythrocytes and striated muscles as well as a subset of neurons in the CNS (Lambert and Bennett, 1993); ankyrin-B (ANK2); (Otto *et al.*, 1991), is expressed in brain, striated muscle, kidney, peripheral blood cells, and the thymus and ankyrin-G (ANK3); (Kordeli *et al.*, 1995; Peters *et al.*, 1995; Devarajan *et al.*, 1996; Thevananther *et al.*, 1998), is expressed in most tissues and includes alternatively spliced forms targeted to Node of Ranvier. It has been shown that ankyrin-G also is associated with sodium (Na) channel clusters in the dystrophic mouse in regions lacking myelination (Deerinck *et al.*, 1997) therefore suggesting a role for ankyrin-G in the localization of the Na channels to specific membrane regions (Bennett and Lambert, 1999).

The function of spectrin and ankyrin-G has been recently studied in mice. βIV spectrin was found specifically at the Node of Ranvier and axon initial segments and was proposed to link voltage-gated Na^+ (Nav) channels to the actin cytoskeleton through ankyrin-G (Berghs *et al.*, 2000; Komada and Soriano, 2002). In βIV spectrin null mice these Nav are distrupted at Node of Ranvier and axon initial segments (Komada and Soriano, 2002). This result indicates the importance of βIV spectrin in the nodal membrane structure and Nav stabilization (Yang *et al.*, 2004). In ankyrin-G knock out mice however, clustering of neurofascin and voltage-gated sodium channel at axon

initial segments is disrupted which lead to the failure in normal action potential firing (Zhou *et al.*, 1998). This indicates that ankyrin-G is essential for localization of neurofascin and voltage-gated sodium channels at these sites.

STRUCTURE AND MOLECULAR ORGANISATION OF NON-MYELINATING SCHWANN CELLS

Each non-myelinating Schwann cell supports a number of axons with a diameter smaller than 1 micron. These small diameter axons or C fibres are produced by many sensory and essentially all postganglionic sympathetic neurons. Each axon lies in membranous channel or trough that may or may not completely surround it and allows it to be separated from other axons (Eames and Gamble, 1970). Gap junctions are found between adjacent non-myelinating Schwann cells as they lie end-to-end along axons at the interphase of two cells. This should facilitate intracellular communication, and suggests that non-myelinating Schwann cells act as a continuous chain of support cells (Konishi, 1990).

The involvement of Nrg1 and ErbB signaling has been also studied in non-myelinating Schwann cells. Using transgenic mice expressing a dominant-negative ErbB receptor, only in non-myelinating Schwann cells, Chen and colleagues were able to demonstrate that lack of the ErbB receptor in adult non-myelinating Schwann cells results in extensive death and proliferation of these cells, similar to that produced by loss of axonal contact. This leads to peripheral neuropathy (Chen et al., 2003). Furthermore, the death of C-fibre sensory neurons by apoptosis in the transgenic animals, at late postnatal stages, has been reported, a process that is possibly due to the reduced expression level of GDNF in the sciatic nerve (Chet et al., 2003). This observation indicates that non-myelinating Schwann cells are involved in the maintenance of C-fibre

sensory neurons by providing essential trophic support. As these Schwann cells do not make myelin high level expression of myelin genes is not seen. Non-myelin forming Schwann cells instead express markers associated with developing Schwann cells. These are, the low affinity neutrophin receptor, p75 (p75NTR), the neural cell adhesion molecule (N-CAM) and L1, and a distinct set of cytoskeletal proteins including glial fibrillary acid protein (GFAP) as well as $\alpha 1\beta 1$ and $\alpha 7\beta 1$ integrins that are not expressed by immature Schwann cells (Jessen and Mirsky, 2005).

P75 neurotrophin receptor (p75NTR)

P75NTR is a 75 kDa cell surface associated glycoprotein, that is able to bind all the neurotrophins including NGF (Jessen and Mirsky, 1980; Hosang and Shooter, 1985; Chao *et al.*, 1986; Radeke *et al.*, 1987). One of the Schwann cell death signals that has been identified in vivo acts through p75NTR, possibly after activation by binding to NGF. This signal is involved in the increased level of Schwann cell death seen in newborn nerves after transection (Syroid *et al.*, 2000).

N-CAM and L1

Both molecules are members of the large Ig superfamily. They have Ig-like domains in combination with fibronectin III-like domains that facilitate homophilic binding (Schachner, 1990; Edelman and Crossin, 1991). N-CAM and L1 have been shown to promote neurite outgrowth in vitro, with L1 being the more potent, suggesting an important function in axonal growth in development and post injury (Schachner, 1990). N-CAM is expressed on the surface of developing Schwann cells, but it is down-regulated on myelinating Schwann cells. Observations have shown that in the mouse, a small amount of N-CAM expression remains in the periaxonal membrane (Martini and

Schachner, 1986) while in the rat it is not detectable on myelin forming Schwann cells (Mirsky *et al.*, 1986; Jessen *et al.*, 1987a). N-CAM has three isoforms (180 kD, 140 kD, and 120 kD) which differ only in their membrane anchors. The two larger proteins are integral membrane proteins while the smallest is tethered by a phosphatidylinositol anchor (Edelman and Crossin, 1991).

L1 is a large cell surface adhesion molecule (200 kD) expressed on mature non-myelinating Schwann cells and their axons (Rathjen and Schachner, 1984; Martini and Schachner, 1986). L1 is expressed on all Schwann cells prior to the onset of myelination and on axons during development, and is down-regulated from all myelinating Schwann cells once myelination is initiated (Faissner *et al.*, 1984; Martini and Schachner, 1986). *In vitro*, L1 binding is required for the process of myelination (*in vitro*) and specifically for the set up of adhesion between axon and Schwann cell (Seilheimer *et al.*, 1989; Wood *et al.*, 1990). However, the development of non-myelin forming Schwann cells and associated unmyelinated axons within the sciatic nerve are essentially normal in L1 deficient mice (Haney *et al.*, 1999). In contrast, in the older sciatic nerve, many of unmyelinated axons were either partially surrounded or completely deprived of Schwann cell processes and these Schwann cells displayed a discontinuous basal lamina. In the mutants, a degree of axonal degeneration was also apparent involving in particular loss of sensory axons (Haney *et al.*, 1999).

SCHWANN CELLS, HEDGEHOG AND PERINEURIUM FORMATION

Developing Schwann cells have an important role as a source of developmental signals in embryonic and neonatal nerves (Jessen and Mirsky, 1999). In addition to Schwann cell survival, signals either from Schwann cells or their precursors are likely to regulate

neurofilament phosphorylation, and hence axonal diameter, Na-channel clustering and the survival of embryonic DRG and motoneurones. The control of perineurium formation is an example of such signals from Schwann cells (Mirsky *et al.,* 2002). Peripheral nerve fibres are surrounded by a nerve sheath made from collagen fibres and a series of cellular tubes called perineurium, that acts as a barrier against unwanted molecules and cellular infiltration (Bunge *et al.,* 1989; Olsson, 1990). It has been shown that Schwann cell derived Desert hedgehog (*dhh*) protein, a member of hedgehog (hh) family of signalling molecules, is involved in the maturation of the epineurium, perineurinm and endoneurium. Desert hedgehog transcripts can be detected by in situ hybridisation in developing nerve in mouse at E11.5 (Bitgood and McMahon, 1995) and are maintained at high levels at least until postnatal day 10 with a decrease in adult nerves (Parmantier *et al.,* 1999).

Hedgehog and its signalling pathway

Hedgehog (Hh) ligands are 19 kDa proteins with two covalent lipid modifications (McMahon *et al.,* 2003; Nusse, 2003; Mann and Beachy, 2004). During the maturation of Hh protein palmitate and cholesterol are added to the N and C termini to enable Hh movement through the tissues. Hh have been shown to have an important role in both vertebrate and invertebrate developmental processes. The hedgehog gene was originally identified in *Drosophila melanogaster* as a protein involved in pattern formation of embryonic and adult fly (Hammerschmidt *et al.,* 1997) by influencing the transcription of many target genes (Hooper and Scott, 2005). In contrast to the single *hh* gene in Drosophila, mammals have three different *hh* genes which are *Sonic* (*Shh*), *Indian* (*Ihh*), and *Dhh*, where *Dhh* is most closely related to *D.melanogaster hh*. They are expressed in different tissues and at different stages of development.

Shh, a well studied hedgehog, controls important developmental processes including dorsoventral neural tube patterning, neural stem cell proliferation, neuronal and glial cell survival, induction of motor neurons (Roelink *et al.*, 1995), as well as somites and limb formation (Ho and Scott, 2002). *Shh* expression is initiated in the midline mesoderm of the head process and notochord at presomite stages and extends into the overlying floorplate region at the ventral midline of the CNS in register with somite stages (Bitgood and McMahon, 1995). In the neural tube, Shh secretion directs cell fate choices in a dose dependent manner as has been demonstrated using various concentrations of purified *Shh* to elicit dose-dependent gene activity in neural tube explants. Shh knockouts are embryonic lethal and targeted gene disruption in the mouse produces cyclopia with absence of ventral neural tube cells including motor neurons (Bitgood and McMahon, 1995).

Indian hedgehog expression has been observed in gut endoderm and cartilage. During early development of the gut, there is an overlap of *Shh* and *Ihh* expression but as differentiation occurs, their expression diverges. High levels of *Ihh* mRNA are detected in cartilage from as early as E11.5, with is highest expression in chondrocytes in the growth region of developing bones (Bitgood and McMahon, 1995). *Ihh* is secreted by the prehypertrophic chondrocytes and acts as an activator of parathyroid hormone-related protein (PTHrP), which negatively regulates the rate of chondrocyte differentiation (Vortkamp *et al.*, 1998). It has been shown that BMPs are located downstream of the Ihh pathway in vertebrates (Pathi *et al.*, 1999; Zou *et al.*, 1999) where their actions can be inhibited by antagonists such as noggin. Furthermore,

noggin knockout mice exhibit fused and malformed joints due to over-proliferation and defective differentiation of chondrocytes (Brunet *et al.*, 1998)

The last member of hedgehog family is *dhh*. *Dhh* is expressed as early as E11.5 in Sertoli cells of the undifferentiated male gonad and in Schwann cell precursors along peripheral nerves. Minor expression of *dhh* is also associated with the developing atrioventricular valve of the heart as well as in endothelial cells of the major blood vessels. There is no expression of *dhh* in the ovary. Since the transcription factor *Sry* is expressed by E10.5 in the testis and Mullerian inhibiting substance, a secreted factor responsible for mediating the loss of female characteristics, is the only other male-specific gene known to be expressed as early as E11.5, dhh could be a gene that is modulated by Sry, downstream of its expression (Pierucci-Alves *et al.*, 2001). Dhh-null female mice are fertile, but males have relatively small embryonic gonads by E18.5 and are sterile into adulthood (Bitgood *et al.*, 1996). Dhh is secreted by Sertoli cells and patched receptors are located on peritubular and Leydig cells. Lack of Dhh results in developmental defects that leads to severe disorganisation of the testis, including anastomotic seminiferous tubules, peritubular cell abnormalities and the absence of Leydig cells (Pierucci-Aves *et al.*, 2001). Furthermore it has been shown, using dhh null mice, that *dhh* is required for the differentiation of foetal Leydig cells in the testis (Ya0 *et al.*, 2002).

Hh signalling in Drosophila melanogaster

Hh signalling and changes in gene expression are mediated by the zinc-finger transcription factor Cubitus interruptus (Ci) in *D.melanogaster* (the Gli proteins are the equivalent in vertebrate, see below) (Fig1.3). Ci can be modified by the Hh signal-

transduction pathway to produce repressing (CiR) and activating (CiA) forms of Ci. In the absence of Hh, its receptor Patched (Ptc), a 12-transmembrane protein, inhibits the activity of an adjacent 7-transmembrane protein known as Smoothened (Smo). The cytoplasmic tail of Smo interacts with Kinesin-related protein Costal2 (Cos2) that acts as a negative regulator of Hh with two large hydrophilic extracellular loops where Hh binding occurs (Stegman *et al.*, 2004). Cos2 acts as the scaffold for Ci and four kinases; protein kinase A (PKA), casein kinase 1(CK1), glycogen synthase kinase-3β (GSK3β) and a serine/threonine kinase known as Fused (Fu) (complex I, Fig1.3) (Zhang *et al.*, 2004).

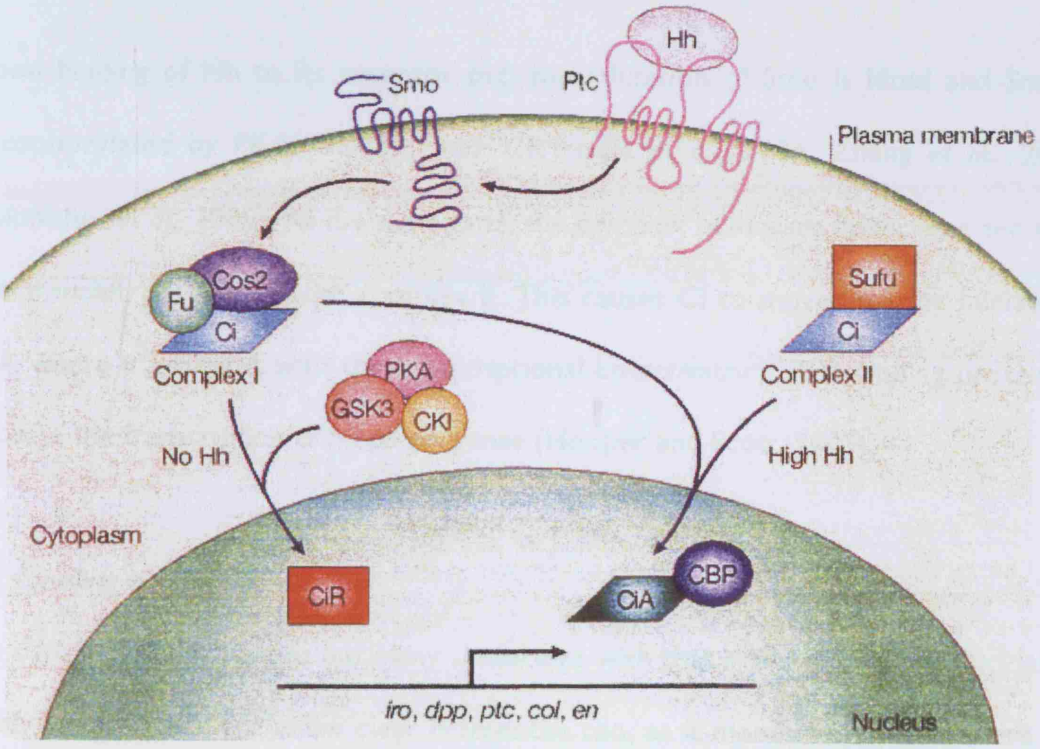

Figure 1.3 Hedgehog signalling in Drosophila melanogaster – The transcription factor Ci is held in the cytoplasm by complex I or complex II. In the absence of hh ligand, ptc inhibits Smo. Complex I promotes the phosphorylation of Ci by PKA, GSK3 and CK1, promoting subsequent processing of Ci to CiR. Higher concentrations of hh function through Ptc, Smo, and Complex I and II to release an active form of Ci (CiA) that leads to downstream signalling. From Hooper and Scott, Nat Rev. 6: 306-316, 2005.

These components, in the resting cell, cause the phosphorylation of Ci which can lead to binding to Supernumerary limbs (Slmb) (Jiang and Struhl, 1998; Dai *et al.*, 2003). This subsequently activates the processing of Ci into the Ci repressor (CiR), which moves into the nucleus and represses the transcription of target genes. In non-activated cells, most of Ci is not associated with Cos2, but is instead associated with suppressor of Fused (Sufu) to form a complex (complex II, Fig1.3) (Lum *et al.*, 2003) which retains Ci in the cytoplasm until it is activated by initiation of Hh signalling (Methot and Basler, 2000; Cheng and Bishop, 2002; Merchant *et al.*, 2004), although is not involved in the processing of Ci to CiR (Hooper and Scott, 2005).

Upon binding of Hh to its receptor ptc, the inhibition of Smo is lifted and Smo is phosphorylated by PKA, GSK3β, and CK1α (Jia *et al.*, 2004; Zhang *et al.*, 2004; Apionishev *et al.*, 2005). At the same time, the complex of kinases dissociates and then preferentially associates with complex II. This causes Ci to move into the nucleus as CiA where it interacts with the transcriptional co-activator CREB-binding protein to activate the transcription of *hh* target genes (Hooper and Scott, 2005).

Hh signalling in vertebrates

Hh signalling in vertebrates has many similarities with that in *D.melanogaster* (McMahon *et al.*, 2003). There are a few clear differences too; as it mentioned earlier, there are three *hh* genes in vertebrates, two *Ptc* genes, and three *Ci* homologues *Gli-1*, *Gli-2*, *Gli-3*. Studies so far suggest that all three hedgehogs use the same intracellular signalling pathway (Fig 1.4), although some signalling differences may occur depending on the hh molecule involved (Osterlund and Kogerman, 2006). The expression and function of *Ptc1* is similar to that of *D.melanogaster* Ptc. However Ptc2 expression is mostly

restricted and in some cases at least, its transcription is independent of Hh signalling (St-Jacques *et al.*, 1998). There is a significant difference in the cytoplasmic tail between *Drosophila*-Smo and vertebrate-Smo which interacts with downstream signalling components. In addition, none of the phosphorylation sites that are important for *Drosophila*-Smo signalling are conserved in mammalian-Smo (Lum *et al.*, 2003). Human Smo is phosphorylated by G-protein-coupled receptor kinase-2 (GRK2), which leads to the recruitment of β-arrestin 2 (Chen *et al.*, 2004). β-arrestin 2 is necessary for hh signalling in zebrafish (Wilbanks *et al.*, 2004). It is a scaffolding protein that links 7-transmembrane proteins to several cellular responses (Lefkowitz and Shenoy, 2005).

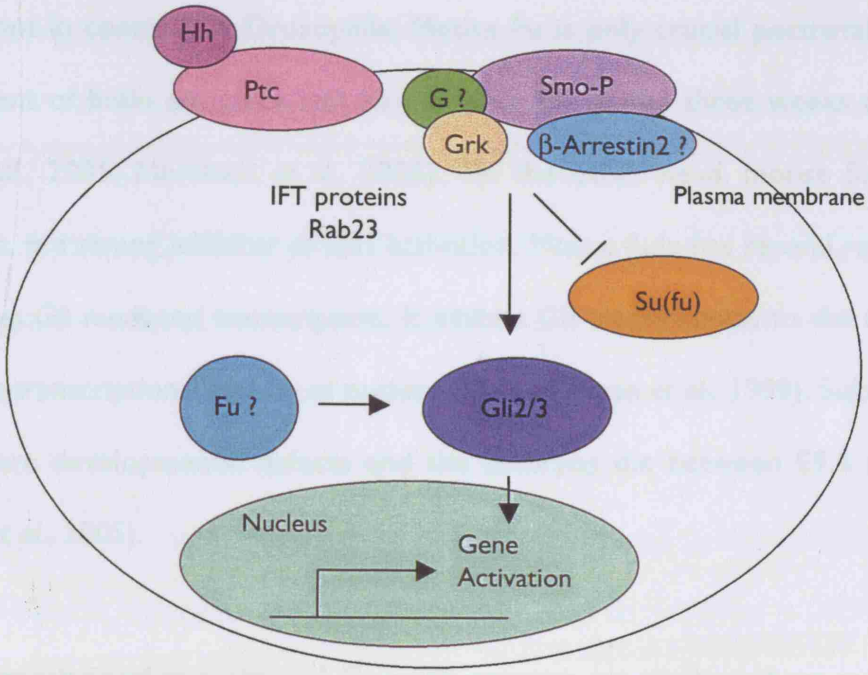

Figure 1.4 Hedgehog signalling in mammals. Stimulation by hh leads to activation of Smo and recruitment of β-Arrestin 2, possibly mediated by the phosphorylation of the Smo C-terminal by Grk2 (Grk). The degree of Fu involvement is not clear and it seems to be dispensable in mammals. Activation of Smo inhibits Sufu and Gli2 and Gli3 activation mediates gene activation – From Osterlund and Kogerman, Trends in Cell Biol. 16,176-180. 2006.

Vertebrate Smo might also link with heterotrimeric G proteins which are associated with other 7-transmembrane proteins. Despite the crucial role of Cos2 in Drosophila Hh signalling, there is no consensus about its mammalian counterpart. In contrast, recent studies have shown that the small G protein Rab23 and intraflagellar transport (IFT) proteins function in hh signalling downstream of mammalian Smo and upstream of Gli (Garcia-Garcia et al., 2005). It has been shown that some Gli2 and Gli3 functions are dependent on IFT proteins and Rab23 is important for suppression of mouse Gli2 activation and processing of mouse Gli3 (Eggrenschwiler *et al.*, 2006). Studies on fused genes revealed that there are significant differences between Drosophila and mouse Fused genes. Recent reports show that the mouse Fu is not required for embryonic development in contrast to Drosophila. Mouse Fu is only crucial postnatally for the development of brain structure and Fu null mice die within three weeks after birth (Chen *et al.*, 2005; Merchant *et al.*, 2005). On the other hand, mouse Sufu, unlike Drosophila, is a strong inhibitor of Gli1 activation. Mouse Sufu has several roles where it influences Gli mediated transcription. It inhibits Gli translocation to the nucleus as well as the transcriptional activity of nuclear Gli (Kogerman *et al.*, 1999). Sufu null mice show severe developmental defects and the embryos die between E9.5 and E10.5 (Cooper *et al.*, 2005).

The post translational regulation of *Ci* and *Gli* proteins are similar, where each resides in the cytoplasm. In the absence of Hh, each is kept in the cytoplasm by Cos2 (KIF7 in Zebrafish and GRK2, b-arrestin2, IFT protein, Rab23 protein in mammals) and Sufu to limit transcriptional activation (Methot and Basler, 2000; Cheng and Bishop, 2002; Merchant *et al.*, 2004). PKA and an SCFE3 ubiquitin ligase (contains SKP1, a member of the cullin family, CUL1, and an F-box containing SKP2 and ring finger protein

ROC1/RBX1) are required by *Ci*, *Gli-3*, and possibly *Gli-2* for the processing to a transcriptional repressor. Individual *Gli* proteins have unique roles; *Gli-3* is mainly a transcriptional repressor, *Gli-2* is mainly a transcriptional activator, and *Gli-1* functions only as a transcriptional activator. Activation of Gli2 and/or Gli3 by Hh often leads to expression of Gli1 that becomes involved in a second wave of activation. Gli1 is not expressed in embryos of Gli2 and Gli3 null mice (Bai *et al.*, 2004) and is not required for development as Gli1 null mice develop normally (Bai *et al.*, 2002).

Hh null mice and their phenotypes

As mentioned earlier, *dhh* null mice were obtained by homologous recombination (Bitgood *et al.*, 1996). In these mice, the structure of the perineurium is severely abnormal and thin (Parmantier *et al.*, 1999). The perineurial cells have a patchy rather than continuous basal lamina, and fail to express the gap junction protein connexin 43 which is normally expressed by perineurial cells. The collagen sheath of the epineurium is also sparse and even absent in some places, whereas there appear to be too many fibroblastic cells within the endoneurium that divide the nerve and form multiple mini-fascicles within the nerve, resembling the mini-fascicles that form in regenerating nerves (Hall, 1989). The permeability of the nerve – tissue barrier to proteins and migratory cells is compromised, and nerve conduction velocity in motor fibres, (saphenous A and C fibres) is on average slightly lowered in *dhh* null mice (Parmantir *et al.*, 1999). The movements of $dhh^{-/-}$ and $dhh^{+/+}$ mice appear indistinguishable when they are running freely (Bitgood and McMahon, 1995). As mentioned earlier, male *dhh* knockout mice are infertile with malformed hypertrophic testes, and abnormalities in the formation of adult-type Leydig cells, peritubular cells and seminiferous tubules (Bitgood *et al.*, 1996; Clark *et al.*, 2000). A similar phenotype, of partial gonadal

dysgenesis with peripheral neuropathy with mini-fascicle formation, has been reported recently in a human patient homozygous for a mutation in the initiation codon of the *dhh* open reading frame (Umehara *et al.*, 2000).

WALLERIAN DEGENERATION AND REGENERATION

Wallerian degeneration is a term used to describe the axonal degeneration and Schwann cell proliferation and de-defferentiation and other events that occur distal to the point of peripheral nerve injury (Terenghi, 1999). Following axotomy, axons in the distal part of the nerve degenerate and this is accompanied by down-regulation of myelin-related genes, de-differentiation and subsequent proliferation of Schwann cells. At the same time NGF, p75NTR, N-CAM, L1, and tenascin-C are up-regulated providing a favourable environment for axonal regeneration (Scherer and Salzer, 2001). During the first week after axotomy, distal axon fragments disappear and myelin breaks down. Myelin debris is partly phagocytosed by Schwann cells, but mainly by macrophages that invade the degenerating nerve (Fernandez-Valle, *et al.*, 1995; Kiefer *et al.*, 2001). The basal lamina persists around the degenerated fibres and comes to surround a column of Schwann cells with an immature phenotype. This structure is referred to as "bands of Bungner" (Scherer and Salzer, 2001). It is still not clear whether Schwann cell de-defferentiation is initiated by active signalling following axonal degeneration or whether it is due to the interruption of the supply of neuronal factors that maintain the myelin phenotype although recent studies favour a process of active signalling. Studies on the slow Wallerian degeneration mouse which is also known as *Ola* mouse have show that myelinated axons remain intact for weeks after axotomy, instead of a few days. These mice also show delayed in Schwann cell proliferation,

macrophage infiltration, down regulation of myelin-related genes, and up-regulation of nerve growth factor (NGF), NGFR/p75 and tenascin-C (Lunn *et al.,* 1989; Thomson *et al.,* 1991; Fruttiger *et al.,* 1995b).

For axonal regeneration to happen, at the proximal site of the injury, axons give rise to one or more sprouts, with a growth cone at the tip which must reach the distal point of nerve stump and once there, will pass through basal lamina and provide the sole pathway for the regenerating axons (Ramon Y Cajal, 1928). Subsequent steps of axon-Schwann cell interactions during nerve regeneration are similar to those during development where initially bundles of axons are surrounded by Schwann cells and eventually segregate to form 1:1 relationship with the larger diameter axons (Scherer and Salzer, 2001). Most of the lipids and cholesterol of the broken down myelin sheath are incorporated into the new myelin sheath by Schwann cells via their lipoprotein receptors (Goodrum and Bouldin, 1996). The presence of macrophages and endoneurial fibroblasts are essential for this process as they are involved in secretion of lipoprotein that contain the recycled cholestrol as well as fatty acids (Goodrum and Bouldin, 1996).

Aims

In a previous study in this laboratory, we demonstrated the existence of a signalling pathway between glia and mesenchymal tissue in peripheral nerve and found that Schwann cell-derived Dhh controls the formation of nerve sheath (Parmantier *et al.*, 1999).

In the present study, my aim is to examine the peripheral nerve of *dhh* null mice (sciatic nerve in particular) further to determine whether the effect of the absence of dhh signalling is confined only to the nerve sheath or whether it has other effects

within the nerve (endoneurium) itself. This would be achieved initially by structural and biochemical examination of sciatic nerves of both wild type and *dhh* null mice.

In particular I aimed to:

1. Determine whether the structure and number of myelinated fibres was normal using immunohistochemistry and electron microscopy
2. Determine whether the morphology and number of unmyelinated fibres was normal.
3. Determine whether the protein composition of the fibres within the nerve was normal, using western blotting and RT-PCR, and whether the molecular and cellular organisation of myelinated fibres was normal.
4. Determine whether there was on-going degeneration and regeneration in injured *dhh* null nerves using electron microscopy and analysis of myelinated fibre profiles.
5. Determine whether macrophages and neutrophil number were normal.
6. Determine whether the endoneurium blood vessels were normal using electron microscopy and permeability tests.
7. Determine whether that rate of degeneration in *dhh* null mice was affected in comparison to the wild types after nerve transection.

CHAPTER 2

MATERIALS AND METHODS

A minimum of two animals per genotype was used for each experiment unless otherwise stated. Since a single copy of *dhh* is sufficient to maintain the normal phenotype (Bitgood *et al.*, 1996; Parmantier *et al.*, 1999; Pierucci-Alves *et al.*, 2001), heterozygous animals were used as controls.

Reagents for molecular biology

Taq DNA-polymerase, RNase H, Reverse Transcriptase (superscript II), dNTPs, 1KB plus ladder, Trizol reagent, Proteinase K and agarose were from Invitrogen (Invitrogen Ltd, Paisley, UK). Glycogen was obtained from Roche Diagnostics (Mannheim, Germany). Ethidium bromide, Tween20, chloroform:isoamyl alcohol 24:1, glycine, trizma base, β-mercaptoethanol, bromophenol blue, and sodium dodecyl sulphate (SDS), were from Sigma (Poole, UK). Random hexamers were from Promega Inc. (Madison, USA). ECL plus kit, western blot stripping kit, and Hybond-N nitrocellulose membrane were from Amersham Pharmacia Biotech (Amersham, UK). Absolute ethanol, isopropanol, methanol, sodium chloride (NaCl), ammonium peroxodisulphate (APS), and glycerol were from BDH Lab Supplies (Poole, UK). Kaleidoscope pre-stained standards were from Bio Rad (Hercules, CA, USA). Diethyl pyrocarbonate (DEPC), and phenol:chloroform:isoamyl alcohol 25:24:1 were from Fluka Chemicals Ltd (Buchs, Switzerland).

Reagents for tissue culture

Dulbecco's modified Eagles medium (DMEM), minimum essential medium (MEM) Ham's F-12 medium, L-15 medium, Hank's balanced salt solution, trypsin, penicillin, and streptomycin were from Invitrogen (Paisley, UK). Foetal calf serum (FCS) was from Bioclear (Calne, UK). Glutamine was from MP Biomedicals Inc (Aurora, Germany). Transferrin, selenium, putrescine, triiodothyronine (T3), thyroxine (T4), Progesterone, insulin, bovine serum albumin (BSA), poly-D-lysine, and laminin were from Sigma (Poole, UK). NDF-b was from R&D systems (Oxford, UK) and collagenase was obtained from Worthington (Lorne Laboratories, Reading, UK). Glucose-D was from BDH and Evans blue from Fluka Chemicals Ltd (Buchs, Switzerland).

Reagents for immunolabelling

Paraformaldehyde was obtained from Fluka Chemicals Ltd (Buchs, Switzerland). Triton X-100 and Hoechst dye H33258 were from Sigma (Poole, UK). Citifluor was from Citifluor Ltd (London, UK). Neutral red solution, DPX mounting medium, and superfrost plus microscope slides were obtained from BDH (Southampton, UK).

Reagents for histology and Electron microscopy

Glutaraldehyde, OCT compound (Tissue Tek), resin (agar, Dodecenyl Succinic Anhydride (DDSA),Methyl Nadic Anhydride (MNA), BDMA-N-Benzyldimethylamine) and embedding moulds were from Agar Scientific (Stansted, UK). Phosphate buffer, uranyl acetate, and propylene oxide were from BDH, osmium tetroxide from Johnson Matthey Chemicals Limited (Royston, UK), Picric acid was from Fluka Chemicals Ltd (Buchs, Switzerland), and Bouin's solution was from Sigma (Poole, UK).

Reagents for in situ hybridisation

Digoxygenin-labeled cRNA antisense probes were generated as described by Parmantier *et al.*, (1999), 4% phosphate-buffered paraformaldehyde, OCT compound (Tissue Tek), 30% sucrose, and superfrost plus microscope slides were from BDH (Southampton, UK).

Animals

Hsd-ICR/CD1 mice were used at postnatal day (p) 3 for Schwann cell purification. Dhh null mice were obtained by homologous recombination (Bitgood *et al.*, 1996), and were from Professor A.P. McMahon (Harvard University). The *dhh* null mutant and wild type mice were on a mixed CD1/C57B16 genetic background. MBP deficient mice (*shiverer*) were obtained from Professor I Griffiths (University of Glasgow Veterinary School). They are on a C3H/101 background. The genotype of all mice was established by PCR on genomic DNA extracted from tail clippings.

Maintenance of transgenic mice

Most of the mice used in this study are derived from a null mutant transgenic line, originally generated by Dr Mark J. Bitgood in the laboratory of Professor Andrew P. McMahon. This transgenic line was created using homologous recombination by removing all of exon 1, 2 and part of exon 3, and replacing them with a neomycin phosphotransferase selection cassette. As a result, no functional protein is produced in mice homozygous for the deletion (Bitgood *et al.*, 1996). Male homozygous mice are viable but sterile due to the absence of mature sperm, and a single copy of *dhh* is sufficient to maintain the normal phenotype (Bitgood *et al.*, 1996).

Generation of Dhh/Shi double mutant mice

MBP null, *shiverer* (*shi*) mice were originally obtained by crossing heterozygous *shi* mice. The offspring were genotyped, and the male *shi* mice were crossed to female *dhh* null mice to generate $dhh^{+/-}/shi^{+/-}$ double heterozygous mice. These mice were then crossed between different litters to obtain $dhh^{-/-}/shi^{-/-}$ double mutant mice (1/16 of offspring). The littermates with phenotypes $dhh^{+/+}/shi^{+/+}$, $dhh^{+/+}/shi^{+/-}$, $dhh^{+/+}/shi^{-/-}$, and $dhh^{-/-}/shi^{+/+}$ were used as controls.

Genomic DNA extraction and genotyping

Tail samples were placed in an eppendorf containing 200 ml of DNA extraction buffer (100 mM Tris pH7.5, 1mM EDTA, 250 mM NaCl, 0.2% SDS) and 8 ml of 10mg/ml proteinase K. They were incubated overnight at 56°C in a water bath. With phenol:chloroform, the next day, the genomic DNAs were vortexed and extracted followed by ethanol precipitation. Each sample was air dried for 10 minutes and re-suspended in 100 ml dH_2O. The samples were either used immediately or stored at –20°C until genotyping could be confirmed.

Genotyping by PCR

1ml of DNA was used for PCR amplification in a standard PCR mix using 1.5 mM $MgCl_2$. The reaction conditions for *Dhh* PCR consist of: 94°C for 3 minutes, followed by 34 cycles of 90°C for 30 seconds, 65°C for 20 seconds, and 72°C for 20 seconds final extension. The primers for *Dhh* were: gDhh1$^{5'}$CCAGGAAGACGAGCACTGGG GTG$^{3'}$; gDhh2$^{5'}$AACTCACTGGCGGTCCGAGCCGG$^{3'}$;gNeo $^{5'}$GGCATGCTGGGGA TGCGGTG$^{3'}$ which produce a single band of 110bp for *Dhh* null mice and a single band of 160 bp for the wild type mice (Parmantier *et al.*, 1999). The reaction conditions for

MBP PCR were: 94°C for 1.5 minutes, followed by 30 cycles of 55°C for 45 seconds, 72°C for 1 minute, 94°C for 45 seconds, followed by hybridisation at 55°C for 1 minute, and extension at 72°C for 5 minutes. Primers in introns flanking exon 6 of the *MBP* gene that is deleted in *Shi* mice were: forward $^{5'}$AGCTCTGGTCTTTCTTGCAG$^{3'}$; reverse $^{5'}$CCCCGTGGTAGGAATATTACATAAC$^{3'}$. Primers on either side of the *shiverer* breakpoint in intron 2 of the *MBP* gene were: forward $^{5'}$CAGGGGA TGGGGAGTCAGAAGTGAG$^{3'}$; reverse $^{5'}$ATGTATGTGTGTGTGTGCTTATCTAGT GTA$^{3'}$. The products are a single band of 380bp unique to *shi* and a single band of ~160bp for the wild type (Gomez *et al.*, 1990).

Immunohistochemistry

Cryostat sections of 10-15 mm were collected on Superfrost Plus microscope slides and air dried for approximately 30 minutes, before fixing in 4% parafomaldehyde in PBS for 10 minutes. Teased nerve preparations were mostly prepared as described by Gould *et al*, (1995). After sacrificing animals, the sciatic nerves were exposed and fixed in situ with fresh 4% phosphate buffered-parafomaldehyde for 30 minutes before dissecting the nerves and transferring them into a bijou containing 4% parafomaldehyde in PBS to post fix them overnight at 4°C. The next day, they were rinsed in 1xPBS, desheathed, and teased into large bundles using fine 27 gauge needles. After teasing, they were either transferred into a 20 mm tissue culture plate for staining with phalloidin labelled with TRITC overnight at 4°C, or directly onto Superfrost Plus slides for further teasing into smaller bundle of fibres. For cx29 staining however, teased nerve preparations were treated slightly differently; after dissecting out sciatic nerves into L15 medium on ice, they were desheathed, teased, and transferred onto the Superfrost Plus slides. They were fixed in 100% ethanol at –20°C for 10 minutes and

rinsed 3 times for 5 minutes in 1xPBS. Teased nerves were then blocked with blocking solutions depending on the antibodies; Cx29: 10% normal goat serum (NGS) and 0.1% Triton X-100 in 1xPBS. For neurofascin (NF155) labelling: teased nerves were treated with Bouin's reagent for 1 minute and rinsed 4 times for 5 minutes in PBS before addition of blocking solution, which was 10% NGS, 0.2% Triton X-100, and 0.1% gelatin in 1x PBS. For MUPP1 nerves were permeabilized in 0.5% Triton X-100 in 1x PBS for 10 minutes before blocking in 10% NGS, 0.1% triton, and 1% glycine; all for one hour at room temperature. Antibodies were diluted in the blocking solution except for NF155 which was diluted in 4% NGS, 0.2% Triton X-100, and 0.1% gelatin and applied overnight at 4°C. The next day the slides were washed three times for five minutes each in 1xPBS and incubated in secondary antibodies for 45 minutes at room temperature. Slides were washed again as before, mounted using Citifluor antifade mountant, and sealed with nail varnish. As control, primary antibody exclusion from a single sample in each experiment was employed to ensure that the second antibody layers used did not cause any non-specific background labelling.

Primary antibodies

Anti neurofascin rabbit polyclonal antibody against neurofascin was a gift from Professor P. J. Brophy, and used at a dilution of 1:100.

Anti MUPP1 rabbit polyclonal antibody against MUPP1 was a gift from Dr E. Peles (Weizmann Institute of Wscience, Rehovot, Israel), and used at a final dilution of 1:100

Anti Cx29 rabbit polyclonal antibody against mouse Cx29 (Zymed Laboratories Inc, South San Francisco, CA, USA) was a gift from Dr C. Meier (Ruhr-University Bochum, Germany), and used at a final dilution of 1:100 (1:1000 for western blotting).

Phalloidin-TRITC toxin binds to F-actin (Sigma, Poole, UK) and was used at a final dilution of 1:100.

F4/80 rat anti-mouse antibody against macrophages (Serotec, Oxford, UK), a gift from Dr Stephen Davis at UCL, was used at a final dilution of 1:500.

GR1-GFP (Ly6-G) antibody (R&D systems, Oxon, UK) to identify neutrophils, a gift from Dr J. Roes was used at a final dilution of 1:300.

Secondary antibodies

Goat anti-rabbit Ig conjugated to fluorescein was from Cappel (Cappel Organon Teknika Corp, PA, USA) and used at a final dilution of 1:600. Goat anti-rat FITC was from Jackson Laboratories (Maine, USA) and used at 1:200. Donkey anti-mouse Ig conjugated to biotin and streptavidin conjugated to fluorescein were from Amersham Pharmacia Biotech (Amersham, UK) and used at 1:100.

Microscopy and quantification

Slides were mounted in Citifluor (Citifluor Ltd, UK) and examined with a fluorescence microscope (Eclipse E800, Nikon). Images were captured with a digital camera (DMX1200, Nikon) and ACT-1 acquisition software (Nikon). For teased nerve analysis, Lucia software (Nikon) was used to capture the image via ACT-1 acquisition software to measure the length of the fibres as well as distances between Schmidt-Lanterman incisures.

Statistical analysis

The statistical significance of data was evaluated using the paired student t-test or the Kolmogorov-Smirnov test.

In situ hybridization

Postnatal day (P) 10 mice were perfused with 4% phosphate-buffered paraformaldehyde for 30 min. The nerves were then removed and fixed for a further 3 hr with fresh 4% paraformaldehyde at 4°C. They were rinsed in PBS, protected in 30% sucrose in PBS overnight prior to mounting in Tissue Tek (sakura-finetek.com). 20 μm frozen sections were mounted on Superfrost slides. The subsequent steps were performed by Professor Mirsky. The sections were prepared for *in situ* hybridization overnight at 65°C using a DIG-labeled antisense probe to *dhh* exactly as described previously (Parmantier *et al.*, 1999). To detect the probe, the background was blocked with 1% fat-free milk in TBST (140mM NaCl, 25 mM Tris-HCl pH 7.5, 5mM levamisole, 0.1% Tween-20) for one hour, before incubation in alkaline phosphatase-conjugated sheep anti-DIG antibody diluted (Amersham, UK) 1:2500 in 1% milk in TBST (Tris-buffered saline containing 0.1% Tween-20) overnight. Before initiating the colour reaction, the tissues were washed thoroughly in PBT (PBS with 0.1% Tween-20) overnight, 20 minutes in TBST with 1-2% Tween-20 and 3 mM levamisole, followed by 10 minutes wash in NTMT (100 mM Tris-Hcl, 100mM NaCl, 50mM $MgCl_2$ pH9.5) before incubation in the colour solution (150 μg/ml nitroblue tetrazolium salt and 75 μg/ml 5-bromo-4-chloro-3-indolylphosphate, toluidinium salt, 100 mM Tris-HCl, 100 mM NaCl, 50 mM $MgCl_2$) in the dark until the colour developed. The reaction was stopped by washes in TE (10 mM Tris, 1 mM EDTA pH 8) buffer. Subsequently, slides were incubated overnight with antibody to human smooth muscle actin, clone 1A4 (1:70) (a gift from L. Morgan, EISAI London Research, London, UK), (dakocytomation.com), then with goat anti-mouse Ig rhodamine for 1 hr (mpbio.com), followed by mouse anti-MBP (1:200) (Sternberger Monoclonals Inc., Baltimore) overnight then by goat anti-mouse Ig fluorescein (jacksonimmuno.com) for 1 hr before

being mounted in Citifluor anti-fade mounting medium (Citifluor, London, UK) prior to examination in an Eclipse 800 Nikon fluorescence microscope.

Western Blotting

Frozen tissues were pulverized, transferred into lysis buffer (25mM tris-HCl, pH 7.4, 95mM NaCl, 10mM EDTA, 2%SDS, 1mM phenylmethylsulphonylfluoride (PMSF) and protease inhibitors), and homogenized with an Ultra-Turrax T8 homogenizer (IKA labortechnik, Staufen, Germany). Protein inhibitor cocktail consists of antipain (0.5μg/ml), pepstatin (0.5μg/ml), amastatin (0.5μg/ml), apoprotein (3U/ml), leupeptin (0.5μg/ml), bestatin (0.5mg/ml), and trypsin inhibitor (0.5μg/ml), all from Roche diagnostics (Mannheim, Germany). The lysates were boiled for five minutes followed by centrifugation for ten minutes, before determination of protein concentration using a Biorad protein assay Kit (Biorad, CA, USA), according to the manufacturer's instructions. Samples (usually 2.5-20 μgs of protein extract) were separated using 8-12% sodium dodecylsulphate polyacrylamide gel electrophoresis (SDS-PAGE) in a mini Protean II gel electrophoresis apparatus (Biorad, CA, USA). Kaleidoscope pre-stained molecular weight standards (Biorad, Hercules, USA) were included for band size identification. Separated proteins were then transferred to a nitrocellulose membrane, Hybond-N, in a mini-gel transfer tank (Biorad, Hercules, USA).

Non-specific binding sites on the membrane were blocked overnight at 4°C using 5% fat free milk powder in PBS/0.05% Tween20. The next day, blocking solutions were replaced with primary antibodies in 1% fat free milk powder dissolved in PBS/0.05% Tween-20, and incubated for one hour at room temperature on a slow rotator (Gallenkamp, UK). The blots were washed in PBS/0.05% Tween20, once for 15 minutes and 3 times, five minutes at room temperature. Following the final wash, the

membranes were incubated with horseradish conjugated secondary antibody diluted in the same solution as the primary antibody and incubated for one hour at room temperature on a slow rotator. The washes were continued as before and the blot was developed with ECL chemoluminescent reagent (Amersham Biosciences Ltd, Amersham, UK). The blots were covered in Saran Wrap film and placed in an autoradiography cassette with intensifying screens (Amersham Biosciences Ltd, Amersham, UK) and visualized by brief exposure to Kodak BioMax MR-1 film. The films were developed after different time exposures, which varied between 15 seconds to 5 minutes, in an X-Ograph Compact X2 automatic developer. This experiment was repeated twice with distal transected nerves and three times with normal nerves.

Primary antibodies for western blotting

Anti protein zero (P0) rabbit polyclonal antibody against rat protein zero was generated and characterized in the laboratory by Louise Morgan essentially as described by Brockes *et al.*, 1980 (Morgan *et al.*, 1991). I purified the antiserum by incubating with chloroform-extracted newborn rat skin for 48 hours, followed by precipitation with caprylic acid and 40% ammonium sulphate. The antibody was used at a final dilution of 1:500.

Anti protein zero (P0) mouse monoclonal antibody against P_0 was a gift from Dr. Juan Archelos (Karl-Franzens-Universitat, Graz, Austria), was used at 1:1000.

Anti MAG mouse monoclonal antibody against myelin associated glycoprotein (Boehringer Mannheim, Mannheim, Germany) was used at 1:1000.

Anti E-cadherin mouse monoclonal antibody against a transmembrane glycoprotein, E-cadherin is localized in the adherens junctions of epithelial cells (BD Biosciences, San Jose, USA) and was used at 1:1000.

Anti MBP mouse monoclonal IgG1 against MBP (Sternberger Monoclonal Incorporated, Lutherville, USA) was used at 1:500.

b-Catenin mouse monoclonal antibody against b-catenin (BD Biosciences, San Jose, USA) was used at 1:1000.

b-Tubulin mouse monoclonal antibody against b-tubulin (Sigma, Poole, UK) was used at 1:500.

Anti TUJ1 rabbit polyclonal antibody against b-tubulin (Covance, Berkeley, CA) was used at 1:1000.

Anti GAPDH mouse monoclonal antibody against glyceraldehyde-3-phosphate dehydrogenase (Abcam Ltd, Cambridge, UK) was used at 1:500.

Primer design

A set of oligonucleotide primers specific for each *mRNA*, usually between 20-25 nucleotides in length, was designed by eye using the sequence information available in the NCBI databases. They were designed in such a way to minimise hairpin structures in individual primers and dimerisation between primer pairs. They were also checked against databases using BLAST software to ensure specificity. The sequence of specific primers that are either designed or used from published literature in this study are listed in table 2.1.

Semi-quantitative Reverse Transcription Polymerase Chain Reaction (RT-PCR)

Total RNA (500ng) was reversed-transcribed in a 50 μl reaction mix containing 20ng random hexamer primers, 1x first strand reaction buffer (50 mM Tris-HCl pH8.3, 75mM KCl, and 3mM $MgCl_2$), 10mM DTT, 0.5mM dNTPs, and 200U reverse

transcriptase (Superscript II) as recommended in the manufacturers protocol (GibcoBRL Life Technologies, Paisley, UK). After incubation for 90 minutes at 42°C, followed by 15 minutes at 70°C, *RNA* was removed by digestion with both RNase H (2U) and RNase A (0.1mg/ml) for 30 minutes at 37°C. The relative amount of cDNA synthesized from each sample was determined by PCR amplification using specific primers for GAPDH mRNA. Equal amounts of cDNA from different samples as well as a water control were used for PCR. PCRs were performed in 50ml reaction volumes containing 1x reaction buffer (20mM Tris-HCl pH8.4, 50mM KCl), 1.5mM $MgCl_2$, 0.5mM dNTPs, 50pmoles of each primer and 2.5U Taq DNA-polymerase. The reaction conditions for each primer pair were optimised with respect to annealing temperature, extension time, concentration of $MgCl_2$, and the number of cycles. PCR reactions were performed in a MWG Biotech Primus96 Thermal Cycler (MWG Biotech, Ebersberg, Germany). Reactions were cycled through one cycle at 94°C for 3 minutes followed by 27-36 rounds at 94 °C for 30 seconds, 30 seconds – 1 minute at specified annealing temperature (Table 2.1), and 30 seconds – 1 minute at 72°C before a final extension time of 5 minutes. Upon completion 10ml of 5x loading buffer (0.25% bromophenol blue, 0.25% xylene cyanol FF, and 30% glycerol in water) was added to each sample and 10ml of each reaction was electrophoresed in a Horizon 58 gel apparatus (BRL-Life Technologies, Gaithersburg, MD) in a 1% agarose gel containing 0.05% ethidium bromide in 1x Tris Acetate EDTA (TAE: 0.89M Tris borate pH8.3 and 20mM Na_2EDTA) buffer. Each RT-PCR preparation was repeated from separate animals three times.

Electron Microscopy (EM)

Homozygous null and control mice from different developmental ages were sacrificed and immediately perfused with 4% paraformaldehyde and 2.5% glutaraldehyde in 0.1M sodium phosphate buffer pH 7.4. The sciatic nerves were dissected out from the mid thigh region, where the number of nerve fascicles is minimal, and post-fixed over night at 4°C. From this point onwards, the preparation was performed by Mark Turmaine in the Electron Microscopy unit in the Anatomy Department at UCL. The next day, samples were rinsed three times for 10 minutes in 0.1M phosphate buffer on ice, and post-fixed in 1% osmium tetroxide (OsO_4) in 0.1M phosphate buffer for 2 hours at 4°C in the dark. They were next washed three times for 10 minutes in 0.1M phosphate buffer followed by three washes for 10 minutes in distilled water. En-block staining was carried out in 1% uranyl acetate in dH_2O for 45 minutes at room temperature in the dark, followed by three times 10 minute washes in dH_2O at room temperature. Samples were dehydrated at room temperature through an ethanol series: five minutes in 30%, 50%, 75%, and 95% ethanol, followed by four times 10 minutes in 100% ethanol and three times 10 minutes in 100% propylene oxide. Tissue samples were mixed and embedded first in 1 part resin to 2 parts propylene oxide for 3 hours and then in 2 parts resin to 1 part propylene oxide for 5 hours. The samples were changed into fresh resin at least twice, each for 8 hours. Finally they were placed in embedding moulds with fresh resin and positioned carefully and cured in an oven at 60°C for 48 hours. Semi-thin sections (1mm), for light microscopy, were cut with a glass knife and stained with toluidine blue. Adjacent thin sections (80-90nm) for electron microscopy, were cut using diamond knife (Diatome) on a Reichert Ultracut E ultramicrotome. These sections were collected on 300 mesh copper grids and formvar coated 2x1 mm slot grids (used for whole nerve counts), counter stained with lead citrate and viewed

in a JEOL 1010 electron microscope. Resin mix were prepared by mixing 20 ml agar 100, 16 ml Dodecenyl Succinic Anhydride (DDSA), 8 ml Methyl Nadic Anhydride (MNA), accelerator, and 1.3 ml BDMA-N-Benzyldimethylamine. They were mixed thoroughly, placed into desiccators and under vacuum for 5-15 minutes to remove gasses from mixture before sectioning could be carried out.

Measurement of myelinated nerve fibre diameter

Dhh null and control mice from postnatal day (p) 30 were sacrificed and perfused as described earlier. Sciatic nerves were dissected out between the mid and the upper thigh region in all mice. They were processed for electron microscopy, and sections were viewed and photographed using a JEOL 1010 electron microscope. Pictures were taken from the lower right hand quadrant of a large transverse nerve section at x2000 magnification, scanned, and imported into Open Lab software where the diameter of myelinated axons and of myelin plus axons was measured. This was used to determine the g-ratio (axon diameter/axon plus myelin sheath diameter). To study the size distribution of axons and of axons plus myelin, the measurements were grouped into increasing size categories separated by 0.1mm, and the number in each category determined.

Quantification of the number of non-myelinated fibres

The sciatic nerves from 2, 4, and 5.5 months old $dhh^{+/+}$ and $dhh^{-/-}$ littermates were prepared for electron microscopy as described previously. The number of unmyelinated axons/Schwann cell unit was counted in one 2 month and one 4 month animal of each genotype and the number of axons in a 1:1, 2:1, etc., ratio was expressed as a percentage of the total number of unmyelinated axons. In addition, the

total number of myelinated and unmyelinated axons in the tibial branch of the sciatic nerve was counted directly in the electron microscope. Nerves from 2, 4, and 5.5 months old *dhh*$^{+/+}$ and *dhh*$^{-/-}$ littermates were counted, a total of 3 nerves for each genotype.

Measurement of endoneurial blood vessel diameter

The sciatic nerves of p30 mice were processed for electron microscopy as before and all the vessels within the endoneurium were viewed and photographed using a JEOL 1010 electron microscope. Pictures were taken from transverse nerve sections at x2000 magnification, scanned, and imported into Open Lab software where the diameter of vessels was measured.

Quantification of the number of myelinated fibres

A montage of the whole transverse section of two normal and two transected sciatic nerves was obtained at x500 magnification to count the total number of myelinated fibres and compare the different categories of myelin profiles in normal and transected nerves.

Investigation of degeneration and regeneration in uninjured sciatic nerve

Sciatic nerves from three different aged mice were processed for electron microscopy except for the 21 month old nerves, which were processed by my collaborator Dr Fujio Umehara (Kagoshima University, Dental School, Japan). Montages of the whole transverse section from each sciatic nerve were obtained at x500 magnification and the numbers of degenerated fibres were counted and compared with the number of

normal myelinated fibres. Degenerated fibres were then identified at higher magnification i.e. <10K for confirmation of their profile.

Measurement of endoneurial blood vessel permeability

The permeability of endoneurial blood vessels (capillaries) was tested using Evans blue solution. 5% bovine albumin was mixed with 1% Evans blue in Hanks' balanced salt solution and dialysed against Hanks' solution overnight at 4°C. The following day, the tracer was filtered and 1ml /kg body weight of mice was injected into the jugular vein of anaesthetised mice. The tracer was left to circulate for 30 minutes and 3 hours before the mice were sacrificed and the sciatic nerve and the brain from each animal were fixed with 4% paraformaldehyde in 0.1M phosphate buffer, sectioned and viewed under the fluorescence microscope.

Peripheral nerve injury experiments

All the experiments where animals were involved were performed following the UK Home Office guidelines.

Sciatic nerve transection

Two months old control and transgenic mice were anaesthetised with halothane and the left sciatic nerve was exposed at mid thigh level. The sciatic nerve was cut and the distal end diverted to limit the possibility of re-ligation. Resulting wounds were sutured with 3/0 black polyamide monofilament, mersilk (Johnson & Johnson Intl, Brussels, Belgium). Two days following transection, the mice were sacrificed and both the distal stump of the transected sciatic nerve and the contralateral control nerve were either

excised, snapped frozen and immediately processed for protein extraction or processed for electron microscopy.

Isolation and culture of Schwann cells

Schwann cells were prepared essentially using the method of Brockes and Raff, (1979). Postnatal mice at 3 days of age (p3) were killed by decapitation and the sciatic nerves were removed using microsurgical instruments and a dissecting microscope. Nerves were transferred into a 35mm tissue culture dish containing L15 medium and kept on ice. The perineurial sheath was removed and the cells were allowed to dissociate by incubation in DMEM containing 0.25% trypsin with 0.4% collagenase at 37°C and 5%CO_2 for 35 minutes. The cells were triturated and then diluted in DMEM with 10% foetal calf serum (FCS) followed by centrifugation for 10 minutes at 1000 rpm and 4°C. The pellet was resuspended in defined medium (DM), and Schwann cells were then purified by immunopanning using antibodies to Thy-1 (Dong *et al.*, 1999), and plated on a 35mm poly-D-lysine (PDL)/ laminin (20 mg/ml) coated tissue culture dishes for 24 hours before addition of hedgehog proteins or analogues.

Defined Medium (DM) contained 1:1 Hams F12/DMEM supplemented with 100mg/ml glutamine, 0.03% bovine serum albumin (BSA), 100mg/ml transferrin, 16mg/ml putrescine, 38ng/ml dexamethasone, 60ng/ml progesterone, 400ng/ml thyroxine (T4), 5ng/ml insulin (low insulin) or 5mg/ml (high insulin), 10ng/ml triiodothyronine (T3), 160ng/ml selenium and 100U/ml each of penicillin/ streptomycin.

Immunopanning

P3 nerve Schwann cells from mouse sciatic nerves were purified by immunopanning using antibodies to Thy1.1 as described in Dong *et al.*, (1997). Two 90mm tissue

culture plates were used and coated with anti-rat IgG at a final concentration of 50-60mg/ml in 7 ml 50 mM tris pH9.5 and incubated at 4°C overnight. The next day, anti-rat IgG solution was removed and the plates were rinsed three times with PBS. T24 solution was prepared by mixing 4.5 ml of T24 monoclonal antibody to Thy1 (The Salk Institute, San Diego, USA) supernatant, 2 ml MEM Hepes buffer, plus 400 ml 35% BSA and added to the plate. After one hour at room temperature T24 solution was removed and the plates were rinsed three times in PBS. The Schwann cells, dissociated from the sciatic nerves as described previously, were resuspended in 7-8 ml DM and transferred to the Thy1.1 coated plates. The plates were incubated at 37°C for 15 minutes followed by three vigorous shakes before being returned to the incubator for a further 15 minutes. The plate was shaken once more and the cell suspension was transferred to another coated plate and the two previous steps were repeated. The cell suspension was then collected, spun, and plated on to a 35mm PDL and laminin coated tissue culture plate in DM with low insulin (Dong *et al.*, 1999), D-glucose (1:100 of 50% solution) and 10ng/ml neuregulin-β1 (R&D Systems). 24 hours prior to the experiment the Schwann cell medium was changed to DMEM and 10% foetal calf serum (Bioclear, Calne, UK). The panning dishes containing fibroblasts were also incubated with DMEM and 10% foetal calf serum (Bioclear, Calne, UK). Cells were then treated either with Dhh protein (a gift from biogen.com at 40nM) or with the Hedgehog pathway agonist Cur-0199567 (40nM) (a gift from Dr L Rubin, Curis Inc., Cambridge) (Frank-Kamenetsky *et al.*, 2002) for 3 hours and 24h followed by *RNA* extraction as described above.

Measurement of motor neuron cell body size and numbers

P30 mice were perfused with 4% paraformaldehyde, 4% picric acid and 0.15M phosphate buffer. The spinal cord was exposed and the tissue from lumbar (L) levels 4-L5 was further dissected and post fixed for 1 hour. Segments were washed in 0.1M phosphate buffer before overnight incubation in 30% sucrose/PBS at 4°C. 40mm sections were cut transversely on a freezing microtome and transferred individually into wells of a 96 well plate containing 0.1M phosphate buffer, 5% sucrose and 0.025 sodium azide. The sections were transferred on to gelatinised slides and allowed to dry for 24 hours before 4-6 minutes immersion in Neutral Red solution (0.5% in 1% acetic acid). Sections were rinsed, dehydrated and mounted in DPX mounting medium and observed at x20/x40 in a Nikon Eclipse 800 microscope. They were analysed in two different ways; first, the number of motor neurons in each lumbar segment was counted, second, images of sections were captured using a digital camera and AKT software (Nikon), and the area of the cell soma of individual motor neurons was measured using Open Lab software.

Table 2.1, Sequence of RT-PCR oligonucleotide primers

Target molecule	Primer sequences	Annealing temp.	Expected size/bp	PCR cycles
MBP-for -rev	5'ACTCACACACGAGAACTACCCA3' 5'CCAGCTAAATCTGCTGAGGG 3'	62°C	169	0030
MAG-for -rev (Nicholson et al. 2001)	5'GGAGACCTGGGC CTACGAAA3' 5'GACGTCCAAACTGGCGTAAC3'	62°C	442	30
Cx32-for -rev (Nicholson et al. 2001)	5'TACGTGGCGTGAATCGGCAC3' 5'GTTGGTGAGCTACGTGCATT3'	62°C	266	30
S100-for -rev	5'GGTGACAAGCACAAGCTGAA3' 5'CTGGAAGTCACACTCCCCA3'	62°C	150	30
Cld5-for -rev (Poliak et al.,2002)	5'GAAGGGGCTGTGGATGTC3' 5'ACCGTCGGATCATAGAAC3'	54°C	314	36
JAM2-for -rev	5'GTCGCACAGATGTGTTTGG3' 5'GAGTTCACATGGAAAGAGG3'	55°C	327	30
JAM3-for -rev (Sohl et al.,2001)	5'TTGGTCTACTACCAACAGG3' 5'TTTCGTGTTCATTGTGTACG3'	55°C	369	30
Cx29-for -rev (Sohl et al.,2001)	5'ATGTGCGGCAGGTTCCTGAGACA3' 5'TCAAA ATGGCTCTTTTGCCTCCA3'	55°C	777	30
E-Cad-for -rev	5'GAAAGGACTTAGAGATTGGCG3' 5'CTGCCTTCAGGTTTTCATCG3'	55°C	488	30
Ptc1-for -rev (Takabatake et al., 1997)	5'AACAAAAATTCAACCAAACCTC3' 5'TGTCTTCATTCCAGTTGATGTG3'	55°C	244	36
Ptc2-for -rev	5'TGCCTCTCTGGAGGGCTTCC3' 5'CAGTTCCTCCTGCCAGTGCA3'	55°C	208	36
Gapdh-for -rev (Clontech)	5'ACCACAGTCCATGCCATCAC3' 5'TCCACCACCCTGTTGCTGTA3'	63°C	451	27

CHAPTER 3

INTODUCTION

Dhh signalling controls the number of SLI in myelinated Schwann cells

It is commonly believed that signals from glial cells play an essential part in establishing and maintaining the structural and functional integrity of the nervous system. Nevertheless, it has proved hard to identify particular signalling molecules that carry out such functions in vivo and to define the consequences of their absence. I have addressed this issue by examining the Schwann cell-derived signalling molecule *dhh* in peripheral nerves. It has been shown previously that *dhh* is required for the correct formation of the connective tissue sheaths around peripheral nerves (Parmantier *et al.*, 1999).

It has been suggested that SLI play a role in myelin formation and although there is not enough information to support this conclusively. MBP-deficient *shi* mice certainly suggest an indirect role for myelin genes in SLI formation. It has been documented that the length from the node to the nearest incisure is greater than the length between two incisures in fibres of all diameters. Furthermore, the microfilament components, F-actin and spectrin co-localize with MAG in periaxonal membrane, SLI, paranodal loops, and inner and outer mesaxons of myelinating Schwann cells. This suggests that Schwann cell spectrin participates in linking F-actin to plasma membranes (Trapp *et al.*, 1989b). There has also been a suggestion that incisures can rapidly form and migrate along internodes, but this translocation has yet to be confirmed as they can dilate and contract in hypotonic or hypertonic environments (Hall and Williams, 1970).

The number of SLI is elevated in *dhh*$^{-/-}$ Schwann cells

Teased nerve fibre preparations were previously used to show that in postnatal nerves, *dhh* is selectively expressed by myelinating Schwann cells (Parmantier *et al.*, 1999). We confirmed this finding using in situ hybridization on transverse sections of P10 sciatic nerve as this allows visualization of other cellular components of the nerve, including blood vessels and the perineurium, both of which were essentially negative (Fig. 3.1 A, B, C).

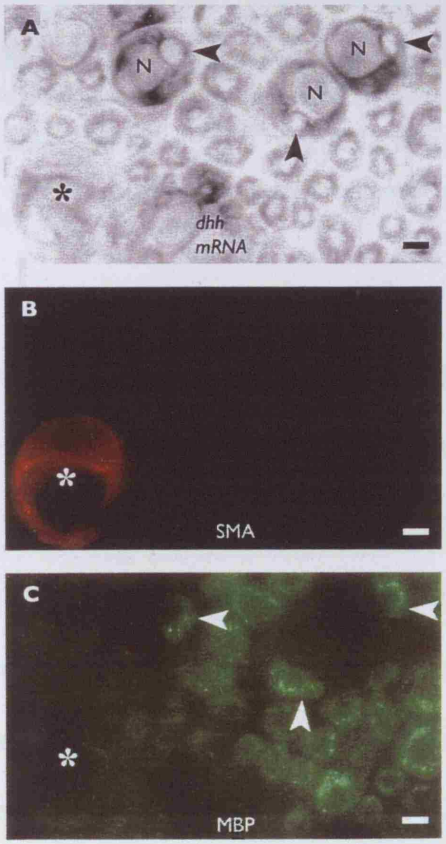

Figure 3.1 *Dhh* mRNA is selectively expressed in myelinating Schwann cells. The same field from a transverse section of a P10 sciatic nerve is shown in **A** (bright field to visualize *dhh* mRNA by *in situ* hybridization), **B** (immunofluorescence using antibodies to smooth muscle actin to visualize blood vessels) and **C** (immunofluorescence using antibodies to MBP to visualize myelin).

(A) Unambiguous Dhh signal is only seen where the section cuts through the nuclei (N) of myelinating cells displacing the myelin sheath (arrow heads) to an eccentric position. (B) The field contains one capillary (asterisk) visualized by SMA antibodies. (C) Myelin sheaths associated shown by MBP antibodies. Myelin sheaths associated with Schwann cell nuclei that are labelled for *Dhh* mRNA (arrow heads).
Scale bars, 4μm.

To investigate the effect of *dhh* on the general architecture of myelinated fibres, nerves were taken from $dhh^{+/-}$ and $dhh^{-/-}$ mice at P10, 23, 30 and 8 months old (n=2 for each genotype at each age). They were fixed, teased and stained with fluorescein-conjugated phalloidin, which binds to F-actin and clearly demarcates Nodes of Ranvier, paranodal loops and SLI (Trapp *et al.*, 1989a; Gould *et al.*, 1995). We found a marked increase in the number of SLI (Fig 3.2 A, B), while the phalloidin labelling in the paranodal and nodal area of the Node of Ranvier appeared normal (not shown). The number of SLI/100 μm at P10, 23 and 30 was more than twice that seen in $dhh^{+/-}$ fibres (Table 3.1).

Figure 3.2 Teased nerve fibres of $dhh^{-/-}$ mice show increased numbers of SLI. Phalloidin-TRITC labelling of SLI, **A**: in a $dhh^{+/-}$ nerve fibre; **B**: in a $dhh^{-/-}$ nerve fibre, showing an increased number of incisures. Some SLI are indicated by arrows. Scale bars, 10μm.

The fibre width, distance between SLI, and the number of SLI in $dhh^{+/+}$ and $dhh^{+/-}$ mice were similar in all ages, showing that a single copy of *dhh* is sufficient to maintain the normal SLI phenotype. Because the number of SLI was increased, the distance between SLI was decreased (Table 3.1). Measurement of the width of teased nerve fibres showed that the fibre width was comparable in all three genotypes, with a tendency to thinner fibres in $dhh^{-/-}$ animals (see below). When visualized by phalloidin labeling, the gross morphology of SLI in $dhh^{-/-}$ nerves differed from that of normal nerves. Whereas the majority of SLI in normal fibres were relatively simple structures, those in $dhh^{-/-}$ fibres were frequently broader and more complex, often consisting of closely spaced doublets

(Fig. 2A, B). Similar observations were made in *shi* mice, where the number of SLI is also increased as a result of lack of MBP (Gould *et al.*, 1995).

	P10		P23		P30	
	$dhh^{+/-}$	$dhh^{-/-}$	$dhh^{+/-}$	$dhh^{-/-}$	$dhh^{+/-}$	$dhh^{-/-}$
Fiber width (μm)	5.6±0.13	5.2±0.11	7.5±0.17	7.4±0.15	8.1±1.1	7.4±0.78
Dist. between SLI (μm)	37.9±1.86	20.9±1.1*	41.2±2.33	21.2±0.9*	40.6±1.6	18.4±0.8*
SLI / 100 μm	2.6±0.9	4.8±0.6*	2.4±0.2	4.7±0.6*	2.5±0.1	5.4±0.5*

Table 3.1 The number and frequency of SLI in $dhh^{-/-}$ and control nerves. At all ages, the number of SLI/100μm in $dhh^{-/-}$ fibres is about double that seen in $dhh^{+/-}$ nerves. The distance between SLI is also smaller in $dhh^{-/-}$ fibres compared with controls. (*) indicates significant difference from same age control $p<0.005$ (student t-test). There is no significant difference in fibre width between $dhh^{+/-}$ and $dhh^{-/-}$ nerve fibres. All data are represented as mean ± standard Error (SE).

Electron microscopic analysis shows a decreased number of large fibers in $dhh^{-/-}$ mice

To test whether the absence of *dhh* changed other structural features of myelinated fibers, electron micrographs from the sciatic nerves of $dhh^{+/+}$, $dhh^{+/-}$, $dhh^{-/-}$ mice (n=3 per genotype) were scanned and the diameter of axons and axons plus myelin of over 1000 fibers for each genotype was measured. We found that the number of larger diameter myelinated axons was reduced in $dhh^{-/-}$ mice compared with $dhh^{+/-}$ mice (Fig. 3A). In these nerves, the number of axons between 6.0 and 7.5 μm in diameter was significantly reduced (P=0.024 Kolmogorov-Smirnov test) and the larger axons were

absent. There was also a trend towards increased numbers of small myelinated axons in the *dhh*$^{-/-}$ animals, although this was not statistically significant. There was no significant difference between any of the genotypes in the average diameter of axons plus myelin (Fig. 3B), although there was a trend towards smaller diameters in *dhh*$^{-/-}$ nerves. This is in line with our previous light microscopic observations on myelinated units in *dhh*$^{-/-}$ and *dhh*$^{+/+}$ nerves (Bajestan *et al.*, 2006).

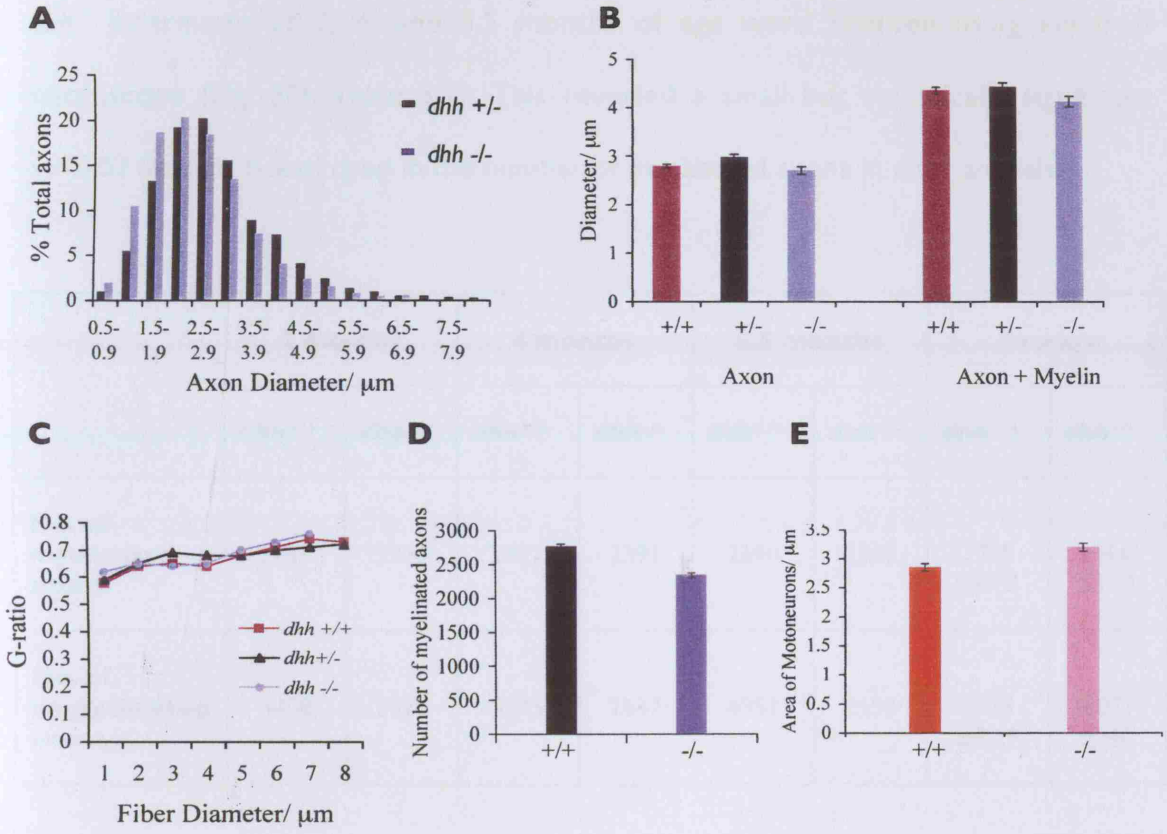

Figure 3.3 Analysis of myelinated fibre diameters and motor neuron cell body size. **A**: Axon diameters in *dhh*$^{+/-}$ and *dhh*$^{-/-}$ nerves; note that myelinated fibres of the largest diameter are absent in *dhh*$^{-/-}$ nerves (n=3 per genotype). **B**: Average diameters of *dhh*$^{+/+}$, *dhh*$^{+/-}$, and *dhh*$^{-/-}$ axons and myelinated profiles are similar, although the *dhh*$^{-/-}$ myelinated profiles are slightly but not significantly smaller (n=2 per genotype). **C**: The g-ratio for each fibre size is similar in all three genotypes. **D**: Counts of the total number of myelinated axons in the tibial nerve of *dhh*$^{+/-}$ and *dhh*$^{+/-}$ mice show that axon numbers are reduced in *dhh*$^{-/-}$ mice (see Table 3.2). **E**: A comparison of the area of motor neuron cell bodies (MN) in the spinal cord of *dhh*$^{+/-}$ and *dhh*$^{+/-}$ mice (n=2 per genotype). The difference between the genotypes is not significant.

There were no significant differences in the g-ratios of myelinated axons between *dhh*$^{+/+}$, *dhh* $^{+/-}$, and *dhh*$^{-/-}$ nerves at any diameter. This accords with previous light microscopic measurements of average g-ratios in *dhh*$^{+/+}$ and *dhh*$^{-/-}$ mice (Bajestan *et al.*, 2006), indicating that although there are more incisures in *dhh*$^{-/-}$ nerves, the myelin thickness in most individual axons remains unaltered (Fig. 3C). To determine whether the total number of myelinated axons was altered in the absence of *Dhh*, the total number of myelinated axons in tibial branch of the sciatic nerve in one pair of *dhh*$^{+/+}$ or *dhh*$^{-/-}$ littermates at 2, 4, and 5.5 months of age were counted using electron microscope (Fig. 3D, Table 3.2). This revealed a small but statistically significant ($p<0.02$ Student t-test) drop in the number of myelinated axons in *dhh*$^{-/-}$ animals.

	2 months		4 months		5.5 months		Average	
	***dhh*$^{+/+}$**	***dhh*$^{-/-}$**	***dhh*$^{+/+}$**	***dhh*$^{-/-}$**	***dhh*$^{+/+}$**	***dhh*$^{-/-}$**	***dhh*$^{+/+}$**	***dhh*$^{-/-}$**
No. of myelinated axons	2783	2280	2822	2391	2690	2363	2765 ±67.8	2344* ±57.7
No. of unmyelinated axons	4408	3026	4245	2847	4353	2550	4335 ±82.9	2807** ±240

Table 3.2 The total number of axons in the tibial branch of the sciatic nerve. In *dhh*$^{-/-}$ nerves, the number of myelinated axons is moderately reduced but the number of unmyelinated axons is reduced by a third. (*) indicates significant difference from the *dhh*$^{+/+}$ control nerve, $p<0.02$. (**) indicates significant difference from the control nerve, $p<0.005$ (Student t-test).

Motor neuron number and cell body size are unchanged in *dhh*$^{-/-}$ mice

The largest diameter axons within the sciatic nerve include those of motor neurons. We therefore investigated whether the observed loss of large diameter axons in *dhh*$^{-/-}$ nerves was due to a loss or change in the size of the motor neurons.

The number and average area of the cell body of motor neurons were compared, as judged by Neutral Red staining, in the L4/5 region of the spinal cord where the largest motor neurons are located (Fig. 3.3E). There was no significant difference in the average size of the motor neurons between *dhh*$^{-/-}$ and *dhh*$^{+/-}$ mice. The average number of motor neurons in the two genotypes was also similar (22.1±1.15 in *dhh*$^{+/+}$ and 23.5±0.86 in *dhh*$^{-/-}$).

Non-myelinating Schwann cells are affected in *Dhh*$^{-/-}$ nerves

In transverse sections of *dhh*$^{-/-}$ nerves, an unusually large number of unmyelinated axons in a 1:1 ratio with a single Schwann cell were observed, while non-myelinating Schwann cells containing large numbers of axons were seldom seen (Fig. 3.4A).

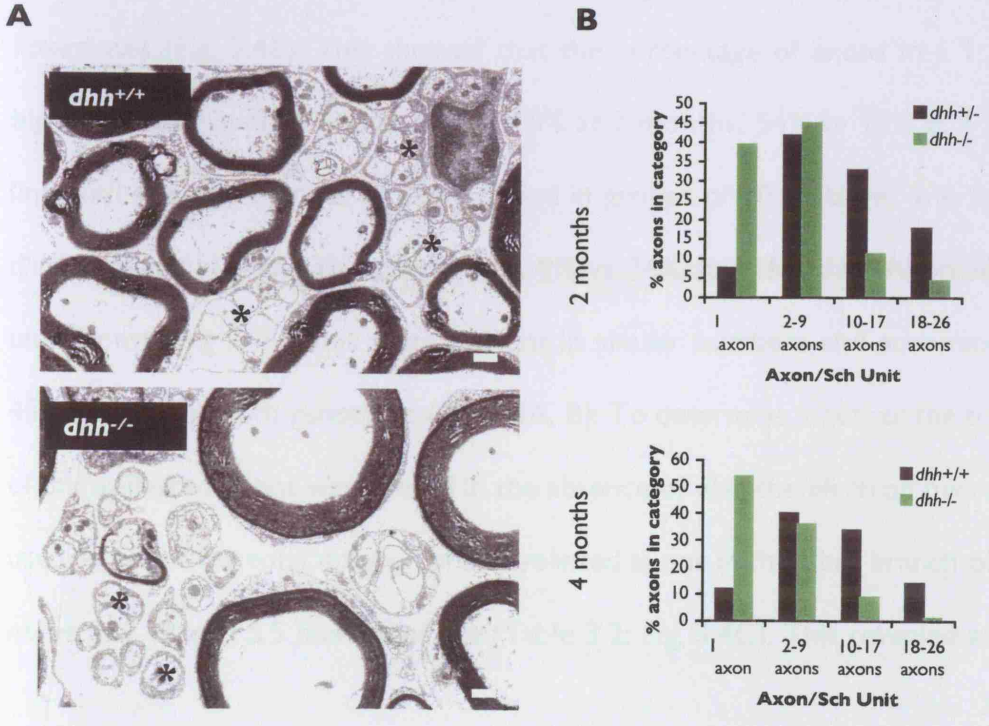

C

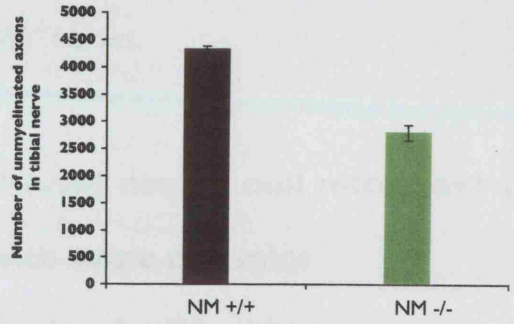

Figure 3.4 **A**: Electron migrographs showing transverse sections of the sciatic nerve of 2 month old mice., illustrating a typical difference in appearance of non-myelinating Schwann cells in *dhh*$^{-/-}$ and *dhh*$^{+/+}$ animals. A few unmyelinated axons are indicated by star. Scale bars, 1μm **B**: The percentage of the total number of small unmyelinated axons that is found in a 1:1 ratio, ratios of 1:2-9 etc., with a non-myelinating Schwann cell in nerves of 2 and 4 month old *dhh*$^{+/-}$ and *dhh*$^{-/-}$ mice. Note the marked increase in the percentage of axons in a 1:1 ratio with a Schwann cell at both ages in *dhh*$^{-/-}$ nerves, and the decrease in the Schwann cell units containing large numbers of axons (*n*=3 per genotype). **C**: Counts of the total number of unmyelinated axons in the tibial nerve of *dhh*$^{+/+}$ and *dhh*$^{-/-}$ mice show that axon numbers are substantially reduced in *dhh*$^{-/-}$ mice (Table 3.2).

This was confirmed by counting the number of unmyelinated axons in a 1:1, 1:2 etc., ratio with Schwann cells in transverse sections of the tibial branch of the sciatic nerve from 2 month old *dhh*$^{-/-}$ and *dhh*$^{+/-}$ littermates and 4 month old *dhh*$^{-/-}$ and *dhh*$^{+/-}$ littermates (Fig. 3.4B). This showed that the percentage of axons in a 1:1 ratio was highly elevated in *dhh*$^{-/-}$ nerves (39% vs 8% at 2 months, 54% vs 12% at 4 months). In line with this, the number of axons found in groups of 10 or larger was lower in the *dhh*$^{-/-}$ nerves (11% vs 33% at 2 months, 9% vs 34% at 4 months). Axon/Schwann cell units containing 2-9 axons were present in similar numbers and accommodated 40-45% of axons in both genotypes (Fig. 3.4A, B). To determine whether the total number of unmyelinated axons was altered in the absence of *dhh*, the electron microscope was used to count the total number of unmyelinted axons in the tibial branch of the sciatic nerve at 2, 4, and 5.5 months of age (Table 3.2; Fig. 3.4C). This revealed a statistically

significant difference ($p<0.005$ Student t-test) in the number of unmyelinated axons in $dhh^{-/-}$ nerves.

dhh/shi double null mice have increased numbers of SLI compared with single null mice

The fact that SLI numbers are increased in both *dhh* and *shi* (MBP) mutants led us to ask whether these conditions were linked. To investigate this genetically, we crossed *dhh* null mice with *shi* mice to obtain mice that were null for both *dhh* and *MBP*. We reasoned that if dhh and MBP acted along an identical pathway to control SLI, there should be little or no increase in the number of SLI in the double mutants when compared with the single mutant mice. On the other hand, if *dhh* and *MBP* were components of two relatively independent and parallel mechanisms, the number of SLI should be further increased. Eleven double null mice were obtained.

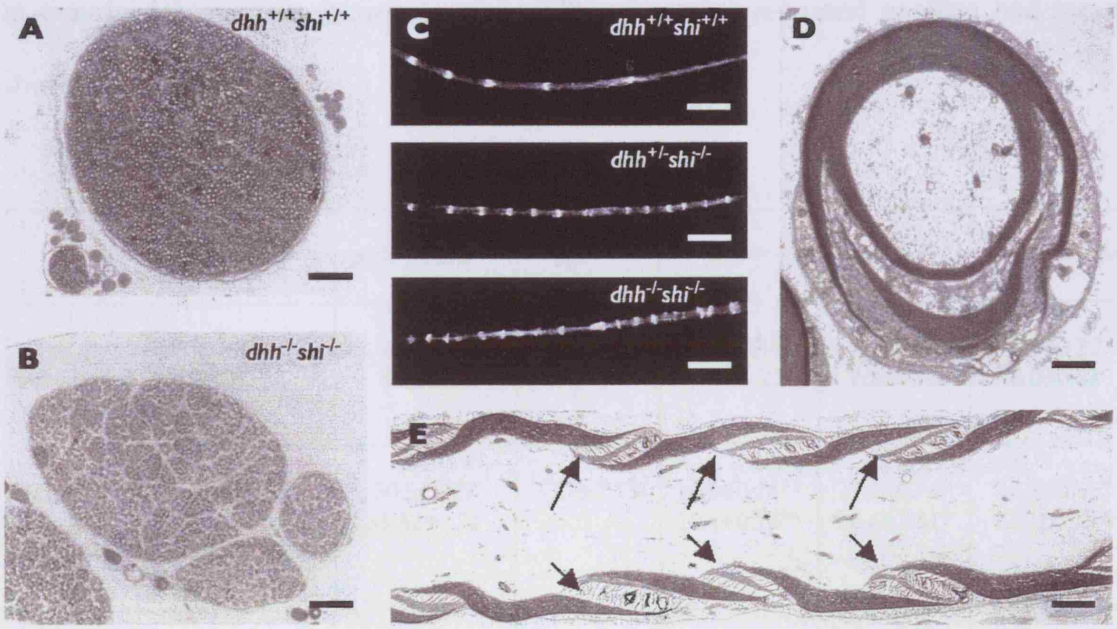

Figure 3.5 $dhh^{-/-}shi^{-/-}$ double null sciatic nerves have increased numbers of SLI. Semi-thin toluidine blue stained sections (x20) of **A**: wild type and **B**; $dhh^{-/-}shi^{-/-}$ nerves. Scale bars, 70μm. Note the arrangement of the double null nerve into mini-fascicles, a phenotype typical of $dhh^{-/-}$ null nerves; **C**: teased

preparations of wild type, double heterozygous and double null nerves from 15 weeks old mice, labelled with phalloidin-TRITC to label SLI. The double null nerve fibres have many more SLI than the wild type one. Scale bars, 66 μm **D**: Electron micrograph showing a complex SLI in a transverse section of double null nerve. Scale bar, 0.9 μm. **E**: Electron micrograph of multiple SLI in a double mutant nerve shown in longitudinal section. Scale bar, 0.7 μm.

Four were used to make teased nerve preparations and for electron microscopy. It was found that the number of SLI was substantially greater in *dhh/shi* double null nerve fibres than either of the single null mice and that, consequently, the distance between incisures was reduced further in the double knockouts (Fig. 3.5C; Table 3.3). As a further measure of myelin disruption, electron micrographs of transversely sectioned nerves were used (Appendix 1-3) to compare the number of continuous, undisrupted compact myelin profiles (sheaths) in normal, single and double null mice with the total number of myelinated fibers, which included profiles that contained incisures or nodal structures (Table 3.4). We found that 92% of the total myelinated axon profiles in normal mice had intact sheaths, while the corresponding figure was 74% in $dhh^{-/-}$ mice. In the double mutants, however, only 22% of total myelinated profiles had intact sheaths.

	$dhh^{+/+}/shi^{+/+}$	$dhh^{+/-}/shi^{+/-}$	$shi^{+/-}$	$shi^{-/-}$	$dhh^{-/-}$	$dhh^{-/-}/shi^{-/-}$
Fiber diameter (μm)	7.4±0.16 9.0±0.26	7.0±0.13 8.9±0.22	7.0±0.15	7.1±0.15 8.4±0.27	7.4±0.15 9.2±0.19	6.9±0.20 8.0±0.23
Distance between SLI (μm)	41.3±2.17 51.6±2.68	30.5±1.27 35.62±1.71	35.3±2.13	18.5±0.74** 20.4±0.74**	21.2±0.94* 26.6±1.61*	14.8±0.66* 13.2±0.35**
SLI/ 100μm	2.4±0.18 2.0±0.1	3.3±0.14 2.8±0.15	2.8±0.74	5.4±0.3* *4.9±0.73*	4.7±0.6 3.8±0.26**	6.8±0.3* 7.6±0.2**

--- 3 weeks --- 15 weeks

Table 3.3 The number of SLI in double mutants. Nerve fibre analysis of the sciatic nerves of indicated genotypes at 3 weeks (blue letters) and 15 weeks of age (n=2 for each genotype at each time point). Note that double null nerves have a greater number of SLI than either *dhh*$^{-/-}$ or *shi*$^{-/-}$ nerves. (*) indicates significant difference from the control nerve at $p<0.002$. (**) indicates significant difference from the control nerve at $p<0.0005$.

This measure of myelin compactness shows a larger difference between *dhh*$^{-/-}$ nerves and *Dhh/shi* double mutant nerves than is evident from counts of SLI numbers (Table 3.3). This suggests that SLI are not only more numerous, but also larger in the *dhh/shi* double mutants. This is in line with the observation that in double mutant nerves, profiles of SLI were more elaborate than in normal fibers as discussed above (see Fig. 3.2) (Fig. 3.5D). Together, these results suggest that *dhh* and MBP control SLI numbers by distinct and relatively independent mechanisms. The intermediate number of SLI in *shi*$^{+/-}$ mice between the wild type and *shi*$^{-/-}$ mice which previously reported, was also confirmed (Smith-Slatas and Barbarese, 2000). Toluidine blue semi-thin sections revealed that the nerves of the double null mice, like those of *dhh*$^{-/-}$ mice, were arranged in mini-fascicles (Fig. 3.4B).

		***dhh*$^{+/+}$/*shi*$^{+/+}$**	***dhh*$^{-/-}$**	***dhh*$^{-/-}$/*shi*$^{-/-}$**
Total number of myelinated axons counted	**Animal 1**	4332	4042	4112
	Animal 2	4071	2323	4323
	AV.	4202	3183	4218
Number of compact myelin profiles	**Animal 1**	4042	3155	1010
	Animal 2	3808	1875	785
	AV.	3925	2515	898
% of compact myelin profiles	**Animal 1**	93	78	25
	Animal 2	94	81	18
	AV.	94	80	22

Table 3.4 The frequency of compact myelin profiles in single and double mutants. Analysis of the number of compact myelin sheaths versus the total number of myelin profiles (including profiles containing SLI or nodes) in transverse electron micrograph sections of wild type, *dhh*$^{-/-}$, and double null nerves (n=3 per genotype). Note the decrease in the number of intact myelin sheaths in the *dhh*$^{-/-}$ nerve and even sharper decrease in the double null nerve when compared with wild type nerve.

The remaining 7 double null mice all died between 4-16 weeks, indicating a shortened life span compared with *shi* mice, which normally do not live past 1 year of age (Peterson and Bray, 1984). Mice that were 6 weeks or older in age had a more pronounced *shi* phenotype than *shi*$^{-/-}$ mice, indicating a possible involvement of *dhh* in CNS myelination.

DISCUSSION

The above results indicate the importance of *Dhh* signaling not only in the formation of nerve sheaths around the sciatic nerve (Parmantier *et al.*, 1999), but also within the nerve itself. Here, I have demonstrated that *dhh* is involved in controlling the number of SLI within the myelinating fibres. The mechanism by which increased number of SLI are formed in *dhh*$^{-/-}$ animals is not clear, but because they are cytoplasmic channels that are likely to be involved in transporting small molecules between the outer part of the myelinating Schwann cell and the inner adaxonal part, it may suggest that they are either responding to increased trafficking of small molecules, or malfunctioning of existing SLI. It may also be speculated that increase in SLI is a part of a more general response of myelinating cells to stress, since in *dhh*$^{-/-}$ animals these cells have less protection from vascular (Chapter 5) and perineurial (Parmantier et al., 1999) diffusion barriers. The possible involvement of MBP in this process was not confirmed, as we have shown that SLI number in MBP and *dhh* null mice are controlled, at least initially, by two independent mechanisms.

The lack of large diameter axons in *dhh*$^{-/-}$ nerves was interesting, and I can only speculate about what the reason could be. The most obvious suggestion would be that the larger myelinated fibres are more vulnerable to the lack of Dhh signalling and are therefore more susceptible to degeneration than the smaller diameter fibres. Subsequently some of the axons that demyelinate and degenerate may regenerate. Regeneration results in thinner myelin sheaths which might shift the average fibre diameter slightly towards smaller diameters, as is in fact seen in Fig3.3. Alternatively, the lack of Dhh might mean that fibres of the largest diameter are never generated during the initial myelination period. Further experiments, perhaps using conditional knockouts could resolve this point.

The slight reduction in the total number of myelinated fibres in the tibial nerve at 2, 4, and 5.5 months suggest that more fibres degenerate than regenerate. In wild type mice degeneration of fibres is normal as mice age (Ceballos *et al.*, 1999; Kanda *et al.*, 1991), and the earlier degeneration seen in *dhh* null mice might suggest that in some unknown way Dhh exerts a protective anti-ageing effect against degeneration. The idea that motor neurons, which give rise to the largest diameter axons might be selectively affected did not appear to be correct as there was no difference in either their number or their area of their cell bodies, although I acknowledge that the method used might not detect subtle changes in either number or diameter.

The loss of large myelinated axons suggested a possible reason for the small reduction in conduction velocity in *dhh*$^{-/-}$ mice reported previously (Parmantier *et al.*, 1999). However it was clear that the myelin thickness relative to axon diameter remained the same in all three genotypes as has been confirmed by g-ratio measurement (Fig3.3). The large and significant loss in the number of unmyelinated axons suggests that Dhh from myelinating Schwann cells may be signalling to non-myelinating Schwann cells,

which express the ptc2 receptor (Bajestan et al., 2006), and which could in turn provide trophic support to the unmyelinated axons.

The increase in the number of fibres that show a 1:1 ratio of Schwann cells to unmyelinated axons and the lack of Schwann cell units enclosing large groups of axons, in *dhh*$^{-/-}$ nerves is also likely to relate to the strong, selective expression of Ptc2 Dhh receptors on these cells (Bajestan *et al.*, 2006). The increase in the number of 1:1 units might also suggest that Dhh signalling could affect Schwann cell proliferation in the period before myelination. This could be tested by injection of BrdU into pregnant mothers at E18 and subsequent comparison of proliferation in sciatic nerves of *dhh* null and normal littermates as has been done previously in this laboratory (D'Antonio et al., J. Neurosci. In press). Alternatively the increased number of 1:1 units may merely reflect the fact that the number of unmyelinated axons is decreased without having any effect on Schwann cell numbers. Moreover, the lack of unmyelinated axons present in large groups could also suggest a possible involvement of adhesion molecules in Dhh signalling pathways which needs to be explored further.

Collectively, the above data suggest that *Dhh* not only has a role in controlling the number of incisures in myelinating Schwann cells but it also, however indirectly, is involved in regulating the number and the grouping of unmyelinated axons. The increased number of SLI in *dhh*$^{-/-}$ nerves acts via mechanisms that are relatively independent of those in *shi*$^{-/-}$ nerves.

It would be interesting to test whether administering Dhh protein to *dhh* null mice would rescue these phenotypes and if it does to what extent the phenotype would be recovered. Furthermore, the extent of Dhh activity and its maintenance during

development could be addressed by the use of SiRNA at different stages of development.

To conclude, this chapter has recognised Dhh signalling to be important in regulating the number of SLI and in the formation and/or maintenance of the correct number and configuration of myelinated and unmyelinated axons.

To explore these data and try to find out some explanations for the above defects, in the next chapter I examine the molecular organisation of SLIs, using immunohistochemistry to determine whether the incisures in *dhh* null mice have the same molecular organisation as that found in nerves of wild-type mice. The expression levels of mRNA and proteins of these genes that are reported to be located at the incisures or that are important components of the myelin sheath will be also examined.

CHAPTER 4

INTRODUCTION

Molecular and cellular organization of SLI

The non-compact regions of myelinating Schwann cells which includes the SLI and the paranodal loops, contain specialized junctions that are also found in epithelial cells, including tight junctions, gap junctions, and adherens junctions (Mugnaini and Schnapp, 1974; Fannon *et al.*, 1995; Balice-Gordon *et al.*, 1998; Spiegel and Peles, 2002). These junctions are found between membrane lamellae of the same cell and called autotypic (Fannon *et al.*, 1995) or reflexive (Balice-Gordon *et al.*, 1998) junctions. Autotypic adherens junctions are abundant in SLIs and contain E-cadherin, a calcium-dependent cell adhesion molecule where the cytoplasmic domain of E-cadherin binds to β-catenin and α-catenin linking it to the actin cytoskeleton (Fannon *et al.*, 1995; Nagafuchi *et al.*, 1993). Furthermore, it has been shown recently that autotypic adherens junctions stabilize SLI via recruitment of p120 catenin to E-cadherin (Tricaud *et al.*, 2005). Both Cx32 and Cx29 are found in autotypic gap junctions (Scherer *et al.*, 1995b; Altevogt *et al.*, 2002; Li *et al.*, 2002). Autotypic tight junctions consist of several adhesion molecules: occludin, PSD95/Disck large/zona occludent (ZO1) allowing the formation of large macromolecular complexes, claudins 1, 2, and 5, integral membrane proteins with four transmembrane domains, two multi-PDZ domain proteins (MUPPs) (MUPP1 and protein associated with lin-7: Pals-associated tight junction protein (PATJ)), and the adaptor protein Par-3 (Poliak *et al.*, 2002). In the adult rat sciatic nerve, Mupp1 and claudin-5 co-localized in the SLI, whereas PATJ and claudin-1 were found at the paranodes (Poliak *et al.*, 2002). The presence of tight junctions, specialized cell-cell contact sites, in epithelia, acts as a selective permeability barrier to restrict movement

across cellular sheaths, from one extracellular compartment to another. In paranodal loops, they prevent the entry of large molecules to the potential space between the layers of the myelin sheath (Hall and Williams, 1971; MacKenzie *et al.,* 1984; Revel and Hamilton, 1969; Tabira *et al.,* 1978). These junctions also consist of junctional adhesion molecule which are a family of glycoproteins where JAM-2 and JAM-3 are the closest relatives which are directly associated with PAR-3, and expressed by endothelial cells (Aurrand-Lions *et al.,* 2000; 2001a; 2001b; Palmeri *et al.,* 2000; Liang *et al.,* 2002).

MAG and S100 are also expressed in SLIs where MAG is enriched between glial loops in the PNS but not CNS (Trapp *et al.,*1989a; 1989b). S100, also a Schwann cell marker, are acidic calcium binding proteins that are found mainly in the cytoplasm of all Schwann cells. Their function in Schwann cells is unclear, but they may be involved in proliferation and regulation of glial cell morphology via cytoskeletal organisation (Kligman and Hilt, 1988).

This chapter will analyse the expression of mRNA and protein as well as localization of some of the above molecules in the Schwann cells of $dhh^{+/-}$ and $dhh^{-/-}$ animals.

To investigate the abundance distribution of some of the molecules associated with compacted and non-compacted myelin, we used western blotting, RT-PCR and immunocytochemmistry.

Cx29 is strongly up-regulated in *dhh*$^{-/-}$ nerves

Since the number of SLI was at least double in *dhh*$^{-/-}$ mice at all ages (Chapter 3), we investigated whether this increase in number had any effect on the expression levels of myelin proteins (P0 and MBP) or proteins that are expressed in the incisures, (MAG, E-cadherin, β-catenin and Cx29 (Gould *et al.*, 1995; Smith-Slatas and Barbarese, 2000; Meier *et al.*, 2004).

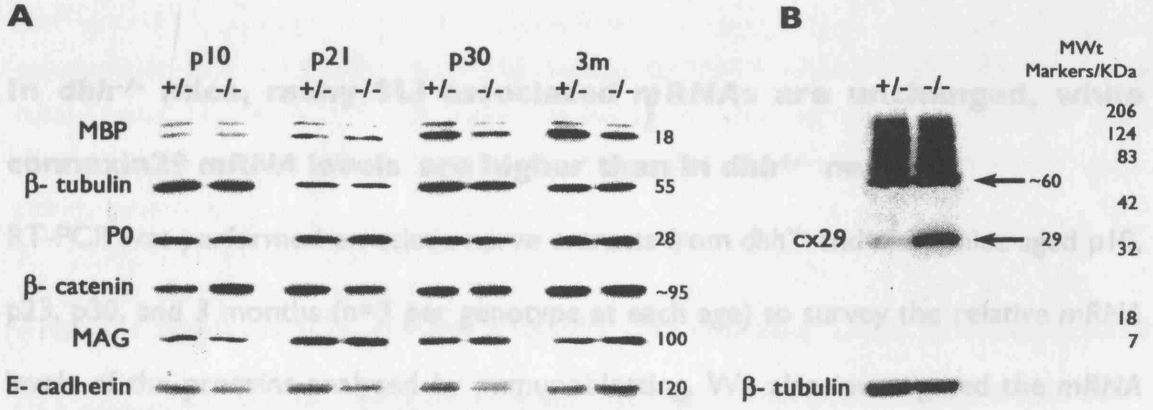

Figure 4.1 Western blot analysis of *dhh*$^{+/-}$ and *dhh*$^{-/-}$ sciatic nerves. **A**: Western blot analysis of MBP, P0, β-catenin, MAG and E-cadherin in sciatic nerves from *dhh*$^{+/-}$ and *dhh*$^{-/-}$ mice at p10, p21, p30, and 3months (n=3 for each genotype at each age). β-tubulin is included to show that samples are equally loaded. Note that MBP levels in *dhh*$^{-/-}$ nerves are lower at p30 and 3 months than in *dhh*$^{+/-}$ nerves while other proteins are unchanged. The size of proteins in kDa are indicated on the side. **B**: Western blot analysis of Cx29 at p21. Note the upregulation of a strong band at ~60kD and a less prominent band at ~29kD in the *dhh*$^{-/-}$ nerves. The above results were obtain from three mice per genotype at each age. Molecular weight markers are indicated to the right of the blot (Biorad, CA, USA).

Protein extracts were prepared from *Dhh*$^{+/-}$ and *Dhh*$^{-/-}$ mouse sciatic nerves at different ages (P10, 21, 30, and 3 months), and analysed by immunoblotting (Figure 4.1A).

In *dhh*$^{-/-}$ nerves the level of MBP was somewhat lower at P30 and 3 months than in *dhh*$^{+/-}$ nerves but there was no apparent difference at earlier ages even though the difference in SLI number is already established by P10 (Table 3.1). There were minimal differences in the expression levels of P0, MAG, and β-catenin protein at all ages, and although E-cadherin levels look slightly lower at p10, p23 and p30, at 3 months the levels look similar in the homo- and heterozygote. Western blotting of Cx29, however, revealed that this protein was markedly up-regulated at P21 (Fig. 4.1B) and other ages (not shown). In agreement with others, I found that Cx29 protein displayed anomalous behaviour on western blotting (Altevogt *et al.*, 2002; Li *et al.*, 2002), showing a strong band at about 60kD and a weaker band at around 30kD, both of which were up-regulated in the *dhh*$^{-/-}$ nerve.

In *dhh*$^{-/-}$ mice, many SLI associated *mRNA*s are unchanged, while connexin29 *mRNA* levels are higher than in *dhh*$^{+/-}$ nerves

RT-PCR was performed on sciatic nerve extracts from *dhh*$^{+/-}$ and *dhh*$^{-/-}$ mice aged p10, p23, p30, and 3 months (n=3 per genotype at each age) to survey the relative *mRNA* levels of the proteins analysed by immunoblotting. We also investigated the *mRNA* levels of other proteins such as Cx32, Cx29, S-100, and claudin5, which are associated with SLI (Gould *et al.*, 1995; Altevogt *et al.*, 2002; Li *et al.*, 2002; Poliak *et al.*, 2002; Poliak and Peles, 2003; Meier *et al.*, 2004), and of JAM2 and JAM3, which are associated with tight junctions and with MUPP1 (Ebnet *et al.*, 2004). After standardization with the housekeeping gene *GAPDH*, samples were run separately with primers against MBP, MAG, Cx32, Cx29, S-100, E-cadherin, claudin5, JAM2 and JAM3 (Fig. 4.2). The results

showed a clear increase in Cx29 *mRNA* expression in *dhh*$^{-/-}$ mice at 3 months with a minor increases detectable at all other ages. The expression level of mRNAs for MBP, Cx32, S-100, JAM2 and JAM3 remained unchanged. MAG and E-cadherin expression levels appeared marginally higher in *dhh*$^{-/-}$ than *dhh*$^{+/-}$ nerves at p13 and p23 but did not appear to be different at older ages.

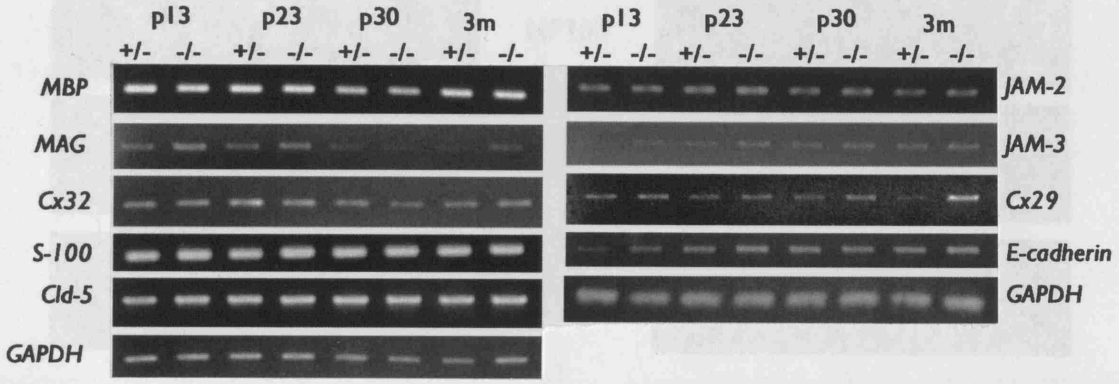

Figure 4.2 RT-PCR analysis of *dhh*$^{+/-}$ and *dhh*$^{-/-}$ sciatic nerves. RT-PCR of mRNA in sciatic nerves from *dhh*$^{+/-}$ and *dhh*$^{-/-}$ mice at p13, p21, p30, and 3 months (n=3 for each genotype at each age) of genes that are expressed either in SLI and/or endothelial junctions. GAPDH is included to show that samples are equally loaded. Note that Cx29 mRNA levels are increased in *dhh*$^{-/-}$ nerve at 3 months. Other genes show either no or minor differences up to p23. Above results were obtained from three mice per genotype at each age.

The SLI associated proteins MUPP1, NF155 and Cx29 are expressed in the additional SLI of *dhh*$^{-/-}$ Schwann cell

To test whether the additional SLI present in *dhh*$^{-/-}$ fibers had the same molecular composition as SLI in normal fibers, sciatic nerves from adult *dhh*$^{+/-}$ and *dhh*$^{-/-}$ animals were teased and immunolabelled with antibodies against a number of SLI proteins. The localisation of Cx29, neurofascin (NF) 155 and MUPP1 is shown in Fig. 4.3. MUPP1 is largely confined to SLI (Poliak *et al.*, 2001), while Cx29 and NF 155 are also present in paranodal loops adjacent to the Node of Ranvier. I found that NF155 and MUPP1 were

seen in essentially all phalloidin labelled SLI in both *dhh*$^{+/+}$ and *dhh*$^{-/-}$ nerve fibers, and immunolabelling for Cx29 showed a similar distribution (Fig. 4.3 A,B,C).

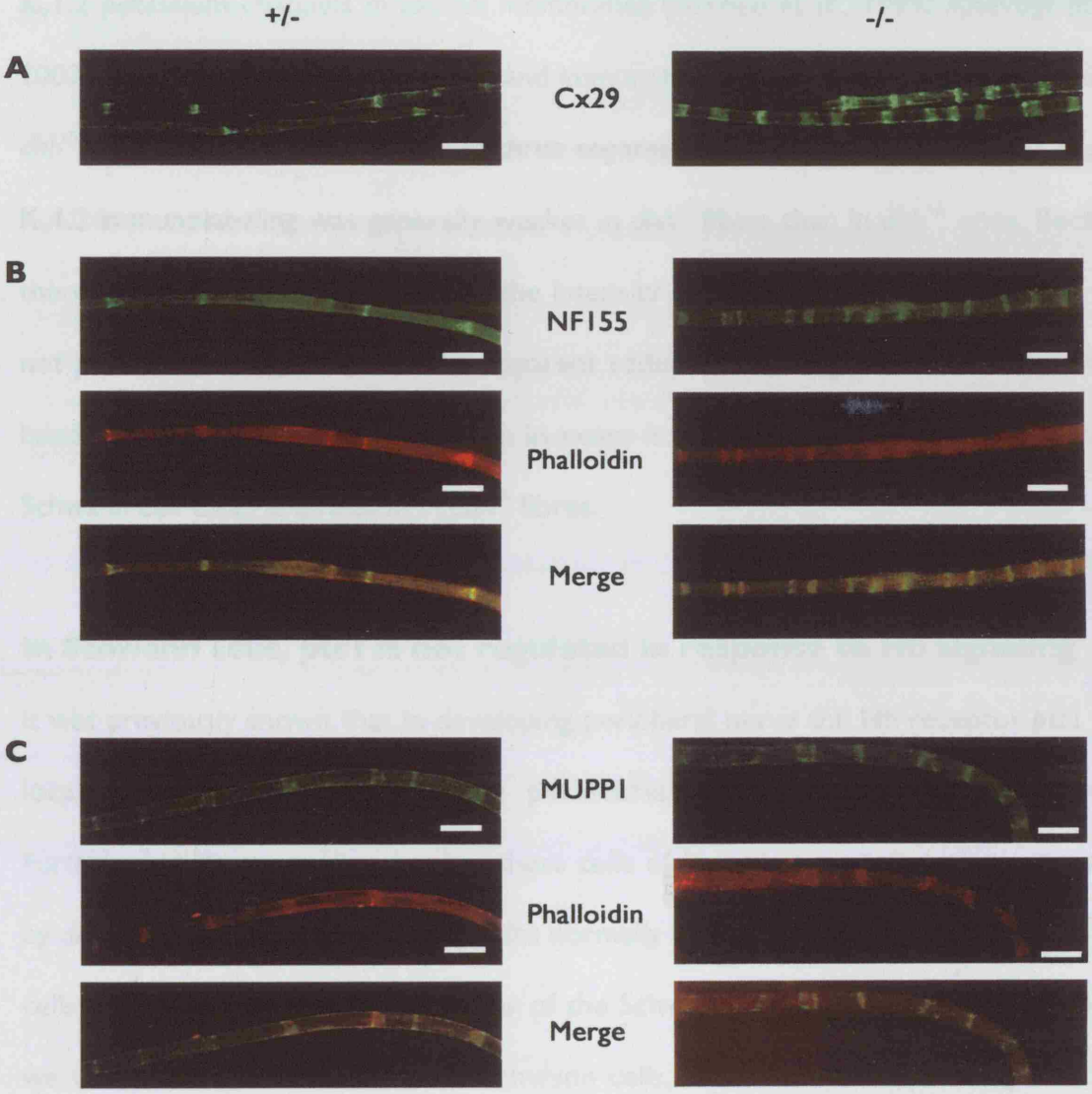

Figure 4.3 Cx29, Mupp1 and NF155 are localized to SLI in nerves of both *dhh*$^{+/-}$ and *dhh*$^{-/-}$ mice. **A**: Cx29 immunolabelling of SLI, showing the increased number of SLI in the *dhh*$^{-/-}$ fibres. **B**: Sciatic nerves were teased and double labelled with phalloidin-TRITC and antibodies to NF155, showing the increased number of SLI in the *dhh*$^{-/-}$ fibres. Note the co-incidence of actin and NF155 labelling. C: Sciatic nerves were teased and double labelled with phalloidin-TRITC and antibodies to MUPP1, showing the increased number of SLI in the *dhh*$^{-/-}$ fibres. Note the co-incidence of actin and MUPP1 labelling. Scale bars, 33μm.

Similar results were obtained previously with S100 and MAG antibodies in the laboratory (not shown). Thus the new incisures that are generated in the absence of

dhh signaling appear to have a largely normal molecular composition. It has been suggested that there is an association between Cx29 in myelinating Schwann cells, and $K_V1.2$ potassium channels in axonal membranes (Arroyo *et al.*, 1999; Altevogt *et al.*, 2002). We therefore used antibodies and immunolabeling to examine $K_V1.2$ channels in *dhh*$^{-/-}$ teased nerves (not shown). In three separate experiments we found that axonal $K_V1.2$ immunolabeling was generally weaker in *dhh*$^{-/-}$ fibers than in *dhh*$^{+/-}$ ones. Because there was considerable variability in the intensity of labeling from fiber to fiber it was not possible to judge whether the apparent reduction was significant. On the other hand, it is clear that $K_V1.2$ expression in axons is not increased commensurately with Schwann cell Cx29 expression in *dhh*$^{-/-}$ fibres.

In Schwann cells, *ptc1* is not regulated in response to Hh signaling

It was previously shown that in developing peripheral nerve the Hh receptor *ptc1* was localized at highest levels in the perineurial cells surrounding nerve fibers. Furthermore its expression level in these cells of fibroblastic origin was up-regulated by *dhh*, as would be expected, since Hhs normally up-regulate *ptc1* expression in target cells (Parmantier *et al.*, 1999). In view of the Schwann cell phenotype reported here, we wished to determine whether Schwann cells, in addition to expressing *dhh*, also expressed *ptc1* receptors that were responsive to Hh signaling. Purified neonatal mouse Schwann cells or nerve-derived fibroblasts were cultured with the Hh ligands or agonists Cur-0199567 (Frank-Kamenetsky *et al.*, 2002) for 3 hours and 24 hours. RT-PCR revealed that Schwann cells expressed detectable levels of *ptc1*, but unlike nerve fibroblastic cells, they did not regulate *ptc1* expression in response to Hh signals (Fig. 4.4).

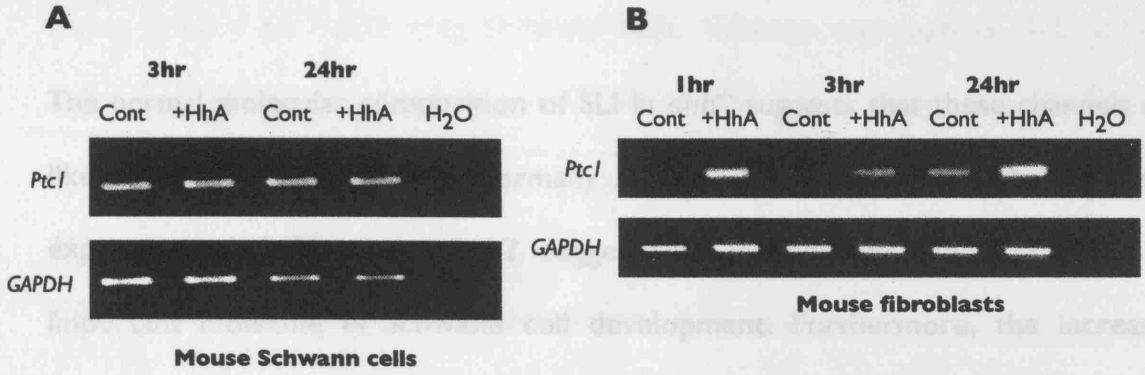

Figure 4.4 RT-analysis showing that Ptc1 mRNA in, **A**: cultured Schwann cells is not up-regulated in response to hedgehog ligands (HhA), **B**: in contrast to that seen in fibroblasts. *Dhh* protein (40nM) was applied to Schwann cells and the hedgehog agonist Cur-019956767 (40nM) to fibroblasts. GAPDH is shown to indicate that samples are equally loaded. Above results were obtained from three different cultures using three p3 pups each time to purify the cells.

In so far as the absence of up-regulation of *ptc1* can be taken to indicate non-functionality of the *ptc1* signaling pathway and the fact that *ptc1* mRNA levels are very low in adult nerves (Parmantier *et al.*, 1999), these observations suggest that the effects of *dhh* on myelinating Schwann cells are most likely to be indirect, perhaps via *dhh*-induced signals from perineurial cells, rather than autocrine.

DISCUSSION

These data suggest that the expression of MBP decreases in $dhh^{-/-}$ after p21, possibly due to an increase in SLIs and reduced compaction of the myelin sheath. While the new SLIs in $dhh^{-/-}$ cells appear to have a broadly normal molecular composition, the mRNA and protein expression of Cx29 in $dhh^{-/-}$ is clearly up-regulated in $dhh^{-/-}$ nerves in contrast to the mRNA of Cx32. I also provide indirect evidence that the effects of *dhh* on myelinated Schwann cells are likely to be indirect, perhaps via perineurial cells.

The normal molecular composition of SLI in *dhh*$^{-/-}$ suggests that these channels are likely to be able to function normally at least to some extent. The increased expression of Cx29, unlike Cx32, suggests the influence of *dhh* signalling on an important molecule in Schwann cell development. Furthermore, the increased expression of Cx29 might be related to the increased number of small diameter fibre, since it has been reported that Cx29 was primarily found in myelin sheaths surrounding small fibres (Altevogt *et al.*, 2002) Unlike Cx32, Cx29 mRNA expression appears early during development and declines to lower level in adulthood and remains at this low level even after nerve transection (Altevogt *et al.*, 2002). Unfortunately, the *shi* and *dhh/shi* double null mice were no longer available at the time I made the observations on Cx29, as it would have been interesting to examine Cx29 expression in these mice as, unlike *dhh*$^{-/-}$ mice, *shi*$^{-/-}$ mice have increased Cx32 expression (Smith-Slatas and Barbarese, 2000). The reduced level of MBP expression is possibly an indication of a decreased level of compaction due to an increase in the number of SLI. Interestingly, the level of P_0, important for compact myelin, is unchanged at all ages of *dhh*$^{-/-}$ that were examined. If the reduction on MBP levels are due to lower amounts of compact myelin, this raises the question of why a similar reduction is not seen in P_0. It is possible to argue that since P_0 is the most abundant protein in myelinated fibres in PNS, it would be hard to observe the small changes in levels using immunobotting technique. As the molecular composition of the incisures in dhh null mice appear normal, it would be appropriate to purseue the analysis of K+ channels in these mice in association with Cx29. The reason for the unchanged level of *ptc1* expression in Schwann cells in response to Hh signals is not clear, but it may indicate that classical ptc1 signalling does not occur in these cells. This in turn, may suggest that rather than

acting directly on myelinating Schwann cells, Schwann cell-derived Dhh induces expression of signals in the perineurium surrounding nerve that in turn acts back on Schwann cells as is seen with Ihh signalling in chondrogenesis (Vortkamp *et al.*, 1996). This could be tested by the use of culture conditioned medium from fibroblasts and Schwann cells and check the mRNA expression level of ptc1.

This chapter has identified some of the molecular differences that has occurred due to the absence of dhh. As dhh is also expressed in the large vessels, my aim is to examine all the vessels within the endoneurium in terms of their diameter and their permabilty to find if dhh has an effect on these vessels.

CHAPTER 5

INTRODUCTION

The role of hedgehog signalling in vasculogenesis and angiogenesis

Vascular formation in the developing nervous system is a highly regulated process. Vascular development usually takes place in two stages; vasculogenesis (the formation of endothelial tubes), and angiogenesis (remodelling of existing blood vessels to form the mature vasculature) (Byrd and Grabel, 2004). Vascular endothelial growth factor (VEGF), its receptors, VEGFR1 or Flt1, VEGFR2 or Flk1, VEGFR3 or Flt4, and angiopoietin/Tie ligands and receptors are some of the molecules that are involved in this process (Yancopoulos et al., 2000). In recent years, other signals and signalling pathways including Notch/Delta (Shawber and Kitajewski, 2004), and ephrin/Eph (Cheng et al., 2002), have been identified to have a role in blood vessel differentiation (Byrd and Grabel, 2004). In the mouse embryo, primitive vessel formation starts at around E7 – E7.5 from localized mesodermal masses lying interior to the visceral endoderm (Boucher and Pedersen, 1996) where the primitive precursors of erythrocytes and endothelial cells are located (Choi et al., 1998). The angiogenic potential of Hh family members has been also investigated in the past few years. It has been shown that the adult vascular system in the mouse can respond to Hh signals. Ptc1-lacz heterozygous mice can be used to measure the expression level of Hh response in both endothelial cells and adventitial fibroblasts surrounding vessels. The data have suggested that hh acts via an intermediate support cell, rather than directly on endothelial cells, to promote vessel remodelling in adults (Byrd and Grabel, 2004). Shh treatment, in a hind limb ischemia model, promotes an increase in capillary density

and blood flow (Pola et al., 2001). Furthermore, addition of Shh in a corneal angiogenesis assay, promotes neovascularization and the formation of large branched vessels (Pola et al., 2001). In regard to Schwann cells, it has been shown that Schwann cell conditioned medium inhibits angiogenesis by producing a potent inhibitor called tissue inhibitor of metalloproteinase-2 (Huang *et al.*, 2000).

Studies on permeability of blood vessels in the PNS of the rat showed that the endoneurial blood vessels (Fig 5.1) do not permit the passage of detectable amounts of fluorescent-labelled albumin, indicating an exchange of albumin across the walls of vessels either does not take place or is insignificant (Olsson, 1966).

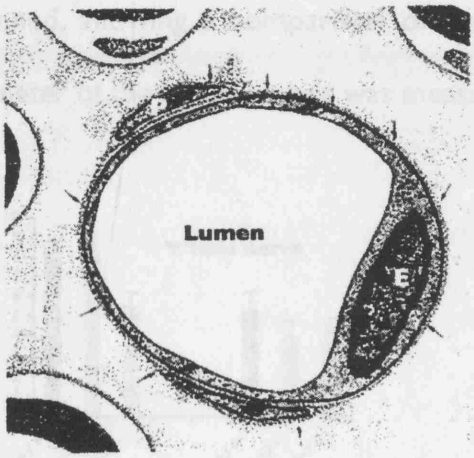

Figure 5.1 Structural basis of blood-nerve barrier. The vessel wall is composed of endothelial cells (E) and a vascular basal lamina (arrows) which surrounds pericytes (P). Outside the vessel, there are large extracellular spaces containing collagen and other constituents of the endoneurial matrix and fluid – Modified from Olsson (1990), *Critical Reviews in Neurobiology* **5,** 265-311.

In the case of epineurial and perineurial blood vessels, the fluorescent albumin is normally found in their walls and in the connective tissue outside (Olsson, 1968). This indicates that the presence of a blood-nerve barrier within peripheral nerves, although it is much more permeable than the blood-brain barrier within the CNS (Olsson, 1990).

The diameter of the blood vessels in *dhh*$^{-/-}$ nerves is reduced compared with wild type nerves

The laboratory has previously shown that the perineurial barrier is defective in *dhh*$^{-/-}$ mice, and that by freeze fracture electron microscopy the tight junctions between perineurial cells are abnormal and allow the passage or proteins and neutrophils (Parmantier *et al.*, 1999). To test whether the endoneurial blood vessels (capillaries) (Bell and Weddell, 1984) within the nerve are abnormal, sciatic nerves from *dhh*$^{+/+}$, *dhh*$^{+/-}$, and *dhh*$^{-/-}$ mice at postnatal day 30 (p30), were fixed and prepared for electron microscopy. Sections cut from both ends of the excised nerve were photographed and scanned, allowing a comparison of proximal and distal sections of the nerve. The diameter of the blood vessels was measured using *Open lab* software.

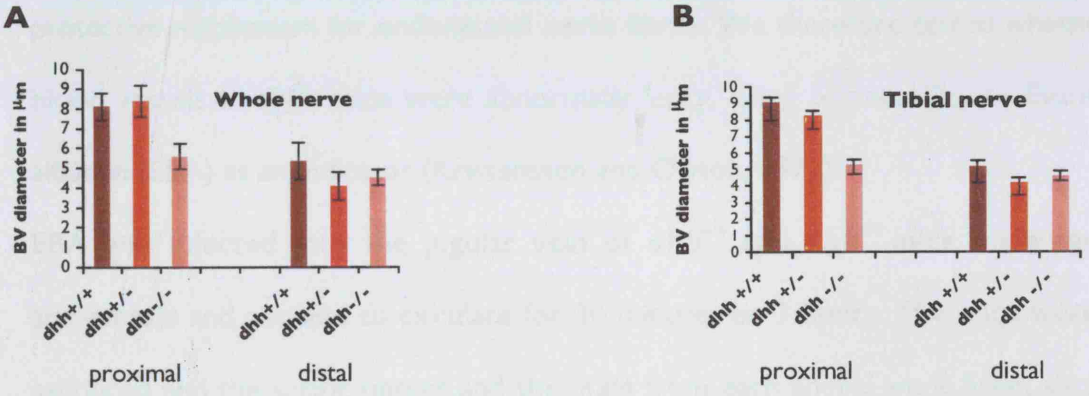

Figure 5.2 Graphs of blood vessel diameter in *dhh*$^{+/+}$, *dhh*$^{+/-}$, and *dhh*$^{-/-}$ sciatic nerve. **A**: Whole nerve; **B**: Tibial nerve. In both nerves the diameter of the vessels at proximal end of *dhh*$^{-/-}$ mice is significantly lower than the controls (8.1±0.7 and 8.4±0.8 in whole nerve of *dhh*$^{+/+}$ and *dhh*$^{+/-}$ respectively in comparison to 5.6±0.6 in *dhh*$^{-/-}$, and 9.1±1.1 in *dhh*$^{+/+}$ and 8.3±0.8 in *dhh*$^{+/-}$ in tibial nerve in comparison to 5.6±0.6 in *dhh*$^{-/-}$), $p<0.05$, However, the diameter of the vessels at distal end of all three genotypes are similar. These results were obtained from 3 mice per genotype.

Furthermore, to further lower the variability, the diameter of blood vessels from the main fascicle alone was also measured separately and compared with vessels from the whole nerve. The results showed that; (i) there was a significant decrease in the diameter of the vessels at the proximal end of *dhh*$^{-/-}$ nerve in comparison to *dhh*$^{+/+}$ and *dhh*$^{+/-}$ nerves (student t-test), (ii) there was no difference between the diameter of the vessels at the distal end, and (iii) analysis of blood vessels in the whole nerve and the main fascicle gave similar results (Fig 5.2).

Blood vessels in peripheral nerves of *dhh*$^{-/-}$ mice are abnormally permeable

In *dhh*$^{-/-}$ nerves, the molecular and cellular composition of the endoneurium is likely to be altered due to the breakdown of the tissue-nerve barrier (Parmantier *et al.*, 1999). The endoneurial capillary-nerve barrier (blood-nerve barrier) constitutes another protective mechanism for endoneurial nerve fibres. We therefore tested whether the blood vessels in *dhh*$^{-/-}$ mice were abnormally leaky, using permeability to Evans Blue albumin (EBA) as an indicator (Kristensson and Olsson, 1971).

EBA was injected into the jugular vein of *dhh*$^{+/+}$ and *dhh*$^{-/-}$ mice under general anaesthesia and allowed to circulate for 30 minutes or 3 hours. The mice were then sacrificed and the sciatic nerves and the brain from each animal were fixed, sectioned and viewed under the fluorescence microscope (Fig. 5.3). In the brain, EBA was confined to blood vessels at both time points and no differences were seen between *dhh*$^{+/+}$ and *dhh*$^{-/-}$ animals. In the sciatic nerve of control mice, EBA was associated with the perineurium/epineurium, presumably reflecting the permeability of epineurial vessels. In the endoneurium, EBA was, however, confined to blood vessels at both time points, demonstrating the existence of the blood-nerve barrier in *dhh*$^{+/+}$ nerves.

But in *dhh*$^{-/-}$ nerves, EBA distribution was markedly different. In this case, EBA was present throughout the nerve at both time points. Thus the double protection offered to endoneurial nerve fibers by the perineurial tissue-nerve barrier and the blood-nerve barrier is absent in *dhh*$^{-/-}$ mice. The permeability of the blood-brain barrier is, however, independent of Dhh signaling. While this is likely to have adverse effects on peripheral nerve fibers, it is probably not a significant cause of the elevated SLI numbers in *dhh*$^{-/-}$ fibers, because SLI numbers are elevated before the perineurial and vascular barriers develop fully (Kristensson and Olsson, 1971; Weerasuriya *et al.*, 1990). Schwann cell-derived Dhh could also be involved in promoting vascularization of peripheral nerves (Kusano et al., 2004) although we did not find any obvious loss of blood vessels in *dhh*$^{-/-}$ nerves

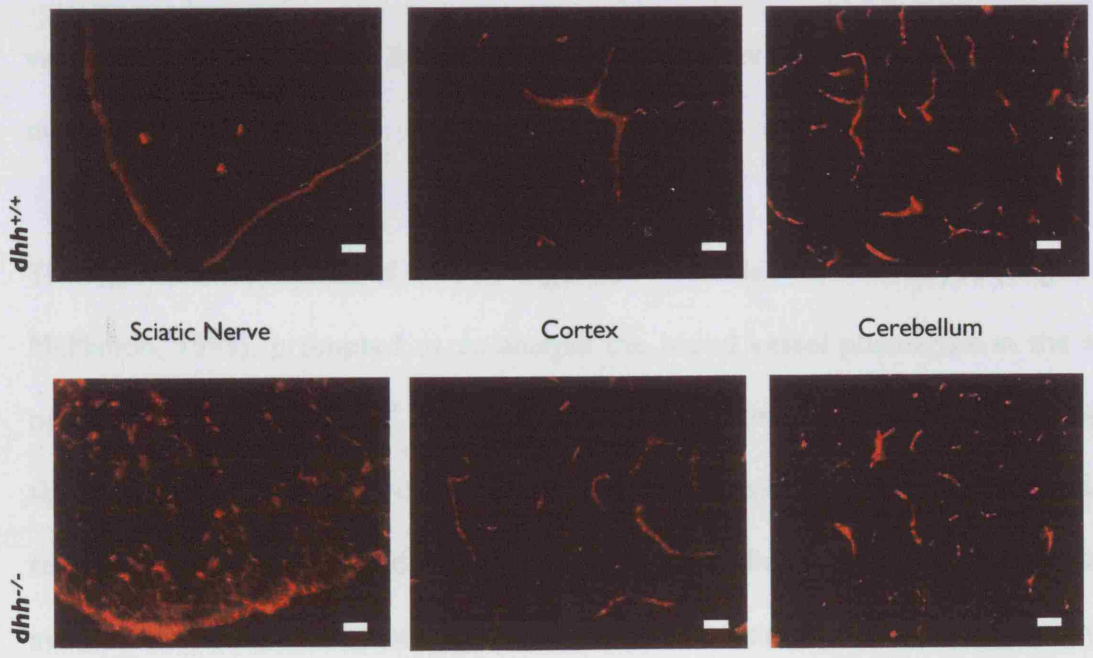

Figure 5.3 Endoneurial blood vessels in *dhh*$^{-/-}$ nerves are permeable to dyes. Comparison of permeability to EBA in *dhh*$^{+/-}$ and *dhh*$^{-/-}$ mouse tissues (x40 oil). Left hand panels; Sciatic nerve. Note the labelling throughout the nerve in the *dhh*$^{-/-}$ nerve (lower panel) while in the *dhh*$^{+/-}$ nerve EBA is confined to the epineurium and three capillaries within the endoneurium. Middle and right hand panels: labelling is confined to capillaries in both cortex and cerebellum, and does not differ between *dhh*$^{+/-}$ and *dhh*$^{-/-}$ mice. Scale bars, 50μm.

DISCUSSION

Dhh signalling is important for the formation of the correct diameter blood vessels within the endoneurial space of the sciatic nerve as well as in the formation of a proper blood-nerve barrier. In *dhh*$^{-/-}$nerve, the vessels closer to the spinal cord were reduced in diameter in comparison to that seen in *dhh*$^{+/+}$ and *dhh*$^{+/-}$ animals, and their permeability was increased.

To date studies on the involvement of Hh in the formation of blood vessels has showed that the target of Hh is either consistent with a direct mode of action for Hh on vessel forming cells, or that it does not directly target angioblast or endothelial cells, but rather targets an intermediate cell type that responds to Hh by expressing a vascular specific growth factor like VEGF. However, it is possible that both mechanisms are involved.

The reported expression of Dhh in large blood vessels of E11 embryos (Bitgood and McMahon, 1995), prompted us to analyse the blood vessel phenotype in the sciatic nerve of wild type and *dhh*$^{-/-}$ mice. In the above experiments, the importance of Dhh signalling for blood vessel diameter and its permeability has been addressed. The reduced vessel diameter and the increase in permeability suggest that Dhh is possibly involved in stability and maintenence of vessels in the endoneurium rather than in their development. *In situ* hybridisation confirmed that the sole source of Dhh secretion is Schwann cells (Fig. 3.1), however it would be important in the future to find out whether vessels or their supporting cells express *ptc1* or *Smo*. The expression of different molecules that are involved in vasculogenesis like VEGF and angiopoietins also

needs to be examined. It is also possible to think that perineurial cells are involved in the formation of blood vessels in the sciatic nerve endoneurium, since it has been reported that the lack of permeability of the endoneurial vessels is established at the point where the vessels enter the innermost layer of the perineurium (Olsson, 1990). Because the perineurium is under-developed, it is possible that this causes abnormal function in the vessels. If this is the case, then one reason for this abnormality might be the diminution in tight junctions between perineurial cells observed in *dhh*$^{-/-}$ nerves (Parmantier *et al.*, 1999). It would also be relevant to examine the tight junctions between endoneurial endothelial cells by freeze fracture to determine whether they are also abnormal. One way to find out whether Dhh has direct effects on blood vessel formation is to use an endothelial cell line that forms blood vessels in culture with a timed and orderly sequence, to determine how conditioned medium from either wild type or *dhh*$^{-/-}$ affects the timing of vessel formation. Alternatively recombinant Dhh could be employed. The above experiments could also be used to examine the formation of tight junctions. Furthermore, the cell line exposed to conditioned medium on Dhh could be tested for the presence of angiogenetic- specific compounds such as VEGF that promote vessel formation.

The abnormal permeability of the endoneurial vessels as well as the lack of large diameter fibres in dhh null mice, led me to investigate in the next chapter the distribution of macrophages within the endoneurium and also to set up nerve injury experiments to compare the degeneration rate in both wild type and *dhh*$^{-/-}$ animals.

CHAPTER 6

INTRODUCTION

Wallerian degeneration and regeneration in *dhh*$^{-/-}$ nerves

Damage and injuries to peripheral nerve initiates a complex set of events. This process begins with the separation of the myelin sheath at incisures to form ovoid structures. The loss of axonal contact initiates the down-regulation of specific genes (Gupta *et al.*, 1988; LeBlanc and Poduslo, 1990). Two main activities are taking place during this process; one is de-differentiation, including proliferation of Schwann cells and the down-regulation of myelin specific genes, and the second is the recruitment of macrophages to the site of the injury. Induction of cytokines in Schwann cells after injury suggests an interaction between Schwann cells and macrophages. Studies have shown that in transected nerve, Schwann cells up-regulate the expression of Leukemia inhibitory factor (LIF) and interleukin-6 (IL-6), and in IL-6 null and LIF null mice, secretion of monocyte chemoattractant protein-1 (MCP-1) is reduced (Banner and Patterson, 1994; Bolin *et al.*, 1995; Kurek *et al.*, 1996; Tofaris *et al.*, 2002). MCP-1 is also induced in Schwann cells after nerve injury and induction of LIF and IL-6 is also seen (Toews et al., 1998; Siebert *et al.*, 2000; Subang and Richardson, 2001). The principle role of macrophages is to phagocytose degenerated myelin (O'Daly and Imaeda, 1967; Stoll *et al.*, 1989), although Schwann cells themselves are able to degrade myelin in vitro (Bigbee *et al.*, 1987; Fernandez-Valle *et al.*, 1995) and, to a limited extent, are involved in myelin clearance in vivo (Stoll *et al.*, 1989). Within the persistent tubes of basal laminae, Schwann cells up-regulated the synthesis of ECM molecules (Patton *et al.*, 1997; Burstyn-Cohen *et al.*, 1998; Chernousov *et al.*, 1999;

Scherer and Salzer, 2001), cell adhesion molecules (Araki and Milbrandt, 1996; Zhang *et al.*, 2000; Scherer and Salzer, 2001), neutotrophins; NGF, BDNF, NT-3 and NT-4 (Fu and Gordon, 1997; Scherer and Salzer, 2001), GAP-43 (Curtis *et al.*, 1992; Woolf *et al.*, 1992), transforming growth factor-β (Scherer and Salzer, 2001), and transcription factors including c-Jun, Krox24 and ATF3 (Topilko *et al.*, 1997; Tsujino *et al.*, 2000). This chapter aims to analyse *dhh*$^{-/-}$ nerve before and during nerve injury to determine whether Dhh signalling has a role to play in this process.

I wished to investigate whether Dhh signalling was involved in the maintenance of myelinated fibres.

Uninjured *dhh*$^{-/-}$ nerves show age-dependent axonal degeneration and myelin breakdown

I first examined uninjured dhh+/+ and dhh-/- nerves from mice of different ages to determine whether there was significant spontaneous degeneration. To investigate this for myelinated fibers, nerves from 2, 5 and 21 month old *dhh*$^{-/-}$ mice were examined by electron microscopy (Fig 6.1A). This revealed that about 1% of the myelinated axons were degenerating at any one time in mutant nerves from 2 and 5 month-old

		2-5 months		21 months	
		dhh$^{+/+}$	*dhh*$^{-/-}$	*dhh*$^{+/+}$	*dhh*$^{-/-}$
Total number of myelinated fibers counted	**Animal 1**	3864	2303	5311	3600
	Animal 2	4176	3424	3486	5288
	AV.	4020	2864	4399	4444
Number of degenerated fibers	**Animal 1**	0	23 (1.0%)	13 (0.2%)	48 (1.3%)
	Animal 2	0	42 (1.2%)	11 (0.3%)	52 (1.0%)
	AV.	0	33 (1.1%)	12 (0.25%)	50 (1.2%)

Table 6.1 The number of degenerating fibres is increased in *dhh*$^{-/-}$ nerves. Counts of degenerated fibres in *dhh*$^{+/+}$ and *dhh*$^{-/-}$ sciatic nerves of 2-5 month and 21 month old mice. No degenerating fibres were found in *dhh*$^{+/+}$ nerves at 2-5 months, whereas degenerating fibres were found in *dhh*$^{-/-}$ nerves. At 21 months, there is a small increase in the number of degenerating profiles in *dhh*$^{+/+}$ nerves, which is still much lower than that found in the null nerve.

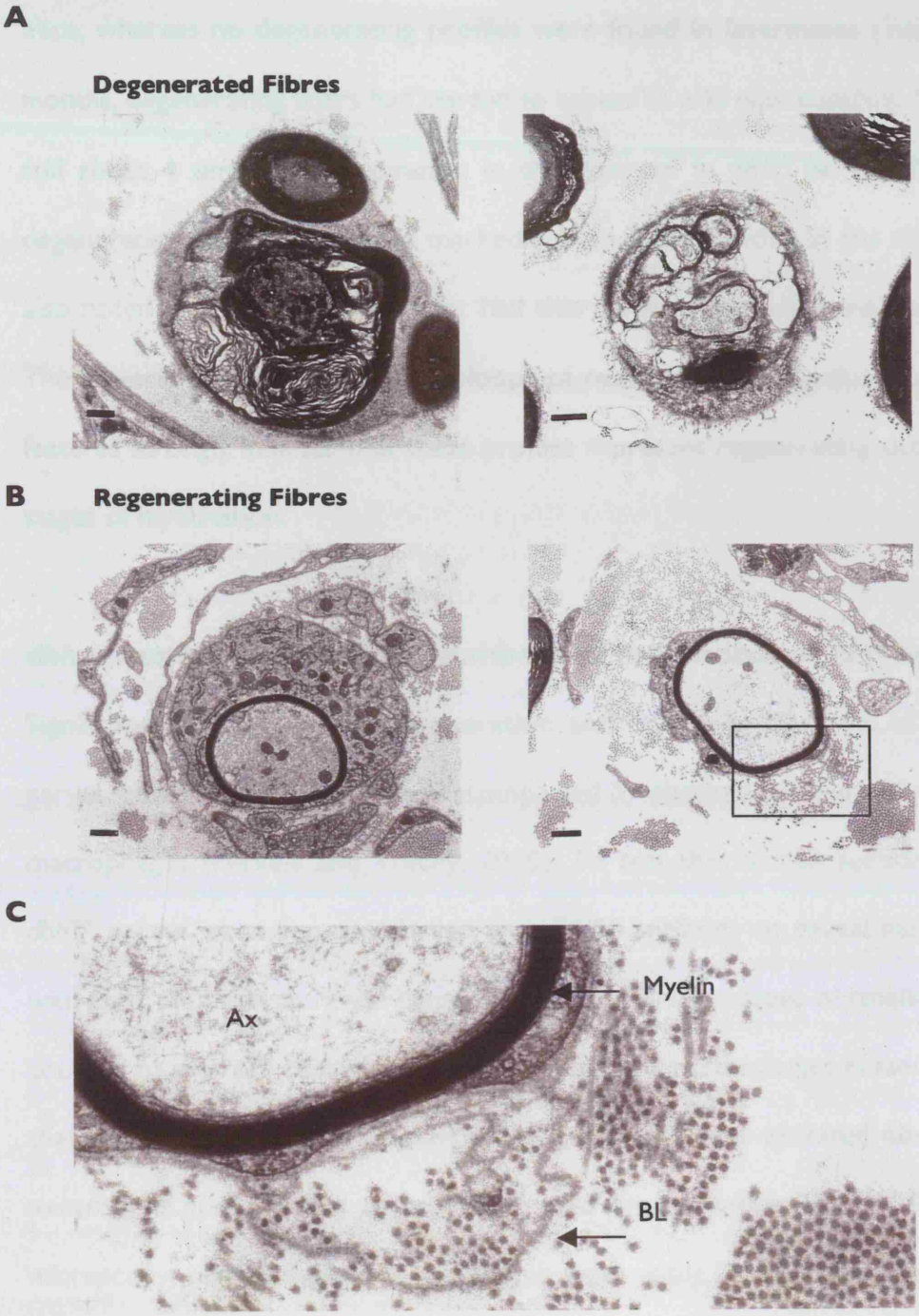

Figure 6.1 *dhh*$^{-/-}$ nerves contain degenerating and regenerating nerve fibres. **A**: Electron micrographs showing two profiles of degenerating fibres. Left hand panel: shrunken axon surrounded by myelin debris; right-hand panel: shrunken axon surrounded by vacuolated Schwann cell. **B**: two profiles of regenerating axons with thin myelin sheaths relative to the axon diameter. **C**: Enlargement of the boxed in area in B. Note redundant basal lamina (BL) associated with a thinly myelinated fibre. Scale bars for **A** and **B**, 1.8µm.

mice, whereas no degenerating profiles were found in littermates (Table 6.1). By 21 months, degenerating fibers had started to appear in wild type controls, but they were still about 4 times more common in *dhh*$^{-/-}$ nerves. In d*hh*$^{-/-}$ nerves, the number of degenerating profiles increased markedly from 5-21 months. In the *dhh*$^{-/-}$ nerves, we also noted a number of axons that had thin myelin sheaths for their size (Fig. 6.1B). These were often associated with loops of redundant basal lamina (Fig. 6.1c). These features strongly indicate that these profiles represent regenerating axons in the early stages of myelination.

dhh$^{-/-}$ nerves contain high numbers of macrophages and neutrophils

Significant, ongoing axonal degeneration and myelin breakdown, as seen in *dhh*$^{-/-}$ nerves, could be expected to be accompanied by elevated numbers of neutrophils and macrophages (Perkins and Tracey, 2000). To test this, frozen sections of *dhh*$^{-/-}$ and *dhh*$^{+/+}$ nerves were immunolabelled with F4/80 antibody to reveal macrophages, and with Gr-1 antibody to reveal neutrophils. Transverse sections of labelled nerves were counted to estimate the number of neutrophils and macrophages present. This showed that in *dhh*$^{-/-}$ nerves, the number of macrophages was elevated about 5 fold and neutrophils about 4 fold compared to wild type controls (Fig. 6.2A). By electron microscopy, macrophages and neutrophils were easily found in *dhh*$^{-/-}$ nerves, but these cells were rarely seen in *dhh*$^{+/+}$ nerves. These cell counts are likely to reflect a chronic, inflammatory cellular response to the ongoing degeneration in *dhh*$^{-/-}$ nerves.

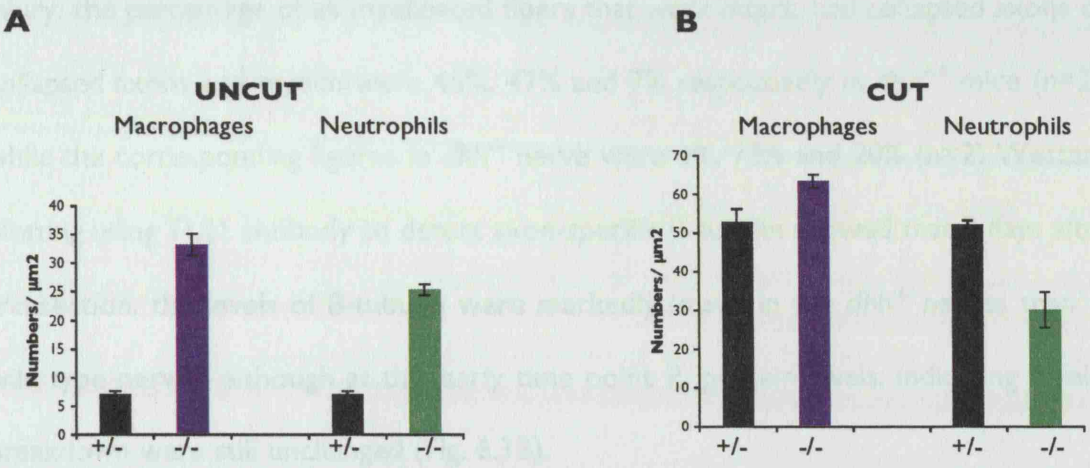

Figure 6.2 Normal and transected *dhh*$^{-/-}$ nerves contain increased numbers of macrophages and neutrophils. **A**: Comparison of macrophage and neutrophil numbers in intact *dhh*$^{+/-}$ and *dhh*$^{-/-}$ nerve. Note the significant increase in the number of macrophages ($p<0.004$) and neutrophils ($p<0.005$) in the *dhh*$^{-/-}$ nerve **B**: Comparison of macrophage and neutrophil numbers in the distal stump of *dhh*$^{+/-}$ and *dhh*$^{-/-}$ nerves 2 days after transection. Both normal and mutant nerves show increased macrophage numbers, Transected normal nerves show a substantial increase in neutrophil numbers as expected, but neutrophil numbers in cut *dhh*$^{-/-}$ nerves are little changed.

Degeneration and inflammatory cell recruitment in transected *dhh*$^{-/-}$ nerves

The elevated number of inflammatory cells, described above, is likely to be a part of the answer to why *dhh*$^{-/-}$ nerves degenerate rapidly following transection (Bajestan *et al.*, 2006), because for myelin breakdown these nerves are less reliant on the macrophage and neutrophil recruitment seen in normal nerves during the first few days after injury.

To examine macrophage and neutrophil recruitment, sciatic nerves of *dhh*$^{-/-}$ and *dhh*$^{+/+}$ mice were transected and processed for cell counts, while other nerves were fixed for electron microscopy or extracted for western blotting to monitor nerve degeneration. Accelerated degeneration of the distal stump was clearly evident by electron microscopy at 2 (Appendix 4-7) and 7 days after transection (Fig 6.3A). Two days after

injury, the percentage of all myelinated fibers that were intact, had collapsed axons or collapsed axons and myelin were 45%, 47% and 7% respectively in *dhh*$^{+/+}$ mice (n=2), while the corresponding figures in *dhh*$^{-/-}$ nerve were 4%, 75% and 20% (n=2) Western blotting using TUJ1 antibody to detect axon-specific β-tubulin showed that 2 days after transection, the levels of ß-tubulin were markedly lower in the *dhh*$^{-/-}$ nerves than in wild type nerves, although at this early time point P_0 protein levels, indicating myelin breakdown were still unchanged (Fig. 6.3B).

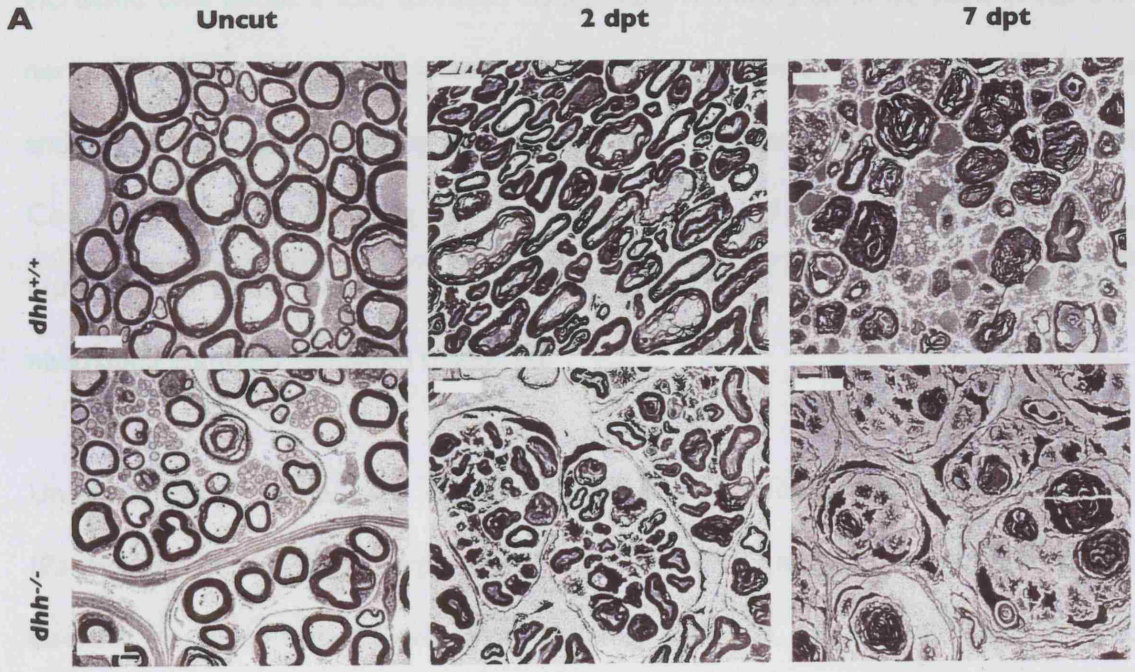

Figure 6.3 *dhh*$^{-/-}$ fibres degenerate rapidly following injury, and the number of minifascicles increases. **A**: Low power (x3000) view of transected nerve, 2 days and 7 days after transection. At both time points, the *dhh*$^{-/-}$ nerve show more advanced degeneration, although the difference is more pronounced at 2 days. Note that an increased number of minifascicles is present in the *dhh*$^{-/-}$ nerve at 2 days and 7 days. Scale bars, 2 μm.

B: TUJ1 immunoblotting reveals that TUJ1 levels, an indicator of axon integrity, show a more marked decrease in *dhh*$^{-/-}$ nerves than in *dhh*$^{+/-}$ nerve at 2 days post-transection. P0 levels are not markedly altered at this time.

This confirms the rapid degeneration of axons in the mutants and agrees with previous observations that axonal degeneration precedes loss of myelin (Koeppen, 2004). Counts of macrophages using F4/80 antibodies showed that in *dhh*$^{+/+}$ nerves their number had increased 7-8 fold at 2 days after cut, in line with previous observations (Clemence *et al,* 1989; Perry *et al.,* 1987), while in mutant nerves, macrophage numbers increased only about 2 fold to reach comparable numbers to those seen in cut *dhh*$^{+/+}$ nerve (Fig. 6.2B). Neutrophil invasion is one of the earliest responses to nerve injury and is followed slightly later by the arrival of macrophages (Perkins and Tracey, 2000). Counts of neutrophils using Gr-1 antibodies revealed that in *dhh*$^{+/+}$ nerves their number had risen 8-9 fold 2 days after transection. In *dhh*$^{-/-}$ nerves, however, neutrophil numbers remained unaltered.

Uninjured *dhh*$^{-/-}$ nerves are organised into mini-fascicles, not found in controls (Parmantier et al 1999). Surprisingly, in injured *dhh*$^{-/-}$ nerves the number of mini-fascicles increased rapidly, even from this high baseline, and was elevated by almost 50% on day 2 after transection (Fig. 6.3A). Thus, the number of mini-fascicles in whole transverse sections of *dhh*$^{-/-}$ uninjured nerves was 140, in 2-day transected nerves this figure was 222 and in 7-day transected nerves it was 260 (n=2). Wild type nerves show slow reorganisation into mini-fascicles associated with nerve transection (Bradley et al., 1998).

These data show that uninjured nerves in *dhh*$^{-/-}$ mice undergo spontaneous degeneration and regeneration of myelinated fibres that is not seen in *dhh*$^{+/+}$ or *dhh*$^{+/-}$ animals. Moreover, in uninjured *dhh*$^{-/-}$ nerve, there is an increased number of neutrophils and macrophages in comparison to the wild type. Although it is not clear whether this is the result of infiltration through the permeable vessels/capillaries resulting from the lack of Dhh signalling, or via signals derived directly from Schwann cells. Furthermore, nerve axotomy causes faster degeneration of the fibres in the distal stump of *dhh*$^{-/-}$ nerve.

The ongoing degeneration and regenerating of fibres in *dhh*$^{-/-}$ nerves is a process which brings together some of the observations that had been collected earlier throughout this project. The increased number of SLI in myelinated axons, and decreased compaction of myelin may result in the loss of contact from axons and de-differentiation of Schwann cells which is followed by degeneration of fibres. This could also explain the absence of large diameter axons in *dhh*$^{-/-}$ nerve. However, it is not clear whether the degeneration happens node to node or throughout the entire fibre. A recent attempt to check whether the expression levels of ATF3 transcription factor and c-Jun, both of which come up after nerve injury, were increased in DRG neurons in *dhh*$^{-/-}$ mice failed due to technical problems. There is extensive evidence that macrophages are involved in clearing myelin from demyelinated axons of injured nerves and in transgenic mice in which there is ongoing demyelination and degeneration, such as in P_0 heterozygotes (Carenini *et al.*, 2001), lack of macrophages retards the degenerative process. It is nevertheless not clear to what extent macrophages are involved in this process in *dhh* null nerves, and their involvement in

accelerating the degeneration of fibres remains to be proved. One approach would be to cross dhh null mice with mice that have reduced levels of macrophages and observe whether the degeneration occurs at the same rate. Taken together these results suggest that, although the mechanism of this process is not clear, the increase in SLI number, reduction in MBP, and increase in macrophage number all seem to be involved as sequential events that come together as a response to the loss of Dhh signalling.

It is clear that vascular and perineurial barriers play an important role in maintaining the stability of peripheral nerves. In this case, the abnormal permeability of *dhh*$^{-/-}$ nerves allows an easy and faster access of macrophages and neutrophils to endoneurial nerve fibres and is likely to cause faster degeneration of these fibres following injury. Although the reason behind the unchanged level of neutrophils after nerve injury in *dhh*$^{-/-}$ nerve is not clear, one could speculate that their involvement in recruiting macrophages to the site of injury is not necessary as the macrophages are already present at the site of injury. The reason for faster degeneration of fibre in *dhh*$^{-/-}$ nerves after transection is not clear, although the presence of additional macrophages within the nerve at the time of injury is likely to lead to a more rapid initiation of degeneration. It is also possible that the increased number of SLI reduces the compaction of myelin and hence may facilitate easier and faster break up of myelin by macrophages. In future experiments it would be important to monitor the degenerative process after injury in a more rigorous manner both at different time points and at different distances from the transection both at the electron and light microscopic levels. It would also be interesting to see whether exogenous application

of recombinant Dhh would prevent the ongoing degeneration in normal nerves and slow the degeneration observed after injury.

In conclusion, this chapter shows that there is increased degeneration and regeneration and increased numbers of both macrophages and neutrophils within dhh null nerves in comparison with wild type nerves. Furthermore, after nerve injury degeneration is more rapid than in wild type nerves.

CHAPTER 7

GENERAL DISCUSSION

This study shows compound tissue abnormalities in nerves that lack the signalling protein Dhh. This indicates that the cell-cell signaling networks that maintain tissue homeostasis in peripheral nerves include, and are crucially dependent on, Dhh. Because Dhh is derived from glial cells, these observations also make the general point that in the PNS, glial signals are essential for broad-spectrum tissue integrity. This is likely to apply to glial cells more generally, although, *in vivo*, signalling molecules with this function in mammalian glia do not appear to have been identified previously.

Myelinated Schwann cells in *dhh*$^{-/-}$ mice have more than double the normal number of SLI. While SLI numbers are also increased in MBP-deficient *shi* mice (Gould et al., 1995), it is found that the number of SLI is substantially increased again in *dhh/shi* double mutants, which suggests that Dhh and MBP are likely to control SLI numbers through distinct mechanisms, although the mechanisms may finally converge in a common pathway. One of the molecular components of SLI, Cx29, is strikingly elevated in *dhh*$^{-/-}$ nerves. Non-myelinating Schwann cells (in Remak fibers) are also affected, since Remak fibers with large numbers of axons are reduced in number, while cells that envelop a single axon only are more numerous. The total number of unmyelinated axons is also reduced by a third, while myelinated axons are lost, albeit to a lesser extent. We show that the blood-nerve barrier is permeable in *dhh*$^{-/-}$ mice, a finding that parallels the breakdown of the perineurial diffusion barrier in these animals (Parmantier et al., 1999). In *dhh*$^{-/-}$ nerves, the number of resident macrophages and

neutrophils is also elevated. Significantly, uninjured *dhh*$^{-/-}$ nerves contain a substantial number of degenerating myelinated fibers, which increases with age. They also contain regenerating axons. In addition to this age-dependent neuropathy, degeneration of injured nerves is more rapid in *dhh* animals than in controls.

While Dhh is expressed in myelinating Schwann cells, Hh receptors are mainly found on the perineurial cells (*ptc1*) (Parmantier *et al.*, 1999) and non-myelinating Schwann cells (*ptc2*) (Bajestan *et al.*, 2006). Very low levels of ptc1 are seen on Schwann cells in tissue sections although they can be detected on neonatal cells in culture by RT-PCR. Even in this case, however, they are not up-regulated in response to Hh agonists as expected for *ptc1* and as seen for *ptc1* in fibrobasts. This argues against an autocrine Dhh circuit in myelinating Schwann cells. A more likely mechanism is indicated by the action of Ihh in cartilage. In this case, Ihh from chondrocytes acts on *ptc1* receptors in the perichondrium that surrounds the cartilage and induces the expression of a second signal that acts back on the chondrocytes (Vortkamp et al., 1996). It is therefore possible that Schwann cell-derived Dhh acts on the perineurium that surrounds the nerve, inducing signals that, in turn, act back on Schwann cells and perhaps other elements in the nerve.

It will be a complex task to untangle Dhh-dependent cell-cell signalling networks in peripheral nerves, and to define the sequences that translate the absence of Dhh in myelinating Schwann cells into the set of tissue changes that have been observed. At this point one can only speculate. The breakdown of the tissue-nerve and blood-nerve barriers is likely to alter the chemical composition of the endoneurial space and therefore the microenvironment of the axon-Schwann cell units (Olsson, 1990;

Beamish et al., 1991; Sinnreich et al., 2005). This, however, is unlikely to be the cause of the adverse changes in myelinating Schwann cells - the increase in SLI - because this is already evident at P10, which is before these barriers are effective (Kristensson and Olsson, 1971; Weerasuriya et al., 1990). Similarly, the abnormalities seen in non-myelinating fibres are likely to relate to the striking and selective expression of ptc2 Hh receptors on these cells (Bajestan et al., 2006). Schwann cell defects, in turn, are likely to contribute to the axon loss seen in *dhh*$^{-/-}$ nerves. In the case of myelinating axons this is accompanied by regeneration as we have observed. But it is also plausible to suggest that the large reduction in unmyelinated axons, likely caused by a lack of *ptc2* activation in these cells, leads to the observed remodeling of Remak fibers to accommodate fewer axons per Schwann cell.

It is unclear to what extent the elevated number of neutrophils and macrophages in uncut *dhh-/-* nerves is due to the absence of vascular and perineurial barriers to their entry, or to what degree they are attracted by the ongoing fibre degeneration. The presence of these cells could contribute to fibre instability, because in another model of demyelinating peripheral neuropathy (i.e. *P0*$^{+/-}$ heterozygote mice) there are increased numbers of macrophages within the endoneurium and both resident and blood-borne macrophages play an active role in the demyelination (Carenini et al., 2001; Maurer et al., 2003). In cut *dhh*$^{-/-}$ nerves, the relatively rapid disappearance of TUJ1 only 2 d after injury indicates abnormally fast axonal degeneration and there is a concomitant increase in myelin degradation. This accelerated deterioration in injured nerves may be caused partly by the same factors that cause ongoing axon loss in intact *dhh-/-* nerves. But it is also likely that the increased numbers of resident macrophages and neutrophils play a part, since these cells are known to be crucial to the

degenerative response (Scheidt et al., 1986; Coleman and Perry, 2002). The effect is the converse of that observed in the C57Bl/Wld mouse where a chromosome translocation results in delayed axonal degeneration and myelin degradation (Lunn et al., 1989; Coleman and Perry, 2002).

Extensive investigation of molecules known to be associated with SLI revealed that cx29 was up-regulated at both the mRNA and protein level in *dhh*$^{-/-}$ nerves. This is intriguing because in adult nerves cx29 is localized to the innermost layers of the myelin sheath, showing a striking coincidence with $K_V1.2$ potassium channels in the underlying axonal membrane (Altevogt et al., 2002; Li et al., 2002). Immunohistochemical experiments (not shown) failed, however, to show any increase in $K_V1.2$ channels corresponding to the strong cx29 up-regulation. A small decrease was observed in MBP protein (but not mRNA) levels at older ages only, with minimal changes in MAG protein level. This contrasts with the findings of Smith-Slatas and Barbarese (2000) in *shi* mice, where increased MAG and cx32 protein levels were found in *shi* nerves relative to wildtype nerves, although mRNA levels were unaltered. We did not see an increase in cx32 mRNA levels or in protein levels (not shown). The SLI increase in *dhh-/-* mice therefore appears to be mechanistically different from that in the *shi* mice, a conclusion reinforced by the elevated SLI numbers found in *shh/shi* double mutants. Increased SLI are also seen in Schwann cells in *Caspr/paranodin* null mice (Bhat et al., 2001) and in the CNS in *ceramide galactosyl transferase* null mice (Dupree et al., 1998).

It has recently been reported that E-cadherin is required to stabilize SLI and that dominant negative mutations in E-cadherin that interfere with binding to p120 catenin

cause destabilization and disappearance of SLI (Tricaud *et al.*, 2005). Since there was no increase in E-cadherin levels on western blot, it seems unlikely that alterations in E-cadherin levels are responsible for the increased number of SLI.

It is of great interest that Dhh levels are reduced in experimental diabetic neuropathy (Calcutt *et al.*, 2003). The present finding that a broad-spectrum neuropathy results from Dhh deficiency indicates that the Dhh loss in the neuropathic model may be a significant cause of the pathological changes. This interpretation is also strongly supported by the finding that external Shh, which activates similar signalling pathways to Dhh, restores nerve function to non-diabetic levels and enhances nerve regeneration after injury (Pepinsky *et al.*, 2002; Calcutt *et al.*, 2003; Kusano *et al.*, 2004). Furthermore, it is noteworthy that a number of the faults caused by Dhh deficiency and described, have previously been identified as age–related changes. These include: axonal loss that involves substantially greater reduction in the number of unmyelinated axons than myelinated ones, the presence of regenerating myelinated fibers, increased numbers of resident macrophages, widening of individual SLI, increase in SLI number, and a shift towards fewer axons per non-myelinating Schwann cell in Remak fibers (Kanda et al., 1991; Ceballos et al., 1999; Tabata et al., 2000).

In conclusion, Dhh is clearly required to maintain proper nerve integrity at many different levels. Some possibilities for future experiments have been suggested in the discussion sections of individual chapters. Overall in the future, the use of conditional null mice in which Dhh or its targets can be excised at different times in development or in maturity is likely to lead to a better understanding of the complex events that lead to the nerve pathology. In view of the strong reduction in adult unmyelinated axons and the strong expression of ptc2 in non-myelinating Schwann cells (Bajestan *et*

al., 2006), it would especially interesting to investigate whether a specific knock-out of ptc2 in peripheral nerve would lead to the same reduction in the numbers of unmyelinated fibres that is seen in the *dhh* null nerve. If the phenotype were similar, this would show a direct effect of Dhh derived from myelinating Schwann cells on neighbouring non-myelinating Schwann cells and unmyelinated fibres.

CHAPTER 8

REFERENCES

Adlkofer, K., Martini, R., Aguzzi, A., Zielasek, J., Toyka, K.V., Suter, U. (1995). Hypermyelination and demyelinating peripheral neuropathy in PMP22-deficient mice. *Nat Genet.* **11,** 274-80.

Adlkofer, K., Frei, R., Neuberg, D.H., Zielasek, J., Toyka, K.V., Suter, U. (1997). Heterozygous peripheral myelin protein 22-deficient mice are affected by a progressive demyelinating tomaculous neuropathy. *J Neurosci.* **17,** 4662-71.

Adlkofer, K., Lai, C. (2000). Role of neuregulins in glial cell development. *Glia* **29,** 104-11.

Afar, D.E., Marius, R.M., Salzer, J.L., Stanners, C.P., Braun, P.E., Bell, J.C. (1991). Cell adhesion properties of myelin-associated glycoprotein in L cell fibroblasts. *J Neurosci Res.* **29,** 429-36.

Agrawal HC, Agrawal D. (1991). Proteolipid protein and DM-20 are synthesized by Schwann cells, present in myelin membrane, but they are not fatty acylated. *Neurochem Res.* **16,** 855-8.

Ainger K, Avossa D, Morgan F, Hill SJ, Barry C, Barbarese E, Carson JH. (1993). Transport and localization of exogenous myelin basic protein mRNA microinjected into oligodendrocytes. *J Cell Biol.* **123,** 431-41.

Airaksinen MS, Saarma M. (2002). The GDNF family: signalling, biological functions and therapeutic value. *Nat Rev Neurosci.* **3,** 383-94.

Alberts, B., Bray, D., Lewis, J., Raff, M., Roberts, K., Watson, J. D. (1994). "Molecular Biology of the cell". Garlan Publishing. New York and London.

Altevogt BM, Kleopa KA, Postma FR, Scherer SS, Paul DL. (2002). Connexin29 is uniquely distributed within myelinating glial cells of the central and peripheral nervous systems. *J. Neurosci.* **22,** 6458-70.

Altevogt BM, Paul DL. (2000). Four classes of intercellular channels between glial cells in the CNS. *J Neurosci.* **24,** 4313-23.

Anderson, D. J. (1997). Cellular and molecular biology of neural crest cell lineage determination. *Trends Genet.* **13,** 276-80.

Anzini P, Neuberg DH, Schachner M, Nelles E, Willecke K, Zielasek J, Toyka KV, Suter U, Martini R. (1997). Structural abnormalities and deficient maintenance of peripheral nerve myelin in mice lacking the gap junction protein connexin 32. *J Neurosci.* **17,** 4545-51.

Apionishev, S., Katanayeva, N.M., Marks, S.A., Kalderon, D., and Tomlinson, A. (2005). Drosophila Smoothened phosphorylation sites essential for Hedgehog signal transduction. *Nat Cell Biol.* **7,** 86-92.

Araki T, Milbrandt J. (1996). Ninjurin, a novel adhesion molecule, is induced by nerve injury and promotes axonal growth. *Neuron* **17,** 353-61.

Arbuthnott ER, Boyd IA, Kalu KU. (1980). Ultrastructural dimensions of myelinated peripheral nerve fibres in the cat and their relation to conduction velocity. *J Physiol.* **308,** 125-57.

Archelos JJ, Previtali SC, Hartung HP. (1999). The role of integrins in immune-mediated diseases of the nervous system. *Trends Neurosci.* **22,** 30-8.

Arquint M, Roder J, Chia LS, Down J, Wilkinson D, Bayley H, Braun P, Dunn R. (1987). Molecular cloning and primary structure of myelin-associated glycoprotein. *Proc Natl Acad Sci U S A.* **84,** 600-4.

Arroyo EJ, Bermingham JR Jr, Rosenfeld MG, Scherer SS. (1998). Promyelinating Schwann cells express Tst-1/SCIP/Oct-6. *J Neurosci.* **18,** 7891-902.

Arroyo EJ, Xu YT, Zhou L, Messing A, Peles E, Chiu SY, Scherer SS. (1999). Myelinating Schwann cells determine the internodal localization of Kv1.1, Kv1.2, Kvbeta2, and Caspr. *J Neurocytol.* 28, 333-47.

Atanasoski S, Shumas S, Dickson C, Scherer SS, Suter U. (2001). Differential cyclin D1 requirements of proliferating Schwann cells during development and after injury. *Mol Cell Neurosci.* **18,** 581-92.

Aurrand-Lions M, Duncan L, Ballestrem C, Imhof BA. (2001b). JAM-2, a novel immunoglobulin superfamily molecule, expressed by endothelial and lymphatic cells. *J Biol Chem.* **276,** 2733-41.

Aurrand-Lions M, Johnson-Leger C, Wong C, Du Pasquier L, Imhof BA. (2001a). Heterogeneity of endothelial junctions is reflected by differential expression and specific subcellular localization of the three JAM family members. *Blood* **98,** 3699-707.

Aurrand-Lions MA, Duncan L, Du Pasquier L, Imhof BA. (2000). Cloning of JAM-2 and JAM-3: an emerging junctional adhesion molecular family? Curr Top Microbiol Immunol. **251,** 91-8.

Baechner D, Liehr T, Hameister H, Altenberger H, Grehl H, Suter U, Rautenstrauss B. (1995). Widespread expression of the peripheral myelin protein-22 gene (PMP22) in neural and non-neural tissues during murine development. *J Neurosci Res.* **42,** 733-41.

Bai CB, Auerbach W, Lee JS, Stephen D, Joyner AL. (2002). Gli2, but not Gli1, is required for initial Shh signalling and ectopic activation of the Shh pathway. *Development.* **129,** 4753-61.

Bai CB, Stephen D, Joyner AL. (2004). All mouse ventral spinal cord patterning by hedgehog is Gli dependent and involves an activator function of Gli3. *Dev Cell.* **6,** 103-15.

Bajestan SN, Umehara F, Shirahama Y, Itoh K, Sharghi-Namini S, Jessen KR, Mirsky R and Osame O. (2006). Desert hedgehog-Patched 2 expression in peripheral nerves during Wallerian degeneration and regeneration. *J. Neurobiol.* **66,** 243-55.

Balice-Gordon, R.J., Bone, L.J., and Sherer, S.S. (1998). Functional Gap-junctions in the Schwann cell myelin Sheath. *J. Cell Biol.* **142,** 1095-1104.

Banner LR, Patterson PH. (1994). Major changes in the expression of the mRNAs for cholinergic differentiation factor/leukemia inhibitory factor and its receptor after injury to adult peripheral nerves and ganglia. *Proc Natl Acad Sci U S A.* **91,** 7109-13.

Barembaum, M., Moreno, T.A., LaBonne, C., Sechrist, J. & Bronner-Fraser, M. (2000). Noelin-1 is a secreted glycoprotein involved in generation of the neural crest. *Nat Cell Biol.* **2,** 219-225.

Baroffio A, Dupin E, Le Douarin NM. (1988). Clone-forming ability and differentiation potential of migratory neural crest cells. *Proc. Natl. Acad. Sci. USA.* **85,** 5325-5329.

Baroffio A, Dupin E, Le Douarin NM. (1991). Common precursors for neural and mesectodermal derivatives in the cephalic neural crest. *Development* **112,** 301-305.

Baron P, Shy M, Honda H, Sessa M, Kamholz J, Pleasure D. (1994). Developmental expression of P0 mRNA and P0 protein in the sciatic nerve and the spinal nerve roots of the rat. *J Neurocytol.* **23,** 249-57.

Barres BA, Raff MC. (1994). Control of oligodendrocyte number in the developing rat optic nerve. *Neuron* **12,** 935-42.

Bartoszewicz ZP, Noronha AB, Fujita N, Sato S, Bo L, Trapp BD, Quarles RH. (1995). Abnormal expression and glycosylation of the large and small isoforms of myelin-associated glycoprotein in dysmyelinating quaking mutants. *J Neurosci Res.* **41,** 27-38.

Beamish NG, Stolinski C, Thomas PK, King RH. (1991). Freeze-fracture observations on normal and abnormal human perineurial tight junctions: alterations in diabetic polyneuropathy. *Acta Neuropathol (Berl).* **81,** 269-79.

Bell MA, Weddell AG. (1984). A descriptive study of the blood vessels of the sciatic nerve in the rat, man and other mammals. *Brain.* **107,** 871-98.

Benjamins, J. A., and Smith, M. E. (1984). *Metabolism of Myelin.* In "Myelin" Morell, P.0, pp. 225-258. Plenum Press, New York.

Bennett V, Baines AJ. (2001). Spectrin and ankyrin-based pathways: metazoan inventions for integrating cells into tissues. *Physiol Rev.* **81,** 1353-92.

Bennett V, Lambert S. (1999). Physiological roles of axonal ankyrins in survival of premyelinated axons and localization of voltage-gated sodium channels. *J Neurocytol.* **28,** 303-18.

Berghs S, Aggujaro D, Dirkx R Jr, Maksimova E, Stabach P, Hermel JM, Zhang JP, Philbrick W, Slepnev V, Ort T, Solimena M. (2000). betaIV spectrin, a new spectrin localized at axon initial segments and nodes of ranvier in the central and peripheral nervous system. *J Cell Biol.* **151,** 985-1002.

Bergoffen J, Scherer SS, Wang S, Scott MO, Bone LJ, Paul DL, Chen K, Lensch MW, Chance PF, Fischbeck KH. (1993). Connexin mutations in X-linked Charcot-Marie-Tooth disease. *Science* **262,** 2039-42.

Bermingham JR Jr, Scherer SS, O'Connell S, Arroyo E, Kalla KA, Powell FL, Rosenfeld MG. (1996). Tst-1/Oct-6/SCIP regulates a unique step in peripheral myelination and is required for normal respiration. *Genes Dev.* **10,** 1751-1762.

Bermingham-McDonogh O, Xu YT, Marchionni MA, Scherer SS. (1997). Neuregulin expression in PNS neurons: isoforms and regulation by target interactions. *Mol Cell Neurosci.* **10,** 184-95.

Bhat MA, Rios JC, Lu Y, Garcia-Fresco GP, Ching W, St Martin M, Li J, Einheber S, Chesler M, Rosenbluth J, Salzer JL, Bellen HJ. (2001). Axon-glia interactions and the domain organization of myelinated axons requires neurexin IV/Caspr/Paranodin. *Neuron* **30,** 369-83.

Bhat RV, Worley PF, Cole AJ, Baraban JM. (1992). Activation of the zinc finger encoding gene krox-20 in adult rat brain: comparison with zif268. *Brain Res Mol Brain Res.* **13,** 263-6.

Bhattacharyya A, Brackenbury R, Ratner N. (1994). Axons arrest the migration of Schwann cell precursors. *Development* **120,** 1411-20.

Bhattacharyya A, Frank E, Ratner N, Brackenbury R. (1991). P0 is an early marker of the Schwann cell lineage in chickens. *Neuron* **7,** 831-44.

Bigbee JW, Yoshino JE, DeVries GH. (1987). Morphological and proliferative responses of cultured Schwann cells following rapid phagocytosis of a myelin-enriched fraction. *J Neurocytol.* **16,** 487-96.

Bignami, A., Chi, N. H., Dahl, D. (1984). First appearance of laminin in the peripheral nerve, cerebral blood vessels and skeletal muscle of the rat embryo. *Int. J. Dev. Neurosci.* **2,** 367-376.

Billings-Gagliardi S, Webster HF, O'Connell MF. (1974). In vivo and electron microscopic observations on Schwann cells in developing tadpole nerve fibers. *Am J Anat.* **141,** 375-91.

Bitgood MJ, Shen L, McMahon AP. (1996). Sertoli cell signaling by Desert hedgehog regulates the male germline. *Curr Biol.* **6,** 298-304.

Bitgood, M.J. and McMahon, A.P. (1995). Hedgehog and bmp genes are co-expressed at many diverse sites of cell-cell interaction in the mouse embryo. *Dev. Biol.* **172,** 126-138.

Bixby S, Kruger GM, Mosher JT, Joseph NM, Morrison SJ. (2002). Cell-intrinsic differences between stem cells from different regions of the peripheral nervous system regulate the generation of neural diversity. *Neuron* **35,** 643-56.

Bizzozero OA, Odykirk TS, McGarry JF, Lees MB. (1989). Separation of the major proteins of central and peripheral nervous system myelin using reversed-phase high-performance liquid chromatography. *Anal Biochem.* **180,** 59-65.

Blanchard AD, Sinanan A, Parmantier E, Zwart R, Broos L, Meijer D, Meier C, Jessen KR, Mirsky R. (1996). Oct-6 (SCIP/Tst-1) is expressed in Schwann cell precursors, embryonic Schwann cells, and postnatal myelinating Schwann cells: comparison with Oct-1, Krox-20, and Pax-3. *J Neurosci Res.* **46,** 630-40.

Boison D, Bussow H, D'Urso D, Muller HW, Stoffel W. (1995). Adhesive properties of proteolipid protein are responsible for the compaction of CNS myelin sheaths. *J Neurosci.* **15,** 5502-13.

Boison D, Stoffel W. (1994). Disruption of the compacted myelin sheath of axons of the central nervous system in proteolipid protein-deficient mice. *Proc Natl Acad Sci U S A.* **91,** 11709-13.

Bolin LM, Verity AN, Silver JE, Shooter EM, Abrams JS. (1995). Interleukin-6 production by Schwann cells and induction in sciatic nerve injury. *J Nerochem.* **64,** 850-8.

Bondurand N, Girard M, Pingault V, Lemort N, Dubourg O, Goossens M. (2001). Human Connexin 32, a gap junction protein altered in the X-linked form of Charcot-Marie-Tooth disease, is directly regulated by the transcription factor SOX10. *Hum Mol Genet.* **10,** 2783-95.

Bosse F, Kury P, Muller HW. (2001). Gene expression profiling and molecular aspects in peripheral nerve regeneration. *Restor Neurol Neurosci.* **19,** 5-18.

Bourguignon LY, Chu A, Jin H, Brandt NR. (1995). Ryanodine receptor-ankyrin interaction regulates internal Ca2+ release in mouse T-lymphoma cells. *J Biol Chem.* **270,** 17917-22.

Bourguignon LY, Jin H, Iida N, Brandt NR, Zhang SH. (1993). The involvement of ankyrin in the regulation of inositol 1,4,5-trisphosphate receptor-mediated internal Ca2+ release from Ca2+ storage vesicles in mouse T-lymphoma cells. *J Biol Chem.* **268,** 7290-7.

Bradley JL, Abernethy DA, King RH, Muddle JR, Thomas PK. (1998). Neural architecture in transected rabbit sciatic nerve after prolonged nonreinnervation. *J Anat.* **192,** 529-38.

Bradley WG, Jenkison M. (1973). Abnormalities of peripheral nerves in murine muscular dystrophy. *J Neurol Sci.* **18,** 227-47.

Braun, P. E., Lee, J., Gravel, M. (2004). 2',3'-Cyclic nucleotide 3'-phosphodiestrase: Structure, Biology, and Function. In "*Myelin biology and disorders*". PP 499-522. Elsevier academic press,

Brennan A, Dean CH, Zhang AL, Cass DT, Mirsky R, Jessen KR. (2000). Endothelins control the timing of Schwann cell generation in vitro and in vivo. *Dev. Biol.* **227,** 545-57.

Britsch, S., Goerich, D.E., Riethmacher, D., Peirano, R.I., Rossner, M., Nave, K.A., Birchmeier, C., and Wegner, M. (2001). The transcription factor Sox10 is a key regulator of peripheral glial development. *Genes Dev.* **15,** 66-78.

Brockes JP, Raff MC. (1979). Studies on cultured rat Schwann cells. II. Comparison with a rat Schwann cell line. *In Vitro* **15,** 772-8.

Bronner-Fraser M, Stern C. (1991). Effects of mesodermal tissues on avian neural crest cell migration. *Dev Biol.* **143,** 213-7.

Brunet LJ, McMahon JA, McMahon AP, Harland RM. (1998). Noggin, cartilage morphogenesis, and joint formation in the mammalian skeleton. *Science* **280,** 1455-7.

Bruzzone R, White TW, Scherer SS, Fischbeck KH, Paul DL. (1994). Null mutations of connexin32 in patients with X-linked Charcot-Marie-Tooth disease. *Neuron* **13,** 1253-60.

Bruzzone R, White TW, Paul DL. (1996). Connections with connexins: the molecular basis of direct intercellular signaling. *Eur J Biochem.* **238,** 1-27.

Bunge, M.B., Wood, P.M., Tynan, L.B., Bates, M.L., and Sanes, J.R. (1989). Perineurium originates from fibroblasts; demonstration *in vitro* with a retroviral marker. *Science* **243,** 229-231.

Bunge RP, Bunge MB, Eldridge CF. (1986). Linkage between axonal ensheathment and basal lamina production by Schwann cells. *Annu Rev Neurosci.* **9,** 305-28.

Burstyn-Cohen T, Frumkin A, Xu YT, Scherer SS, Klar A. (1998), Accumulation of F-spondin in injured peripheral nerve promotes the outgrowth of sensory axons. *J Neurosci.* **18,** 8875-85.

Bushdid PB, Brantley DM, Yull FE, Blaeuer GL, Hoffman LH, Niswander L, Kerr LD. (1998). Inhibition of NF-kappaB activity results in disruption of the apical ectodermal ridge and aberrant limb morphogenesis. *Nature* **392,** 615-658.

Byrd N, Grabel L. (2004). Hedgehog signaling in murine vasculogenesis and angiogenesis. *Trends Cardiovasc Med.* **14,** 308-13.

Calcutt NA, Allendoerfer KL, Mizisin AP, Middlemas A, Freshwater JD, Burgers M, Ranciato R, Delcroix JD, Taylor FR, Shapiro R, Strauch K, Dudek H, Engber TM, Galdes A, Rubin LL, Tomlinson DR. (2003). Therapeutic efficacy of sonic hedgehog protein in experimental diabetic neuropathy. *J Clin Invest.* **111,** 507-14.

Campagnoni AT, Pribyl TM, Campagnoni CW, Kampf K, Amur-Umarjee S, Landry CF, Handley VW, Newman SL, Garbay B, Kitamura K. (1993). Structure and developmental regulation of Golli-mbp, a 105-kilobase gene that encompasses the myelin basic protein gene and is expressed in cells in the oligodendrocyte lineage in the brain. *J Biol Chem.* **268,** 4930-8.

Campana WM, Darin SJ, O'Brien JS. (1999). Phosphatidylinositol 3-kinase and Akt protein kinase mediate IGF-I- and prosaptide-induced survival in Schwann cells. *J Neurosci Res.* **57,** 332-341.

Carenini S, Maurer M, Werner A, Blazyca H, Toyka KV, Schmid CD, Raivich G, Martini R. (2001). The role of macrophages in demyelinating peripheral nervous system of mice heterozygously deficient in p0. *J Cell Biol.* **152,** 301-8.

Carpenter, D., Stone, D.M., Brush, J., Ryan, A., Armanian, M., Frantz, G., Rosenthal, A., and De Sauvage, F.J. (1998). Characterization of two patched receptor for the vertebrate hedgehog protein family. Proc. *Natl. Acad. Sci. USA.* **95,** 13630-13634.

Carpenter EM, Hollyday M. (1992a). The location and distribution of neural crest-derived Schwann cells in developing peripheral nerves in the chick forelimb. *Dev Biol.* **150,** 144-59.

Carpenter EM, Hollyday M. (1992b). The distribution of neural crest-derived Schwann cells from subsets of brachial spinal segments into the peripheral nerves innervating the chick forelimb. *Dev Biol.* **150,** 160-70.

Carraway KL, Carraway CA, Carraway KL 3rd. (1997). Roles of ErbB-3 and ErbB-4 in the physiology and pathology of the mammary gland. *J Mammary Gland Biol Neoplasia.* **2,** 187-98.

Carraway KL III, Cantley LC. (1994). A neu acquaintance for erbB3 and erbB4: a role for receptor heterodimerization in growth signaling. *Cell* **78,** 5-8.

Carroll SL, Miller ML, Frohnert PW, Kim SS, Corbett JA. (1997). Expression of neuregulins and their putative receptors, ErbB2 and ErbB3, is induced during Wallerian degeneration. *J Neurosci.* **17,** 1642-59.

Ceballos D, Cuadras J, Verdu E, Navarro X. (1999). Morphometric and ultrastructural changes with ageing in mouse peripheral nerve. *J Anat.* **195,** 563-76.

Ceccherini I, Zhang AL, Matera I, Yang G, Devoto M, Romeo G, Cass DT. (1995). Interstitial deletion of the endothelin-B receptor gene in the spotting lethal (sl) rat. *Hum Mol Genet.* **4,** 2089-96.

Chao MV, Bothwell MA, Ross AH, Koprowski H, Lanahan AA, Buck CR, Sehgal A. (1986). Gene transfer and molecular cloning of the human NGF receptor. *Science* **232,** 518-21.

Chavrier P, Zerial M, Lemaire P, Almendral J, Bravo R, Charnay P. (1988). A gene encoding a protein with zinc fingers is activated during G0/G1 transition in cultured cells. *EMBO J.* **7,** 29-35.

Chen MS, Bermingham-McDonogh O, Danehy FT Jr, Nolan C, Scherer SS, Lucas J, Gwynne D, Marchionni MA. (1994). Expression of multiple neuregulin transcripts in postnatal rat brains. *J Comp Neurol.* **349,** 389-400.

Chen MH, Gao N, Kawakami T, Chuang PT. (2005). Mice deficient in the fused homolog do not exhibit phenotypes indicative of perturbed hedgehog signalling during embryonic development. *Mol Cell Biol.* **25,** 7042-53.

Chen S, Rio C, Ji RR, Dikkes P, Coggeshall RE, Woolf CJ, Corfas G. (2003). Disruption of ErbB receptor signaling in adult non-myelinating Schwann cells causes progressive sensory loss. *Nat Neurosci.* **6,** 1186-93.

Chen W, Ren XR, Nelson CD, Barak LS, Chen JK, Beachy PA, de Sauvage F, lefkowitz RJ. (2004). Activity-dependent internalization of smoothened mediated by beta-arrestin 2 and GRK2. *Science.* **306,** 2257-60.

Cheng HL, Feldman EL. (1997). Insulin-like growth factor-I (IGF-I) and IGF binding protein-5 in Schwann cell differentiation. *J Cell Physiol.* **171,** 161-7.

Cheng HL, Shy M, Feldman EL. (1999). Regulation of insulin-like growth factor-binding protein-5 expression during Schwann cell differentiation. *Endocrinology.* **140,** 4478-85.

Cheng HL, Steinway M, Delaney CL, Franke TF, Feldman EL. (2000). IGF-I promotes Schwann cell motility and survival via activation of Akt. *Mol Cell Endocrinol.* **170,** 211-215.

Cheng L, Esch FS, Marchionni MA, Mudge AW. (1998). Control of Schwann cell survival and proliferation: autocrine factors and neuregulins. *Mol Cell Neurosci.* **12,** 141-56.

Cheng N, Brantley DM, Liu H, Lin Q, Enriquez M, Gale N, Yancopoulos G, Cerretti DP, Daniel TO, Chen J. (2002). Blockade of EphA receptor tyrosine kinase activation inhibits vascular endothelial cell growth factor-induced angiogenesis. *Mol Cancer Res.* **1,** 2-11.

Cheng, S.Y., and Bishop, J.M. (2002). Suppressor of Fused represses Gli-mediated transcription by recruiting the SAP18-mSin3 corepressor complex. *Proc. Natl. Acad. Sci. USA.* **99,** 5442-7.

Chernousov MA, Scherer SS, Stahl RC, Carey DJ. (1999). p200, a collagen secreted by Schwann cells, is expressed in developing nerves and in adult nerves following axotomy. *J Neurosci Res.* **56,** 284-94.

Choi K, Kennedy M, Kazarov A, Papadimitriou JC, Keller G. (1998). A common precursor for hematopoietic and endothelial cells. *Development* **125,** 725-32.

Christy BA, Lau LF, Nathans D. (1988). A gene activated in mouse 3T3 cells by serum growth factors encodes a protein with "zinc finger" sequences. *Proc Natl Acad Sci U S A.* **85,** 7857-61.

Clark, A.M., Garland, K.K., Russell, L.D. (2000). Desert hedgehog (Dhh) gene is required in the mouse testis for formation of adult-type Leydig cells and normal development of peritubular cells and seminiferous tubules. *Biol Reprod.* **63,** 825-38.

Clemence A, Mirsky R, Jessen KR. (1989). Non-myelin-forming Schwann cells proliferate rapidly during Wallerian degeneration in the rat sciatic nerve. *J Neurocytol.* **18,** 185-92.

Coetzee T, Dupree JL, Popko B. (1998). Demyelination and altered expression of myelin-associated glycoprotein isoforms in the central nervous system of galactolipid-deficient mice. *J Neurosci Res.* **54,** 613-22.

Coetzee T, Fujita N, Dupree J, Shi R, Blight A, Suzuki K, Suzuki K, Popko B. (1996a). Myelination in the absence of galactocerebroside and sulfatide: normal structure with abnormal function and regional instability. *Cell* **86,** 209-19.

Coetzee T, Li X, Fujita N, Marcus J, Suzuki K, Francke U, Popko B. (1996b). Molecular cloning, chromosomal mapping, and characterization of the mouse UDP-galactose:ceramide galactosyltransferase gene. *Genomics* **35,** 215-22.

Coleman MP, Perry VH. (2002). Axon pathology in neurological disease: a neglected therapeutic target. *Trends Neurosci.* **25,** 532-7.

Colman DR, Kreibich G, Frey AB, Sabatini DD. (1982). Synthesis and incorporation of myelin polypeptides into CNS myelin. *J Cell Biol.* **95,** 598-608.

Conlon IJ, Dunn GA, Mudge AW, Raff MC. (2001). Extracellular control of cell size. *Nat Cell Biol.* **3,** 918-21.

Cooper AF, Yu KP, Brueckner M, Brailey LL, Johnson L, McGrath JM, Bale AE. (2005). Cardiac and CNS defects in a mouse with targeted disruption of suppressor of fused. *Development.* **132,** 4407-17.

Cornbrooks CJ, Carey DJ, McDonald JA, Timpl R, Bunge RP. (1983). In vivo and in vitro observations on laminin production by Schwann cells. *Proc Natl Acad Sci U S A.* **80,** 3850-4.

Court FA, Sherman DL, Pratt T, Garry EM, Ribchester RR, Cottrell DF, Fleetwood-Walker SM, Brophy PJ. (2004). Restricted growth of Schwann cells lacking Cajal bands slows conduction in myelinated nerves. *Nature* **431,** 191-5.

Crovello CS, Lai C, Cantley LC, Carraway KL 3rd. (1998). Differential signaling by the epidermal growth factor-like growth factors neuregulin-1 and neuregulin-2. *J Biol Chem.* **273,** 26954-61.

Curtis R, Stewart HJ, Hall SM, Wilkin GP, Mirsky R, Jessen KR. (1992). GAP-43 is expressed by nonmyelin-forming Schwann cells of the peripheral nervous system. *J Cell Biol.* **116,** 1455-64.

D'Urso D, Brophy PJ, Staugaitis SM, Gillespie CS, Frey AB, Stempak JG, Colman DR. (1990). Protein zero of peripheral nerve myelin: biosynthesis, membrane insertion, and evidence for homotypic interaction. *Neuron* **4,** 449-60.

D'Urso D, Ehrhardt P, Muller HW. (1999). Peripheral myelin protein 22 and protein zero: a novel association in peripheral nervous system myelin. *J Neurosci.* **19,** 3396-403.

D'Urso D, Prior R, Greiner-Petter R, Gabreels-Festen AA, Muller HW. (1998). Overloaded endoplasmic reticulum-Golgi compartments, a possible pathomechanism of peripheral neuropathies caused by mutations of the peripheral myelin protein PMP22. *J Neurosci.* **18,** 731-40.

Dai, P., Akimaru, H., and Ishii, S.A. (2003). A hedgehog-responsive region in the Drosophila wing disc is defined by debra-mediated ubiquitination and lysosomal degradation of Ci. *Dev. Cell.* **4,** 917-928.

Davis JQ, Bennett V. (1994). Ankyrin binding activity shared by the neurofascin/L1/NrCAM family of nervous system cell adhesion molecules. *J Biol Chem.* **269,** 27163-6.

Davis JQ, McLaughlin T, Bennett V. (1993). Ankyrin-binding proteins related to nervous system cell adhesion molecules: candidates to provide transmembrane and intercellular connections in adult brain. *J Cell Biol.* **121,** 121-133.

de Ferra F, Engh H, Hudson L, Kamholz J, Puckett C, Molineaux S, Lazzarini RA. (1985). Alternative splicing accounts for the four forms of myelin basic protein. *Cell* **43,** 721-7.

De Leon M, Nahin RL, Mendoza ME, Ruda MA. (1994). SR13/PMP-22 expression in rat nervous system, in PC12 cells, and C6 glial cell lines. *J Neurosci Res.* **38,** 167-81.

De Leon M, Welcher AA, Suter U, Shooter EM. (1991). Identification of transcriptionally regulated genes after sciatic nerve injury. *J Neurosci Res.* **29,** 437-48.

de Waegh SM, Lee VM, Brady ST. (1992). Local modulation of neurofilament phosphorylation, axonal caliber, and slow axonal transport by myelinating Schwann cells. *Cell* **68,** 451-63.

Debby-Brafman, A., Burstyn-Cohen, T., Klar, A., and Kalcheim, C. (1999). F-spondin, expressed in somite regions avoided by neural crest cells, mediates inhibition of distinct somite domains to neural crest migration. *Neuron* **22,** 475-488.

DeBellard ME, Tang S, Mukhopadhyay G, Shen YJ, Filbin MT. (1996). Myelin-associated glycoprotein inhibits axonal regeneration from a variety of neurons via interaction with a sialoglycoprotein. *Mol Cell Neurosci.* **7,** 89-101.

Deerinck TJ, Levinson SR, Bennett GV, Ellisman MH. (1997). Clustering of voltage-sensitive sodium channels on axons is independent of direct Schwann cell contact in the dystrophic mouse. *J Neurosci.* **17,** 5080-8.

Delaney CL, Cheng HL, Feldman EL. (1999). Insulin-like growth factor-I prevents caspase-mediated apoptosis in Schwann cells. *J. neurobiol.* **41,** 540-548.

Delaunay, J. (2002). Molecular basis of red cell membrane disorders. *Acta Haematol.* **108,** 210-8.

Devarajan P, Stabach PR, Mann AS, Ardito T, Kashgarian M, Morrow JS. (1996). Identification of a small cytoplasmic ankyrin (AnkG119) in the kidney and muscle that binds beta I sigma spectrin and associates with the Golgi apparatus. *J Cell Biol.* **133,** 819-30.

Diehl HJ, Schaich M, Budzinski RM, Stoffel W. (1986). Individual exons encode the integral membrane domains of human myelin proteolipid protein. *Proc Natl Acad Sci U S A.* **83,** 9807-11.

Diner, O. (1965). The Schwann cells during mitosis and their relation to the axons during the development of the sciatic nerve in the rat. *C R Acad Sci Hebd Seances Acad Sci D.* **261,** 1731-34.

Dong Z, Brennan A, Liu N, Yarden Y, Lefkowitz G, Mirsky R, Jessen KR. (1995). Neu differentiation factor is a neuron-glia signal and regulates survival, proliferation, and maturation of rat Schwann cell precursors. *Neuron* **15,** 585-96.

Dong Z, Dean C, Walters JE, Mirsky R, Jessen KR. (1997). Response of Schwann cells to mitogens in vitro is determined by pre-exposure to serum, time in vitro, and developmental age. *Glia* **20,** 219-30.

Dong Z, Sinanan A, Parkinson D, Parmantier E, Mirsky R, Jessen KR. (1999). Schwann cell development in embryonic mouse nerves. *J Neurosci Res.* **56,** 334-48.

Dowsing BJ, Morrison WA, Nicola NA, Starkey GP, Bucci T, Kilpatrick TJ. (1999). Leukemia inhibitory factor is an autocrine survival factor for Schwann cells. *J Nerochem.* **73,** 96-104.

Dubreuil RR, MacVicar G, Dissanayake S, Liu C, Homer D, Hortsch M. (1996). Neuroglian-mediated cell adhesion induces assembly of the membrane skeleton at cell contact sites. *J Cell Biol.* **133,** 647-55.

Duncan ID, Hammang JP, Trapp BD. (1987). Abnormal compact myelin in the myelin-deficient rat: absence of proteolipid protein correlates with a defect in the intraperiod line. *Proc Natl Acad Sci U S A.* **84,** 6287-91.

Dupin E, Baroffio A, Dulac C, Cameron-Curry P, Le Douarin NM. (1990). Schwann-cell differentiation in clonal cultures of the neural crest, as evidenced by the anti-Schwann cell myelin protein monoclonal antibody. *Proc. Natl. Acad. Sci. USA.* **87,** 1119-1123.

Dupin E, Real C, Glavieux-Pardanaud C, Vaigot P, Le Douarin NM. (2003). Reversal of developmental restrictions in neural crest lineages: transition from Schwann cells to glial-melanocytic precursors in vitro. Proc. *Natl. Acad. Sci. USA.* **100,** 5229-33.

Dupin E, Ziller C, Le Douarin NM. (1998). The avian embryo as a model in developmental studies: chimeras and in vitro clonal analysis. *Curr. Top. Dev. Biol.* **36,** 1-35.

Dupree JL, Coetzee T, Suzuki K, Popko B. (1998). Myelin abnormalities in mice deficient in galactocerebroside and sulfatide. *J Neurocytol.* **27,** 649-59.

Dytrych L, Sherman DL, Gillespie CS, Brophy PJ. (1998). Two PDZ domain proteins encoded by the murine periaxin gene are the result of alternative intron retention and are differentially targeted in Schwann cells. *J Biol Chem.* **273,** 5794-800.

Eames RA, Gamble HJ. (1970). Schwann cell relationships in normal human cutaneous nerves. *J Anat.* **106,** 417-35.

Ebnet K, Suzuki A, Ohno S, Vestweber D. (2004). Junctional adhesion molecules (JAMs): more molecules with dual functions? *J Cell Sci.* **117,** 19-29.

Edelman, GM. (1983). Cell adhesion molecules. *Science.* **219,** 450-7.

Edelman GM, Crossin KL. (1991). Cell adhesion molecules: implications for a molecular histology. *Annu Rev Biochem.* **60,** 155-90.

Eichberg, J. (2002). Myelin P0: new knowledge and new roles. *Neurochem Res.* **27,** 1331-40.

Einheber S, Milner TA, Giancotti F, Salzer JL. (1993). Axonal regulation of Schwann cell integrin expression suggests a role for alpha 6 beta 4 in myelination. *J Cell Biol.* **123,** 1223-36.

Einheber S, Zanazzi G, Ching W, Scherer S, Milner TA, Peles E, Salzer JL. (1997). The axonal membrane protein Caspr, a homologue of neurexin IV, is a component of the septate-like paranodal junctions that assemble during myelination. *J Cell Biol.* **139,** 1495-506.

Eldridge CF, Bunge MB, Bunge RP. (1989). Differentiation of axon-related Schwann cells in vitro: II. Control of myelin formation by basal lamina. *J Neurosci.* **9,** 625-38.

Epstein DJ, Vekemans M, Gros P. (1991). Splotch (Sp2H), a mutation affecting development of the mouse neural tube, shows a deletion within the paired homeodomain of Pax-3. *Cell* **67,** 767-774.

Erickson CA, Duong TD, Tosney KW. (1992). Descriptive and experimental analysis of the dispersion of neural crest cells along the dorsolateral path and their entry into ectoderm in the chick embryo. *Dev Biol.* **151,** 251-72.

Erickson CA, Goins TL. (1995). Avian neural crest cells can migrate in the dorsolateral path only if they are specified as melanocytes. *Development* **121,** 915-24.

Faissner A, Kruse J, Nieke J, Schachner M. (1984). Expression of neural cell adhesion molecule L1 during development, in neurological mutants and in the peripheral nervous system. *Brain Res.* **17,** 69-82.

Falls D.L., Rosen K.M., Corfas G.,Lane W.S., Fischbach G.D. (1993). ARIA, a protein that stimulates acetylcholine receptor synthesis, is a member of the neu ligand family. *Cell* **72,** 801-815.

Fannon AM, Sherman DL, Ilyina-Gragerova G, Brophy PJ, Friedrich VL Jr, Colman DR. (1995). Novel E-cadherin-mediated adhesion in peripheral nerve: Schwann cell architecture is stabilized by autotypic adherens junctions. *J Cell Biol.* **129,** 189-202.

Feltri ML, Graus Porta D, Previtali SC, Nodari A, Migliavacca B, Cassetti A, Littlewood-Evans A, Reichardt LF, Messing A, Quattrini A, Mueller U, Wrabetz L. (2002). Conditional disruption of beta 1 integrin in Schwann cells impedes interactions with axons. *J Cell Biol.* **156,** 199-209.

Feltri ML, Scherer SS, Nemni R, Kamholz J, Vogelbacker H, Scott MO, Canal N, Quaranta V, Wrabetz L. (1994). Beta 4 integrin expression in myelinating Schwann cells is polarized, developmentally regulated and axonally dependent. *Development* **120,** 1287-301.

Feltri ML, Wrabetz L. (2005). Laminins and their receptors in Schwann cells and hereditary neuropathies. *J Peripher Nerv Syst.* **10,** 128-43.

Fernandez-Valle C, Bunge RP, Bunge MB. (1995). Schwann cells degrade myelin and proliferate in the absence of macrophages: evidence from in vitro studies of Wallerian degeneration. *J Neurocytol.* **24,** 667-79.

Ferri CC, Bisby MA. (1999). Improved survival of injured sciatic nerve Schwann cells in mice lacking the p75 receptor. *Neurosci Lett.* **272,** 191-4.

ffrench-Constant, C. (2004). Integrins. In "Myelin biology and disorders". PP 609-632. Elsevier academic press.

Figlewicz DA, Quarles RH, Johnson D, Barbarash GR, Sternberger NH. (1981). Biochemical demonstration of the myelin-associated glycoprotein in the peripheral nervous system. *J Neurochem.* **37,** 749-58.

Filbin MT, Walsh FS, Trapp BD, Pizzey JA, Tennekoon GI. (1990). Role of myelin P0 protein as a homophilic adhesion molecule. *Nature* **344,** 871-2.

Fischer I, Sapirstein VS. (1994). Molecular cloning of plasmolipin. Characterization of a novel proteolipid restricted to brain and kidney. *J Biol Chem.* **269,** 24912-9.

Frank M, Schaeren-Wiemers N, Schneider R, Schwab ME. (1999). Developmental expression pattern of the myelin proteolipid MAL indicates different functions of MAL for immature Schwann cells and in a late step of CNS myelinogenesis. *J Nerochem.* **73,** 589-97.

Franz, T. (1993). The Splotch (Sp1H) and Splotch-delayed (Spd) alleles: differential phenotypic effects on neural crest and limb musculature. *Anat Embryol (Berl).* **187,** 371-377.

Frei R, Dowling J, Carenini S, Fuchs E, Martini R. (1999). Myelin formation by Schwann cells in the absence of beta4 integrin. *Glia* **27,** 269-74.

Fressinaud C, Rigaud M, Vallat JM. (1986). Fatty acid composition of endoneurium and perineurium from adult rat sciatic nerve. *J Neurochem.* **46,** 1549-54.

Fruttiger M, Montag D, Schachner M, Martini R. (1995). Crucial role for the myelin-associated glycoprotein in the maintenance of axon-myelin integrity. *Eur J Neurosci.* **7,** 511-5.

Fruttiger M, Schachner M, Martini R. (1995b). Tenascin-C expression during wallerian degeneration in C57BL/Wlds mice: possible implications for axonal regeneration. *J Neurocytol.* **24,** 1-14.

Fu SY, Gordon T. (1997). The cellular and molecular basis of peripheral nerve regeneration. *Mol Neurobiol.* **14,** 67-116.

Galili N, Davis RJ, Fredericks WJ, Mukhopadhyay S, Rauscher FJ 3rd, Emanuel BS, Rovera G, Barr FG. (1993). Fusion of a fork head domain gene to PAX3 in the solid tumour alveolar rhabdomyosarcoma. *Nat Genet.* **5,** 230-5.

Gammill, L.S. & Bronner-Fraser, M. (2003). Neural crest specification: migrating into genomics. *Nat. Rev. Neurosci.* **4,** 795-805.

Garbay B, Heape AM, Sargueil F, Cassagne C. (2000). Myelin synthesis in the peripheral nervous system. *Prog Neurobiol.* **61,** 267-304.

Garbern JY, Cambi F, Tang XM, Sima AA, Vallat JM, Bosch EP, Lewis R, Shy M, Sohi J, Kraft G, Chen KL, Joshi I, Leonard DG, Johnson W, Raskind W, Dlouhy SR, Pratt V, Hodes ME, Bird T, Kamholz J. (1997). Proteolipid protein is necessary in peripheral as well as central myelin. *Neuron* **19,** 205-18.

Garcia-Castro MI, Marcelle C, Bronner-Fraser M. (2002). Ectodermal Wnt function as a neural crest inducer. *Science* **297,** 848-51.

Garcia-Garcia MJ, Eggenschwiler JT, Caspary T, Alcorn HL, Wyler MR, Huangfu D, Rakeman AS, Lee JD, Feinberg EH, Timmer JR, Anderson KV. (2005). Analysis of mouse embryonic patterning and mophogenesis by forward genetics. *Proc Natl Acad Sci USA.* **102,** 5910-2.

Garratt AN, Britsch S, Birchmeier C. (2000a). Neuregulin, a factor with many functions in the life of a schwann cell. *Bioessays.* **11,** 987-96.

Garratt AN, Voiculescu O, Topilko P, Charnay P, Birchmeier C. (2000b). A dual role of erbB2 in myelination and in expansion of the schwann cell precursor pool. *J Cell Biol.* **148,** 1035-46.

Gassmann M, Casagranda F, Orioli D, Simon H, Lai C, Klein R, Lemke G. (1995). Aberrant neural and cardiac development in mice lacking the ErbB4 neuregulin receptor. *Nature* **378,** 390-4.

Geren, B. B., and Raskind, J. (1953). Development of the fine structure of the myelin sheath in sciatic nerves of chick embryo. *Proc Natl Acad Sci U S A.* **39,** 880-884.

Ghabriel, M.N., and Allt, G. (1981). Incisures of Schmidt-Lanterman. *Progress in neurobiology.* **17,** 25-58.

Ghazvini M, Mandemakers W, Jaegle M, Piirsoo M, Driegen S, Koutsourakis M, Smit X, Grosveld F, Meijer D. (2002). A cell type-specific

allele of the POU gene Oct-6 reveals Schwann cell autonomous function in nerve development and regeneration. *EMBO J.* **21,** 4612-20.

Ghislain J, Desmarquet-Trin-Dinh C, Jaegle M, Meijer D, Charnay P, Frain M. (2002). Characterisation of cis-acting sequences reveals a biphasic, axon-dependent regulation of Krox20 during Schwann cell development. *Development* **129,** 155-166.

Giancotti FG, Stepp MA, Suzuki S, Engvall E, Ruoslahti E. (1992). Proteolytic processing of endogenous and recombinant beta 4 integrin subunit. *J Cell Biol.* **18,** 951-9.

Giese KP, Martini R, Lemke G, Soriano P, Schachner M. (1992). Mouse P0 gene disruption leads to hypomyelination, abnormal expression of recognition molecules, and degeneration of myelin and axons. *Cell* **71,** 565-76.

Gillen C, Gleichmann M, Greiner-Petter R, Zoidl G, Kupfer S, Bosse F, Auer J, Muller HW. (1996). Full-lenth cloning, expression and cellular localization of rat plasmolipin mRNA, a proteolipid of PNS and CNS. *Eur J Neurosci.* **8,** 405-14.

Gillespie CS, Lee M, Fantes JF, Brophy PJ. (1997). The gene encoding the Schwann cell protein periaxin localizes on mouse chromosome 7 (Prx). *Genomics* **41,** 297-8.

Gillespie CS, Sherman DL, Blair GE, Brophy PJ. (1994). Periaxin, a novel protein of myelinating Schwann cells with a possible role in axonal ensheathment. *Neuron* **12,** 497-508.

Gillespie CS, Sherman DL, Fleetwood-Walker SM, Cottrell DF, Tait S, Garry EM, Wallace VC, Ure J, Griffiths IR, Smith A, Brophy PJ. (2000). Peripheral demyelination and neuropathic pain behavior in periaxin-deficient mice. *Neuron* **26,** 523-31.

Golding JP, Cohen J. (1997). Border controls at the mammalian spinal cord: late-surviving neural crest boundary cap cells at dorsal root entry sites may regulate sensory afferent ingrowth and entry zone morphogenesis. *Mol Cell Neurosci.* **9,** 381-96.

Gomez CM, Muggleton-Harris AL, Whittingham DG, Hood LE, Readhead C. (1990). Rapid preimplantation detection of mutant (shiverer) and normal alleles of the mouse myelin basic protein gene allowing selective implantation and birth of live young. *Proc Natl Acad Sci U S A.* **87,** 4481-4.

Goodrum JF, Bouldin TW. (1996). The cell biology of myelin degeneration and regeneration in the peripheral nervous system. *J Neuropathol Exp Neurol.* **55,** 943-53.

Gould RM, Byrd AL, Barbarese E. (1995). The number of Schmidt-Lanterman incisures is more than doubled in shiverer PNS myelin sheaths. *J Neurocytol.* **24,** 85-98.

Goulding MD, Chalepakis G, Deutsch U, Erselius JR, Gruss P. (1991). Pax-3, a novel murine DNA binding protein expressed during early neurogenesis. *EMBO J.* **10,** 1135-1147.

Greenfield S, Brostoff S, Eylar EH, Morell P. (1973). Protein composition of myelin of the peripheral nervous system. *J Neurochem.* **20,** 1207-16.

Griffiths IR, Dickinson P, Montague P. (1995). Expression of the proteolipid protein gene in glial cells of the post-natal peripheral nervous system of rodents. *Neuropathol Appl Neurobiol.* **21,** 97-110.

Griffiths IR, Mitchell LS, McPhilemy K, Morrison S, Kyriakides E, Barrie JA. (1989). Expression of myelin protein genes in Schwann cells. *J Neurocytol.* **18,** 345-52.

Grim M, Halata Z, Franz T. (1992). Schwann cells are not required for guidance of motor nerves in the hindlimb in Splotch mutant mouse embryos. *Anat Embryol (Berl).* **186,** 311-8.

Grinspan JB, Marchionni MA, Reeves M, Coulaloglou M, Scherer SS. (1996). Axonal interactions regulate Schwann cell apoptosis in developing peripheral nerve: neuregulin receptors and the role of neuregulins. *J Neurosci.* **16,** 6107-18.

Gruss P, Walther C. (1992). Pax in development. *Cell* **69,** 719-722.

Guilbot A, Williams A, Ravise N, Verny C, Brice A, Sherman DL, Brophy PJ, LeGuern E, Delague V, Bareil C, Megarbane A, Claustres M. (2001). A mutation in periaxin is responsible for CMT4F, an autosomal recessive form of Charcot-Marie-Tooth disease. *Hum Mol Genet.* **10,** 415-21.

Guillory, G., Bronner-Fraser, M. (1986). An in vitro assay for neural crest cell migration through the somites. *J. Embryol. Exp. Morphol.* **98,** 85-97.

Gupta SK, Poduslo JF, Mezei C. (1988). Temporal changes in PO and MBP gene expression after crush-injury of the adult peripheral nerve. *Brain Res.* **464,** 133-41.

Gupta SK, Pringle J, Poduslo JF, Mezei C. (1993). Induction of myelin genes during peripheral nerve remyelination requires a continuous signal from the ingrowing axon. *J Neurosci Res.* **34,** 14-23.

Hagedorn L, Suter U, Sommer L. (1999). P0 and PMP22 mark a multipotent neural crest-derived cell type that displays community effects in response to TGF-beta family factors. *Development* **126,** 3781-94.

Hall, S.M. (1989). Regeneration in the peripheral nervous system. *Neuropathol Appl Neurobiol.* **15,** 513-29.

Hall SM, Williams PL. (1970). Studies on the "incisures" of Schmidt and Lanterman. *J Cell Sci.* **6,** 767-91.

Hall SM, Williams PL. (1971). The distribution of electron-dense tracers in peripheral nerve fibres. *J Cell Sci.* **8,** 541-55.

Hamacher M, Pippirs U, Kohler A, Muller HW, Bosse F. (2001). Plasmolipin: genomic structure, chromosomal localization, protein expression pattern, and putative association with Bardet-Biedl syndrome. *Mamm Genome.* **12,** 933-7.

Hammerschmidt, M., Brook, A., and McMahon, A.P. (1997). The world according to hedgehog. *Trends Genet.* **13,** 14-21.

Haney C, Snipes GJ, Shooter EM, Suter U, Garcia C, Griffin JW, Trapp BD. (1996). Ultrastructural distribution of PMP22 in Charcot-Marie-Tooth disease type 1A. *J Neuropathol Exp Neurol.* **55,** 290-9.

Haney CA, Sahenk Z, Li C, Lemmon VP, Roder J, Trapp BD. (1999). Heterophilic binding of L1 on unmyelinated sensory axons mediates Schwann cell adhesion and is required for axonal survival. *J Cell Biol.* **146,** 1173-84.

Harrison, RG. (1924). Neuroblast versus sheath cell in the development of peripheral nerves. *J. Comp. Neurol.* **37,** 123-205.

Hazel TG, Nathans D, Lau LF. (1988). A gene inducible by serum growth factors encodes a member of the steroid and thyroid hormone receptor superfamily. *Proc Natl Acad Sci U S A.* **85,** 8444-8.

He X, Treacy MN, Simmons DM, Ingraham HA, Swanson LW, Rosenfeld MG. (1989). Expression of a large family of POU-domain regulatory genes in mammalian brain development. *Nature* **340,** 35-41.

Henion PD, Weston JA. (1997). Timing and pattern of cell fate restrictions in the neural crest lineage. *Development* **124,** 4351-4359.

Herbarth B, Pingault V, Bondurand N, Kuhlbrodt K, Hermans-Borgmeyer I, Puliti A, Lemort N, Goossens M, Wegner M. (1998). Mutation of the Sry-related Sox10 gene in Dominant megacolon, a mouse model for human Hirschsprung disease. *Proc Natl Acad Sci U S A.* **95,** 5161-5.

Herdegen T, Kiessling M, Bele S, Bravo R, Zimmermann M, Gass P. (1993). The KROX-20 transcription factor in the rat central and peripheral nervous systems: novel expression pattern of an immediate early gene-encoded protein. *Neuroscience* **57,** 41-52.

Hiscoe, H.B. (1947). Distribution of nodes and incisures in normal and regenerated nerve fibers. *Anat. Rec.* **99,** 447-475.

Ho KS and Scott MP. (2002). Sonic hedgehog in the nervous system : functions, modifications and mechanisms. *Curr Opin Neurobiol.* **12,** 57-63.

Hodgkin AL, Huxley AF. (1952). A quantitative description of membrane current and its application to conduction and excitation in nerve. *J Physiol.* **117,** 500-44.

Holmes W.E., Sliwkowski M.X., Akita R.W., henzel W.J., Lee J., Park J.W., Yansura D., Abadi N., Raab H., Lewis G.D., Shepard H.M., Kuang W.J., Wood W.I., Goeddel D.V., Vandlen R.I. (1992). Identification of heregulin, a specific activator of p185erbB2. *Science* **256,** 1205-1210.

Hooper, J.E., and Scott, M.P. (2005). Communicating with hedgehog. *Nat Rev Mol Cell Biol.* **6,** 306-317.

Hosang M, Shooter EM. (1985). Molecular characteristics of nerve growth factor receptors on PC12 cells. *J Biol Chem.* **260,** 655-62.

Hsieh ST, Kidd GJ, Crawford TO, Xu Z, Lin WM, Trapp BD, Cleveland DW, Griffin JW. (1994). Regional modulation of neurofilament organization by myelination in normal axons. *J Neurosci.* **14,** 6392-401.

Huang D, Rutkowski JL, Brodeur GM, Chou PM, Kwiatkowski JL, Babbo A, Cohn SL. (2000). Schwann cell-conditioned medium inhibits angiogenesis. *Cance Res.* **60,** 5966-71.

Hudson, L. D. (2004). Proteolipid protein gene. In "Myelin biology and disorders". PP 401-420. Elsevier academic press,

Huxley C, Passage E, Manson A, Putzu G, Figarella-Branger D, Pellissier JF, Fontes M. (1996). Construction of a mouse model of Charcot-

Marie-Tooth disease type 1A by pronuclear injection of human YAC DNA. *Hum Mol Genet.* **5,** 563-9.

Huxley C, Passage E, Robertson AM, Youl B, Huston S, Manson A, Saberan-Djoniedi D, Figarella-Branger D, Pellissier JF, Thomas PK, Fontes M. (1998). Correlation between varying levels of PMP22 expression and the degree of demyelination and reduction in nerve conduction velocity in transgenic mice. *Hum Mol Genet.* **7,** 449-58.

Hynes, RO. (2002). Integrins: bidirectional, allosteric signaling machines. *Cell* **110,** 673-87.

Hynes, R. O. (1992). Integrins: versatility, modulation, and signaling in cell adhesion. *Cell* **69,** 11-25.

Ikenaka, K., Kagawa, T., Mikoshiba, K. (1992). Selective expression of DM-20, an alternatively spliced myelin proteolipid protein gene product, in developing nervous system and in nonglial cells. *J Neurochem.* **58,** 2248-53.

Ikeya, M., Lee, S.M., Johnson, J.E., McMahon, A.P. &Takada, S. (1997). Wnt signalling required for expansion of neural crest and CNS progenitors. *Nature* **389,** 966-970.

Inuzuka T, Fujita N, Sato S, Baba H, Nakano R, Ishiguro H, Miyatake T. (1991). Expression of the large myelin-associated glycoprotein isoform during the development in the mouse peripheral nervous system. *Brain Res.* **562,** 173-5.

Ionasescu V, Searby C, Ionasescu R. (1994). Point mutations of the connexin32 (GJB1) gene in X-linked dominant Charcot-Marie-Tooth neuropathy. *Hum Mol Genet.* **3,** 355-8.

Ionasescu VV, Searby C, Ionasescu R, Neuhaus IM, Werner R. (1996). Mutations of the noncoding region of the connexin32 gene in X-linked dominant Charcot-Marie-Tooth neuropathy. *Neurology.* **47,** 541-4.

Jacobson, M. (1993). Developmental Neurobiology, 3rd edition. Plenum Press. New York.

Jaegle M, Ghazvini M, Mandemakers W, Piirsoo M, Driegen S, Levavasseur F, Raghoenath S, Grosveld F, Meijer D. (2003). The POU proteins Brn-2 and Oct-6 share important functions in Schwann cell development. *Genes Dev.* **17,** 1380-91.

Jaegle M, Meijer D. (1998). Role of Oct-6 in Schwann cell differentiation. *Microsc Res Tech.* **41,** 372-8.

Jaegle M, Mandemakers W, Broos L, Zwart R, Karis A, Visser P, Grosveld F, Meijer D. (1996). The POU factor Oct-6 and Schwann cell differentiation. *Science* **273,** 507-510.

Jessen, K.R., and Mirsky, R. (1999). Schwann cells and their precursors emerge as major regulators of nerve development. *Trends in neuroscience.* **22,** 402-410.

Jessen KR, Brennan A, Morgan L, Mirsky R, Kent A, Hashimoto Y, Gavrilovic J. (1994). The Schwann cell precursor and its fate: a study of cell death and differentiation during gliogenesis in rat embryonic nerves. *Neuron* **12,** 509-27.

Jessen KR, Morgan L, Brammer M, Mirsky R. (1985). Galactocerebroside is expressed by non-myelin-forming Schwann cells in situ. *J Cell Biol.* **101,** 1135-43.

Jessen KR, Mirsky R. (1980). Glial cells in the enteric nervous system contain glial fibrillary acidic protein. *Nature* **286,** 736-7.

Jessen KR, Mirsky R, Morgan L. (1987a). Myelinated, but not unmyelinated axons, reversibly down-regulate N-CAM in Schwann cells. *J Neurocytol.* **16,** 681-8.

Jessen KR, Mirsky R, Morgan L. (1987b). Axonal signals regulate the differentiation of non-myelin-forming Schwann cells: an immunohistochemical study of galactocerebroside in transected and regenerating nerves. *J Nerosci.* **7,** 3362-9.

Jessen KR, Mirsky R. (1991). Schwann cell precursors and their development. *Glia* **4,** 185-94.

Jessen KR, Mirsky R. (2004). Schwann Cell Development. In "Myelin biology and disorders". PP 329-370. Elsevier academic press.

Jessen KR, Mirsky R. (2005). The origin and development of glial cells in peripheral nerves. *Nat Rev Neurosci.* **6,** 671-82.

Jetten AM, Suter U (2000). The peripheral myelin protein 22 and epithelial membrane protein family. *Prog Nucleic Acid Res Mol Biol.* **64,** 97-129.

Jia, J., Tong, C., Wang, B., Luo, L., and Jiang, J. (2004). Hedgehog signalling activity of Smoothened requires phosphorylation by protein kinase A and casein kinase I. *Nature* **432,** 1045-50.

Jiang J, Struhl G. (1998). Regulation of the Hedgehog and Wingless signalling pathways by the F-box/WD40-repeat protein Slimb. *Nature* **391,** 493-6.

Johnson PW, Abramow-Newerly W, Seilheimer B, Sadoul R, Tropak MB, Arquint M, Dunn RJ, Schachner M, Roder JC. (1989). Recombinant myelin-associated glycoprotein confers neural adhesion and neurite outgrowth function. *Neuron* **3,** 377-85.

Jones JT, Akita RW, Sliwkowski MX. (1999). Binding specificities and affinities of egf domains for ErbB receptors. *FEBS Lett.* **447,** 227-31.

Kadlubowski M, Hughes RA, Gregson NA. (1984). Spontaneous and experimental neuritis and the distribution of the myelin protein P2 in the nervous system. *J Nerochem.* **42,** 123-9.

Kalomiris EL, Bourguignon LY. (1988). Mouse T lymphoma cells contain a transmembrane glycoprotein (GP85) that binds ankyrin. *J Cell Biol.* **106,** 319-27.

Kamholz J, Sessa M, Scherer S, Vogelbacker H, Mokuno K, Baron P, Wrabetz L, Shy M, Pleasure D. (1992). Structure and expression of proteolipid protein in the peripheral nervous system. *J Neurosci Res.* **31,** 231-44.

Kanda T, Tsukagoshi H, Oda M, Miyamoto K, Tanabe H. (1991). Morphological changes in unmyelinated nerve fibres in the sural nerve with age. *Brain* **114,** 585-99.

Keller MP, Chance PF. (1999). Inherited neuropathies: from gene to disease. *Brain Pathol.* **9,** 327-41.

Khursigara G, Bertin J, Yano H, Moffett H, DiStefano PS, Chao MV. (2001). A prosurvival function for the p75 receptor death domain mediated via the caspase recruitment domain receptor-interacting protein 2. *J Neurosci.* **21,** 5854-63.

Kiefer R, Kieseier BC, Stoll G, Hartung HP. (2001). The role of macrophages in immune-mediated damage to the peripheral nervous system. *Prog Neurobiol.* **64,** 109-27.

Kim HA, Pomeroy SL, Whoriskey W, Pawlitzky I, Benowitz LI, Sicinski P, Stiles CD, Roberts TM. (2000). A developmentally regulated switch directs regenerative growth of Schwann cells through cyclin D1. *Neuron* **26,** 405-16.

Kim T, Fiedler K, Madison DL, Krueger WH, Pfeiffer SE. (1995). Cloning and characterization of MVP17: a developmentally regulated myelin protein in oligodendrocytes. *J Neurosci Res.* **42,** 413-22.

Kingsley, D. M. (1994). The TGF-beta superfamily: new members, new receptors, and new genetic tests of function in different organisms. *Genes Dev.* **8,** 133-46.

Kioussi C, Gross MK, Gruss P. (1995). Pax3: a paired domain gene as a regulator in PNS myelination. *Neuron* **15,** 553-62.

Kirschner DA, Ganser AL. (1980). Compact myelin exists in the absence of basic protein in the shiverer mutant mouse. *Nature* **283,** 207-10.

Kirschner DA, Wrabetz L, Feltri ML. (2004). The P0 Gene. In "Myelin biology and disorders". PP 523-545. Elsevier academic press.

Kligman D, Hilt DC. (1988). The S100 protein family. *Trends Biochem Sci.* **13,** 437-43.

Klugmann M, Schwab MH, Puhlhofer A, Schneider A, Zimmermann F, Griffiths IR, Nave KA. (1997). Assembly of CNS myelin in the absence of proteolipid protein. *Neuron* **18,** 59-70.

Koeppen, AH. (2004). Wallerian degeneration: history and clinical significance. *J Neurol Sci.* **220,** 115-7.

Kogerman P, Grimm T, Kogerman L, Krause D, Unden AB, Sandstedt B, Toftgard R, Zaphiropoulos PG. (1999). Mammalian suppressor-of-fused modulates nuclear-cytoplasmic shuttling of Gli-1. *Nat Cell Biol.* **1**(5): 312-9.

Komada M, Soriano P. (2002). [Beta]IV-spectrin regulates sodium channel clustering through ankyrin-G at axon initial segments and nodes of Ranvier. *J Cell Biol.* **156,** 337-48.

Konishi, T (1990). Dye coupling between mouse Schwann cells. *Brain Res.* **508,** 85-92.

Kordeli E, Lambert S, Bennett V. (1995). AnkyrinG. A new ankyrin gene with neural-specific isoforms localized at the axonal initial segment and node of Ranvier. *J Biol Chem.* **270,** 2352-9.

Kristensson K, Olsson Y. (1971). The perineurium as a diffusion barrier to protein tracers. Differences between mature and immature animals. *Acta Neuropathol (Berl).* **17,** 127-38.

Kruger GM, Mosher JT, Tsai YH, Yeager KJ, Iwashita T, Gariepy CE, Morrison SJ. (2003). Temporally distinct requirements for endothelin receptor B in the generation and migration of gut neural crest stem cells. *Neuron* **40,** 917-29.

Krull, C.E. (2001). Segmental organization of neural crest migration. *Mech. Dev.* **105,** 37-45.

Kubu CJ, Orimoto K, Morrison SJ, Weinmaster G, Anderson DJ, Verdi JM. (2002). Developmental changes in Notch1 and numb expression mediated by local cell-cell interactions underlie progressively increasing delta sensitivity in neural crest stem cells. *Dev Biol.* **244,** 199-214.

Kuhlbrodt K, Herbarth B, Sock E, Hermans-Borgmeyer I, Wegner M. (1998). Sox10, a novel transcriptional modulator in glial cells. *J Neurosci.* **18,** 237-50.

Kuhn G, Lie A, Wilms S, Muller HW. (1993). Coexpression of PMP22 gene with MBP and P0 during de novo myelination and nerve repair. *Glia* **8,** 256-64.

Kumar NM, Gilula NB. (1986). Cloning and characterization of human and rat liver cDNAs coding for a gap junction protein. *J Cell Biol.* **103,** 767-76.

Kurek JB, Austin L, Cheema SS, Bartlett PF, Murphy M. (1996). Up-regulation of leukaemia inhibitory factor and interleukin-6 in transected sciatic nerve and muscle following denervation. *Neuromuscul Disord.* **6,** 105-14.

Kurihara T, Tsukada Y. (1967). The regional and subcellular distribution of 2',3'-cyclic nucleotide 3'-phosphohydrolase in the central nervous system. *J nerochem.* **14,** 1167-74.

Kurtz A, Zimmer A, Schnutgen F, Bruning G, Spener F, Muller T. (1994). The expression pattern of a novel gene encoding brain-fatty acid binding protein correlates with neuronal and glial cell development. *Development* **120,** 2637-49.

Kury P, Greiner-Petter R, Cornely C, Jurgens T, Muller HW. (2002). Mammalian achaete scute homolog 2 is expressed in the adult sciatic nerve and regulates the expression of Krox24, Mob-1, CXCR4, and p57kip2 in Schwann cells. *Neurosci.* **22,** 7586-95.

Kusano KF, Allendoerfer KL, Munger W, Pola R, Bosch-Marce M, Kirchmair R, Yoon YS, Curry C, Silver M, Kearney M, Asahara T, Losordo DW. (2004). onic hedgehog induces arteriogenesis in diabetic vasa nervorum and restores function in diabetic neuropathy. *Arterioscler Thromb Vasc Biol.* **24,** 2102-7.

LaBonne C, Bronner-Fraser M. (1998). Neural crest induction in Xenopus: evidence for a two-signal model. *Development* **125**, 2403-14.

Lai C, Brow MA, Nave KA, Noronha AB, Quarles RH, Bloom FE, Milner RJ, Sutcliffe JG. (1987a). Two forms of 1B236/myelin-associated glycoprotein, a cell adhesion molecule for postnatal neural development, are produced by alternative splicing. *Proc Natl Acad Sci U S A.* **84,** 4337-41.

Lai C, Watson JB, Bloom FE, Sutcliffe JG, Milner RJ. (1987b). Neural protein 1B236/myelin-associated glycoprotein (MAG) defines a subgroup of the immunoglobulin superfamily. *Immunol Rev.* **100,** 129-51.

Lallier T, Leblanc G, Artinger KB, Bronner-Fraser M. (1992). Cranial and trunk neural crest cells use different mechanisms for attachment to extracellular matrices. *Development* **116,** 531-41.

Lambert S, Bennett V. (1993). Postmitotic expression of ankyrinR and beta R-spectrin in discrete neuronal populations of the rat brain. *J Neurosci.* **13,** 3725-35.

Lambert S, Yu H, Prchal JT, Lawler J, Ruff P, Speicher D, Cheung MC, Kan YW, Palek J. (1990). cDNA sequence for human erythrocyte ankyrin. *Proc Natl Acad Sci U S A.* **87,** 1730-4.

Lappe-Siefke C, Goebbels S, Gravel M, Nicksch E, Lee J, Braun PE, Griffiths IR, Nave KA. (2003). Disruption of Cnp1 uncouples oligodendroglial functions in axonal support and myelination. *Nat. Genet.* **33,** 366-74.

D. S. Latchman. (1999). POU family transcription factors in the nervous system. J *Cell Physiol.* **179,** 126-33.

Lau LF, Nathans D. (1987). Expression of a set of growth-related immediate early genes in BALB/c 3T3 cells: coordinate regulation with c-fos or c-myc. *Proc Natl Acad Sci U S A.* **84,** 1182-86.

Lawson SN, Caddy KW, Biscoe TJ. (1974). Development of rat dorsal root ganglion neurones. Studies of cell birthdays and changes in mean cell diameter. *Cell Tissue Res.* **153,** 399-413.

Le Douarin, N. (1973). A biological cell labeling technique and its use in expermental embryology. *Dev Biol.* **30,** 217-22.

Le Douarin, N. (1982). The Neural Crest. New York, NY. Cambridge University Press.

Le Douarin, NM. (1986). Cell line segregation during peripheral nervous system ontogeny. *Science* **231,** 1515-22.

Le Douarin, NM. (2004). The avian embryo as a model to study the development of the neural crest: a long and still ongoing story. *Mech Dev.* **121,** 1089-102.

Le Douarin N, Dulac C, Dupin E, Cameron-Curry P. (1991). Glial cell lineages in the neural crest. *Glia* **4,** 175-84.

Le Douarin NM, Kalcheim C. (1999). The Neural Crest. 2nd edition. New York, NY: Cambridge University Press.

Le Douarin NM, Smith J. (1988). Development of the peripheral nervous system from the neural crest. *Annu Rev Cell Biol.* **4,** 375-404.

Le Douarin NM, Teillet MA. (1974). Experimental analysis of the migration and differentiation of neuroblasts of the autonomic nervous system and of neurectodermal mesenchymal derivatives, using a biological cell marking technique. *Dev Biol.* **41,** 162-84.

Le N, Nagarajan R, Wang JY, Svaren J, LaPash C, Araki T, Schmidt RE, Milbrandt J. (2005). Nab proteins are essential for peripheral nervous system myelination. *Nat Neurosci.* **8,** 932-40.

LeBlanc AC, Poduslo JF. (1990). Axonal modulation of myelin gene expression in the peripheral nerve. *J Neurosci Res.* **26,** 317-26.

Lee KF, Simon H, Chen H, Bates B, Hung MC, Hauser C. (1995). Requirement for neuregulin receptor erbB2 in neural and cardiac development. *Nature* **378,** 394-8.

Lee M, Brennan A, Blanchard A, Zoidl G, Dong Z, Tabernero A, Zoidl C, Dent MA, Jessen KR, Mirsky R. (1997). P0 is constitutively expressed in the rat neural crest and embryonic nerves and is negatively and positively regulated by axons to generate non-myelin-forming and myelin-forming Schwann cells, respectively. *Mol Cell Neurosci.* **8,** 336-50.

Lee MJ, Calle E, Brennan A, Ahmed S, Sviderskaya E, Jessen KR, Mirsky R. (2001). In early development of the rat mRNA for the major myelin protein P(0) is expressed in nonsensory areas of the embryonic inner ear, notochord, enteric nervous system, and olfactory ensheathing cells. *Dev Dyn.* **222,** 40-51.

Lees, M. B., and Brostoff, S. W. (1984). Proteins of myelin. In "Myelin" (P. Morrell, ed.), pp. 197-224. Plenum Press, New York.

Lefkowitz RJ, Shenoy SK. (2005) Transduction of receptor signals by beta-arrestins. *Science.* **308,** 512-7.

Lemaire P, Revelant O, Bravo R, Charnay P. (1988). Two mouse genes encoding potential transcription factors with identical DNA-binding domains are activated by growth factors in cultured cells. *Proc Natl Acad Sci U S A.* **85,** 4691-95.

Lemke, G. (1996). Neuregulins in development. *Mol. Cell Neurosci.* **7,** 247-262.

Lemke, G. (2001). Glial control of neuronal development. *Annu Rev Neurosci.* **24,** 87-105.

Lemke G, Axel R. (1985). Isolation and sequence of a cDNA encoding the major structural protein of peripheral myelin. *Cell* **40,** 501-8.

Lemke G, Barde YA. (1998). Neuronal and glial cell biology. *Curr Opin Neurobiol.* **8,** 567-569.

Lemke G, Lamar E, Patterson J. (1988a). Isolation and analysis of the gene encoding peripheral myelin protein zero. *Neuron* **1,** 73-83.

Li H, Wigley C, Hall SM. (1998). Chronically denervated rat Schwann cells respond to GGF in vitro. *Glia* **24,** 290-303.

Li M, Shibata A, Li C, Braun PE, McKerracher L, Roder J, Kater SB, David S. (1996). Myelin-associated glycoprotein inhibits neurite/axon growth and causes growth cone collapse. *J Neurosci Res.* **46,** 404-14.

Li X, Lynn BD, Olson C, Meier C, Davidson KG, Yasumura T, Rash JE, Nagy JI. (2002). Connexin29 expression, immunocytochemistry and freeze-fracture replica immunogold labelling (FRIL) in sciatic nerve. *Eur J Neurosci.* **16,** 795-806.

Li ZP, Burke EP, Frank JS, Bennett V, Philipson KD. (1993). The cardiac Na+-Ca2+ exchanger binds to the cytoskeletal protein ankyrin. *J Biol Chem.* **16,** 11489-91.

Liang TW, Chiu HH, Gurney A, Sidle A, Tumas DB, Schow P, Foster J, Klassen T, Dennis K, DeMarco RA, Pham T, Frantz G, Fong S. (2002). Vascular endothelial-junctional adhesion molecule (VE-JAM)/JAM 2 interacts with T, NK, and dendritic cells through JAM 3. *J Immunol.* **168,** 1618-26.

Lim RW, Varnum BC, Herschman HR. (1987). Cloning of tetradecanoyl phorbol ester-induced 'primary response' sequences and their expression in density-arrested Swiss 3T3 cells and a TPA non-proliferative variant. *Oncogene* **1,** 263-70.

London, Y (1971). Ox peripheral nerve myelin membrane. Purification and partial characterization of two basic proteins. *Biochim Biophys Acta.* **249,** 188-96.

Loring JF, Erickson CA. (1987). Neural crest cell migratory pathways in the trunk of the chick embryo. *Dev Biol.* **121,** 220-36.

Lum, L., Zhang, C., Oh, S., Mann, R.K., von Kessler, D.P., Taipale, J., Weis-Garcia, F., Gong, R., Wang, B., and Beachy, P.A. (2003). Hedgehog signal transduction via Smoothened association with a cytoplasmic complex scaffolded by the atypical kinesin, Costal-2. *Mol. Cell.* **12,** 1261-74.

Lunn ER, Perry VH, Brown MC, Rosen H, Gordon S. (1989). Absence of Wallerian Degeneration does not Hinder Regeneration in Peripheral Nerve. *Eur J Neurosci.* **1,** 27-33.

Lunn ER, Scourfield J, Keynes RJ, Stern CD. (1987). The neural tube origin of ventral root sheath cells in the chick embryo. *Development* **101,** 247-54.

Lux SE, John KM, Bennett V. (1990). Analysis of cDNA for human erythrocyte ankyrin indicates a repeated structure with homology to tissue-differentiation and cell-cycle control proteins. *Nature* **344**, 36-42.

Mack KJ, Cortner J, Mack P, Farnham PJ. (1992). krox 20 messenger RNA and protein expression in the adult central nervous system. *Brain Res Mol Brain Res.* **14,** 117-23.

Mackenzie ML, Shorer Z, Ghabriel MN, Allt G. (1984). Myelinated nerve fibres and the fate of lanthanum tracer: an in vivo study. *J Anat.* **138,** 1-14.

Macklin WB, Campagnoni CW, Deininger PL, Gardinier MV. (1987). Structure and expression of the mouse myelin proteolipid protein gene. *J Neurosci Res.* **18,** 383-94.

Madrid RE, Jaros E, Cullen MJ, Bradley WG. (1975). Genetically determined defect of Schwann cell basement membrane in dystrophic mouse. *Nature* **257,** 319-21.

Magyar JP, Martini R, Ruelicke T, Aguzzi A, Adlkofer K, Dembic Z, Zielasek J, Toyka KV, Suter U. (1996). Impaired differentiation of Schwann cells in transgenic mice with increased PMP22 gene dosage. *J Neurosci.* **16,** 5351-60.

Maier M, Berger P, Suter U. (2002). Understanding Schwann cell-neurone interactions: the key to Charcot-Marie-Tooth disease? *J Anat.* **200,** 357-66.

Mann, R.K. & Beachy, P.A. (2004). Novel lipid modifications of secreted protein signals. *Annu Rev Biochem.* **73,** 891-923.

Mansouri A, Hallonet M, Gruss P. (1996). Pax genes and their roles in cell differentiation and development. *Curr Opin Cell Biol.* **8,** 851-857.

Marchesi VT, Steers E Jr. (1968). Selective solubilization of a protein component of the red cell membrane. *Science* **159,** 203-4.

Marchionni M.A., Goodearl A.D., Chen M.S., Bermingham-McDonogh O., Kirk C., Hendricks M., Danehy F., Misnmi D., Sudhalter J., kobayashi K., Wroblewski D., lynch C., Baldassare M., Hiles I., Davis J.B., Hsuan J.J., Totty N.F., Otsu M., McBurney R.N., Waterfiled M.D., Stroobant P., Gwynne D. (1993). Glial growth factors are alternatively spliced erbB2 ligands expressed in the nervous system. *Nature* **362,** 312-318.

Maro G.S., Vermeren M., Voiculescu O., Melton L., Cohen J., Charnay P., and Topilko p. (2004). Neural crest boundary cap cells constitute a source of neuronal and glial cells of the PNS. *Nat neurosci.* **7,** 930-938.

Martini R, Mohajeri MH, Kasper S, Giese KP, Schachner M. (1995). Mice doubly deficient in the genes for P0 and myelin basic protein show that both proteins contribute to the formation of the major dense line in peripheral nerve myelin. *J Neurosci.* **15,** 4488-95.

Martini R, Schachner M. (1986). Immunoelectron microscopic localization of neural cell adhesion molecules (L1, N-CAM, and MAG) and their shared carbohydrate epitope and myelin basic protein in developing sciatic nerve. *J Cell Biol.* **103,** 2439-48.

Matsumura K, Yamada H, Saito F, Sunada Y, Shimizu T. (1997). Peripheral nerve involvement in merosin-deficient congenital muscular dystrophy and dy mouse. *Neuromuscul Disord.* **7,** 7-12.

Mattson MP, Culmsee C, Yu Z, Camandola S. (2000). Roles of nuclear factor kappaB in neuronal survival and plasticity. *J Neurochem.* **74,** 443-56.

Maurer M, Muller M, Kobsar I, Leonhard C, Martini R, Kiefer R. (2003). Origin of pathogenic macrophages and endoneurial fibroblast-like cells in an animal model of inherited neuropathy. *Mol Cell Neurosci.* **23,** 351-9.

Mayor R, Morgan R, Sargent MG. (1995). Induction of the prospective neural crest of Xenopus. *Development* **121,** 767-77.

Mazumder R, Iyer LM, Vasudevan S, Aravind L. (2002). Detection of novel members, structure-function analysis and evolutionary classification of the 2H phosphoesterase superfamily. *Nucleic Acids Res.* **30,** 5229-43.

McMahon, A.P., Ingham, P.W., and Tabin, C.J. (2003). Developmental roles and clinical significance of hedgehog signaling. *Curr. Top. Dev. Biol.* **53,** 1-114.

McMahon AP, Champion JE, McMahon JA, Sukhatme VP. (1990). Developmental expression of the putative transcription factor Egr-1 suggests that Egr-1 and c-fos are coregulated in some tissues. *Development* **108,** 281-17.

Meier C, Dermietzel R, Davidson KG, Yasumura T, Rash JE. (2004). Connexin32-containing gap junctions in Schwann cells at the internodal zone of partial myelin compaction and in Schmidt-Lanterman incisures. *J Neurosci.* **24,** 3186-98.

Meier C, Parmantier E, Brennan A, Mirsky R, Jessen KR. (1999). Developing Schwann cells acquire the ability to survive without axons by establishing an autocrine circuit involving insulin-like growth factor, neurotrophin-3, and platelet-derived growth factor-BB. *J Neurosci.* **19,** 3847-59.

Meijer D, Graus A, Kraay R, Langeveld A, Mulder MP, Grosveld G. (1990). The octamer binding factor Oct6: cDNA cloning and expression in early embryonic cells. *Nucleic Acids Res.* **18,** 7357-65.

Menegoz M, Gaspar P, Le Bert M, Galvez T, Burgaya F, Palfrey C, Ezan P, Arnos F, Girault JA. (1997). Paranodin, a glycoprotein of neuronal paranodal membranes. *Neuron* **19,** 319-31.

Merchant M, Vajdos FF, Ultsch M, Maun HR, Wendt U, Cannon J, Desmarais W, Lazarus RA, de Vos AM, de Sauvage FJ. (2004). Suppressor of fused regulates Gli activity through a dual binding mechanism. *Mol. Cell Biol.* **24,** 8627-41.

Merchant M, Evangelista M, Luoh SM, Franyz GD, Chalasani S, Carano RA, van Hoy M, Ramirez J, Ogasawara AK, McFarland LM, Filvaroff EH, French DM, de Sauvage FJ. (2005). Loss of the serine/threonine kinase fused results in postnatal growth defects and lethality due to progressive hydrocephalus. *Mol Cell Biol.* **25,** 7054-68.

Methot N., and Basler K. (2000). Suppressor of fused opposes hedgehog signal transduction by impeding nuclear accumulation of the activator form of Cubitus interruptus. *Development* **27,** 4001-10.

Meyer D, Birchmeier C. (1995). Multiple essential functions of neuregulin in development. *Nature* **378,** 386-90.

Michailov GV, Sereda MW, Brinkmann BG, Fischer TM, Haug B, Birchmeier C, Role L, Lai C, Schwab MH, Nave KA. (2004). Axonal neuregulin-1 regulates myelin sheath thickness. *Science* **304,** 700-3.

Milbrandt, J. (1987). A nerve growth factor-induced gene encodes a possible transcriptional regulatory factor. *Science* **238,** 797-799.

Milbrandt, J. (1988). Nerve growth factor induces a gene homologous to the glucocorticoid receptor gene. *Neuron* **1,** 183-8.

Milner RJ, Lai C, Nave KA, Lenoir D, Ogata J, Sutcliffe JG. (1985). Nucleotide sequences of two mRNAs for rat brain myelin proteolipid protein. *Cell* **42,** 931-9.

Mirsky, R., Jessen, K.R., Brennan, A., Parkinson, D., Dong, Z., Meier, C., Parmantier, E., Lawson, D. (2002). Schwann cells as regulators of nerve development. *J. Physiology.* **96,** 17-24.

Mirsky R, Jessen KR, Schachner M, Goridis C. (1986). Distribution of the adhesion molecules N-CAM and L1 on peripheral neurons and glia in adult rats. *J Neurocytol.* **15,** 799-815.

Mirsky R, Jessen KR. (1996). Schwann cell development, differentiation and myelination. *Curr Opin Neurobiol.* **6,** 89-96.

Moase CE, Trasler DG. (1990). Delayed neural crest cell emigration from Sp and Spd mouse neural tube explants. *Teratology.* **42,** 171-182.

Monsoro-Burg, A.H., Fletcher, R. & Harland, R. (2003). Neural cell induction by paraxial mesoderm in Xenopus embryo requires FGF signals. *Development* **130,** 3111-3124.

Monuki ES, Kuhn R, Weinmaster G, Trapp BD, Lemke G. (1990). Expression and activity of the POU transcription factor SCIP. *Science* **249,** 1300-3.

Monuki ES, Weinmaster G, Kuhn R, Lemke G. (1989). SCIP: a glial POU domain gene regulated by cyclic AMP. *Neuron* **3,** 783-93.

Morgan L, Jessen KR, Mirsky R. (1991). The effects of cAMP on differentiation of cultured Schwann cells: progression from an early phenotype (04+) to a myelin phenotype (P0+, GFAP-, N-CAM-, NGF-receptor-) depends on growth inhibition. *J Cell Biol.* **112,** 457-67.

Morris JK, Lin W, Hauser C, Marchuk Y, Getman D, Lee KF. (1999). Rescue of the cardiac defect in ErbB2 mutant mice reveals essential roles of ErbB2 in peripheral nervous system development. *Neuron* **23,** 273-83.

Morrison, SJ. (2001). Neuronal potential and lineage determination by neural stem cells. *Curr Opin Cell Biol.* **13,** 666-72.

Morrison SJ, Perez SE, Qiao Z, Verdi JM, Hicks C, Weinmaster G, Anderson DJ. (2000). Transient Notch activation initiates an irreversible switch from neurogenesis to gliogenesis by neural crest stem cells. *Cell* **101,** 499-510.

Morrison SJ, White PM, Zock C, Anderson DJ. (1999). Prospective identification, isolation by flow cytometry, and in vivo self-renewal of multipotent mammalian neural crest stem cells. *Cell* **96**, 737-49.

Morrissey TK, Levi AD, Nuijens A, Sliwkowski MX, Bunge RP. (1995). Axon-induced mitogenesis of human Schwann cells involves heregulin and p185erbB2. *Proc Natl Acad Sci U S A.* **92,** 1431-5.

Mugnaini, E. (1982). Membrane specializations in neuroglial cells and at neuron-glia contacts. In: Sears, T. A., Neuronal-glial cell interrelationships. pp. 39-56. Springer-Verlag, Berlin, Heidelberg, New York.

Mugnaini E, Schnapp B. (1974). Possible role of zonula occludens of the myelin sheath in demyelinating conditions. *Nature* **251,** 725-7.

Muse ED, Jurevics H, Toews AD, Matsushima GK, Morell P. (2001). Parameters related to lipid metabolism as markers of myelination in mouse brain. *J Neurochem.* **76,** 77-86.

Musso M, Balestra P, Bellone E, Cassandrini D, Di Maria E, Doria LL, Grandis M, Mancardi GL, Schenone A, Levi G, Ajmar F, Mandich P.

(2001). The D355V mutation decreases EGR2 binding to an element within the Cx32 promoter. *Neurobiol Dis.* **8,** 700-6.

Nagafuchi A, Tsukita S, Takeichi M. (1993). Transmembrane control of cadherin-mediated cell-cell adhesion. *Semin Cell Biol.* **4,** 175-81.

Nagarajan R, Svaren J, Le N, Araki T, Watson M, Milbrandt J. (2001). EGR2 mutations in inherited neuropathies dominant-negatively inhibit myelin gene expression. *Neuron* **30,** 355-68.

Narayanan V, Barbosa E, Reed R, Tennekoon G. (1988). Characterization of a cloned cDNA encoding rabbit myelin P2 protein. *J Biol Chem.* **263,** 8332-7.

Nelson WJ, Veshnock PJ. (1987). Ankyrin binding to (Na+ + K+)ATPase and implications for the organization of membrane domains in polarized cells. *Nature* **328,** 533-6.

Newman S, Kitamura K, Campagnoni AT. (1987). Identification of a cDNA coding for a fifth form of myelin basic protein in mouse. *Proc Natl Acad Sci U S A.* **84,** 886-90.

Nicholson SM, Gomes D, de Nechaud B, Bruzzone R. (2001). Altered gene expression in Schwann cells of connexin32 knockout animals. *J Neurosci Res.* **66,** 23-36.

Nickols JC, Valentine W, Kanwal S, Carter BD. (2003). Activation of the transcription factor NF-kappaB in Schwann cells is required for peripheral myelin formation. *Nat Neurosci.* **6,** 161-167.

Niemann S, Sereda MW, Suter U, Griffiths IR, Nave KA. (2000). Uncoupling of myelin assembly and schwann cell differentiation by transgenic overexpression of peripheral myelin protein 22. *J Neurosci.* **20,** 4120-8.

Niessen CM, Cremona O, Daams H, Ferraresi S, Sonnenberg A, Marchisio PC. (1994). Expression of the integrin alpha 6 beta 4 in peripheral nerves: localization in Schwann and perineural cells and different variants of the beta 4 subunit. *J Cell Sci.* **107,** 543-52.

Nieto M, Schuurmans C, Britz O, Guillemot F. (2001). Neural bHLH genes control the neuronal versus glial fate decision in cortical progenitors. *Neuron* **29,** 401-413.

Noakes PG, Bennett MR. (1987). Growth of axons into developing muscles of the chick forelimb is preceded by cells that stain with Schwann cell antibodies. *J Comp Neurol.* **259,** 330-47.

Norton, W. T., Cammer, W. (1984). Isolation and characterization of myelin. In: "Myelin" (Morell, P). PP. 147-195. Plenum Press, New York,.

Notterpek L, Shooter EM, Snipes GJ. (1997). Upregulation of the endosomal-lysosomal pathway in the trembler-J neuropathy. *J Neurosci.* **17,** 4190-200.

Notterpek L, Snipes GJ, Shooter EM. (1999). Temporal expression pattern of peripheral myelin protein 22 during in vivo and in vitro myelination. *Glia* **25,** 358-69.

Nusse, R. (2003). Wnts and hedgehogs: lipid-modified proteins and similarities in signaling mechanisms at the cell surface. *Development* **130,** 5297-5305.

O'Daly JA, Imaeda T. (1967). Electron microscopic study of Wallerian degeneration in cutaneous nerves caused by mechanical injury. *Lab Invest.* **17,** 744-66.

Oakley RA, Tosney KW. (1991). Peanut agglutinin and chondroitin-6-sulfate are molecular markers for tissues that act as barriers to axon advance in the avian embryo. *Dev Biol.* **147,** 187-206.

Olafson RW, Drummond GI, Lee JF. (1969). Studies on 2',3'-cyclic nucleotide-3'-phosphohydrolase from brain. *Can J Biochem.* **47,** 961-6.

Olsson, Y. (1966). Studies on vascular permeability in peripheral nerves. I. Distribution of circulating fluorescent serum albumin in normal, crushed and sectioned rat sciatic nerve. *Acta Neuropathol (Berl).* **7,** 1-15.

Olsson, Y. (1968). Topographical differences in the vascular permeability of the peripheral nervous system. *Acta Neuropathol (Berl).* **10,** 26-33.

Olsson, Y. (1971). Studies on vascular permeability in peripheral nerves. IV. Distribution of intravenously injected protein tracers in the peripheral nervous system of various species. *Acta Neuropathol (Berl).* **17,** 114-26.

Olsson, Y. (1990). Microenvironment of the peripheral nervous system under normal and pathological conditions. *Crit. Rev. Neurobiol.* **5,** 265-311.

Omlin FX, Webster HD, Palkovits CG, Cohen SR. (1982). Immunocytochemical localization of basic protein in major dense line regions of central and peripheral myelin. *J Cell Biol.* **95,** 242-8.

Opdecamp K, Kos L, Arnheiter H, Pavan WJ. (1998). Endothelin signalling in the development of neural crest-derived melanocytes. *Biochem Cell Biol.* **76,** 1093-99.

Osterlund T, and Kogerman P. (2006). Hedgehog signalling: how to get from Smo to Ci and Gli. *Trends Cell Biol.* **16,** 176-180.

Otto E, Kunimoto M, McLaughlin T, Bennett V. (1991). Isolation and characterization of cDNAs encoding human brain ankyrins reveal a family of alternatively spliced genes. *J Cell Biol.* **114,** 241-53.

Owens GC, Bunge RP. (1989). Evidence for an early role for myelin-associated glycoprotein in the process of myelination. *Glia* **2,** 119-28.

Palmeri D, van Zante A, Huang CC, Hemmerich S, Rosen SD. (2000). Vascular endothelial junction-associated molecule, a novel member of the immunoglobulin superfamily, is localized to intercellular boundaries of endothelial cells. *J Biol Chem.* **275,** 19139-45.

Paratore C, Hagedorn L, Floris J, Hari L, Kleber M, Suter U, Sommer L. (2002). Cell-intrinsic and cell-extrinsic cues regulating lineage decisions in multipotent neural crest-derived progenitor cells. *Int J Dev Biol.* **46,** 193-200.

Parkinson DB, Bhaskaran A, Droggiti A, Dickinson S, D'Antonio M, Mirsky R, Jessen KR. (2004). Krox-20 inhibits Jun-NH2-terminal kinase/c-Jun to control Schwann cell proliferation and death. *J Cell Biol.* **164,** 385-94.

Parkinson DB, Dickinson S, Bhaskaran A, Kinsella MT, Brophy PJ, Sherman DI, Sharghi-Namini S, Duran Alonso MB, Jessen KR, Mirsky R. (2002b). Krox20 activates a set of complex changes in Schwann cells that characterise myelination. *Glia* **Supplement 1** (S69)

Parkinson DB, Dickinson S, Bhaskaran A, Kinsella MT, Brophy PJ, Sherman DL, Sharghi-Namini S, Duran Alonso MB, Mirsky R, Jessen KR. (2003). Regulation of the myelin gene periaxin provides evidence for Krox-20-independent myelin-related signalling in Schwann cells. *Mol Cell Neurosci.* **23,** 13-27.

Parkinson DB, Dong Z, Bunting H, Whitfield J, Meier C, Marie H, Mirsky R, Jessen KR. (2001). Transforming growth factor beta (TGFbeta)

mediates Schwann cell death in vitro and in vivo: examination of c-Jun activation, interactions with survival signals, and the relationship of TGFbeta-mediated death to Schwann cell differentiation. *J Neurosci.* **21,** 8572-85.

Parkinson DB, Langner K, Namini SS, Jessen KR, Mirsky R. (2002a). beta-Neuregulin and autocrine mediated survival of Schwann cells requires activity of Ets family transcription factors. *Mol Cell Neurosci.* **20,** 154-67.

Parmantier, E., Lynn, B., lawson, D., Turmain, M., Sharghi-Namini, S., Chakrabarti, L., McMahon, A.P., Jessen, K.R. and Mirsky, R. (1999). Schwann cell derived desert hedgehog controls the development of peripheral nerve sheaths. *Neuron* **23,** 713-724.

Patel PI, Roa BB, Welcher AA, Schoener-Scott R, Trask BJ, Pentao L, Snipes GJ, Garcia CA, Francke U, Shooter EM, Lupski JR, Suter U. (1992). The gene for the peripheral myelin protein PMP-22 is a candidate for Charcot-Marie-Tooth disease type 1A. *Nat Genet.* **1,** 159-65.

Pathi S, Rutenberg JB, Johnson RL, Vortkamp A. (1999). Interaction of Ihh and BMP/Noggin signalling during cartilage differentiation. *Dev. Biol.* **209,** 239-253.

Patton BL, Miner JH, Chiu AY, Sanes JR. (1997). Distribution and function of laminins in the neuromuscular system of developing, adult, and mutant mice. *J Cell Biol.* **139,** 1507-21.

Paul, DL. (1995). New functions for gap junctions. *Curr Opin Cell Biol.* **7,** 665-72.

Paul, D. L. (1986). Molecular cloning of cDNA for rat liver gap junction protein. *J Cell Biol.* ***103,*** 123-34.

Pedraza L, Huang JK, Colman DR. (2001). Organizing principles of the axoglial apparatus. *Cell* **30,** 335-44.

Peirano RI, Goerich DE, Riethmacher D, Wegner M. (2000a). Protein zero gene expression is regulated by the glial transcription factor Sox10. *Mol Cell Biol.* **20,** 3198-209.

Peirano RI, Wegner M. (2000b). The glial transcription factor Sox10 binds to DNA both as monomer and dimer with different functional consequences. *Nucleic Acids Res.* **28,** 3047-55.

Peles E, Nativ M, Lustig M, Grumet M, Schilling J, Martinez R, Plowman GD, Schlessinger J. (1997). Identification of a novel contactin-associated transmembrane receptor with multiple domains implicated in protein-protein interactions. *EMBO J.* **16,** 978-88.

Pepinsky RB, Shapiro RI, Wang S, Chakraborty A, Gill A, Lepage DJ, Wen D, Rayhorn P, Horan GS, Taylor FR, Garber EA, Galdes A, Engber TM. (2002). Long-acting forms of Sonic hedgehog with improved

pharmacokinetic and pharmacodynamic properties are efficacious in a nerve injury model. *J Pharm Sci.* **91,** 371-87.

Perkins NM, Tracey DJ. (2000). Hyperalgesia due to nerve injury: role of neutrophils. *Neuroscience* **101,** 745-57.

Perris, R., Krotoski, D., Bronner-Fraser, M. (1991). Collages in avian neural crest development: distribution in vivo and migration-promoting ability in vitro. *Development* **113,** 969-84.

Perris, R. (1997). The extracellular matrix in neural crest-cell migration. *Trends Neurosci.* **20,** 23-31.

Perry VH, Brown MC, Gordon S. (1987). The macrophage response to central and peripheral nerve injury. A possible role for macrophages in regeneration. *J Exp Med.* **165,** 1218-23.

Peters LL, John KM, Lu FM, Eicher EM, Higgins A, Yialamas M, Turtzo LC, Otsuka AJ, Lux SE. (1995). Ank3 (epithelial ankyrin), a widely distributed new member of the ankyrin gene family and the major ankyrin in kidney, is expressed in alternatively spliced forms, including forms that lack the repeat domain. *J Cell Biol.* **130,** 313-30.

Peterson AC, Bray GM. (1984). Hypomyelination in the peripheral nervous system of shiverer mice and in shiverer in equilibrium normal chimaera. *J Comp Neurol.* **227,** 348-56.

Pham-Dinh D, Birling MC, Roussel G, Dautigny A, Nussbaum JL. (1991). Proteolipid DM-20 predominates over PLP in peripheral nervous system. *Neuroreport.* **2,** 89-92.

Pierucci-Alves F, Clark AN, Russell LD. (2001). A developmental Study of the desert hedgehog-null mouse testis. *Biol. Reproduction* **65,** 1392-1402.

Pingault V, Bondurand N, Kuhlbrodt K, Goerich DE, Prehu MO, Puliti A, Herbarth B, Hermans-Borgmeyer I, Legius E, Matthijs G, Amiel J, Lyonnet S, Ceccherini I, Romeo G, Smith JC, Read AP, Wegner M, Goossens M. (1998). SOX10 mutations in patients with Waardenburg-Hirschsprung disease. *Nat genet.* **18,** 171-173.

Pinkas-Kramarski R, Shelly M, Guarino BC, Wang LM, Lyass L, Alroy I, Alimandi M, Kuo A, Moyer JD, Lavi S, Eisenstein M, Ratzkin BJ, Seger R, Bacus SS, Pierce JH, Andrews GC, Yarden Y. (1998). ErbB tyrosine kinases and the two neuregulin families constitute a ligand-receptor network. *Mol Cell Biol.* **18,** 6090-101.

Podratz JL, Rodriguez E, Windebank AJ. (2001). Role of the extracellular matrix in myelination of peripheral nerve. *Glia* **35,** 35-40.

Pola R, Ling LE, Silver M, Corbley MJ, Kearney M, Blake Pepinsky R, Shapiro R, Taylor FR, Baker DP, Asahara T, Isner JM. (2001). The morphogen Sonic hedgehog is an indirect angiogenic agent upregulating two families of angiogenic growth factors. *Nat Med.* **7,** 706-11.

Poliak, S., Peles, E. (2003). The local differentiation of myelinated axons at nodes of Ranvier. *Nat Rev Neurosci.* **4,** 968-80.

Poliak S, Matlis S, Ullmer C, Scherer SS, Peles E. (2002). Distinct claudins and associated PDZ proteins form different autotypic tight junctions in myelinating Schwann cells. *J Cell Biol.* ***159,*** 361-72.

Poltorak M, Sadoul R, Keilhauer G, Landa C, Fahrig T, Schachner M. (1987). Myelin-associated glycoprotein, a member of the L2/HNK-1 family of neural cell adhesion molecules, is involved in neuron-oligodendrocyte and oligodendrocyte-oligodendrocyte interaction. *J Cell Biol.* **105,** 1893-9.

Pratt JH, Berry JF, Kaye B, Goetz FC. (1969). Lipid class and fatty acid composition of rat brain and sciatic nerve in alloxan diabetes. *Diabetes* **18,** 556-61.

Previtali SC, Feltri ML, Archelos JJ, Quattrini A, Wrabetz L, Hartung H. (2001). Role of integrins in the peripheral nervous system. *Prog Neurobiol.* **64,** 35-49.

Pribyl TM, Campagnoni CW, Kampf K, Kashima T, Handley VW, McMahon J, Campagnoni AT. (1993). The human myelin basic protein gene is included within a 179-kilobase transcription unit: expression in the immune and central nervous systems. *Proc Natl Acad Sci U S A.* **90,** 10695-9.

Privat A, Jacque C, Bourre JM, Dupouey P, Baumann N. (1979). Absence of the major dense line in myelin of the mutant mouse "shiverer". *Neurosci Lett.* **12,** 107-12.

Puckett C, Hudson L, Ono K, Friedrich V, Benecke J, Dubois-Dalcq M, Lazzarini RA. (1987). Myelin-specific proteolipid protein is expressed in myelinating Schwann cells but is not incorporated into myelin sheaths. *J Neurosci Res.* **18,** 511-8.

Qian X, Shen Q, Goderie SK, He W, Capela A, Davis AA, Temple S. (2000). Timing of CNS cell generation: a programmed sequence of neuron and glial cell production from isolated murine cortical stem cells. *Neuron* **28,** 69-80.

Quarles RH, Everly JL, Brady RO. (1973). Evidence for the close association of a glycoprotein with myelin in rat brain. *J Neurochem.* **21,** 1177-91.

Radeke MJ, Misko TP, Hsu C, Herzenberg LA, Shooter EM. (1987). Gene transfer and molecular cloning of the rat nerve growth factor receptor. *Nature* **325,** 593-7.

Raff MC, Abney E, Brockes JP, Hornby-Smith A. (1978). Schwann cell growth factors. *Cell* **15,** 813-22.

Raine, C. S. (1984). Morphology of myelin and myelination. In "P. Morell (ed.), Myelin". PP. 1–41. New York: Plenum.

Ramon Y Cajal, S. (1928). Degeneration and regeneration of the nervous system. Oxford, Oxford University Press.

Ranscht B, Bronner-Fraser M. (1991). T-cadherin expression alternates with migrating neural crest cells in the trunk of the avian embryo. *Development* **111,** 15-22.

Rathjen FG, Schachner M. (1984). Immunocytological and biochemical characterization of a new neuronal cell surface component (L1 antigen) which is involved in cell adhesion. *EMBO J.* **3,** 1-10.

Reichardt LF, Tomaselli KJ. (1991). Extracellular matrix molecules and their receptors: functions in neural development. *Annu Rev Neurosci.* **14,** 531-70.

Revel JP, Hamilton DW. (1969). The double nature of the intermediate dense line in peripheral nerve myelin. *Anat Rec.* **163,** 7-15.

Reynolds ML, Fitzgerald M, Benowitz LI. (1991). GAP-43 expression in developing cutaneous and muscle nerves in the rat hindlimb. *Neuroscience* **41,** 201-11.

Rickmann M, Fawcett JW, Keynes RJ. (1985). The migration of neural crest cells and the growth of motor axons through the rostral half of the chick somite. *J Embryol Exp Morphol.* **90,** 437-55.

Riese DJ, van Raaij TM, Plowman GD, Andrews GC, Stern DF. (1995). The cellular response to neuregulins is governed by complex interactions of the erbB receptor family. *Mol Cell Biol.* **15,** 5770-6.

Riethmacher D, Sonnenberg-Riethmacher E, Brinkmann V, Yamaai T, Lewin GR, Birchmeier C. (1997). evere neuropathies in mice with targeted mutations in the ErbB3 receptor. *Nature* **389,** 725-30.

Ritchie, JM. (1982). On the relation between fibre diameter and conduction velocity in myelinated nerve fibres. *Proc R Soc Lond B Biol Sci.* **217,** 29-35.

Roach A, Takahashi N, Pravtcheva D, Ruddle F, Hood L. (1985). Chromosomal mapping of mouse myelin basic protein gene and structure and transcription of the partially deleted gene in shiverer mutant mice. *Cell* **42,** 149-55.

Robertson AM, Huxley C, King RH, Thomas PK. (1999). Development of early postnatal peripheral nerve abnormalities in Trembler-J and PMP22 transgenic mice. *J Anat.* **195,** 331-9.

Rosenbluth, J. (1980). Peripheral myelin in the mouse mutant Shiverer. *J Comp Neurol.* **193,** 729-39.

Rosenbluth, J. (1999). A brief history of myelinated nerve fibers: one hundred and fifty years of controversy. *J Neurocytol.* **28,** 251-62.

Ryseck RP, Macdonald-Bravo H, Mattei MG, Ruppert S, Bravo R. (1989). Structure, mapping and expression of a growth factor inducible gene encoding a putative nuclear hormonal binding receptor. *EMBO J.* **8,** 3327-35.

Sakamoto Y, Kitamura K, Yoshimura K, Nishijima T, Uyemura K. (1987). Complete amino acid sequence of PO protein in bovine peripheral nerve myelin. *J Biol Chem.* **262,** 4208-14.

Salzer JL, Holmes WP, Colman DR. (1987). The amino acid sequences of the myelin-associated glycoproteins: homology to the immunoglobulin gene superfamily. *J Cell Biol.* **104,** 957-65.

Sancho S, Magyar JP, Aguzzi A, Suter1 U. (1999). Distal axonopathy in peripheral nerves of PMP22-mutant mice. *Brain* **122,** 1563-77.

Sancho S, Young P, Suter U. (2001). Regulation of Schwann cell proliferation and apoptosis in PMP22-deficient mice and mouse models of Charcot-Marie-Tooth disease type 1A. *Brain* **124,** 2177-87.

Sandri, C., Van Buren, J. M., and Akert, K. (1982). Membrane morphology of the vertebrate nervous system. *Prog Brain Res.* **46,** 201-265.

Schachner, M. (1990). Functional implications of glial cell recognition molecules. *Sem Neurosci.* **2,** 497-507.

Schaeren-Wiemers N, Valenzuela DM, Frank M, Schwab ME. (1995). Characterization of a rat gene, rMAL, encoding a protein with four hydrophobic domains in central and peripheral myelin. *J Neurosci.* **15,** 5753-64.

Scheidt P, Waehneldt TV, Beuche W, Friede RL. (1986). Changes of myelin proteins during Wallerian degeneration in situ and in millipore diffusion chambers preventing active phagocytosis. *Brain Res.* **379,** 380-4.

Scherer, S. S. (1996). Molecular specializations at nodes and paranodes in peripheral nerve. *Microsc Res Tech.* **34,** 452-61.

Scherer, S. S. (1997). The biology and pathobiology of Schwann cells. *Curr Opin Neurol.* **10,** 386-97.

Scherer, S. S., Paul, D. L. (2004). Functional Organization of the Nodes of Ranvier. In "Myelin biology and disorders". PP 89-116. Elsevier academic press.

Scherer SS, Deschenes SM, Xu YT, Grinspan JB, Fischbeck KH, Paul DL. (1995b). Connexin32 is a myelin-related protein in the PNS and CNS. *J Neurosci.* **15,** 8281-94.

Scherer SS, Kamholz J, Jakowlew SB. (1993). Axons modulate the expression of transforming growth factor-betas in Schwann cells. *Glia* **8,** 265-76.

Scherer SS, Wang DY, Kuhn R, Lemke G, Wrabetz L, Kamholz J. (1994). Axons regulate Schwann cell expression of the POU transcription factor SCIP. *J Neurosci.* **14,** 1930-42.

Scherer SS, Xu YT, Bannerman PG, Sherman DL, Brophy PJ. (1995a). Periaxin expression in myelinating Schwann cells: modulation by axon-glial interactions and polarized localization during development. *Development* **121,** 4265-73.

Scherer SS, Xu YT, Nelles E, Fischbeck K, Willecke K, Bone LJ. (1998). Connexin32-null mice develop demyelinating peripheral neuropathy. *Glia* **24,** 8-20.

Scherer SS., Salzer JL. (2001). Axon-Schwann cell interactions during peripheral nerve degeneration and regeneration. In "Glial cell development". PP 299-331. Oxford University Press.

Schindler P, Luu B, Sorokine O, Trifilieff E, Van Dorsselaer A. (1990). Developmental study of proteolipids in bovine brain: a novel proteolipid and DM-20 appear before proteolipid protein (PLP) during myelination. *J Neurochem.* **55,** 2079-85.

Schneider-Maunoury S, Topilko P, Seitandou T, Levi G, Cohen-Tannoudji M, Pournin S, Babinet C, Charnay P. (1993). Disruption of Krox-

20 results in alteration of rhombomeres 3 and 5 in the developing hindbrain. *Cell* **75,** 1199-214.

Schneider-Schaulies J, von Brunn A, Schachner M. (1990). Recombinant peripheral myelin protein P0 confers both adhesion and neurite outgrowth-promoting properties. *J Neurosci Res.* **27,** 286-97.

Seilheimer B, Persohn E, Schachner M. (1989). Antibodies to the L1 adhesion molecule inhibit Schwann cell ensheathment of neurons in vitro. *J Cell Biol.* **109,** 3095-103.

Sela-Donenfeld D, Kalcheim C. (1999). Regulation of the onset of neural crest migration by coordinated activity of BMP4 and Noggin in the dorsal neural tube. *Development* **126,** 4749-62.

Selleck MA, Garcia-Castro MI, Artinger KB, Bronner-Fraser M. (1998). Effects of Shh and Noggin on neural crest formation demonstrate that BMP is required in the neural tube but not ectoderm. *Development* **125,** 4919-30.

Selleck, M. & Bronner-fraser, M. (1995). Origins of the avian neural crest: the role of neural plate/epidermal interactions. *Development* **121,** 525-538.

Sen R, Baltimore D. (1986). Inducibility of kappa immunoglobulin enhancer-binding protein Nf-kappa B by a posttranslational mechanism. *Cell* **47,** 921-28.

Serbedzija GN, Bronner-Fraser M, Fraser SE. (1994). Developmental potential of trunk neural crest cells in the mouse. *Development* **120,** 1709-18.

Serbedzija GN, Fraser SE, Bronner-Fraser M. (1990). Pathways of trunk neural crest cell migration in the mouse embryo as revealed by vital dye labelling. *Development* **108,** 605-12.

Sereda M, Griffiths I, Puhlhofer A, Stewart H, Rossner MJ, Zimmerman F, Magyar JP, Schneider A, Hund E, Meinck HM, Suter U, Nave KA. (1996). A transgenic rat model of Charcot-Marie-Tooth disease. *Neuron* **16,** 1049-60.

Shah NM, Anderson DJ. (1997). Integration of multiple instructive cues by neural crest stem cells reveals cell-intrinsic biases in relative growth factor responsiveness. *Proc. Natl. Acad. Sci. USA.* **94,** 11369-74.

Shah NM, Marchionni MA, Isaacs I, Stroobant P, Anderson DJ. (1994). Glial growth factor restricts mammalian neural crest stem cells to a glial fate. *Cell* **77,** 349-60.

Shapiro DN, Sublett JE, Li B, Downing JR, Naeve CW. (1993). Fusion of PAX3 to a member of the forkhead family of transcription factors in human alveolar rhabdomyosarcoma. *Cancer Res.* **53,** 5108-12.

Shapiro L, Doyle JP, Hensley P, Colman DR, Hendrickson WA. (1996). Crystal structure of the extracellular domain from P0, the major structural protein of peripheral nerve myelin. *Neuron* **17,** 435-49.

Shawber CJ, Kitajewski J. (2004). Notch function in the vasculature: insights from zebrafish, mouse and man. *Bioessays* **26,** 225-34.

Shen YJ, DeBellard ME, Salzer JL, Roder J, Filbin MT. (1998). Myelin-associated glycoprotein in myelin and expressed by Schwann cells inhibits axonal regeneration and branching. *Mol Cell Neurosci.* **12,** 79-91.

Sherman DL, Brophy PJ. (2000). A tripartite nuclear localization signal in the PDZ-domain protein L-periaxin. *J Biol Chem.* **275,** 4537-40.

Sherman DL, Fabrizi C, Gillespie CS, Brophy PJ. (2001). Specific disruption of a schwann cell dystrophin-related protein complex in a demyelinating neuropathy. *Neuron* **30,** 677-87.

Sherman, D. L. and Brophy, P. J. (2004). The periaxin gene. In "Myelin biology and disorders". Elsevier academic press.

Shuman S, Hardy M, Pleasure D. (1983). Peripheral nervous system myelin and Schwann cell glycoproteins: identification by lectin binding and partial purification of a peripheral nervous system myelin-specific 170,000 molecular weight glycoprotein. *J Neurochem.* **41,** 1277-85.

Sieber-Blum, M. (1990). Mechanism of neural crest diversification. *Comm. Dev. Neurobiol.* **1,** 225-249.

Siebert H, Sachse A, Kuziel WA, Maeda N, Bruck W. (2000). The chemokine receptor CCR2 is involved in macrophage recruitment to the injured peripheral nervous system. *J Neuroimmunol.* **110,** 177-85.

Sim FJ, Zhao C, Li WW, Lakatos A, Franklin RJ. (2002). Expression of the POU-domain transcription factors SCIP/Oct-6 and Brn-2 is associated with Schwann cell but not oligodendrocyte remyelination of the CNS. *Mol Cell Neurosci.* **20,** 669-82.

Simons K, Ikonen E. (2000). How cells handle cholesterol. *Science* **290,** 1721-26.

Singh H, Pfeiffer SE. (1985). Myelin-associated galactolipids in primary cultures from dissociated fetal rat brain: biosynthesis, accumulation, and cell surface expression. *J Neurochem.* **45,** 1371-81.

Sinnreich M, Taylor BV, Dyck PJ. (2005). Diabetic neuropathies. Classification, clinical features, and pathophysiological basis. *Neurologist.* **11,** 63-79.

Skoff AM, Lisak RP, Bealmear B, Benjamins JA. (1998). TNF-alpha and TGF-beta act synergistically to kill Schwann cells. *J Neurosci Res.* **53,** 747-56.

Sliwkowski MX, Schaefer G, Akita RW, Lofgren JA, Fitzpatrick VD, Nuijens A, Fendly BM, Cerione RA, Vandlen RL, Carraway KL 3rd.

(1994). Coexpression of erbB2 and erbB3 proteins reconstitutes a high affinity receptor for heregulin. *J Biol Chem.* **269,** 14661-5.

Smith-Slatas C, Barbarese E. (2000). Myelin basic protein gene dosage effects in the PNS. *Mol Cell Neurosci.* **15,** 343-54.

Snipes GJ, Orfali W. (1998). Common themes in peripheral neuropathy disease genes. *Cell Biol Int.* **22,** 815-35.

Snipes GJ, Suter U, Welcher AA, Shooter EM. (1992). Characterization of a novel peripheral nervous system myelin protein (PMP-22/SR13). *J Cell Biol.* **117,** 225-38.

Snipes GJ, Suter U. (1995). Molecular anatomy and genetics of myelin proteins in the peripheral nervous system. *J Anat.* **186,** 483-94.

Sohl G, Eiberger J, Jung YT, Kozak CA, Willecke K. (2001). The mouse gap junction gene connexin29 is highly expressed in sciatic nerve and regulated during brain development. *Biol Chem.* **382,** 973-8.

Soilu-Hanninen M, Ekert P, Bucci T, Syroid D, Bartlett PF, Kilpatrick TJ. (1999). Nerve growth factor signaling through p75 induces apoptosis in Schwann cells via a Bcl-2-independent pathway. *J Neurosci.* **19,** 4828-38.

Southard-Smith EM, Angrist M, Ellison JS, Agarwala R, Baxevanis AD, Chakravarti A, Pavan WJ. (1999). The Sox10(Dom) mouse: modeling the genetic variation of Waardenburg-Shah (WS4) syndrome. *Genome Res.* **9,** 215-25.

Spiegel I, Peles E. (2002). Cellular junctions of myelinated nerves (Review). *Mol Membr Biol.* **19,** 95-101.

Sporkel O, Uschkureit T, Bussow H, Stoffel W. (2002). Oligodendrocytes expressing exclusively the DM20 isoform of the proteolipid protein gene: myelination and development. *Glia* **37,** 19-30.

Srinivasan Y, Elmer L, Davis J, Bennett V, Angelides K. (1988). Ankyrin and spectrin associate with voltage-dependent sodium channels in brain. *Nature* **333,** 177-80.

St-Jacques, B., Dassule, H.R., Karavanova, I., Botchkarev, V.A., Li, J., Danielian, P.S., McMahon, J.A., Lewis, P.M., Paus, R., and McMahon, A.P. (1998). Sonic hedgehog signaling is essential for hair development. *Curr Biol.* **8,** 1058-68.

Stahl N, Harry J, Popko B. (1990). Quantitative analysis of myelin protein gene expression during development in the rat sciatic nerve. *Brain Res Mol Brain Res.* **8,** 209-12.

Stecca B, Southwood CM, Gragerov A, Kelley KA, Friedrich VL Jr, Gow A. (2000). The evolution of lipophilin genes from invertebrates to tetrapods: DM-20 cannot replace proteolipid protein in CNS myelin. *J Neurosci.* **20,** 4002-10.

Stefansson H, Sigurdsson E, Steinthorsdottir V, Bjornsdottir S, Sigmundsson T, Ghosh S, Brynjolfsson J, Gunnarsdottir S, Ivarsson O, Chou TT, Hjaltason O, Birgisdottir B, Jonsson H, Gudnadottir VG, Gudmundsdottir E, Bjornsson A, Ingvarsson B, Ingason A, Sigfusson S, Hardardottir H, Harvey RP, Lai D, Zhou M, Brunner D, Mutel V, Gonzalo A, Lemke G, Sainz J, Johannesson G, Andresson T, Gudbjartsson D, Manolescu A, Frigge ML, Gurney ME, Kong A, Gulcher JR, Petursson H, Stefansson K. (2002). Neuregulin 1 and susceptibility to schizophrenia. *Am J Hum Genet.* **71,** 877-92.

Stegman, M.A., Goetz, J.A., Ascano, M.Jr., Ogden, S.K., Nybakken, K.E., and Robbins, D.J. (2004). The kinesin-related protein Costal2 associates with membranes in a hedgehog-sensitive, Smoothened-independent manner. *J. Biol. Chem* **279,** 7064-71.

Stemple DL, Anderson DJ. (1992). Isolation of a stem cell for neurons and glia from the mammalian neural crest. *Cell* **71,** 973-85.

Stewart HJ, Brennan A, Rahman M, Zoidl G, Mitchell PJ, Jessen KR, Mirsky R. (2001). Developmental regulation and overexpression of the transcription

factor AP-2, a potential regulator of the timing of Schwann cell generation. *Eur J Neurosci.* **14,** 363-72.

Stewart HJ, Bradke F, Tabernero A, Morrell D, Jessen KR, Mirsky R. (1996). Regulation of rat Schwann cell Po expression and DNA synthesis by insulin-like growth factors in vitro. *Eur J Neurosci.* **8,** 553-64.

Stewart HJ, Morgan L, Jessen KR, Mirsky R. (1993). Changes in DNA synthesis rate in the Schwann cell lineage in vivo are correlated with the precursor--Schwann cell transition and myelination. *Eur J Neurosci.* **5,** 1136-44.

Stewart HJ, Rougon G, Dong Z, Dean C, Jessen KR, Mirsky R. (1995). TGF-betas upregulate NCAM and L1 expression in cultured Schwann cells, suppress cyclic AMP-induced expression of O4 and galactocerebroside, and are widely expressed in cells of the Schwann cell lineage in vivo. *Glia* **15,** 419-36.

Stewart HJ, Turner D, Jessen KR, Mirsky R. (1997b). Expression and regulation of alpha1beta1 integrin in Schwann cells. *J Neurobiol.* **33,** 914-28.

Stewart HJ, Zoidl G, Rossner M, Brennan A, Zoidl C, Nave KA, Mirsky R, Jessen KR. (1997a). Helix-loop-helix proteins in Schwann cells: a study of regulation and subcellular localization of Ids, REB, and E12/47 during embryonic and postnatal development. *J Neurosci Res.* **50,** 684-701.

Stoffel W, Hillen H, Giersiefen H. (1984). Structure and molecular arrangement of proteolipid protein of central nervous system myelin. *Proc Natl Acad Sci U S A.* **81,** 5012-6.

Stoll G, Griffin JW, Li CY, Trapp BD. (1989). Wallerian degeneration in the peripheral nervous system: participation of both Schwann cells and macrophages in myelin degradation. *J Neurocytol.* **18,** 671-83.

Storey KG, Goriely A, Sargent CM, Brown JM, Burns HD, Abud HM, Heath JK. (1998). Early posterior neural tissue is induced by FGF in the chick embryo. *Development* **125,** 473-84.

Streit A, Berliner AJ, Papanayotou C, Sirulnik A, Stern CD. (2000). Initiation of neural induction by FGF signalling before gastrulation. *Nature* **406,** 74-78.

Streit, A. & Stern, C. (1999). Establishment and maintenance of the border of the neural plate in the chick: involvement of FGF and BMP activity. *Mech. Dev.* **82,** 51-66.

Subang MC, Richardson PM. (2001). Synthesis of leukemia inhibitory factor in injured peripheral nerves and their cells. *Brain Res.* **900,** 329-31.

Suh JG, Ichihara N, Saigoh K, Nakabayashi O, Yamanishi T, Tanaka K, Wada K, Kikuchi T. (1997). An in-frame deletion in peripheral myelin protein-22 gene causes hypomyelination and cell death of the Schwann cells in the new Trembler mutant mice. *Neuroscience* **79,** 735-44.

Sukhatme VP, Cao XM, Chang LC, Tsai-Morris CH, Stamenkovich D, Ferreira PC, Cohen DR, Edwards SA, Shows TB, Curran T, et al. (1988). A zinc finger-encoding gene coregulated with c-fos during growth and differentiation, and after cellular depolarization. *Cell* **53,** 37-43.

Sukhatme VP, Kartha S, Toback FG, Taub R, Hoover RG, Tsai-Morris CH. (1987). A novel early growth response gene rapidly induced by fibroblast, epithelial cell and lymphocyte mitogens. *Oncogene Res.* **1,** 343-355.

Sulaiman OA, Gordon T. (2002). Transforming growth factor-beta and forskolin attenuate the adverse effects of long-term Schwann cell denervation on peripheral nerve regeneration in vivo. *Glia* **37,** 206-218.

Sunada Y, Bernier SM, Utani A, Yamada Y, Campbell KP. (1995). Identification of a novel mutant transcript of laminin alpha 2 chain gene responsible for muscular dystrophy and dysmyelination in dy2J mice. *Hum Mol Genet.* **4,** 1055-61.

Suter U, Moskow JJ, Welcher AA, Snipes GJ, Kosaras B, Sidman RL, Buchberg AM, Shooter EM. (1992a). A leucine-to-proline mutation in the putative first transmembrane domain of the 22-kDa peripheral myelin protein in the trembler-J mouse. *Proc Natl Acad Sci U S A.* **89,** 4382-6.

Suter U, Snipes GJ, Schoener-Scott R, Welcher AA, Pareek S, Lupski JR, Murphy RA, Shooter EM, Patel PI. (1994). Regulation of tissue-specific

expression of alternative peripheral myelin protein-22 (PMP22) gene transcripts by two promoters. *J Biol Chem.* **269,** 25795-808.

Suter U, Welcher AA, Ozcelik T, Snipes GJ, Kosaras B, Francke U, Billings-Gagliardi S, Sidman RL, Shooter EM. (1992b). Trembler mouse carries a point mutation in a myelin gene. *Nature* **356,** 241-4.

Suter U, Welcher AA, Snipes GJ. (1993). Progress in the molecular understanding of hereditary peripheral neuropathies reveals new insights into the biology of the peripheral nervous system. *Trends Neurosci.* **16,** 50-6.

Suzuki N, Rohdewohld H, Neuman T, Gruss P, Scholer HR. (1990). Oct-6: a POU transcription factor expressed in embryonal stem cells and in the developing brain. *EMBO J.* **9,** 3723-32.

Svennerholm, L. (1980). Ganglioside designation. *Adv Exp Med Biol.* **125.**

Swirnoff AH, Apel ED, Svaren J, Sevetson BR, Zimonjic DB, Popescu NC, Milbrandt J. (1998). Nab1, a corepressor of NGFI-A (Egr-1), contains an active transcriptional repression domain. *Mol Cell Biol.* **18,** 512-24.

Syroid DE, Maycox PR, Burrola PG, Liu N, Wen D, Lee KF, Lemke G, Kilpatrick TJ. (1996). Cell death in the Schwann cell lineage and its regulation by neuregulin. *Proc Natl Acad Sci U S A.* **93,** 9229-34.

Syroid DE, Maycox PJ, Soilu-Hanninen M, Petratos S, Bucci T, Burrola P, Murray S, Cheema S, Lee KF, Lemke G, Kilpatrick TJ. (2000). nduction of postnatal schwann cell death by the low-affinity neurotrophin receptor in vitro and after axotomy. *J Neurosci.* **20,** 5741-47.

Syroid DE, Zorick TS, Arbet-Engels C, Kilpatrick TJ, Eckhart W, Lemke G. (1999). A role for insulin-like growth factor-I in the regulation of Schwann cell survival. *J Neurosci.* **19,** 2059-2068.

Tabata H, Ikegami H, Kariya K. (2000). Spontaneous age-related peripheral neuropathy in B6C3F1 mice. *J Toxicol Sci.* **25,** 95-104.

Tabira T, Cullen MJ, Reier PJ, Webster H deF. (1978). An experimental analysis of interlamellar tight junctions in amphibian and mammalian C.N.S. myelin. *J Neurocytol.* **7,** 489-503.

Takabatake T, Ogawa M, Takahashi TC, Mizuno M, Okamoto M, Takeshima K. (1997). Hedgehog and patched gene expression in adult ocular tissues. *FEBS Lett.* **410,** 485-9.

Takahashi M, Osumi N. (2005). dentification of a novel type II classical cadherin: rat cadherin19 is expressed in the cranial ganglia and Schwann cell precursors during development. *Dev Dyn.* **232,** 200-8.

Takahashi N, Roach A, Teplow DB, Prusiner SB, Hood L. (1985). Cloning and characterization of the myelin basic protein gene from mouse: one gene can encode both 14 kd and 18.5 kd MBPs by alternate use of exons. *Cell* **42,** 139-48.

Tang S, Woodhall RW, Shen YJ, deBellard ME, Saffell JL, Doherty P, Walsh FS, Filbin MT. (1997). Soluble myelin-associated glycoprotein (MAG) found in vivo inhibits axonal regeneration. *Mol Cell Neurosci.* **9,** 333-46.

Tay SY, Ingham PW, Roy S. (2005). A homologue of the Drosophila kinesin-like protein Costal2 regulates Hedgehog signal transduction in the vertebrate embryo. *Development* **132**, 625-634.

Taylor, C.M., Marta, C.B., Bansal, R., and Pfeiffer, S.E. (2004). The transport, assembly, and function of myelin lipids. In "Myelin Biology and Disorders". PP 57-88. Elsevier Academic Press.

Taylor V, Welcher AA, Program AE, Suter U. (1995). Epithelial membrane protein-1, peripheral myelin protein 22, and lens membrane protein 20 define a novel gene family. *J Biol Chem.* **270**, 28824-33.

Terenghi, G. (1999). Peripheral nerve regeneration and neurotrophic factors. *J Anat.* **194,** 1-14.

Tetzlaff, W. (1982). Tight junction contact events and temporary gap junctions in the sciatic nerve fibres of the chicken during Wallerian degeneration and subsequent regeneration. *J Neurocytol.* **11,** 839-58.

Thatikunta P, Qin W, Christy BA, Tennekoon GI, Rutkowski JL. (1999). Reciprocal Id expression and myelin gene regulation in Schwann cells. *Mol Cell Neurosci.* **14,** 519-528.

Thevananther S, Kolli AH, Devarajan P. (1998). Identification of a novel ankyrin isoform (AnkG190) in kidney and lung that associates with the plasma membrane and binds alpha-Na, K-ATPase. *J Biol Chem.* **273,** 23952-8.

Thomson CE, Mitchell LS, Griffiths IR, Morrison S. (1991). Retarded Wallerian degeneration following peripheral nerve transection in C57BL/6/Ola mice is associated with delayed down-regulation of the P0 gene. *Brain Res.* **538,** 157-60.

Timsit S, Martinez S, Allinquant B, Peyron F, Puelles L, Zalc B. (1995). Oligodendrocytes originate in a restricted zone of the embryonic ventral neural tube defined by DM-20 mRNA expression. *J Neurosci.* **15,** 1012-24.

Timsit SG, Bally-Cuif L, Colman DR, Zalc B. (1992). DM-20 mRNA is expressed during the embryonic development of the nervous system of the mouse. *J Neurochem.* **58,** 1172-5.

Tobler AR, Notterpek L, Naef R, Taylor V, Suter U, Shooter EM. (1999). Transport of Trembler-J mutant peripheral myelin protein 22 is blocked in the intermediate compartment and affects the transport of the wild-type protein by direct interaction. *J Neurosci.* **19,** 2027-36.

Toews AD, Barrett C, Morell P. (1998). Monocyte chemoattractant protein 1 is responsible for macrophage recruitment following injury to sciatic nerve. *J Neurosci Res.* **53,** 260-7.

Tofaris GK, Patterson PH, Jessen KR, Mirsky R. (2002). Denervated Schwann cells attract macrophages by secretion of leukemia inhibitory factor (LIF) and monocyte chemoattractant protein-1 in a process regulated by interleukin-6 and LIF. *J Neurosci.* **22,** 6696-703.

Topilko P, Levi G, Merlo G, Mantero S, Desmarquet C, Mancardi G, Charnay P. (1997). Differential regulation of the zinc finger genes Krox-20 and Krox-24 (Egr-1) suggests antagonistic roles in Schwann cells. *J Neurosci Res* **50,** 702-712.

Topilko P, Schneider-Maunoury S, Levi G, Baron-Van Evercooren A, Chennoufi AB, Seitanidou T, Babinet C, Charnay P. (1994). Krox-20 controls myelination in the peripheral nervous system. *Nature* **371,** 796-9.

Topilko P, Schneider-Maunoury S, Levi G, Trembleau A, Gourdji D, Driancourt MA, Rao CV, Charnay P. (1998). Multiple pituitary and ovarian defects in Krox-24 (NGFI-A, Egr-1)-targeted mice. *Mol Endocrinol.* **12,** 107-122.

Touraine RL, Attie-Bitach T, Manceau E, Korsch E, Sarda P, Pingault V, Encha-Razavi F, Pelet A, Auge J, Nivelon-Chevallier A, Holschneider AM, Munnes M, Doerfler W, Goossens M, Munnich A, Vekemans M, Lyonnet S. (2000). Neurological phenotype in Waardenburg syndrome type 4 correlates with novel SOX10 truncating mutations and expression in developing brain. *Am J Hum Genet.* **66,** 1496-503.

Trachtenberg JT, Thompson WJ. (1996). Schwann cell apoptosis at developing neuromuscular junctions is regulated by glial growth factor. *Nature* **379,** 174-7.

Trapp, BD. (1988a). Distribution of the myelin-associated glycoprotein and P0 protein during myelin compaction in quaking mouse peripheral nerve. *J cell Biol.* **107,** 675-685.

Trapp, B. D., Pfeiffer, S. E., Anitei, M., Kidd, G. J. (2004). Cell Biology of Myelin Assembly. In "Myelin biology and disorders". PP 29-55. Elsevier academic press.

Trapp BD, Andrews SB, Wong A, O'Connell M, Griffin JW. (1989a). Co-localization of the myelin-associated glycoprotein and the microfilament components, F-actin and spectrin, in Schwann cells of myelinated nerve fibres. *J Neurocytol.* **18,** 47-60.

Trapp BD, Andrews SB, Cootauco C, Quarles R. (1989b). The myelin-associated glycoprotein is enriched in multivesicular bodies and periaxonal membranes of actively myelinating oligodendrocytes. *J Cell Biol.* **109,** 2417-26.

Trapp BD, Dubois-Dalcq M, Quarles RH. (1984b). Ultrastructural localization of P2 protein in actively myelinating rat Schwann cells. *J Nerochem.* **43,** 944-8.

Trapp BD, McIntyre LJ, Quarles RH, Sternberger NH, Webster HD. (1979). Immunocytochemical localization of rat peripheral nervous system myelin proteins: P2 protein is not a component of all peripheral nervous system myelin sheaths. *Proc Natl Acad Sci U S A.* **76,** 3552-56.

Trapp BD, Moench T, Pulley M, Barbosa E, Tennekoon G, Griffin J. (1987). Spatial segregation of mRNA encoding myelin-specific proteins. *Proc Natl Acad Sci U S A.* **84,** 7773-7.

Trapp BD, Quarles RH. (1982). Presence of the myelin-associated glycoprotein correlates with alterations in the periodicity of peripheral myelin. *J cell Biol.* **92,** 877-882.

Trapp BD, Quarles RH, Suzuki K. (1984a). Immunocytochemical studies of quaking mice support a role for the myelin-associated glycoprotein in forming and maintaining the periaxonal space and periaxonal cytoplasmic collar of myelinating Schwann cells. *J cell Biol.* **99,** 594-606.

Tricaud N, Perrin-Tricaud C, Bruses JL, Rutishauser U. (2005). Adherens junctions in myelinating Schwann cells stabilize Schmidt-Lanterman incisures via recruitment of p120 catenin to E-cadherin. *J Neurosci.* **25,** 3259-69.

Tropak MB, Johnson PW, Dunn RJ, Roder JC. (1988). Differential splicing of MAG transcripts during CNS and PNS development. *Brain Res.* **464,** 143-55.

Tsujino H, Kondo E, Fukuoka T, Dai Y, Tokunaga A, Miki K, Yonenobu K, Ochi T, Noguchi K. (2000). Activating transcription factor 3 (ATF3) induction by axotomy in sensory and motoneurons: A novel neuronal marker of nerve injury. *Mol Cell Neurosci.* **15,** 170-82.

Umehara, F., Tate, G., Itoh, K., Yamaguchi, N., Douchi, T., Mitsuya, T., Osame, M. (2000). A novel mutation of desert hedgehog in a patient with 46,XY partial gonadal dysgenesis accompanied by minifascicular neuropathy. *Am J Hum Genet.* **67,** 1302-5.

Uschkureit T, Sporkel O, Bussow H, Stoffel W. (2001). Rumpshaker-like proteolipid protein (PLP) ratio in a mouse model with unperturbed structural and functional integrity of the myelin sheath and axons in the central nervous system. *Glia* **35,** 63-71.

Uyemura K, Tobari C, Hirano S, Tsukada Y. (1972). Comparative studies on the myelin proteins of bovine peripheral nerve and spinal cord. *J nerochem.* **19,** 2607-14.

Uyemura K, Yoshimura K, Suzuki M, Kitamura K. (1984). Lipid binding activities of the P2 protein in peripheral nerve myelin. *Neurochem Res.* **9,** 1509-14.

Uziyel Y, Hall S, Cohen J. (2000). Influence of laminin-2 on Schwann cell-axon interactions. *Glia* **32,** 109-21.

Valentijn LJ, Baas F, Wolterman RA, Hoogendijk JE, van den Bosch NH, Zorn I, Gabreels-Festen AW, de Visser M, Bolhuis PA. (1992). Identical point mutations of PMP-22 in Trembler-J mouse and Charcot-Marie-Tooth disease type 1A. *Nat Genet.* **2,** 288-91.

Vermeren M, Maro GS, Bron R, McGonnell IM, Charnay P, Topilko P, Cohen J. (2003). Integrity of developing spinal motor columns is regulated by neural crest derivatives at motor exit points. *Neuron* **37,** 403-15.

Vortkamp, A., Pathi, S., Peretti, G.M., Caruso, E.M., Zaleske, D.J., and Tabin, C.J. (1998). Recapitulation of signals regulating embryonic bone formation during postnatal growth and in fracture repair. *Mech. Dev.* **71,** 65-76.

Vortkamp A, Lee K, Lanske B, Segre GV, Kronenberg HM, Tabin CJ. (1996). Regulation of rate of cartilage differentiation by Indian hedgehog and PTH-related protein. *Science* **273,** 613-22.

Wakamatsu Y, Maynard TM, Weston JA. (2000). Fate determination of neural crest cells by NOTCH-mediated lateral inhibition and asymmetrical cell division during gangliogenesis. *Development* **127,** 281-21.

Watson MA, Milbrandt J. (1990). Expression of the nerve growth factor-regulated NGFI-A and NGFI-B genes in the developing rat. *Development* **110,** 173-83.

Waxman SG, Bennett MV. (1972). Relative conduction velocities of small myelinated and non-myelinated fibres in the central nervous system. *Nat New Biol.* **238,** 217-9.

Webster, H.D. (1965). The relationship between schmidt-lantermann incisures and myelin segmentation during wallerian degeneration. *Ann N Y Acad Sci.* **122,** 29-38.

Webster, H. D. (1971). The geometry of peripheral myelin sheaths during their formation and growth in rat sciatic nerves. *J Cell Biol.* **48,** 348-367.

Weerasuriya A, Curran GL, Poduslo JF. (1990). Developmental changes in blood-nerve transfer of albumin and endoneurial albumin content in rat sciatic nerve. *Brain Res.* **521,** 40-6.

Wegner, M. (1999). From head to toes: the multiple facets of Sox proteins. *Nucleic Acids Res.* **27,** 1409-20.

Wegner, M. (2000). Transcriptional control in myelinating glia: flavors and spices. *Glia* **31,** 1-14.

Weiner JA, Chun J. (1999). Schwann cell survival mediated by the signaling phospholipid lysophosphatidic acid. *Proc. Natl. Acad. Sci. USA.* **96,** 5233-8.

Weiss MD, Luciano CA, Quarles RH. (2001). Nerve conduction abnormalities in aging mice deficient for myelin-associated glycoprotein. *Muscle Nerve.* **24,** 1380-7.

Welcher AA, Suter U, De Leon M, Snipes GJ, Shooter EM. (1991). A myelin protein is encoded by the homologue of a growth arrest-specific gene. *Proc Natl Acad Sci U S A.* **88,** 7195-9.

Wen D, Peles E, Cupples R, Suggs S.V., Bacus S.S., Luo Y., Trail G., Hu S., Silbiger S.M., Levy R.B., Koski R.A., Lu H.S., Yarden Y. (1992). Neu differentiation factor: a transmembrane glycoprotein containning an EGF domain and an immunoglobulin homology unit. *Cell* **69,** 559-72.

Weston, J. A. (1963). A radioautographic analysis of the migration and localization of trunk neural crest cells in the chick. *Dev. biol.* **6,** 279-310.

White PM, Morrison SJ, Orimoto K, Kubu CJ, Verdi JM, Anderson DJ. (2001). Neural crest stem cells undergo cell-intrinsic developmental changes in sensitivity to instructive differentiation signals. *Neuron* **29,** 57-71.

White TW, Paul DL. (1999). Genetic diseases and gene knockouts reveal diverse connexin functions. *Annu Rev Physiol.* **61,** 283-30.

Wilkinson DG, Bhatt S, Chavrier P, Bravo R, Charnay P. (1989a). Segment-specific expression of a zinc-finger gene in the developing nervous system of the mouse. *Nature* **337,** 461-4.

Willecke K, Eiberger J, Degen J, Eckardt D, Romualdi A, Guldenagel M, Deutsch U, Sohl G. (2002). Structural and functional diversity of connexin genes in the mouse and human genome. *Biol Chem.* **383,** 725-37.

Windebank AJ, Wood P, Bunge RP, Dyck PJ. (1985). Myelination determines the caliber of dorsal root ganglion neurons in culture. *J Neurosci.* **5,** 1563-9.

Woldeyesus MT, Britsch S, Riethmacher D, Xu L, Sonnenberg-Riethmacher E, Abou-Rebyeh F, Harvey R, Caroni P, Birchmeier C. (1999). Peripheral nervous system defects in erbB2 mutants following genetic rescue of heart development. *Genes Dev.* **13,** 2538-48.

Wood PM, Schachner M, Bunge RP. (1990). Inhibition of Schwann cell myelination in vitro by antibody to the L1 adhesion molecule. *J Neurosci.* **10,** 3635-45.

Woolf CJ, Reynolds ML, Chong MS, Emson P, Irwin N, Benowitz LI. (1992). Denervation of the motor endplate results in the rapid expression by terminal Schwann cells of the growth-associated protein GAP-43. *J Neurosci.* **12,** 3999-4010.

Wrabetz L, Feltri ML, Quattrini A, Imperiale D, Previtali S, D'Antonio M, Martini R, Yin X, Trapp BD, Zhou L, Chiu SY, Messing A. (2000). P(0) glycoprotein overexpression causes congenital hypomyelination of peripheral nerves. *J Cell Biol.* **148,** 1021-34.

Wrabetz, L; Feltri, M. L; Suter, U. (2004). Models of Charcot-Marie-Tooth disease. in "Myelin biology and disorders". pp. 1143-68. Elsevier academic press.

Xu H, Wu XR, Wewer UM, Engvall E. (1994). Murine muscular dystrophy caused by a mutation in the laminin alpha 2 (Lama2) gene. *Nat. Genet.* **8,** 297-302.

Yanagisawa M, Kurihara H, Kimura S, Goto K, Masaki T. (1988). A novel peptide vasoconstrictor, endothelin, is produced by vascular endothelium and modulates smooth muscle Ca2+ channels. *J Hypertens Suppl.* **6,** 188-91.

Yancopoulos GD, Davis S, Gale NW, Rudge JS, Wiegand SJ, Holash J. (2000). Vascular-specific growth factors and blood vessel formation. *Nature* **407,** 242-8.

Yang Y, Lacas-Gervais S, Morest DK, Solimena M, Rasband MN. (2004). BetaIV spectrins are essential for membrane stability and the molecular organization of nodes of Ranvier. *J Neurosci.* **24,** 7230-40.

Yin X, Crawford TO, Griffin JW, Tu P, Lee VM, Li C, Roder J, Trapp BD. (1998). Myelin-associated glycoprotein is a myelin signal that modulates the

caliber of myelinated axons. *J Neurosci.* **18,** 1953-62.

Yool D, Klugmann M, Barrie JA, McCulloch MC, Nave KA, Griffiths IR. (2002). Observations on the structure of myelin lacking the major proteolipid protein. *Neuropathol Appl Neurobiol.* **28,** 75-8.

Yoshida H, Kunisada T, Grimm T, Nishimura EK, Nishioka E, Nishikawa SI. (2001). Review: melanocyte migration and survival controlled by SCF/c-kit expression. *J Investig Dermatol Symp Proc.* **6,** 1-5.

Yoshino JE, Dinneen MP, Sprinkle TJ, DeVries GH. (1985). Localization of 2',3'-cyclic nucleotide 3'-phosphodiesterase on cultured Schwann cells. *Brain Res.* **325,** 199-203.

Yoshino JE, Griffin JW, DeVries GH. (1983). Identification of an axolemma-enriched fraction from peripheral nerve. *J nerochem.* **41,** 1126-30.

Young HM, Hearn CJ, Farlie PG, Canty AJ, Thomas PQ, Newgreen DF. (2001). GDNF is a chemoattractant for enteric neural cells. *Dev Biol.* **229,** 503-16.

Zanazzi G, Einheber S, Westreich R, Hannocks MJ, Bedell-Hogan D, Marchionni MA, Salzer JL. (2001). Glial growth factor/neuregulin inhibits Schwann cell myelination and induces demyelination. *J Cell Biol.* **152,** 1289-99.

Zhang C, Williams EH, Guo Y, Lum L, Beachy PA. (2004). Extensive phosphorylation of Smoothened in Hedgehog pathway activation. *Proc Natl Acad Sci U S A.* **101,** 17900-7.

Zhang X, Davis JQ, Carpenter S, Bennett V. (1998). Structural requirements for association of neurofascin with ankyrin. *J Biol Chem.* **273,** 30785-94.

Zhang Y, Roslan R, Lang D, Schachner M, Lieberman AR, Anderson PN. (2000). Expression of CHL1 and L1 by neurons and glia following sciatic nerve and dorsal root injury. *Mol Cell Neurosci.* **16,** 71-86.

Zhou D, Lambert S, Malen PL, Carpenter S, Boland LM, Bennett V. (1998). AnkyrinG is required for clustering of voltage-gated Na channels at axon initial segments and for normal action potential firing. *J Cell Biol.* **143,** 1295-304.

Zimmermann, H. (1996). Accumulation of synaptic vesicle proteins and cytoskeletal specializations at the peripheral node of Ranvier. *Microsc Res Tech.* **34,** 462-73.

Zorick TS, Syroid DE, Arroyo E, Scherer SS, Lemke G. (1996). The Transcription Factors SCIP and Krox-20 Mark Distinct Stages and Cell Fates in Schwann Cell Differentiation. *Mol Cell Neurosci.* **8,** 129-45.

Zorick TS, Syroid DE, Brown A, Gridley T, Lemke G. (1999). Krox-20 controls SCIP expression, cell cycle exit and susceptibility to apoptosis in developing

myelinating Schwann cells. *Development* **126,** 1397-406.

Zou H, Wieser R, Massague J, Niswander L. (1997). Distinct roles of type I bone morphogenetic protein receptors in the formation and differentiation of cartilage. *Genes Dev.* **11,** 2191-203.